Isolation of Affimers against biomarkers of *Clostridium difficile* infection for use as diagnostic tools

Modupe Oluwabunmi Ajayi

MSc. (Hons)

Submitted in accordance with the requirements for the degree of Doctor of Philosophy

The University of Leeds

School of Molecular and Cellular Biology

February, 2017

The candidate confirms that the work submitted is her own and that appropriate credit has been given where reference has been made to the work of others.

This copy has been supplied on the understanding that it is copyright material and that no quotation from the thesis may be published without proper acknowledgement.

The right of Modupe Oluwabunmi Ajayi to be identified as Author of this work has been asserted by her in accordance with the Copyright, Designs and Patents Act 1988.

Acknowledgement

First, I would like to express my sincere gratitude to my supervisor, Professor Michael J. McPherson. Thank you for painstakingly tutoring me despite the several turns in this PhD; you have been a true inspiration. I appreciate your guidance, motivation and immense knowledge. Thanks to my co-supervisor, Dr Darren Tomlinson for your help. To Dr Christian Tiede, who is also part of my supervisory team, I deeply appreciate your support and helpful discussions throughout this PhD. Especially for providing guidance during the phage display screening of GDH, toxin A and toxin B. Thanks to Dr Thembaninkosi Gaule for all your encouragements and scientific expertise. Many thanks to my home university Adekunle Ajasin University Akungba-Akoko, Ondo State Nigeria, for nominating me for TETFUND sponsorship, which funded my PhD.

I appreciate Dr Iain Manfield for providing useful discussions on data analysis during the biophysical characterisation of my samples using gel filtration, Surface Plasmon Resonance, Differential Scanning Calorimetry and OpTim techniques. I would like to acknowledge Dr Cliff Shone from Public Health England (PHE) for providing me with generous amount of toxin A and toxin B.

No true success can be achieved in isolation; therefore, I greatly appreciate the support, fun and memories shared with the current members of the McPherson research group and the BioScreening Technology group (Hannah, Anna, Michal, Heather, Janice, Danah, Rob, Sophie, Lia, Kasia and Tom) and past (Sarah and Suja). Thank you to the two students I supervised during my PhD for their contribution to the project: Mr Samuel Rhoden and Ms Glenys Lewis.

I would like to thank members of DLBC Leeds; you have made Leeds to be home away from home. Thanks for the fellowship and true love I found in you. Special thanks go to Dr Victor Ebenuwa and family for the uplifting messages. I sincerely appreciate the Tsiga, Daranijo and Oluwi families for helping me with childminding during those tough days - thank you so much. To all my amazing friends and everyone in DLCF Leeds especially Grace, Faith, Mercy, Wole, Lekan, George,

Telema, Taiwo and Pelumi, thanks for the cooperation and support you have shown during my leadership.

To my amazing parents, Mr Ayodele Abel Afun and Mrs Mercy Funmilola Afun, I am deeply grateful for all your labour of love, your sacrifices, and prayers. Dad, you taught me how to be resilient, courageous and to fight against life challenges to achieve my goal in life. You are my hero. To my siblings - Busayo, David and Daniel - thanks for been so close even when we are physically far apart. A big thank you to my friends and family in Nigeria - Pastor Meshack, my in-laws, Lekan Onisuuru and Kenny Aruleba.

I would especially like to thank my husband, Toluleke Ajayi (Teminikan) for the great sacrifice he paid during this 4 years of PhD. Thanks for taking care of Tim and Jerry and sustaining our home. You've been my rock, my comfort, my helper and counsellor - you are a rare gem. To my lovely sons, Timothy, Jeremiah and Samuel, I love you so much and proud to be your mum. I always look forward with joy to seeing you no matter what I've faced in the laboratory.

Finally, yet importantly, this thesis is dedicated to God Almighty, the Alpha and Omega. Thank you Lord for opening the door for the funding of my PhD against all odds, for giving me the accomplishing strength and for fulfilling your promise in Job 8:7 – Though my beginning was small, yet my latter end has greatly increased.

Abstract

Clostridium difficile is one of the leading causal agents of hospital acquired infection and antibiotic-associated diarrhoea. The treatment and control of *Clostridium difficile* infection (CDI) is critically dependent on accurate laboratory diagnosis. However, current diagnostic methods have limitations including cost, potential over-sensitivity, lack of detection of toxin protein associated with nucleic acid amplification techniques, and long turnaround time for toxigenic cultures. Detection of toxins in faecal samples of patients suffering from CDI is a highly significant and necessary criterion for the diagnosis of CDI. Rapid enzyme immunoassays are used for toxin detection and can be completed in less than an hour, however, their low sensitivities make them unacceptable for use as a stand-alone test. To date, no one-step diagnostic that is low cost, sensitive and specific is available for CDI diagnosis. Leeds has developed a non-antibody binding protein called Affimer type II (Affimer). From phage display libraries, Affimer binders against >350 targets have been identified.

This thesis investigates the isolation of Affimers against biomarkers of *Clostridium difficile* infection for use as diagnostic tools. Phage display screening yielded high affinity Affimers against the three well-established biomarkers of CDI (toxin A, toxin B and glutamate dehydrogenase). Characterisation of the Affimer binders show that they bind to their target with low nanomolar affinity. Through sandwich phage ELISA, two toxin B Affimers have been established for use as a pair in sandwich assay format. This thesis has also explored the ability of Affimers to function as novel reagents for the potential development of a point-of-care diagnostic tool for *C. difficile* infection. The most exciting result include the development of a toxin B hybrid assay which shows improved sensitivity and specificity by switching one of the molecular recognition elements of a clinically used *C. difficile* detection kit from antibodies to Affimers.

Table of content

List of Figures

List of Tables

Abbreviations

Ab	Antibody
ABP	Artificial binding proteins
Abs	Absorbance
ADH-3	Affimer (ataxin binder) with 3 mutations
ADH-5	Affimer (ataxin binder) with 5 mutations
Ag:	Antigen
APS	Ammonium persulfate
ATP	Adenosine 5'-triphosphate
Ax	Absorbance at x nm
BCM	Barycentric Mean
BLAST	Basic local alignment search tool
bp/kb	Base pairs/ kilobase pairs
bp:	Base pair
BSA	Bovine serum albumin
CCNA	cell culture cytotoxicity assay
CDAD	*Clostridium difficile* Associated Disease
CDI	*Clostridium difficile* Infection
CDR	Complementarity determining regions
CROPS:	Combined repetitive oligopeptides
CV	Column volume
Da	Daltons
Deg	Degree
DLS	Dynamic Light Scattering
DNA:	Deoxyribonucleic acid
dNTP:	Deoxyribonucleotide triphosphate
DSC	Differential Scanning Calorimetry
ds-DNA	Double-stranded DNA
EDTA	Ethylenediamine tetra-acetic acid
ELISA	Enzyme-linked Immunosorbent assay

g	Gram
GC	Gas chromatography
GDH	Glutamate dehydrogenase
GO	Galactose oxidase
GTP	Guanosine Triphosphate
h	Hour
HRP	Horseradish peroxidase
Ig	Immunoglobulin
InsP6	Inositol Hexakisphosphate
IPTG	Isopropyl-β-D-thiogalactopyranoside
JD-F12 (3)	JD-F12 with mutations N16D, Q50E and N94D
JD-F12 DED	JD-F12 with DED mutations pre and post variable loops
JD-F12	Ataxin Affimer binder
Kb	Kilobase
kDa	kilodalton
L	Litre
LB	Luria-Bertani Broth
LCT	Large Clostridial Toxins
LR	Long repeat
m	Metre
M	Molar
M.W	Molecular weight
MAb	Monoclonal clonal antibodies
MT	Mutant
mg	Milligram
min	Min
mL	Millilitre
mM	Millimolar
mV	Millivolt
NAAT	Nucleic acid amplification Test
N16D	JD-F12 with N16D point mutation

N16D-N94D	JD-F12 with N16D and N94D point mutations
N16D-Q50E	JD-F12 with N16D and Q50E point mutations
N94D	JD-F12 with N94D point mutation
NAD(H)	Nicotinamide adenine dinucleotide (reduced)
NEB	New England biolabs
ng	Nanogram
nm	Nanometre
nM	Nanomolar
ºC	Degree celsius
OD	Optical Density
OD_{600}	Optical density at 600 nm
PAGE	Polyacrylamide gel electrophoresis
PBS	Phosphate buffered saline
PCR	Polymerase chain reaction
PDB	Protein Data Bank
PEG	Polyethylene Glycol
PHE	Public Health England
pM	Picomolar
PMC	Pseudomembranous Colitis
Q50E	JD-F12 with Q50E point mutation
Q50E-N94D	JD-F12 with Q50E and N94D point mutations
RNA	Ribonucleic acid
rpm	Revolutions per min
s	Second
SAXS	Small-Angle X-ray Scattering
scFv	single chain variable fragment
SDS	Sodium dodecyl sulphate
SDS-PAGE	Sodium Dodecyl Sulphate Polyacrylamide Gel
SEC	Size Exclusion Chromatography
SLS	Static Light Scattering
SOB	Super Optimal Broth

SR	Short repeat
TAE	Tris Acetate EDTA
TB	Terrific Broth
TBS-T	Tris Buffered saline with Tween
TEMED	Tetramethylenediamine
TMB:	Trimethyl borate
Tris-HCl	Tris (hydroxymethyl) aminomethane pH adjusted with 0.2 M HCl
TXN	Toxin
UV/Vis	Ultraviolet-visible
V	Volt
WT	Wild Type
µg	Microgram
µL	Micro litre
µM	Micromolar

Chapter 1: Introduction

1.0 *Clostridium difficile* Infection (CDI)

It is a great concern when hospitals known as a "place of care" are also seen as a "place of contracting infection". *Clostridium difficile* infection has become a global public health challenge (Lessa *et al*., 2012), and it is the leading cause of hospital-acquired (nosocomial) infection and antibiotic-associated diarrhoea in developed countries with significant rise worldwide. Generally, when patient colonised by *Clostridium difficile* become exposed to broad-spectrum antibiotics, the normal microflora in the gut is altered allowing *C. diff*, an opportunistic bacteria to colonise the gut and produce its toxins, enterotoxin toxin A and cytotoxin toxin B, thereby leading to *Clostridium difficile* infection (see Figure 1.1) (Ghose, 2013). *Clostridium difficile* associated diseases range from mild diarrhoea, inflammation, to severe and life-threatening pseudomembranous colitis.

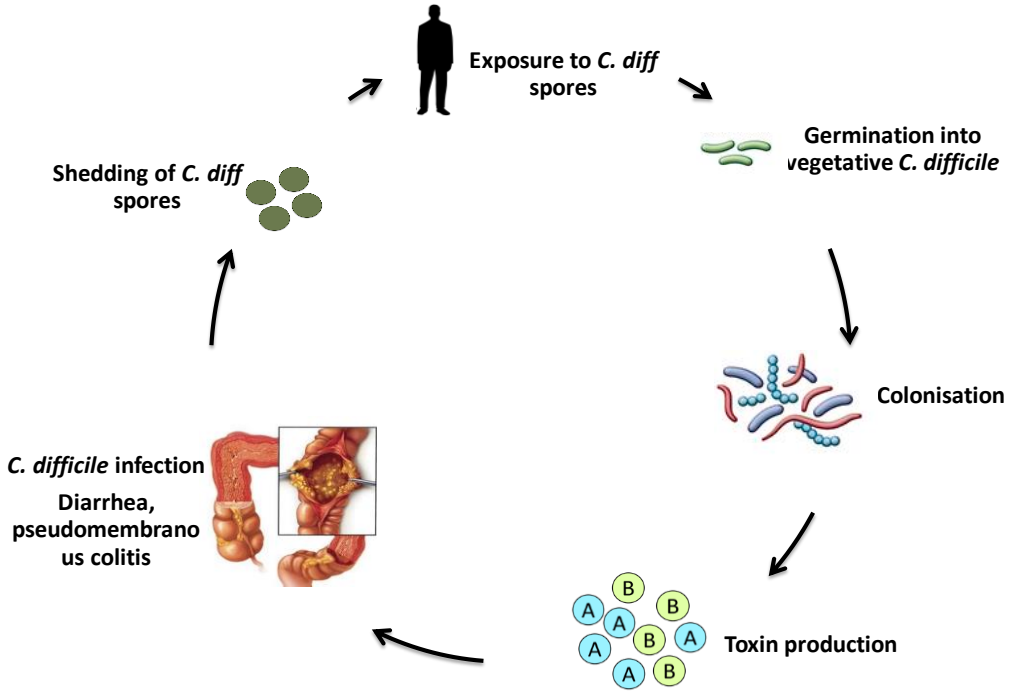

Figure 1.1: The life cycle of *Clostridium difficile* infection. The development *Clostridium difficile* infection is dependent on the different stages of *C. difficile* life cycle. Following exposure to *Clostridium difficile* spores, perturbance of the normal flora in the gut leads to germination of the spores and then the eventual colonisation of *C. difficile*. Toxin producing *C. difficile* then produce toxin A and B which are the virulence factor that causes *C. difficile* infection symptoms such as diarrhea or life threatening pseudomembranous colitis. Spores are released into the environment, and transmission to new hosts continues the infectious cycle.

In the United States, *Clostridium difficile* is the most frequently reported nosocomial pathogen. According to the data obtained from US death certificates, *Clostridium difficile* infection accounted for 14,000 deaths in 2007 (Hall *et al*., 2012) which has risen to 29,000 deaths in 2011 (Lessa *et al*., 2015) as reported in the surveillance study carried out by Lessa *et al*. (2015) as part of the Centers for Disease Control and Prevention (CDC) Emerging Infections Program. In the United Kingdom, *Clostridium difficile* infection causes an estimate of 3,000 deaths per year (Planche *et al*., 2013). Increased surge in the number of cases of *Clostridium difficile* infection has led to increased financial burden. It has been estimated that $9,000 to $13,000 is spent per case (McGlone *et al*., 2012, Zimlichman *et al*., 2013) while the health care cost per year is $500 million to $1.5 billion (Schroeder *et al*., 2014) in the United States. This rise in *C. diff* incidence has been spurred by the outbreak of hypervirulent strains NAP1/ribotype 027 in 2000, and increased antibiotic resistance in *C. diff* strains.

Further researches have also indicated a rise in CDI in classes of people considered previously as low-risk such as children and postpartum women (Freeman *et al*., 2010). More recently, increases in *C. diff* incidence have also been linked to the switch from toxin assays to more sensitive molecular testing which detects the toxin A and toxin B genes but do not differentiate asymptomatic colonised carriers from patients suffering from *Clostridium difficile* infection (Fong *et al*., 2011, Burnham and Carroll, 2013, Koo *et al*., 2014). Therefore, accurate and reliable diagnosis of *Clostridium difficile* infection is needed more than ever before.

1.1 The bacteria

Clostridium difficile is an anaerobic gram-positive, spore-forming bacterium that can be found in the gastrointestinal tracts of humans, animals and in the environment. It was first described in 1935 (Hall and O'Toole, 1935) as a component of the faecal flora in neonates. Due to the difficulty experienced with the isolation and culturing of this bacterium, it was initially called *Bacillus difficile.* Infact, up to 60 % - 70 % of newborn babies and infants have been shown to be colonised with *C. difficile* asymptomatically (Bolton *et al*., 1984), then the colonisation rate continues to drop off to 0 to 3 % at 3 years of age (Antonara and

Leber, 2016, Jangi and Lamont, 2010). Though the titre of *C. difficile* toxin found in healthy children and adults suffering from *Clostridium difficile* infection were similar (Viscidi *et al*., 1981), it has been proposed that lack of toxin receptors on the surface of infant intestinal wall, and the protective action of breast milk, play major roles in protecting infants from developing *Clostridium difficile* infection (Eglow *et al*, 1992, Cerquetti *et al*., 1995, Jangi and Lamont, 2010).

C. difficile was not considered a particularly harmful pathogen until a rise in the number of cases of pseudomembranous colitis (PMC) in the 1970s. It was Bartlett *et al*. (1978) that identified toxin-producing *C. difficile* as the causative agent of PMC in patients receiving Clindamycin (Bartlett *et al*., 1978 1974, Tedesco *et al*., 1974). Today, *Clostridium difficile* is one of the most common causes of antibiotic-associated diarrhoea in the world (Wong *et al*., 2017, Karen C and John G, 2011, Kyne, 2010) and a number of intestinal diseases known as *C. difficile* associated disease (CDAD) or *C. difficile* infections (Kyne, 2010).

1.1.1 Risk factor

Clostridium difficile infection is commonly referred to as a hospital-acquired infection because of its prevalence in hospitals and healthcare settings. The major risk factors for *Clostridium difficile* associated diseases are antibiotic use, hospitalisation, and age. Exposure to antibiotics have been linked to CDI, especially to broad-spectrum antibiotics clindamycin, cephalosporines, penicillins and floroquinolones (Dingle *et al*., 2017, Lessa *et al*., 2015). The human colon contains 10^{12} bacteria per gram of content (referred to as the normal gut microflora) which provides an important host defense against the growth and colonisation of pathogenic organisms such as *Clostridium difficile* (Owens *et al*., 2008a, Owens *et al*., 2008b). In *C. diff* infection, the use of antibiotics disrupts this defense by suppressing the growth of normal gut flora, leading to the overgrowth of toxigenic *Clostridium difficile*.

Advanced age is also one of the most important risk factors for CDI. Studies by Pepin *et al*. (2005) observed a 10 fold higher risk for developing CDI in people older than 65 years old compared to younger population (Pépin *et al*., 2005). The

prevalence of *C. difficile* spores in hospitals and care homes are higher than in the general community. Therefore, non-surprisingly, adult patients with long stay in these facilities have higher rate of colonisation (20 % -25 %), than healthy adults in the society (2 %-3 %) (Simor *et al*., 2002, McFarland *et al*., 1989). When combined with their low immunity status and use of antimicrobial agents, exposure to *C. difficile spores*, ultimately poses a great danger of acquiring *C. difficile* infection.

Additionally, certain drugs have been implicated as risk factors for CDI such as proton pump inhibitors and hydrogen blockers (Francis *et al*., 2013, Tleyjeh *et al*., 2012). This is because they alter the pH of the stomach by decreasing the acidity of the stomach which facilitates the transition of *C. difficile* spores from the stomach to the gut where it germinates into toxin-producing state (Ghose, 2013).

1.1.2 Epidemiology

Historically, *C. difficile* infection has been underestimated as a healthcare-associated disease for these three major reasons. First, *C. diff* was identified as a normal component in the gut of healthy babies (Hall and O'Toole, 1935). Second, since its association as the causative agent of pseudomembranous colitis in 1978, there was low rate of severe disease and death reported (less than 3 %) (Rubin *et al*., 1995). Finally, by late 1980's, research already conducted on the clinical features, diagnostic test, effective therapies and epidemiologic studies made many to believe that there is little else to be known about *Clostridium difficile* infection (Barlett, 1988, Gerding, 2009).

The turn of the 21st century has witnessed a dramatic change in the epidemiology of *Clostridium difficile* infection due to a marked increase in incidence, severity and mortality. Of particular interest was the outbreak reported in Quebec, Canada in 2003. According to the research by Pepin *et al*. (2005), the incidence of CDI in Quebec was stable from 1991 (22.2 per 100,000) till 2002 (25.2 per 100,000) but rose four-fold in 2003 (92.2 per 100,000) (Pépin *et al*., 2005). Aside the increase in incidence, the greater concern was the simultaneous occurrence of outbreaks in major acute care hospitals in the region, then the increase in severity and mortality of the infection (Kelly and LaMont, 2008). The increase incidence of CDI was

attributed to the outbreak of a hypervirulent strain designated restriction endonuclease analysis type BI, North American pulsed-field gel electrophoresis type 1 (NAP1), polymerase chain reaction (PCR) ribotype 027 (BI/NAP1/027) which accounted for 82 % of the strain isolated from outbreak in Quebec, Canada (Karen and John, 2011). The hypervirulent strain exhibited high level of resistance to floroquinolones, an increased production of toxin A and toxin B *in vitro*, production of binary toxin and has emerged as a dominant strain globally (Ghose, 2013).

The outbreak of increased incidence of CDI is not limited to the United States, several outbreaks have been reported in the England, Netherlands and across Europe (Kuijper *et al*., 2006). In the United Kingdom, *C. difficile* was listed as the primary cause of death for 499 patients in 1999, 1,998 in 2005 and 3,393 in 2006. Higher mortality has also been reported in Australia and Asia (Clements *et al*., 2010). A closer look at the epidemiology of CDI incidence in England, when compared with other countries revealed that there has been a remarkable decrease over the past decade (Lessa *et al*., 2015, Ghose, 2013). This has been attributed to the introduction of national CDI prevention and management policies in 2007. Figure 1.2 below, which was taken from the most recent paper published in 2017 (Dingle *et al*., 2017), showed that the incidence of CDI in England increased from 1998 to 2006 then decreased drastically since 2007.

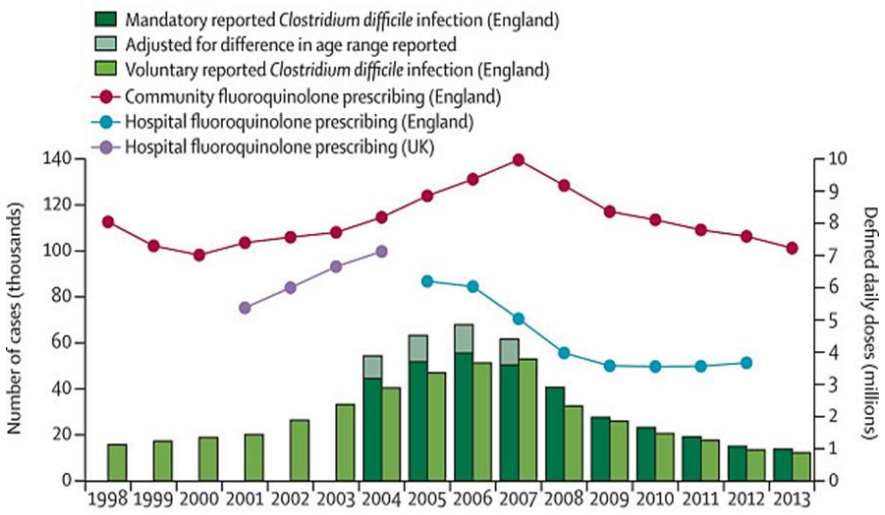

Figure 1.2: Incidence of *Clostridium difficile* infection in England and fluoroquinolone prescription (Dingle *et al*., 2017).

Summarily, despite the decrease in CDI incidence in the United Kingdom, the changing epidemiology of *C. difficile* infection calls for worldwide surveillance to avoid a repeat of the CDI complacency witnessed in the 1980s.

1.2 Pathogenicity

1.2.1 Toxin A and toxin B

During *C. difficile* infection, the bacteria produce two major toxins: toxin A and toxin B which are recognised as the major virulence factor. These two toxins are readily detected in faecal samples and have become the primary biomarkers used for the diagnosis of the infection. Due to their high molecular weight, toxin A (308 kDa) and toxin B (270 kDa) belong to the family of large clostridial toxins (LCTs) alongside *Clostridium sordellii* lethal toxin (TcsL- 300 kDa), *Clostridium sordellii* hemorrhagic toxin (TcsH- 270 kDa) and *Clostridium novyi* alpha toxin (Tcnα- 250 kDa) (Jank and Aktories, 2008).

1.2.2 Pathogenicity Loci

The genes encoding toxin A (tcdA) and toxin B (tcdB) are located on the 19.6 kb pathogenicity locus (PaLoc) (Figure 1.3) along with three other regulatory genes (tcdD, tcdE and tcdC) involved in toxin production in all toxigenic strains of *C. difficile* (Voth *et al*., 2005; Govind and Dupuy, 2012; Aubry *et al*., 2012). However, in non-toxigenic strains, the PaLoc is replaced by 115 bp of non-coding sequence (Rupnik *et al*., 2009).

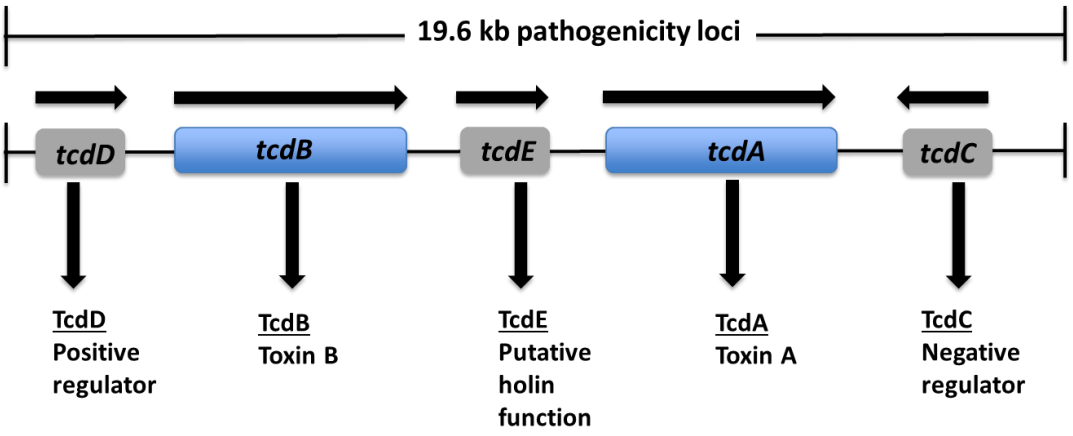

Figure 1.3: Schematic diagram illustrating the genetic organisation of the pathogenicity Loci.

The role of the regulatory genes in *C. difficile* infection has been investigated (Matamourous *et al.,* 2007; Rupnik *et al*., 1998; Govind and Dupuy, 2012). The gene encoding tcdC is found upstream of tcdA gene and is regarded as the negative regulator for toxin production during the exponential growth phase (Voth *et al*., 2005). However, in hypervirulent strains, the negative toxin regulation of tcdC was elucidated to contain an 18 bp deletion and a frame-shift which leads to increased toxin production (Matamouros *et al*., 2007). tcdD is located downstream of tcdB and it is coordinately expressed with toxin A and B. It has been suggested that tcdD functions as a major positive regulator for toxin A and B expression. The gene encoding tcdE is located in between tcdB and tcdA, and has been speculated to facilitate the release of toxin A and B through permeability of the cell wall of *Clostridium difficile* (Cohen *et al*., 2000).

1.2.3 Structure and function of toxin A and toxin B

Toxin A and toxin B are large single-chain proteins with four functional domains. At the primary structure level, toxin A and toxin B exhibit overall sequence similarity of 74 % and a sequence identity of 49 % (von Eichel-Streiber *et al*., 1991, Voth *et al*., 2005, Pruitt and Lacy, 2012). Structurally, toxin A (TcdA) and toxin B (TcdB) contain four distinct domains with specific functions. They are, the N-terminal catalytic domain, a cysteine proteinase domain, a central hydrophobic region, and the C-terminal receptor binding domain.

High resolution structures of the holotoxin for toxin A and B has not been solved. However, a low resolution three-dimensional structure for TcdA (308kDa) and TcdB (270 kDa) has been solved by electron microscopy, small angle x-ray scattering and crystallization (Pruitt *et al*., 2010, Ho *et al*., 2005, Albesa-Jové *et al*., 2010). Most recently, the crystal structure of toxin A refined to 3.25 Å resolution (residues 1-1832) has been determined by Chumbler *et al* (2016). The successfully solved structures of toxin A domains are displayed in Figure 1.4 and that of toxin B is displayed in Figure 1.5.

The function of each domain can be explained using the mode of entry and mechanism of action of the toxin as illustrated in Figure 1.6 (Pruitt and Lacy, 2012). Upon secretion from the bacteria, *C. diff* toxins utilise the C-terminal receptor

binding domain (RBD) as binding sites for cell surface receptor carbohydrate and enter the cell by clathrin-mediated endocytosis (Burnham and Carroll, 2013). Following internalisation of the toxins, the acidification of the endosome induces structural changes in the toxin causing the exposure of the hydrophobic region of the central delivery domain which forms a pore for the passage of the N-terminal catalytic domain. Before the release of the catalytic domain into the cytosol, the toxin undergoes autoproteolysis.

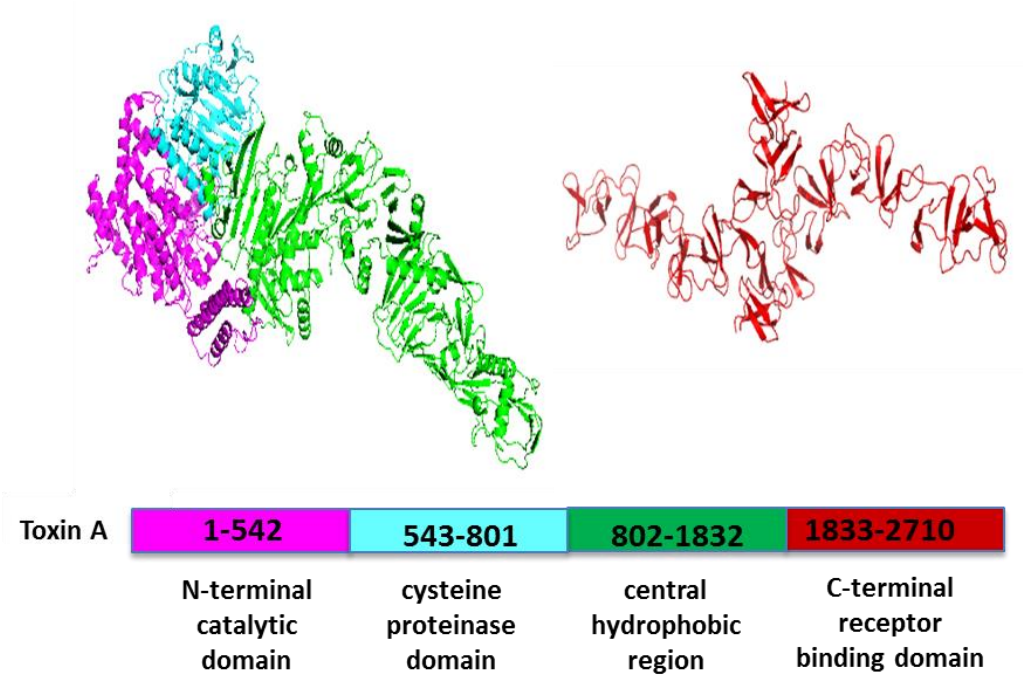

Figure 1.4: Crystal structure of Toxin A domains. Each structure is colour coded to correspond with the schematic representation of domain organisation. PDB code: 4R04 for toxin A residues 1-1832 and PDB code: 2QJ6 for toxin A residues 2390-2706 which is part of the C-terminal receptor binding domain. Images were created using PyMOL.

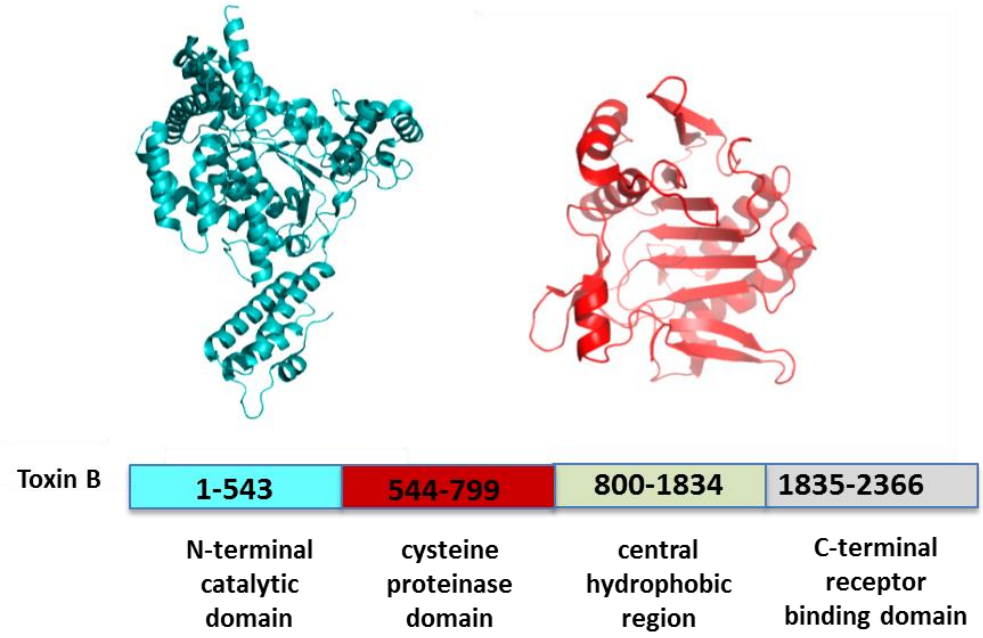

Figure 1.5: Crystal structure of the catalytic and cysteine proteinase domain of Toxin B. Each structure is colour coded to correspond with the schematic representation of domain organisation. PDB code: 2BVL for toxin B N-terminal catalytic domain and PDB code: 3PEE for for the cysteine proteinase domain. Images were created using PyMOL.

The cysteine proteinase domain is the self-cleavage proteolytic site required for the release of the N-terminal enzymatic domain (Pruitt and Lacy, 2012, Voth and Ballard, 2005). This cleavage is initiated and dependent on the binding of host factor Inositol hexakisphosphate (InsP6) to the catalytic site of the cysteine proteinase domain resulting in the release of the biologically active toxin, a glucosyltransferase (63 kDa). The N-terminal domain of toxin A and B possesses the glucosyltransferase enzymatic activity which once released into the cytosol catalyses the transfer of glucose or N-acetylglucosamine residues to host cell Ras and Rho GTPases (Just *et al*., 1995) leading to their inactivation. This causes disruption to the interactions of host cell Ras and Rho GTPases with regulatory molecules which consequently interrupts vital signalling pathways. Inactivating GTPases compromises their integrity and leads to disorganisation of actin cytoskeleton and cell death ultimately.

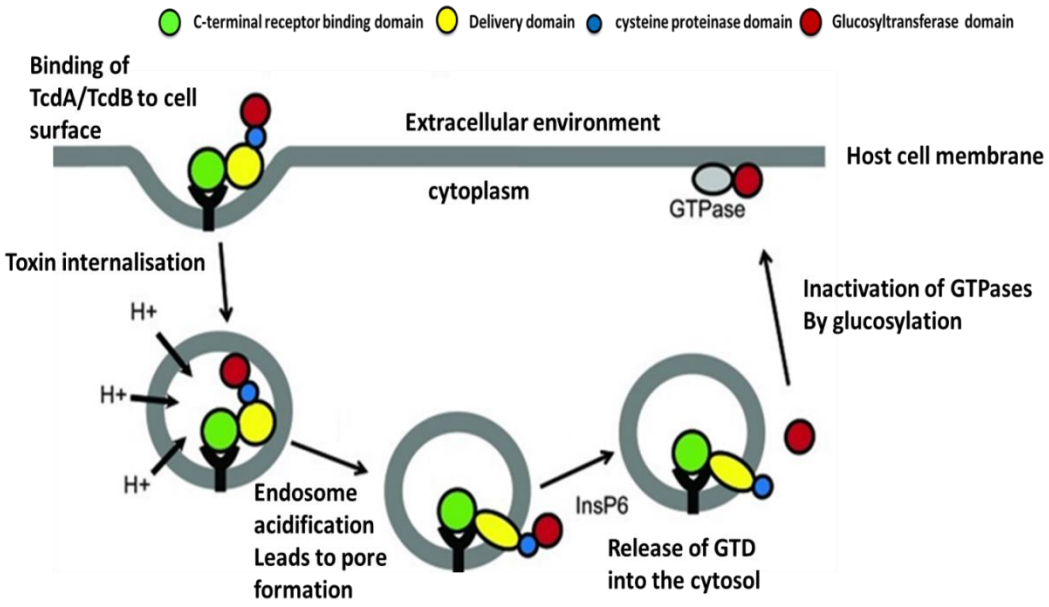

Figure 1.6: Mechanism of action of toxin A and toxin B *in vivo*. Toxin A or Toxin B binds to the surface of the cell and is internalised by receptor-mediated endocytosis. Acidification of the endosome triggers the formation of a pore through which the GTD is translocated. The GTD is released into the cytosol by InsP6 dependent autoproteolysis which then glucosylates the Rho family GTPases at the cell membrane. The image was adapted from Pruitt and Lacy (2012).

1.2.4 Role of toxin A and B in pathogenicity

Initial studies carried out by Lyerly and colleagues (Lyerly *et al*., 1985) on the role played by toxin A and toxin B in the pathogenicity of *C. diff* suggested that only strains producing toxin A are toxigenic and able to cause disease in undamaged gut, while those producing only toxin B are unable to independently cause disease. Paradoxically, twenty-four years later, Lyras and colleagues published their research findings (Lyras *et al*., 2009) that toxin B is the virulence-determining factor and that strains with only toxin A are avirulent. This finding put forward again the question of the role of toxin A and B in *C. diff* pathogenicity. The first study to ascertain the toxin roles was conducted by (Kuehne *et al*., 2010), wherein the ClosTron knockout system was used to investigate the role of each toxin. The study confirms that bacteria producing either toxin A or toxin B or both toxins can cause acute severe colitis in the hamster model of infection used; therefore, they possess cytotoxic activity, *in vitro*, which translated directly to virulence *in vivo*. Further studies (Steele *et al*., 2012, Carter *et al*., 2010) have substantiated this result.

1.2.5 CDT Binary toxin

In addition to toxin A and B, approximately 6 to 12.5 % of *C. difficile* strains produce another toxin called *C. difficile* transferase (CDT) also known as binary toxin, which has been associated with high mortality rate in *C. difficile* infection (Barth *et al*., 2004). It is called binary toxin because it is composed of two subunits, CDTa and CDTb, which are separately produced and secreted, but combine into a potent cytotoxin CDT (Burnham and Carroll, 2013). The precise role of binary toxin in conferring virulence remains unclear (Geric *et al*., 2006, Bacci *et al*., 2011) however, production of CDT has been associated with hypervirulent strains (McDonald *et al*., 2005, Bella *et al*., 2016). One study by Lim *et al* (2014) described an Australian outbreak caused by a binary toxin-producing strain (ribotype 244) which was associated with higher mortality than others. Another study by Androga *et al* (2015) reported the isolation of toxin-negative, binary toxin-positive strains ($A^-B^-CDT^+$) of *Clostridium difficile* infection from a 15-year old patient with ulcerative colitis and severe diarrhea.

1.3 Diagnosis of *Clostridium difficile* infection

The accurate diagnosis of *Clostridium difficile* infection is essential for treatment, prevention and control, but it is critically dependent on the sensitivity and specificity of the diagnostic method used (Burnham and Carroll, 2013). Having a diagnostic test with limited sensitivity implies that some patients who are CDI positive will obviously be missed, and may not receive optimum treatment (Barbut *et al*., 2013). Missed CDI positive patients would not be effectively isolated which leads to further spread of CDI. On the other hand, having a diagnostic test with limited specificity implies that there would be a high rate of false positives. This means that some patients who do not have CDI would be classified as CDI positive, and placed on unnecessary treatment. These patients would be wrongly isolated and placed with genuine cases. This exposes such patients to greater risk of infection (Barbut *et al*., 2013). Highly sensitive and specific diagnostic tests are therefore pivotal in *Clostridium difficile* infection diagnosis and control.

To diagnose *Clostridium difficile* infection, patients suffering from the symptoms of CDI (diarrhoea, abdominal pain, and fever) are tested for the presence of the bacteria, *C. diff* toxins, and glutamate dehydrogenase enzyme (GDH) which is the common antigen in faecal samples, or examined by colonoscopy to demonstrate pseudomembranous colitis (Bauer *et al*., 2009, Lloyd *et al*., 2015). The diagnostic approaches employed in clinical laboratories can be classified based on the target detected. Some detect the presence of the bacteria, some detect the presence of toxins and GDH while others detect nucleic acids for genes associated with toxin production. These classifications are:

1. Microbiological cultures; which include the cell culture cytotoxicity neutralisation assay (CCNA) and toxigenic culture of *C. difficile*.
2. Enzyme immunoassays for the detection of *C. difficile* products in faecal samples such as Toxin A, Toxin B and GDH.
3. Nucleic acid amplification tests (NAATs) which identify the toxin genes, GDH genes and 16S RNA, in faecal samples.

An overview of each diagnostic method is presented diagrammatically in figure 1.7, and discussed in the sections below.

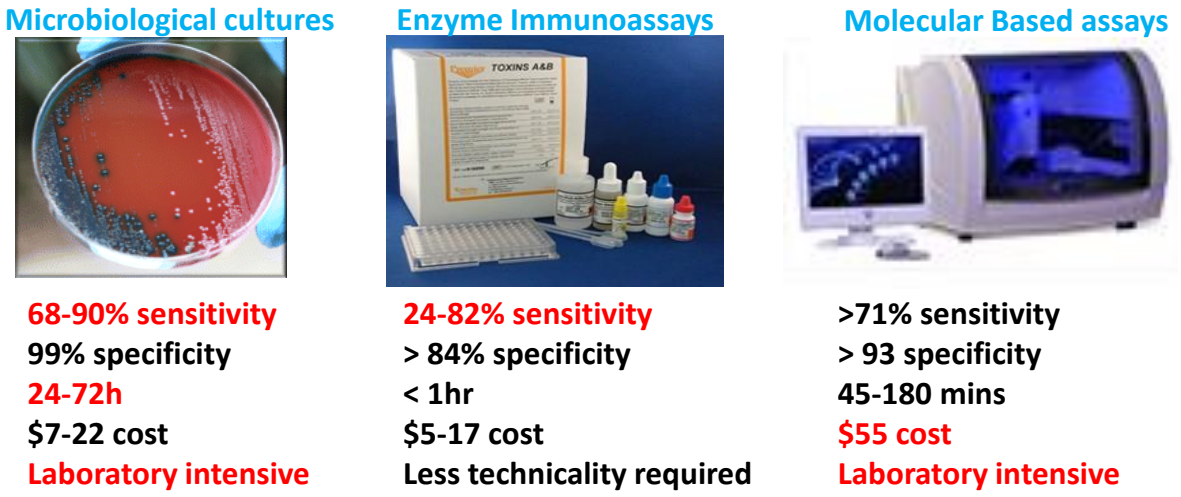

Figure 1.7: Diagnostic methods for *Clostridium difficile* infection. The three types of diagnostics are presented. These are the microbiological cultures, enzyme immunoassays and molecular based assays.

1.3.1 Microbiological cultures

The two cultures, cell culture cytotoxicity neutralisation assays (CCNA) and the toxigenic cultures remain the gold standards for the *C. difficile* infection diagnosis (Planche and Wilcox, 2011). They also serve as a reference for the evaluation of other diagnostic methods.

1.3.1.1 Cell culture cytotoxicity neutralization assay (CCNA)

The earliest diagnostic method for *Clostridium difficile* infection was the cell culture neutralisation assay (Chang *et al*., 1978) which was developed contemporaneously with the discovery of *Clostridium difficile* as the causative agent for *C. difficile* infection. In this assay, a stool filtrate is prepared and applied onto sensitive tissue culture cells and incubated for 24-48 h. Different cell lines such as human fibroblast cells, Vero cells, MRC-5 and Hep2 cells have been used for this purpose (Burnham and Carroll, 2013). Following incubation, cells are observed for cell rounding which is characteristic of the toxin induced cytopathic effect (CPE). To verify that the cytopathic effect was indeed caused by *C. difficile* toxins and not by nonspecific toxicity, a neutralisation assay is performed. In the neutralisation assay, *Clostridium Sordellii* antitoxin or *Clostridium difficile* antitoxin is added. The absence of the cytopathic effect in the cell cultures provides evidence that the cellular changes were caused by *C. difficile* toxin.

Cell culture cytotoxicity neutralisation assays (CCNA) detect toxin B primarily, although it has been reported that toxin A is also detected to some extent (Lyerly *et al*., 1988). It can detect faecal toxin at 1 to 10 pg/ mL and is still recognised as the gold standard with sensitivity and specificity of 98 % and 99 % respectively. However, the outbreak of hypervirulent strains and researches that compared the sensitivity and specificity of CCNA with nucleic acid amplification tests concluded that the overall sensitivity and specificity of CCNA is 68-86 % and 97-100 % respectively. Thus, challenging its use as an acceptable gold standard (Cohen *et al*., 2010, Barbut *et al*., 2009, Eastwood *et al*., 2009, de Jong *et al*., 2012).

The sensitivity of CCNA is affected by several factors. *Clostridium difficile* toxins are temperature sensitive and can degrade in the specimen, so improper storage of

faecal sample can lead to false negative results. As described above, different cell lines have been used to perform CCNA which would result in varying sensitivity of the assay. In addition, slow turnaround time, and the lack of a generally accepted standardised procedure has limited the use of CCNA as a routine test.

1.3.1.2 Toxigenic culture (TC)

The toxigenic culture method was developed after CCNA for the detection of *C. difficile* in late 1979 (Chang *et al*., 1979, George *et al*, 1979). Toxigenic culture comprises an anaerobic culture of *C. difficile* bacteria from faecal samples, and it detects the presence of toxigenic bacteria rather than the toxin itself. This means that the bacteria *Clostridium difficile* is recovered from spores in faecal samples and then tested for toxin-producing ability.

For the assay, *C. difficile* spores are enriched by subjecting faecal samples to alcohol shock which removes vegetative bacteria that may overgrow *C. difficile (*Riley *et al.,* 1987*)*. An enriched specimen is then cultured onto an anaerobic culture medium. Media used for this purpose include cycloserine, cefoxitin and fructose agar (CCFA), or cefoxitin cycloserine egg yolk agar (CCEY). Sometimes lysozyme and taurocholate are added to the medium to enhance spore germination. The culture is then incubated at least for 48 h and could be held up to 7 days, colonies are examined and typical *C. difficile* colonies are identified and isolated. Once confirmed as *C. difficile*, they are tested for toxin-producing ability. *C. difficile* isolates are grown in pre-reduced brain heart infusion broth, then the culture supernatant would be tested for cytopathic effect of toxin B using cell culture cytotoxicity neutralization assay. Alternatively, enzyme immunoassays are used to detect the presence of toxin in culture supernatant.

Since toxigenic culture is cultured from *C. difficile* spores to identify toxigenic strains, it has a very high sensitivity (94 %-100 %) and specificity (99 %). When the sensitivity of cell culture cytotoxicity neutralisation assays (CCNA) was compared with toxigenic culture (TC), CCNA has a sensitivity of 75 %-85 % (Barbut *et al*., 2009; Eastwood *et al*., 2009; Kelly *et al*., 1987; Delmee *et al*., 2005). For this reason,

toxigenic culture has remained one of the two gold standards for the validation of new diagnostic methods and very importantly in epidemiological studies.

Although toxigenic assay is very sensitive (94 %-100 %) and specific (99 %) for the detection of toxigenic strains of *C. diff*, it lacks the specificity to differentiate between patients with CDI or merely colonised because acquisition of toxigenic *C. diff* strain alone does not diagnose CDI. A high rate of false positive for TC has been reported in asymptomatic carriers (*C. diff* colonised), infants and in patients who were recently exposed to antibiotics (Su *et al.,* 2013). Besides, toxigenic culture is time-consuming, taking 2-7 days, is laborious and does not have a standardised protocol. Also, toxigenic culture requires specialised facilities. Based on these limitations, toxigenic culture is too slow, and lacks specificity to be used in routine assays for patient management.

1.3.2 Enzyme immunoassays

Due to the above limitations associated with cultures, enzyme immunoassays (its principle and types are described in section 1.4) were developed to increase the speed of diagnosis. Enzyme immunoassays for CDI diagnosis use antibodies for the detection of biomarkers of *Clostridium difficile* infection. A biomarker is a physiological or pathological measurable object, which is related to a particular disease, and any change, increase or decrease, in concentration can be indicative of a particular disease (WHO, 2001). For *Clostridium difficile* infection diagnosis, the three validated biomarkers used as targets in immunoassays are toxin A, toxin B, and glutamate dehydrogenase. Enzyme immunoassays are widely in use for clinical diagnosis because of cost effectiveness, rapid turnaround time and ease of use.

1.3.2.1 GDH enzyme immunoassays

Glutamate dehydrogenase (GDH) is a metabolic enzyme that is encoded by the *glu*D gene. In *Clostridium difficile*, GDH is produced at high levels in both toxigenic and non-toxigenic strains and therefore referred to as *C. difficile* common antigen (Carroll, 2011, Delmee *et al*., 2005). This makes GDH a useful screening biomarker to rule out the presence of *C. difficile* during clinical diagnosis. Carman *et al*. (2012) evaluated how conserved GDH is in 77 different ribotypes from both toxigenic and

non-toxigenic strains from around the world. From the study (Carman *et al*., 2012), they found out that all the strains contained gluD, the gene encoding GDH, with almost identical protein sequences. Similarly, another study by Goldernberg *et al*., (2011) found no significant difference when GDH was assayed from different ribotypes.

Consistently, studies have shown that GDH assays possess high sensitivity (80 % - 100 %) and a high negative predictive value (NPV) when used as a screening test. This implies that patients with a negative screening test result truly don't have the disease, regardless of the assay type or reference method used (Planche *et al*., 2013, Quinn *et al*., 2010, Shetty *et al*., 2011). GDH assays are available in microwell enzyme immunoassay format, for example *C. diff* CheK-60, and *C. diff* Quik Chek, and in the lateral flow immnuo-chromatographic format such as *C. diff* Quik Chek complete. They provide a rapid turnaround time, are inexpensive and require minimal hands-on time. The sensitivity of GDH assays makes them attractive in diagnostic algorithms (see section 1.3.4).

1.3.2.2 Toxin A and toxin B immunoassays

Toxin immunoassays use monoclonal or polyclonal antibodies raised against toxin A and/ or B for the diagnosis of CDI. In 1983, Lyerly and colleagues (Lyerly *et al,* 1983) developed the first toxin enzyme immunoassay for the detection of toxin A. The toxin immunoassay was favoured over culture for CDI diagnosis because of its inherent advantages over culture (cheap, quick, and easy to use). However, in the early 1990s, the latex agglutination test developed for toxin A was confirmed to be detecting a common antigen for *Clostridium difficile*- glutamate dehydrogenase (GDH), and not toxin A (Lyerly *et al.,* 1991, Anderson *et al.,* 1993). Toxin A specific immunoassays were reintroduced and widely used until pathogenic *C. difficile* strains which were toxin A^-B^+ (producing only toxin B) were identified and associated with outbreaks in 2000 because these strains were missed by the toxin A immunoassays (Alfa *et al.,* 2000, Kim *et al.,* 2008, Shin *et al.,* 2008). Enzyme immunoassays for toxin A and B soon replaced immunoassays for toxin A only. However, production of monoclonal antibodies against toxin B was challenging (Deng *et al.,* 2003). Therefore, as described in more details in Chapter 5, >85 % of

commercially available toxin immunoassays utilise polyclonal antibodies as capturing molecules for toxin B which limits their sensitivity. Toxin assays are available in either microwell EIA format or lateral flow immune-chromatographic format.

For the microwell format, the capturing antibody (either monoclonal or polyclonal) is coated onto the walls of the microwell. Faecal samples diluted in buffers provided are added together with the conjugate (detection antibody conjugated to an enzyme). Enzyme substrates are added and optical density measured after an incubation period. Toxin immunoassays are easily performed and results are available within an hour and are easily interpreted which makes them widely used as a routine diagnostic test for CDI. However, the sensitivity of toxin immunoassays has been reported to be unsatisfactorily low ranging from 40 % to 99 % when compared to the two gold standards (CCNA and TC) or nucleic acid amplification tests (NAATs). It has been concluded that they cannot be used as stand-alone diagnostic for CDI due to poor sensitivity. Table 1.1 below gives a summary of some papers that evaluated the sensitivity and specificity of toxin EIA.

Table 1.1: Comparison of sensitivity and specificity of toxin EIA

Reference	Toxin enzyme immunoassay	Gold standard	Sensitivity (%)	Specificity (%)
van den Berg *et al*., 2005	Meridian Premier Toxin A & B	CCNA	96.8	94.8
Chapin *et al*., 2011	Meridian Premier Toxin A & B	NAATs	42.3	100
Eastwood *et al*., 2009	Meridian Premier Toxin A & B	CCNA	91.7	97.1
Eastwood *et al*., 2009	Techlab Tox A/B Quik Chek	CCNA	84.3	98.6
Eastwood *et al*., 2009	Techlab Tox A/B Quik Chek	TC	74.4	98.9
Eastwood *et al*., 2009	Remel ProSpecT	TC	81.6	93.3
Eastwood *et al*., 2009	Remel ProSpecT	CCNA	89.8	92.6
Novak-Weekley *et al*., 2010	Meridian Premier Toxin A & B	TC	58.3	94.7
Sloan *et al*., 2008	Meridian Premier Toxin A & B	TC	48	98
Sloan *et al*., 2008	Immunocard Toxin A & B	TC	48	99
Sloan *et al*., 2008	Remel Xpect *C. difficile* A/B	TC	48	84

Based on the evaluation of the sensitivity and specificity of the toxin immunoassay, a common trend can be observed. The sensitivity of the assay depends on the gold

standard used. When CCNA test was used as the gold standard, the sensitivity ranged from 84.3 % - 96.8 %, but when toxigenic culture (TC) or NAATs was used, the sensitivity fell to 42.3 % - 81.6 %. The main reason for this disparity in sensitivity is because the two gold standards detect different targets. Planche and Wilcox (2011) in their paper argued that when evaluating the sensitivity of a diagnostic method, a gold standard that detects the same target must be used (Planche and Wilcox, 2011). This means that since CCNA detects the presence of toxins in faecal samples, it represents a true standard for toxin immunoassays and not toxigenic culture which only identifies toxigenic strains of *C. difficile*.

Detection of toxins in faecal samples is critical for the diagnosis of *C. difficile*, however, use of rapid, cheap and easy-to-use toxin immunoassays as a stand-alone test have been limited by their low sensitivity (Cohen *et al*., 2010, Eastwood *et al*., 2009, Carroll, 2011, Crobach *et al*., 2009). In 2012, Polage and his colleagues published a paper to evaluate the clinical significance of lower sensitivity of toxin immunoassays on the diagnosis of CDI (Polage *et al*., 2012). In their paper, they reviewed the chart of patients at the Davis Medical Centre, University of California, who had a toxin testing between a 4-year period (January 2005 and December 2009). A total of 7,076 patients were included, 625 patients were toxin-positive while 6,121 were toxin-negative. After reviewing the chart, only 1/6,121 of the toxin-negative patients developed pseudomembranous colitis (PMC) and a small proportion of the total population (5.3 %) received treatment regardless of the toxin result. This result suggests that though toxin immunoassays have reduced sensitivity, the clinical significance of this was minimal because it has a good correlation with patients truly suffering from CDI. This has led the landscape of CDI diagnosis to be shifted in recent years to the use of Nucleic Acid Amplification Tests (NAATs).

1.3.3 Nucleic Acid Amplification tests (NAATs).

Nucleic acid amplification tests (NAATs) are molecular methods for the detection of *Clostridium difficile* toxin genes but not the presence of toxin in faecal samples. These assays use conventional PCR for the identification of tcdA, tcdB and 16S rRNA genes. As early as the 1990s, the use of NAATs was described in the literature.

However, the FDA approved the first NAATs for *C. difficile* detection, BD GeneOhm *C. diff* assay (BD diagnostics Inc., Sparks, MD) in 2009. Since then, NAATs that detect toxin A, toxin B genes have been commercially available (Swindells *et al*., 2010). Molecular testing for the detection of toxigenic organisms are increasingly employed for the diagnosis of *Clostridium difficile* infection in many institutions (especially in the US), because of its superior sensitivity and specificity (90-100 %), and rapid turnaround time (<3 h) compared to other toxin immunoassays and microbiological cultures.

Since NAATs detects only the gene encoding toxin A and B, thereby identifying toxigenic strains capable of producing these toxins regardless of toxin production, a few questions have been raised.

(i) What is the clinical significance of detecting toxigenic strains and not the actual toxins, and its impact on the CDI diagnosis, epidemiology and treatment?
(ii) Will strains emerge that are not detected by a particular assay?
(iii) Can NAATs be used as a stand-alone test?

Several studies have repeatedly reported that NAAT lacks specificity since it cannot distinguish infected patients from asymptomatic *C. diff* colonised patients (Song *et al*., 2015, Polage *et al*., 2015, Burnham and Carroll, 2013, Fong *et al*., 2011, Koo *et al*., 2014, Gould and McDonald, 2008). Since the percentage of patients colonised with toxigenic strain is 5 to 10 times higher than patients suffering from CDI, testing asymptomatic carriers through NAATs, whose cause of diarrhea is not *C. difficile* related would lead to them been diagnosed with CDI (Polage *et al*., 2015). In fact, up to 50 % of elderly patients who are residents in care homes carry toxigenic strains.

Of interest, Polage *et al*., (2015) compared the history of patients who are PCR-positive with those who are toxin negative, to investigate if PCR-positve/toxin-negative patients need treatment. In this study, 1416 hospitalised adults at the University of California Davis Medical centre between December 2010 and October 2012 were included. Patients were categorised as tox+/PCR+ (131), tox-/PCR+ (162)

and tox-/PCR- (1123) which implied that 55.3 % (162/293) of patients who had PCR positive results did not produce toxin. Patients in the tox-/PCR+ group had outcome comparable to the tox-/PCR- group. Only one death (0.6 %) in the tox-/PCR+ group was attributed to be CDI related while 18 out of 19 (94.7 %) deaths in the tox+/PCR+ group were CDI related. This study offered compelling evidence that up to half of patients diagnosed using NAATs are likely to be asymptomatically colonised with *C. difficile*, leading to overdiagnosis of CDI and undue exposure of such patients to antibiotics, and unnecessary treatments. Switching to molecular testing platforms has contributed to the higher incidence of CDI reported in the US (Moehring *et al*., 2013). Although NAATs have very high sensitivity and specificity, recommendations from authors and official guidelines in the UK (Planche *et al*., 2013, Department of Health, 2012) is that NAATs should not be used as a stand-alone diagnostic test for *Clostridium difficile* infection but diagnosis must be defined with a positive toxin test.

1.3.4 Multiple algorithms for *C. difficile* diagnosis

With the complexity surrounding the diagnostic methods discussed in the above sections, clinical practice guidelines have been put forward by the Society for Healthcare Epidemiology of America (SHEA), the Infectious Diseases Society of America (IDSA) (Cohen *et al*., 2010), the American College of Gastroenterology (ACG) (Surawicz *et al*., 2013), and the United Kingdom National Health Service (NHS) (Ticehurst *et al*., 2006) to suggest diagnostic approaches for *C. difficile* infection. Since toxin immunoassays cannot be used as stand-alone test, a combination of testing methods is used as part of multiple testing algorithms. The two diagnostic algorithms currently in use are illustrated below in Figure 1.8.

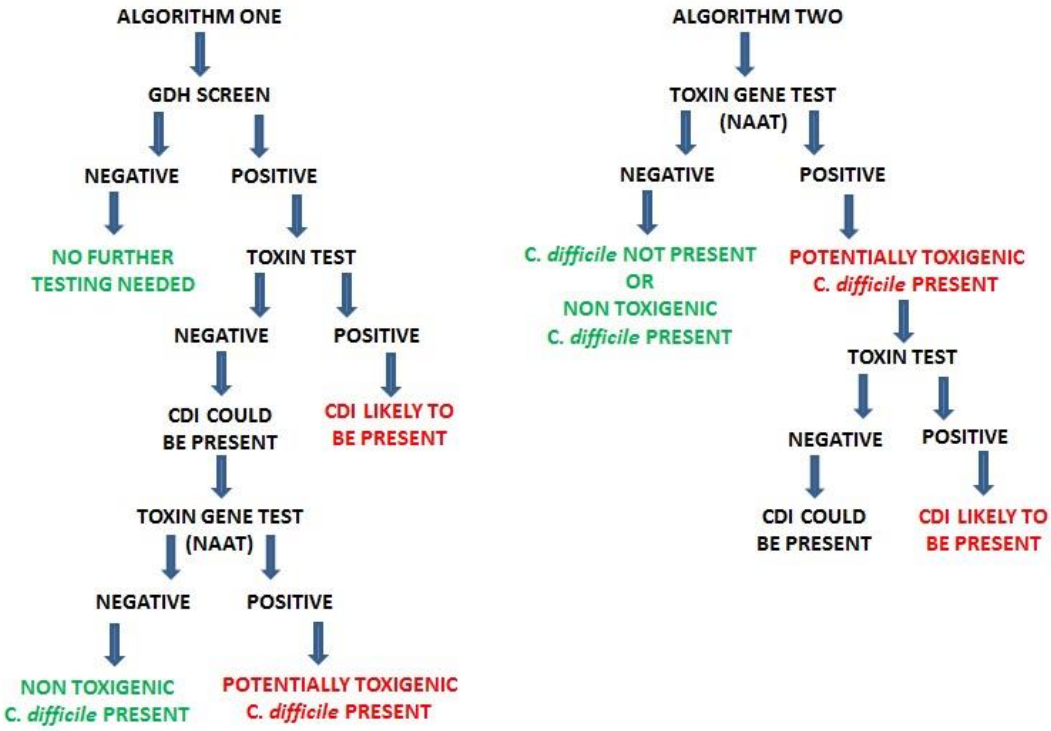

Figure 1.8: The two algorithms for *C. difficile* testing. Algorithm one includes the use of GDH as a screening method in two or three-step algorithm, while Algorithm 2 uses NAATs as either a standalone test or part of two step algorithm.

The use of GDH immunoassay as a screening method, followed by a confirmatory test to test for the presence of toxin in clinical samples (either CCNA and/or toxin immunoassays) in two or three-step algorithm has been the acceptable algorithm in the UK (Wilcox, 2012). In the US, clinical laboratories are switching to the use of NAATs as stand-alone or in combination with either toxin immunoassays or toxigenic cultures (Polage *et al*., 2015). In the words of Avila *et al*., (2016), "Laboratory testing for CDI is an exciting and rapid changing field: however, it remains an area of confusion". As described in the sections above, CDI diagnosis has no generally acceptable gold standard and no single best test that is cheap, sensitive, specific, fast and in a user-friendly format. With the complexity surrounding the clinical diagnosis of *C. difficile* infection, some salient facts remain

- Detection of the physical toxin in faecal sample is required for clinical diagnosis.
- Toxin immunoassays represent the best potential platform for toxin detection however it has limited sensitivity.

One of the areas less explored in *C. difficile* infection diagnosis is how to improve the sensitivity of toxin immunoassays. Therefore, this forms one of the main objectives of this thesis; to carry out experiments on how to improve the sensitivity of toxin immunoassays. A brief overview of enzyme immunoassays and antibodies is given in section 1.4 and 1.5 respectively.

1.4 Enzyme-Linked immuno-sorbent assay (ELISA)

Enzyme-linked immunosorbent Assay (ELISA) is an immunoassay technique that is widely used for the detection and quantification of specific target such as peptides, proteins, hormones and antibodies in a sample. Before the invention of ELISA, radioimmunoassay (RIA) was the only method for detecting and quantifying various biological molecules (Yalow and Berson, 1960). However, the use of radioactivity became a major safety concerns and so RIA techniques were modified by the replacement of the radioactive molecules with enzymes, giving rise to the widely used Enzyme-linked immunosorbent assay (Gan and Patel, 2013).

The format of ELISA was developed independently in 1971 by two research groups: Peter Perlmann and Eva Engvall at Stockholm University (Engvall and Perlmann, 1971), and the Dutch research group of Anton Schuurs and Bauke van Weemen (Van Weemen and Schuurs, 1971). van Weemen and Schuurs described the quantification of human chorionic gonadotrophin (HCG) in female patients' samples. Here, they conjugated the target (HCG) with the enzyme horseradish peroxidase followed by the addition of the antibody bound to a molecule that would change the colour of a substrate when oxidised by horseradish peroxidase. They termed their assay enzyme immunoassay (EIA). In Engvall's paper, antibody conjugated to the enzyme alkaline phosphatase was used for the successful quantification of immunoglobulin. Therefore, they named the assay enzyme-linked immunosorbent assay (ELISA).

1.4.1 Principle and protocol of ELISA

The principle of ELISA is based on the affinity and specificity of antibodies to the selected target (antigen) and the use of enzyme systems as the reporter label to detect the presence of the target of interest. The target is immobilised directly

onto the surface of a microtitre plate or through capture antibodies already coated onto the plate for target binding, then a secondary, enzyme-coupled antibody is introduced to detect the captured antigen (Figure 1.9). Chromogenic enzyme substrates are added which yields visible colour change or fluorescence thereby indicating the presence of the antigen (Hornbeck, 2001). The major components of an ELISA are antigen, antibodies (primary or secondary) and the enzyme. There are different types of ELISA format based on the arrangement of the target and the antibodies, these are described below.

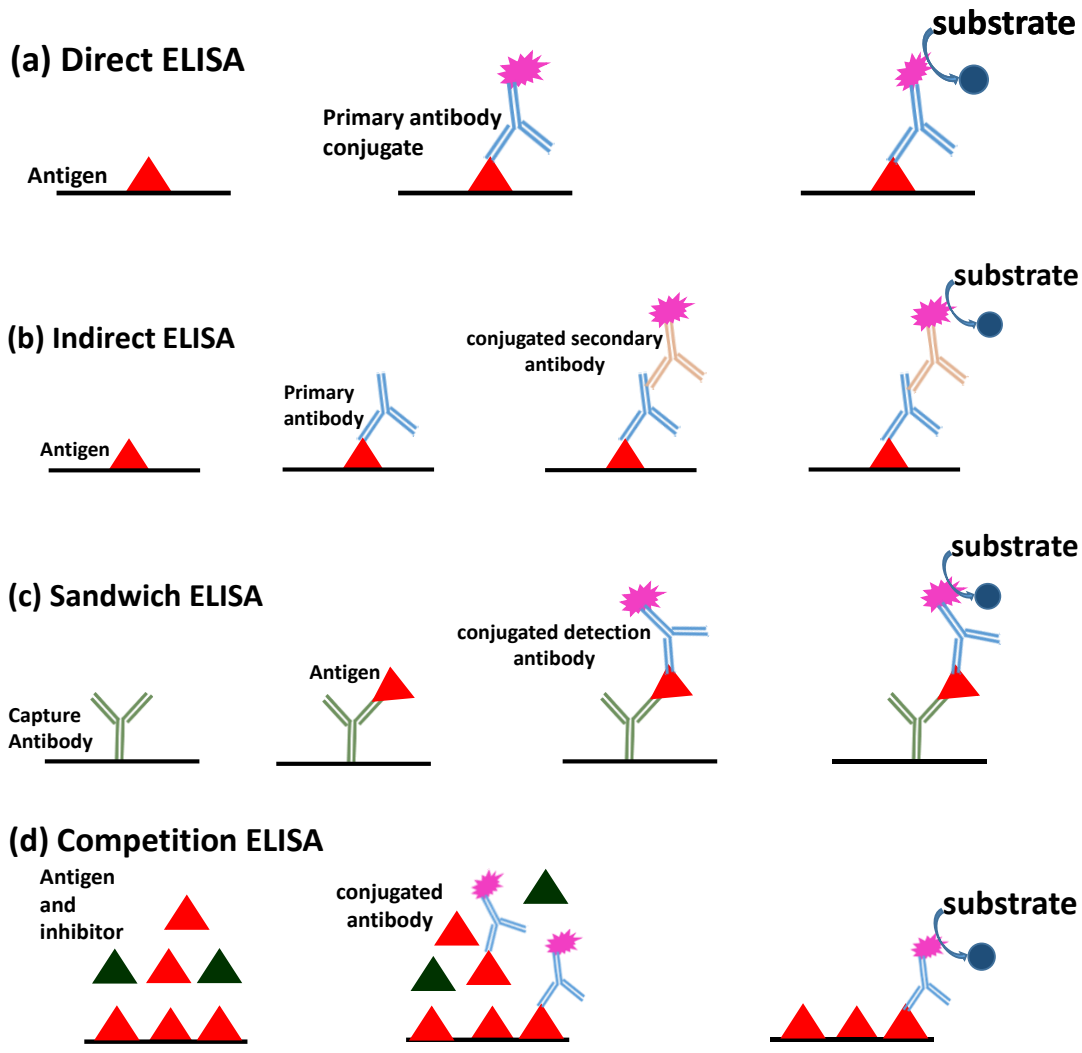

Figure 1.9: Schematic representation of the types of ELISA. The protocol for each type of ELISA (a) Direct ELISA (b) Indirect ELISA (c) Sandwich ELISA and (d) Competition ELISA is illustrated.

1.4.2 Types of ELISA

1.4.2.1 Direct ELISA

In direct ELISA also referred to as antigen screening, the target (antigen) is adsorbed directly onto the surface of the plate and detected by an enzyme-linked antibody (Figure 1.9a). With the addition of chromogenic enzyme substrate, a visible colour change is obtained and its intensity can be measured spectrophotometrically (Engvall, 2010). It has been successfully used for the quantification of high molecular weight antigens (Xu *et al*., 2006), and the detection of non-structural 1 (NS1) protein, and for the diagnosis of west Nile virus infection (Saxena *et al*., 2013). Direct ELISA is the simplest form of ELISA and faster to perform as it contains fewer steps. However, direct ELISA has some disadvantages. Immobilisation of antigen is non-specific which can lead to unavailability of the epitope on the target. Also, labelling the primary antibodies for each ELISA is expensive and time-consuming. The signal amplification obtained from direct ELISA is minimal compared to other formats of ELISA.

1.4.2.2 Indirect ELISA

For the indirect ELISA, the antigen of interest is coated on the surface of the plate, and captured by an unlabelled primary antibody. The complex is then detected by the introduction of enzyme-conjugated secondary antibody raised against the primary antibody (Figure 1.9b). This method is particularly useful when it is difficult to get an enzyme-linked primary antibody specific for the target of interest and has been used more commonly in endocrinology (Lin *et al*., 2015). Advantages of the indirect format of ELISA include: flexibility and versatility since different primary antibody can be used with the same labelled secondary antibody, which also saves cost. There is also increased sensitivity since more than one labelled antibody is bound per primary antibody. The major limitation of indirect ELISA is potential cross-reactivity of the antigen to the secondary antibody which might cause high non-specific background signals.

1.4.2.3 Sandwich ELISA

Sandwich ELISA was developed by Kato and his colleagues (Kato *et al*., 1977). In this assay, the antigen to be detected or quantified is sandwiched between two antibodies - the capture antibody and the detection antibody (Figure 1.9c). The capture antibody is immobilised onto the surface of the plate by direct adsorption or oriented immobilisation. When a sample containing the antigen of interest is added, the antigen gets bound to the capture antibody, and non-bound antigens are washed off. Addition of enzyme-conjugated detection antibody leads to the detection of the antigen–antibody complex. Sandwich ELISA has been the major format used in diagnostic kits for clinical and research purposes (Kragstrup *et al*., 2008). One major advantage of sandwich ELISA is that the antigen does not have to be purified, but can be detected even in complex samples such as blood samples and faecal samples (Park *et al*., 2013). Also, the use of both capture and detection antibody in sandwich ELISA makes it 2 to 5 times more sensitive and specific than direct or indirect ELISA. The major disadvantage of sandwich ELISA is the requirement of a pair of antibodies that bind to non-overlapping epitope on the target molecule.

1.4.2.4 Competition ELISA

Competition ELISA is used to measure the concentration of the target by detecting interferences in an expected signal output. In this assay (Figure 1.9d), sample antigen and a reference (or inhibitor) compete for binding to a known amount of labelled antibody. Therefore, the more the reference, the less free antibody will be available to bind the immobilised antigen, and the less the signal obtained. Though Competitive ELISA is the most complex of the types of ELISA, however it is useful for the identification of antibodies binding to non-overlapping epitopes and can be based on either direct, indirect or sandwich ELISA.

1.5 Antibodies, use and limitations

1.5.1 Structures

The discovery of antitoxins (later dubbed antibodies) can be dated to 1890 when Von Behring and Kitasato reported the existence of an agent in the blood that

could neutralise diphtheria toxin (Von Behring and Kitasato 1890). Antibodies also called immunoglobulins are structurally complex proteins produced by the humoral immune system in the higher organism (Schroeder Jr and Cavacini, 2010). They function to identify and destroy toxins and invading pathogens that are harmful to the organism.

Structurally, antibodies (150 kDa) comprise of two identical light chains (25 kDa each) and two identical heavy chains (50 kDa each). Each light chain pairs with a heavy chain, and each heavy chain pair with another heavy chain, and is held together by disulphide bonds to form a Y-shape as depicted in Figure 1.6 below. Each of the chains is divided into two regions, the variable regions and the constant regions. The light chain consists of one variable region V_L and one constant region C_L while the heavy chain consists of one variable region V_H and three constant regions C_H1, C_H2 and C_H3. When digested with papain, antibodies are cleaved into two fragments, the antigen binding fragment (Fab) and the constant region fragment (Fc).

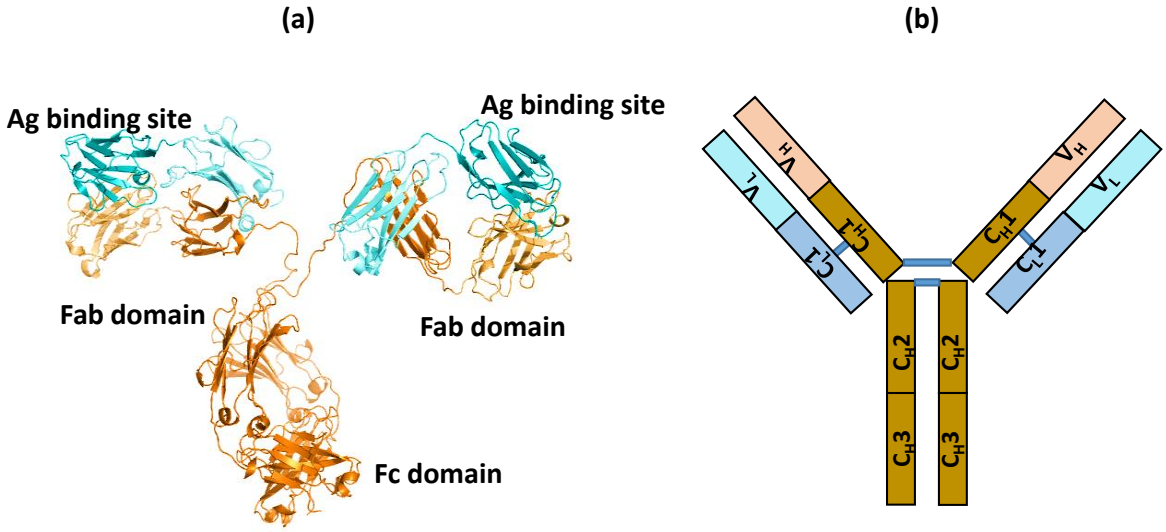

Figure 1.10: The structure of an antibody protein. The two identical heavy chains are connected by disulphide linkages. The antigen-combining site is composed of the variable regions (purple) of the heavy and light chains, which contains the hypervariable region (light blue) whereas the effector site Fc region of the antibody controls whether it agglutinates antigens, binds to macrophages, or enters mucous secretions.

The variable regions of the light and heavy chain is made of the first 110 amino acid residues of the amino terminal region are called the Complementarity Determining

Regions (CDR) which forms the antigen (Ag) binding site (Wang *et al*., 2007). To achieve antibody diversity, the three gene segments of the CDR called the Variable, Diversity, and Joining (V,D,J) segments are recombined to bind different target with great affinity and specificity through germ line gene recombination and somatic hypermutation (Jung *et al*., 2006). Through this recombination, human can make at least 10^{15} different antibodies, each with unique antigen specificity. Antibody diversity has made them very useful in the field of diagnostics as biological recognition molecules against nucleic acids, peptides, proteins, or carbohydrates etc.

Polyclonal and monoclonal antibodies

Antibodies are produced by the B-lymphocytes of the immune system in response to the presence of an antigen. Traditionally, when an animal is immunised with an antigen, several different B-lymphocyte clones produce a pool of antibodies, which is referred to as polyclonal antibody, that can be isolated from the sera (Stahl *et al*., 2013). Polyclonal antibodies recognise the same target but binds different epitopes (antibody binding site) on the target. In addition to their ability to detect multiple epitopes, they can be generated rapidly with fewer technicalities involved. In assays such as sandwich ELISA, polyclonal antibodies used as capture antibody offer high sensitivity for detecting targets that are present even in low quantities since they can bind multiple epitopes. However, the use of polyclonal antibodies in assays has limitations. The major ones are: variability between different batches of polyclonal antibody produced in the same animal at different times. Each polyclonal serum produced is unique and not reproducible even when produced from the same animal. Also, since they recognise multiple epitopes on the same target, this heterogeneous mixture has higher potential for cross-reactivity with biomolecules containing similar epitopes which limits specificity in diagnostic assays.

These limitations were overcome with the development of monoclonal antibodies by Köhler and Milstein in 1975 (Köhler and Milstein, 1975) through the hybridoma technology. A monoclonal antibody represents a specific antibody produced from a single antibody secreting B-cells and therefore only binds one unique epitope. In

the hybridoma technology, Köhler and Milstein fused a single antibody secreting B-cells to immortal myeloma cells to produce a hybridoma cell capable of continuous production of a specific monoclonal antibody (mAb) (Kohler and Milstein, 1975). Monoclonal antibodies can be produced in large quantities and there is batch to batch homogeneity and consistency. Since they bind with high specificity to a single epitope, there is a reduced probability of cross-reactivity seen with polyclonal antibodies. However, monoclonal antibodies also have limitations. They are significantly more expensive to produce and time consuming. Their sensitivity is affected with small changes in the epitope of the target molecule. They also have more demanding storage conditions as they are sensitive to pH and buffer conditions.

Summarily, production of monoclonal antibodies has been useful especially in diagnostic applications that require the production of unique antibody to a specific epitope in large quantities.

1.5.2 Recombinant antibodies and fragments

To overcome immunogenicity experienced when antibodies derived from murine sources are administered, scientists sought to humanise the monoclonal antibodies (Roque *et al*., 2004). This allows the generation of humanised chimeric antibodies containing 60-70 % of human antibody sequence and the antigen specificity from murine construct. Chimeric antibodies have been developed as therapeutics with rare adverse responses reported (van dijk, 2001, Brekke and Sandlie, 2003). Advances have been made in the development of highly humanised antibody through CDR grafting (Jones *et al*., 1986) in which sequences for the human CDR are replaced with those from the original murine antibody (Figure 1.11).

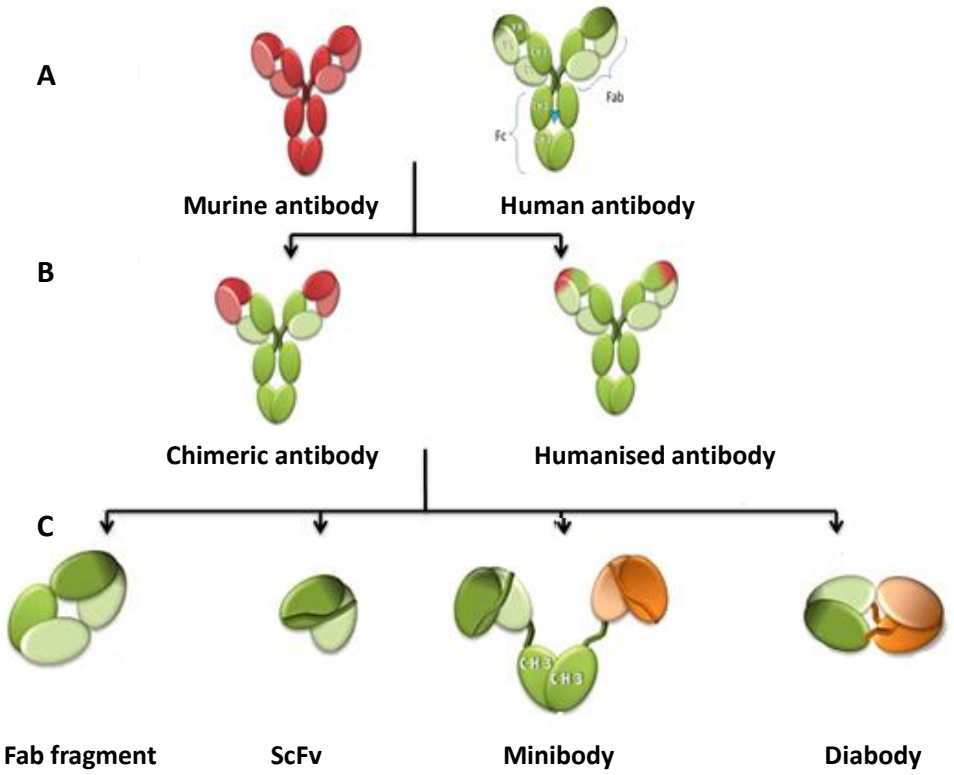

Figure 1.11: Antibody and their derivatives. Adapted from Chames *et al* (Chames *et al*., 2009). (a) Full-length antibodies from murine (red) and human (green), using light colours for light chain and dark colours for heavy chains. (b) The improvement on immunogenicity of monoclonal murine antibodies gave rise to chimeric antibody (human antibody with the murine variable region) and humanised antibodies (human antibody with murine hypervariable region grafting). (c) The derived fragments which are engineered to maintain the affinity and specificity of full-length antibody but are smaller in size, examples include the antigen-binding fragment (Fab) and single chain variable fragment (scFv), minibody and diabody.

Through antibody protein engineering, fragments of antibodies such as Fab and scFv have been developed. Fab fragment 55 kDa (consisting of the light chains, variable region of the heavy chain and CH1 of the heavy chain) retained antigen-binding activity but lack an effector function. They can be used as alternative to full length antibodies because they are monovalent and are rapidly cleared from the body. scFv fragments (single-chain variable fragments) 28 kDa, which is the variable domains of the heavy and light chains linked by a flexible linker (Bird *et al*., 1988), has also been in use as attractive alternative to full-size antibodies. A diagrammatic flow of the generations of antibodies and some of their derivatives is given in Figure 1.11.

1.5.3 Uses of antibodies

Development of the hybridoma technology has greatly enhanced the use of antibodies alongside with advancement in antibody protein engineering such as chimerisation of antibodies (Morrison *et al*., 1984), development of humanised antibodies (Jones *et al*., 1986), phage display (McCafferty *et al*., 1990), as well as the discovery of single chain antibodies in camelids (Skerra, 2000, Grönwall and Ståhl, 2009, Hamerscasterman *et al*., 1993). About 100,000 antibodies have been used in research and diagnostics and they are available commercially , more than 30 antibody-based products have been approved for use while over 240 antibodies aimed to be used therapeutically are in clinical development (Reichert, 2010, Beck *et al*., 2008).

The high sensitivity, specificity, and binding versatility of antibodies have made them valuable reagents in various diagnostic applications. Monoclonal antibodies have been developed for the diagnosis of animal viruses such as rotavirus, bovine herpes virus, *Trichomonas vaginalis* (Siddiqui, 2010); for the detection of mouse lymphocyte surface glycoprotein (Trowbridge, 1978). Antibodies have remained the mainstream of molecular recognition elements against different targets in FDA approved diagnostic kits for use in clinical laboratories. However, despite the many uses of antibodies in therapeutic and diagnostic approaches, there are limitations with antibody use.

1.5.3 Limitations in the use of antibodies for diagnostic application

1.5.3.1 Structural Limitations

Antibodies are relatively large multimeric proteins (150 kDa). Structurally, they are made up of complex multiple domains that require disulphide bonds and post-translational modification such as glycosylation, for stability (Banta *et al*., 2013). The heavy chains and light chains are held by disulphide bridges which make it difficult to be expressed in the reducing cytosol of microbial expression hosts (Frenzel *et al*., 2013). Consequently, the expression must be directed to the periplasmic space of prokaryotes, which leads to poor yield.

1.5.3.2 Production Limitations

Antibodies are often highly sensitive to elevated temperature, become susceptible to irreversible denaturation, prone to aggregation, therefore, limiting their shelf life. The behaviour of antibodies seems to vary, even though they have similar structures leading to batch-to-batch variation (Wang *et al*., 2007). In addition to these, monoclonal antibodies may take up to six months to produce and they are expensive.

1.5.3.3 Patent Issues

Biopharmaceutical companies, who have successfully produced recombinant antibodies, have protected intellectual property rights which makes the commercialisation of antibody derived products complicated (Stahl *et al*., 2013).

1.6 Antibody mimetics: Scaffold proteins

To overcome the limitations identified in the structure and function of antibodies and their derivatives, naturally occurring binding proteins of non-immunoglobulin origin have been tested as backbone for affinity molecules. These affinity molecules must possess comparable sensitivity, specificity, mimicking the molecular recognition of antibodies, and better properties but overcoming the limitations identified in antibodies (Skerra, 2007). To be used as an alternative to antibody, the binding protein must meet most of the criteria listed below as compiled from various papers (Binz *et al*., 2005, Caravella and Lugovskoy, 2010, Carter, 2011, Hey *et al*., 2005, Löfblom *et al*., 2011).

1.6.1 Characteristics of alternative binding proteins.

Artificial binding proteins are in general small (less than 200 amino acids), monomeric, stable and easy to express in *E. coli*. Most do not contain cysteines, enabling the introduction of a cysteine for site-specific coupling of biotin, fluorescent labels or polyethylene glycol (PEG) to enhance their utility or stability. They are thermostable, they have a high level of expression in microbial host leading to high yield in bacterial system. They exhibit high sensitivity and specificity to targets, have a good method for selection and show robustness. Artificial binding proteins tolerate diversification, and for use as therapeutics, they should

have good Immunogenicity record, no undesired side effect, extended plasma half-life, and ease of tissue penetration.

In 1992, the first report of alternative binding protein from non-antibody sources was reported by Roberts *et al* (Roberts *et al*., 1992), they used the Bovine (or basic) pancreatic trypsin inhibitor, BPTI, a Kunitz-type protease inhibitor as a scaffold to select binders against human neutrophil elastase target protein. Since then, more than 50 novel non-antibody protein scaffolds have been developed (Wurch *et al*., 2008) but only a handful have proved robust. These alternative antibody binding proteins (see section 1.6.4) have proven to be viable solutions to some of the roadblocks faced by antibodies thus triggering a paradigm shift in so far as antibodies are no longer considered as the unique and universal class of receptor proteins in biotechnology and medicine (Gebauer and Skerra, 2009, Skerra, 2003). They offer structurally diverse frameworks as starting points for engineering. Steps involved in the engineering of non-antibody binding proteins are discussed in the section 1.6.4.

Binding proteins that are non-immunoglobulin in origin have been called by different terminologies such as affinity protein (Grönwall *et al*., 2009), antibody mimetics (Baloch *et al*., 2016), alternative scaffolds (Stahl *et al*., 2012), scaffold proteins (Hosse *et al*., 2006) and non-antibody binding proteins (Löfblom *et al*., 2011). These names have been used interchangeably in this thesis.

1.6.2 Protein engineering of alternative binding proteins

Understanding the relationship between protein sequences, structure and their functions and thereby improving these properties forms the core of protein engineering (Banta *et al*., 2013). It involves identifying residues in a protein that are responsible for its catalytic activities, stability when subjected to high temperatures, binding capacity and other functional properties. This insight has helped protein engineers to develop new mutant proteins with enhanced or even novel properties, desired physical and chemical properties of the proteins which do not occur in nature and enzymes with improved thermostability, enzymatic activities and folding properties (Lehmann *et al*., 2000, Jackel *et al*., 2008). For engineering an

alternative binding protein, the major steps involved are described schematically in Figure 1.12

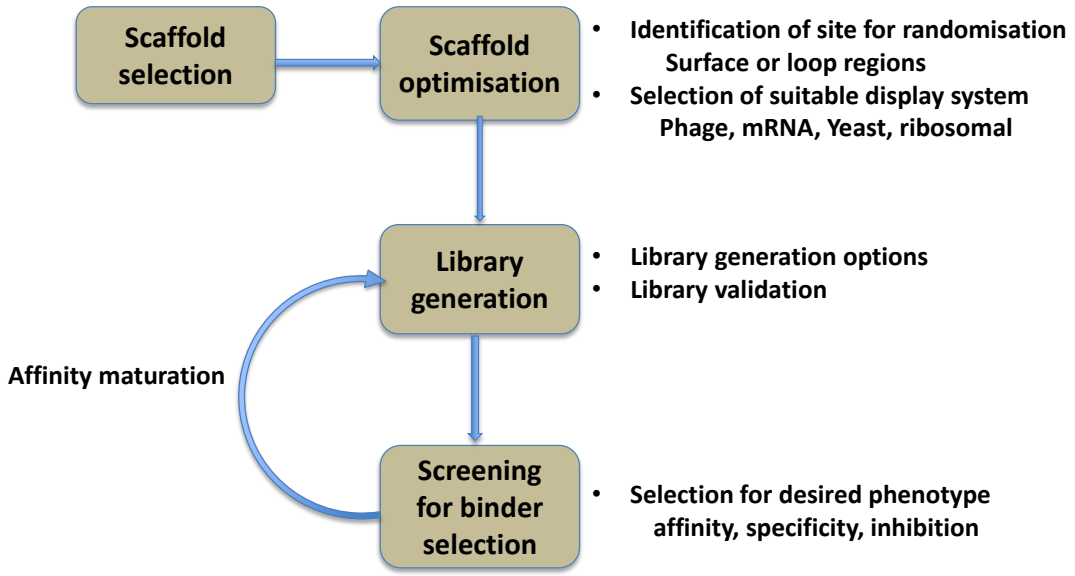

Figure 1.12: Steps in engineering new protein scaffold. The process of designing new protein scaffold begins with the selection of a scaffold protein, then the optimisation of the scaffold, followed by the generation of a diverse library using a suitable display system. From this library, screening is carried out for the selection of binders with desired phenotype. To achieve affinity maturation, library of the selected binder can be generated by adding further diversification through PCR.

1.6.2.1 Scaffold selection and optimisation

The process of designing a new alternative binding protein begins with the selection of a suitable scaffold. A protein scaffold is defined as a polypeptide framework with a well-defined three-dimensional structure that tolerates mutations or insertions without a trade-off of its structural integrity (Skerra, 2007). Together with the other characteristics outlined in section 1.6.1, researchers began to explore proteins that exhibit natural binding abilities for use as protein scaffolds. One approach for designing a protein scaffold is the consensus design concept (Steipe *et al*., 1994). This is because in nature, conserved sequences arise from the desire to maintain stability during evolution. When non-antibody protein scaffolds exhibit natural binding abilities, the protein sequence of its homologous family members is aligned and analysed to identify regions in the sequence that are conserved (Binz *et al*., 2005). The amino acid positions in these conserved regions are thought to contribute to the stability of the proteins than the positions that do

not have clear consensus sequence (Jacobs *et al*., 2012). From these alignments, the consensus design concept results in the production of an optimally packed protein core structure which is the major determinant of the stability of the protein. This approach in protein engineering has been reported successful to improve the thermostability of antibodies (Knappik *et al*., 2000), enzymes (Komor *et al*., 2012), DNA binding proteins, fluorescent proteins and also for the optimisation of scaffold proteins (Binz *et al*., 2005, Jacobs *et al*., 2012, Tiede *et al*., 2014).

1.6.2.2 Introduction of diversity into protein scaffold

Once a suitable scaffold has been selected, it is then optimised for the display system of choice followed by the introduction of variation and diversity to create a library. Binding residues on protein scaffolds that naturally participate in biomolecular recognition are an obvious choice for mutagenesis. For example, the inhibitory sequences within the Gln Val Val Ala Gly and Pro Trp Glu variable regions of the Affimer scaffold were selected for randomisation (Tiede *et al*., 2014). Other sites on protein scaffolds considered for variation include exposed surface loops as in Adnectin (Koide *et al*., 1998) and Lipocalins (Schlehuber *et al*., 2000), or exposed hydrophobic residues, stacked Beta sheets, and faces formed by alpha helical bundles (Banta *et al*., 2013). Examples of scaffold with surface rensomised residues include designed Ankyrin repeats proteins (Darpins) and Affibodies (Binz *et al*., 2003, Nord *et al*., 1997). The scaffolds mentioned here are discussed in more details in section 1.6.4. Once the appropriate site or region for randomisation has been selected, a mutagenic strategy is selected for the generation of mutant libraries, typically by using synthetic oligonucleotides and degenerate codons (Krumpe, *et al*., 2007, Stahl *et al*., 2013).

1.6.2.3 Display systems for novel affinity properties

Through combinatorial protein design, new proteins with new characteristics can be created *in vitro.* Nevertheless, predicting the combinations involved to design such a novel functionality is challenging (Grönwall and Ståhl, 2009). Thus, all protein selection systems are based on linking the genotype (the nucleic acid coding for the protein) to the phenotype (the expressed protein itself) of each protein which increases the ease of identification, screening, selection and

amplification of individual protein variant (Grönwall and Ståhl, 2009). Different protein selection systems have been developed, each of which has its pros and cons. The choice of a selection system depends largely on the diversity, size of the library and also on specific characteristics of the protein scaffold. Basically, there are three categories of protein selection systems which are (i) Cell-dependent display system (such as phage display, yeast display, *E. coli* surface display) where proteins are displayed on cellular surfaces or phage particles (Willats, 2002). (ii) Cell-free display systems (such as ribosomal display, mRNA display and DNA CIS display) which employs the transcription and translation machinery in cells for display (Gronwall, 2009, Binz, 2004, Odegrip, 2004). (iii) Non-display system (such as the protein complementation assay and yeast-two-hybrid display) where *in vivo* selection system relies on affinity between protein and their target to generate cell growth survival (Michnick, 2000).

1.6.3 Phage display technology

Phage display technology is used for the study of interactions between macromolecules. It was first described by George Smith in 1985 (Smith, 1985) when he fused the peptide of interest onto the gene gIII of filamentous phage, therefore demonstrating the display of the peptide on the phage. One crucial principle in phage display is the physical linkage of the properties of a polypeptide (phenotype) to the sequence encoding it (genotype). In this technique, a foreign gene sequence is spliced into the gene of one of the phage coat proteins creating a hybrid coat protein. As phage are released from the cell, the hybrid coat protein is incorporated into the phage particles and displayed on the outer surface (Smith and Petrenko, 1997). Thus, the foreign proteins are displayed on surfaces of phage particles.

The major filamentous phage strains used as vectors used in phage display are M13, fd and f1. The filamentous bacteriophage is flexible rod-like shape containing a single stranded genome of about 6400 nucleotides. The phage particle is encapsulated by the major coat protein pVIII, there are 2700 copies of the major coat protein on each virion. On one end of the cylinders, there are 5 copies of the minor coat protein pIII and pVI, while at the other end, there are 5 copies of pVII

and pIX (Petrenko *et al*., 1996, Scott and Smith, 1990). For phage display, the most widely used coat proteins are minor coat protein pIII and the major coat protein pVIII. One major difference in the use of either coat protein is the size of peptide that can be displayed. In pVIII, inserts more than 6-8 residues are less efficiently packaged into the capsid, however, peptide displayed on pVIII benefit from the avidity effect of being present in 2700 copies. On the other hand, larger inserts (>100 amino acids) can be readily packaged into the capsid when displayed on pIII (Sidhu *et al*., 2000).

Phage display technique allows for the generation of combinatorial libraries with up to 10^{10} different variants. This peptide library could be used for screening of molecules (called target of interest) to select, study and characterise ligands selected from the affinity screening of the phage display library. The process of selecting binders from the phage display library is called biopanning (Ehrlich *et al*., 2000). It involves the incubation of the phage library with the target of interest, unbound phages are washed off, and then bound phages are eluted for characterisation. Further rounds of panning are included to obtain highest target-binding clone. A schematic illustration of the steps involved in phage display is presented in Figure 1.13.

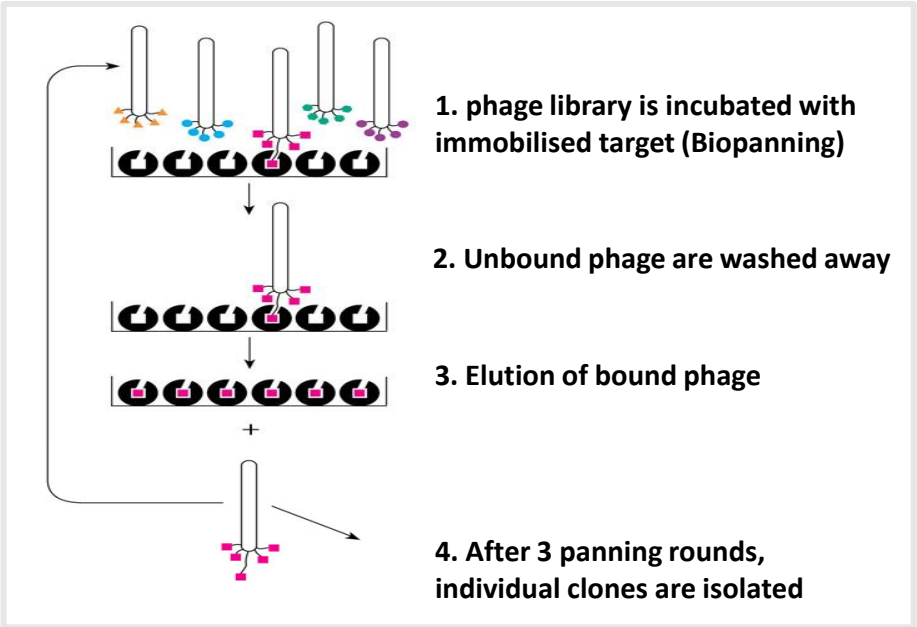

Figure 1.13: A schematic illustration of the steps involved in phage display screening. This occurs in three major steps of binding, washing, and eluting.

1.6.4 Examples of Protein Scaffolds.

1.6.4.1 Fibronectin

They are one of the most frequent mediators of protein-protein interaction. Structurally, they resemble antibodies in that they contain complementarity-determining region-like loops but unlike antibodies, they do not rely on disulphide bonds (Jones *et al*., 2008). The fibronectin type III domain is a 94-amino acid residue protein that is made up of seven strands with three connecting loops at one end of the beta sheet (Figure 1.14b) (Koide *et al*., 1998). The scaffold tenth fibronectin type III protein scaffold results from the randomization of the three N-terminal loop of the 10^{th} repeating structure in human fibronectin (Hey *et al*., 2005). Engineered Adnectin from the ^{10}Fn3 domain has been designed with high affinity and specificity to generate binders against various therapeutic targets (Lipovšek, 2011), such as the angiogenesis-related human vascular endothelial growth factor receptor 2 (VEGFR2), rheumatoid arthritis, psoriasis and Crohn's disease (Hey *et al*., 2005).

1.6.4.2 Lipocalin

The Lipocalins just like the fibronectin belongs to the antibody-like scaffolds. They are a diverse beta- barrel protein that contains disulphide bonds (Figure 1.14c). Naturally, they bind small molecules in their barrels and thus involved in the transport or storage of small hydrophobic molecules such as steroids and lipids (Stahl *et al*., 2013). Lipocalins due to their properties have been engineered and found as a suitable scaffold for recognising low molecular weight targets or haptens (Hosse *et al*., 2006)

1.6.4.3 Affibodies

They are derived from an immunoglobin Fc binding domain of *Staphylococcus aureus* protein A, which exhibits protein binding properties naturally. Thus the engineered version is referred to as Z domain of Staphylococcal protein-A (Hosse *et al*., 2006). They belong to the non-β sheet protein scaffold, consisting of three α-helices, which are arranged in an antiparallel three-helix bundle (Figure 1.14a). Thirteen surface exposed residues identified as necessary for binding were chosen

for randomisation to create the affibody library. The engineered Z domain lost almost all binding ability to the Fab of immunoglobulin but retained its binding ability to the Fc region of immunoglobulin (Löfblom *et al*., 2010). Unlike antibodies, they do not have disulphide bonds, yet they exhibit reversible folding. It is noteworthy that affibodies molecules can also be produced by chemical peptide synthesis (Löfblom *et al*., 2010). The application of affibodies has been reported for separation, purification, diagnostics, *in vivo* tumour imaging, therapeutic (Grönwall and Ståhl, 2009, Löfblom *et al*., 2010).

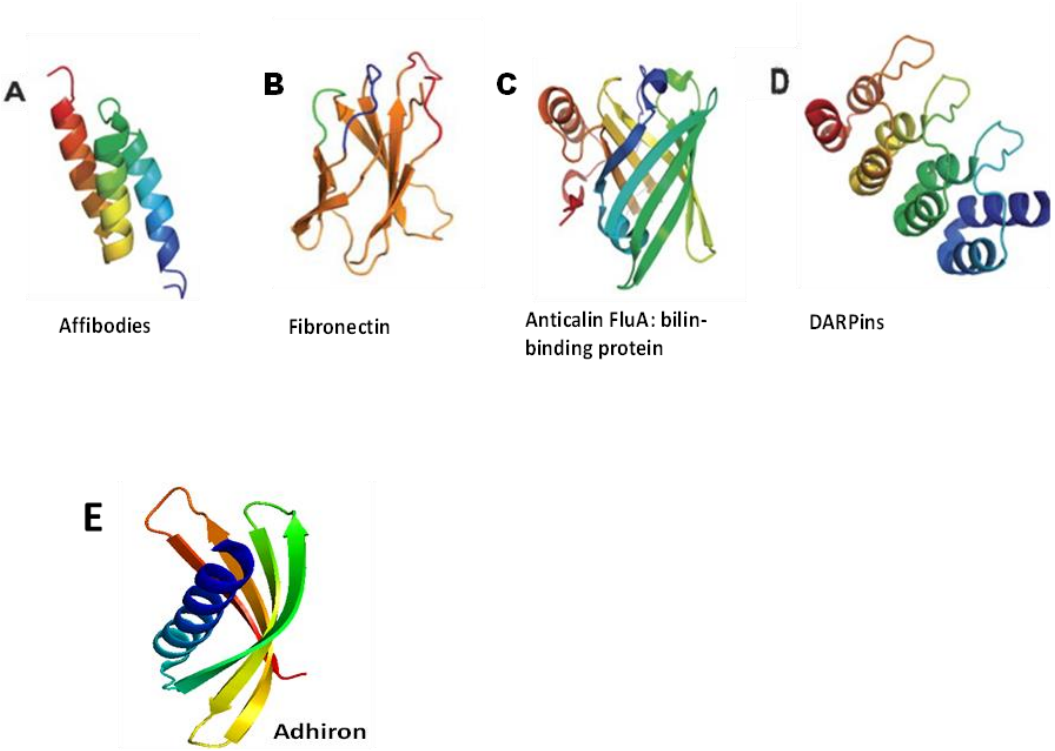

Figure 1.14: The schematic 3D structures of selected scaffolds. The structure of (a) affibodies, (c) anticalin and (d) DARPins were adapted from (Nuttall and Walsh, 2008); the structure of (b) fibronectin was adapted from (Lipovšek, 2011) while the structure of Affimer was generated through PyMol using PDB file: 4N6U.

1.6.4.4 DARPins

Repeat proteins are proteins that are built upon consecutive units of small amino acid residues (20-40 residues) which form contiguous domains. Naturally, they exhibit binding abilities in many biological processes. Due to their structure, they can easily be adapted to the size of their targets by adjusting the number of repeats in the proteins.

The ankyrin repeat protein belongs to the repeat protein group. As a naturally occurring binding protein, they mediate various protein-protein interactions. Binz and his group (Binz *et al*., 2005, Binz *et al*., 2004) generated the designed ankyrin repeats of varying sizes called DARPins (14-18 kDa) through the combinatorial consensus design approach. DARPins use both the beta-turns and a randomised surface for binding (Figure 1.14d). They show high thermodynamic stability, reversible folding properties. They show the highest expression levels for soluble functional proteins in *E. coli*, they do not contain cysteines, low aggregation tendencies. They are used for novel fusions for both extracellular and intracellular targeting (Binz *et al*., 2004).

1.6.4.5 Affimers (also referred to as Adhirons)

Scientists at the University of Leeds have developed a non-antibody binding protein called Affimer also known as Adhirons (Tiede *et al*., 2014). The Affimer scaffold is based on consensus from phytocystatin sequence which are small (ca. 100 amino acids) protein inhibitors of cysteine proteases (Kondo *et al*., 1991). This consensus protein displayed very good protease inhibitor activity and meets the requirements to be a good scaffold for peptide presentation (small, monomeric, high solubility and high stability and the lack of disulphide bonds and glycosylation sites). The inhibitory sequences comprising the QVVAG and PWE loops of the novel phytocystatin for peptide presentation were replaced with nine randomised residues in each loop.

Previous work on variants of human stefin A were shown to tolerate peptide insertion within surface exposed loops (Hoffmann *et al*., 2010, Stadler *et al*., 2011). Despite having a similar overall fold, Affimer shares only about 23 % pair-wise amino acid sequence identity with the human stefin variants. The consensus sequence of Adhiron was derived and constructed from multiple alignments of 57 phytocystatin sequences (Tiede *et al*., 2014). An Affimer scaffold library was built by splice overlap extension (SOE) of two PCR products, the degenerate positions (NNN) were introduced as trimers representing a single codon for each of the 19 amino acids excluding cysteine and there were no termination codons.

The Affimer library (10^{10}) has been presented in phage display for screening and selection of high affinity binders. It has been screened against various targets such as yeastSUMO, the fibroblast growth factor (FGF1), receptor (CD31). It has been tested as a valuable research agent for high specificity binding. Using the bio-layer interferometry technology (BLItz™) and surface plasmon resonance, analysis of the binding kinetics of selected Affimers to their targets gave K_D between 9 and 103 nM (Tiede *et al*., 2014, Kyle *et al*., 2015, Sharma *et al*., 2016). The introduction of 9 additional amino acids residue within its two variable regions retained high thermostability with a melting temperature of 101°C. The work in this thesis has been based on the use of Affimer as the alternative scaffold protein

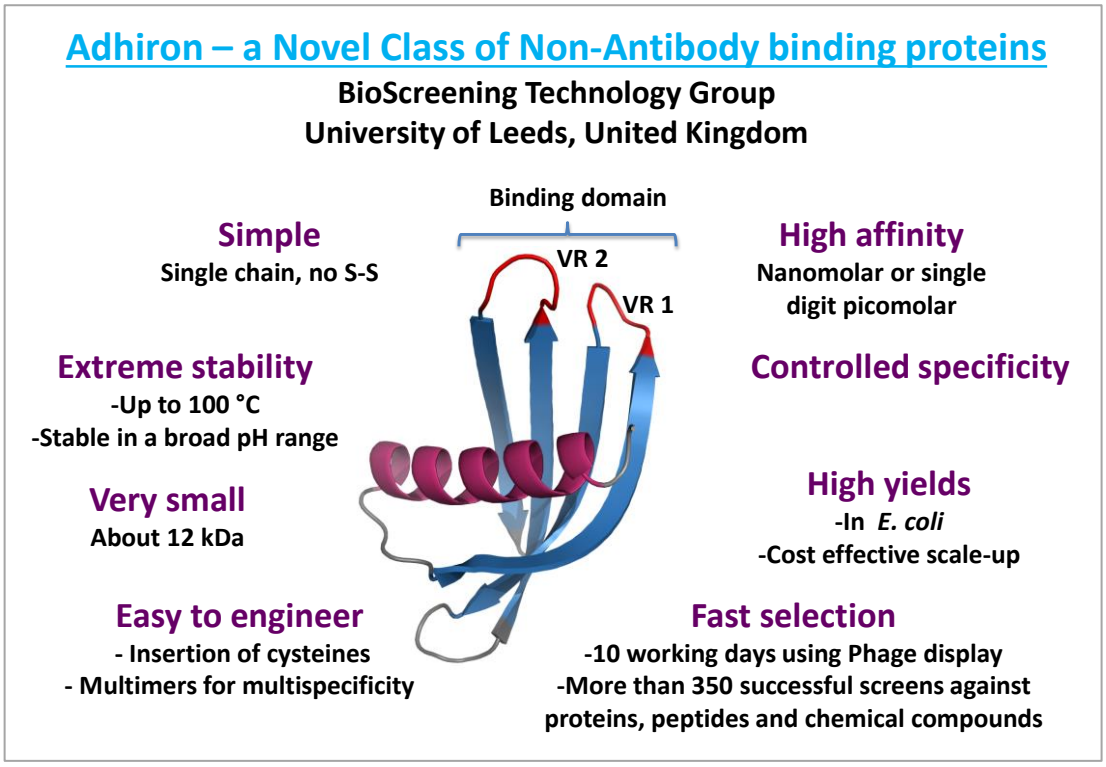

Figure 1.15: Characteristics of the Affimer (Adhiron) scaffold. This shows the structure and characteristics of the Affimer scaffold.

1.7 Applications of scaffold proteins

The characteristics of non-antibody binding proteins highlighted earlier have made them powerful tools in a wide range of applications broadly classified as therapeutic or non-therapeutic applications such as diagnostics, and basic and applied research.

1.7.1 Scaffold proteins in therapeutic applications.

Application of scaffold proteins for therapeutic use has been the most common goal, which is stimulated by the large commercial success and therapeutic use of monoclonal antibodies (Škrlec *et al*., 2015). In therapeutic applications, scaffold proteins are directed against targets that are relevant in diseases such as biomarkers, surface receptors and signalling molecules with examples of these scaffold proteins advancing into clinical development discussed briefly. Angiocal is a PEGylated Anticalin that has been tested in Phase I clinical trials for targeting and antagonising a VEGFR-2 ligand, VEGF-A in patients with advanced solid tumours (Mross *et al*., 2013). Adnectin CT-322 was successfully tested against VEGFR-2 for the treatment of recurrent glioblastoma in a Clinical trial (Mamluk *et al*., 2010). Similarly, scaffold proteins have been used in the treatment of inflammatory diseases- Affibody against TNF-alpha (Johnson *et al*., 2009), and Repebodies against human IL-6 (Lee *et al*., 2014), cardiovascular disease and for the treatment of blood disorders- DX88 (Ecallantide) which is a selective inhibitor of plasma kallikrein based on a Kunitz domain (Dennis *et al*., 1995). DX88 remains the only protein scaffold that has been successfully approved for therapeutic use.

1.7.2 Diagnostic use of scaffold proteins

The high affinity, specificity and sensitivity with which antibodies interact with antigens make them a useful reagent not only in therapeutic applications but also as diagnostics (Skerra, 2000). Current diagnostic formats popularly used are Enzyme-Linked Immunosorbent Assay (ELISA), flow cytometry, immunohistochemistry (Binz *et al*., 2005). More recently, diagnostics are taking new approaches in which non-antibody binding proteins are immobilised onto the surface of miniature chips for screening (Chan *et al*., 2013). Scaffold proteins possess many qualities that makes them more suitable than antibodies for *in vivo* and *in vitro* diagnostics. The small size of scaffold proteins enhances better tissue penetration and more rapid blood clearance better than antibodies. A radiolabeled EGFR-binding Affibody molecule was used as a tumor imaging agent in malignancy (Nordberg *et al*., 2007). In *in vitro* diagnostic applications, like antibodies, scaffold proteins with high specificity and affinity has been selected against various targets

in many types of samples (Škrlec *et al*., 2015); they can be used in conjunction with multiple detection technologies such as microarrays, electronic chips and dip-sticks (Grönwall and Ståhl, 2009, Stahl *et al*., 2013). However, they have edge over antibodies for use as diagnostics because of the absence of cysteine in their structure which gives them flexibility of introducing unique cysteines for site-directed immobilization when coupling to detectors for biosensor applications (Chan *et al*., 2013), their tolerance to fusion proteins such as fluorescent proteins or enzymes and their ease of being engineered to contain intrinsic detection means. Protein scaffold such as Affibodies (Löfblom *et al*., 2010), Darpins (Binz *et al*., 2005), and Affimer (Affimer), have been successfully used for diagnostics (Škrlec *et al*., 2015).

1.8 Molecular Recognition Elements for diagnosing *C. difficile Infection.*

Since the introduction of enzyme immunoassays for the diagnosis of *C. difficile* infection over three decades ago, antibodies have been the only molecular recognition element used for capturing and detection of toxin A, toxin B and GDH in commercially available diagnostic kit for CDI (Vanpoucke *et al*., 2001, Carroll, 2011). The inherent limitations of antibodies as described in Section 1.6.3 directly impact the performance of antibody-based toxin immunoassay, in fact, the sensitivity and specificity of such assays is critically dependent on the sensitivity and specificity of the molecular recognition elements used. Ochsner and colleagues (Oschner *et al*., 2013) reported the use of slow-off rate aptamers (SOMAmers) as replacement for antibody for toxin A and B detection in CDI diagnosis. More recently, Hong and colleagues (Hong *et al*., 2015), reported the selection and characterisation of single-stranded DNA Aptamers as antibody alternatives for the detection of toxin B at nanomolar concentration in clinical samples. Although no other antibody alternatives have been reported in the literature for *Clostridium difficile* infection, these studies strongly suggest that replacement of antibodies with novel affinity reagent have the potential to significantly enhance the performance of current toxin immunoassays and emerging diagnostic techniques for *Clostridium difficile* infection.

1.9 Aims of the thesis

The aims of this thesis are

(i) To identify and isolate Affimers with high sensitivity and specificity against the three validated biomarkers (toxin A, toxin B and glutamate dehydrogenase) of *Clostridium difficile* infection.

(ii) To characterise selected Affimers for their stability, affinity and ability to function as novel reagent for the development of point-of-care diagnostic tool for *Clostridium difficile* infection.

1.10 Structure of the thesis

Chapter 2 details the materials and methods used throughout in this thesis.

Chapter 3 describes mutational studies of aggregation-prone Affimers, using Ataxin binder as a case study. Selected point mutations were tested in other aggregation-prone Affimers to see if they could be used as a generic approach for engineering aggregation-resistant Affimers. Secondly, since the Affimer scaffold was developed from plant cystatin, this chapter details the engineering of bacterial cystatin using the consensus design approach, then describes the optimisation trials for the protein expression of bacterial cystatin.

Chapter 4 describes work done using glutamate dehydrogenase from *C. difficile* as the biomarker of interest. This chapter is structured into three main parts: the first part details the design, production and characterisation of recombinant glutamate dehydrogenase (GDH) from *clostridium difficile*, which is the common antigen, used in the screening for the presence of the bacteria. The second part describes the selection of Affimers against GDH using phage display technology, then the cloning, expression and purification of unique Affimers. Then the third part details the various characterisation carried out, that led to the selection of the best Affimer for GDH and finally the sensitivity of Affimer-based assay was compared to a commercially available and clinically used GDH ELISA kit.

Chapter 5 details the work done using toxin A and toxin B from *C. difficile* as biomarkers of interest. This chapter is structured into three main parts: the first

describes the identification, isolation and selection of Affimers against toxin A and B using phage display technology. The second part details the description of the cloning, expression and purification of unique Affimers. The last part of this chapter gives an extensive characterisation of the selected Binders using a range of biophysical and biochemical approaches, then the identification of Affimer pairs possessing high affinity and specificity for toxin A and toxin B.

Chapter 6 details conjugation of the Affimers to detection enzymes to produce a one-step detection system and testing this against the current state-of-the art clinical ELISA tests used in the NHS in the UK. Finally, the chapter describes the development of an Affimer-based hybrid assay for toxin B that shows higher sensitivity and discriminate between Toxin A and Toxin B compared to commercial test kits.

Chapter 7 is a summary of the findings of Chapter 3 to 6 and placing the work presented here in context with the literature. Then discusses future work and applications for the research carried out in this thesis.

Chapter 2: Materials and Methods

2.1 Introduction

This chapter outlines the materials and methods used throughout the project. It gives an overview of the principles of each technique and a description of how it was carried out. Unless otherwise stated, all chemicals were purchased from Sigma-Aldrich or Fisher Scientific; randomised oligonucleotide primers were generated by IDT while other oligonucleotide primers were generated by Sigma-Aldrich. Synthetic genes were generated by GenScript.

2.1 *E. coli*

2.1.1 XL10-Gold

Genotype: $Tet_r\Delta$ (mcrA)183 Δ(mcrCB-hsdSMR-mrr)173 endA1 supE44 thi-1 recA1 gyrA96 relA1 lac Hte [F' proAB $lacI_qZ$ ΔM1 Tn10 (Tet_r) Amy Cam^r]

Source: Stratagene

XL10-Gold cells were used routinely for replication, purification and storage of plasmid DNA as they have been optimised by a number of mutations: (i) the *recA1* mutation improves insert stability as unwanted recombination is reduced; (ii) non-specific digestion by endonuclease I is prevented by incorporation of the *endA1* mutation thereby greatly improves the quality of the miniprep; (iii) incorporation of the *hsdR* mutation prevents the cleavage of cloned DNA by the *EcoK* endonuclease system; (iv) the *supE44* mutation suppresses amber (UAG) stop codons by insertion of glutamines therefore, the termination of translation is reduced; (v) Exhibit *Hte* phenotype, which increases transformation efficiency of large and ligated DNA molecules. The other mutations in the genotype were not relevant for the work presented here.

2.1.2 XL1-Blue

Genotype: *recA1 endA1 gyrA96 thi-1 hsdR17 supE44 relA1 lac [F´ proAB $lacI_qZ$ ΔM15 Tn10 (Tet_r)]*

Source: Stratagene

XL1-Blue cells were also used for replication, purification and storage of plasmid DNA as they have been optimised by a number of mutations: the *recA1*, *endA1,*

hsdR and *supE44* mutations as described for XL10-Gold. The other mutations in the genotype were not relevant for the work presented here.

2.1.3 BL21 (DE3) Star

Genotype*: F- ompT hsdSB (rB-mB-) gal dcm rne131 (DE3)*

Source: Invitrogen

BL21 (DE3) Star cells were used for protein expression as they have been optimised by a number of mutations: (i) the *ompT* mutation in outer membrane protease VII as well as the absence of the *Ion* protease reduces the proteolytic cleavage of the expressed protein; (ii) the *hsdSB* mutation reduces degradation of transformed plasmids which are 'foreign' to the host cell; (iii) the *rne* gene (rne131) mutation encodes a truncated ribonuclease E enzyme that lacks the ability to degrade mRNA, thereby increasing the stability of mRNA, with a resultant increase in the yield of the recombinant protein; (iv) the DE3 designation means that the BL21 strain contains λ DE3 lysogen which carries the gene for T7 RNA polymerase under the control of the IPTG-inducible *lacUV5* promoter for which it is used to induce expression in a T7 promoter-based system (for example pET vectors used here).

2.1.4 ER2738 electrocompetent cells

Genotype: [F´*proA+B+ lacIq Δ*(*lacZ*)M15 *zzf::Tn10* (tetr)] *fhuA2 glnV*_(*lac-proAB*) *thi-1*_(*hsdS-mcrB*)5

Source: Lucigen

The *E. coli* host strain ER2738 is an F+ strain, which produces highly efficient electrocompetent cells and was used for phage propagation during phage display library screening. ER2738 is a suppressor strain, it contains the *supE (GlnV)* mutation which suppresses the amber (UAG) stop codons within the library by insertion of glutamine (CAG). This generates a fusion of the pIII protein and the binding molecule displayed on the surface of the phage. The F-factor of ER2738 contains a mini-transposon which confers tetracycline resistance, so that cells harbouring the F-factor can be selected by plating and propagating in tetracycline-containing medium.

2.2 Plasmids

2.2.1 pDHis phagemid vector

The pDHis phagemid vector used in this project was derived from pDHis II that was developed from pHEN1 (Hoogenboom *et al.,* 1991). The vector contains a recombinant coding sequence for Affimer flanked by NheI and NotI restriction sites, and an ampicillin (*amp*) resistant gene for selection (Figure 2.1). The presence of the DsbA secretion signal peptide allows for efficient translocation to the periplasm. The in-frame amber (TAG) stop codon allows translational read-through to create an Affimer-truncated-pIII fusion protein.

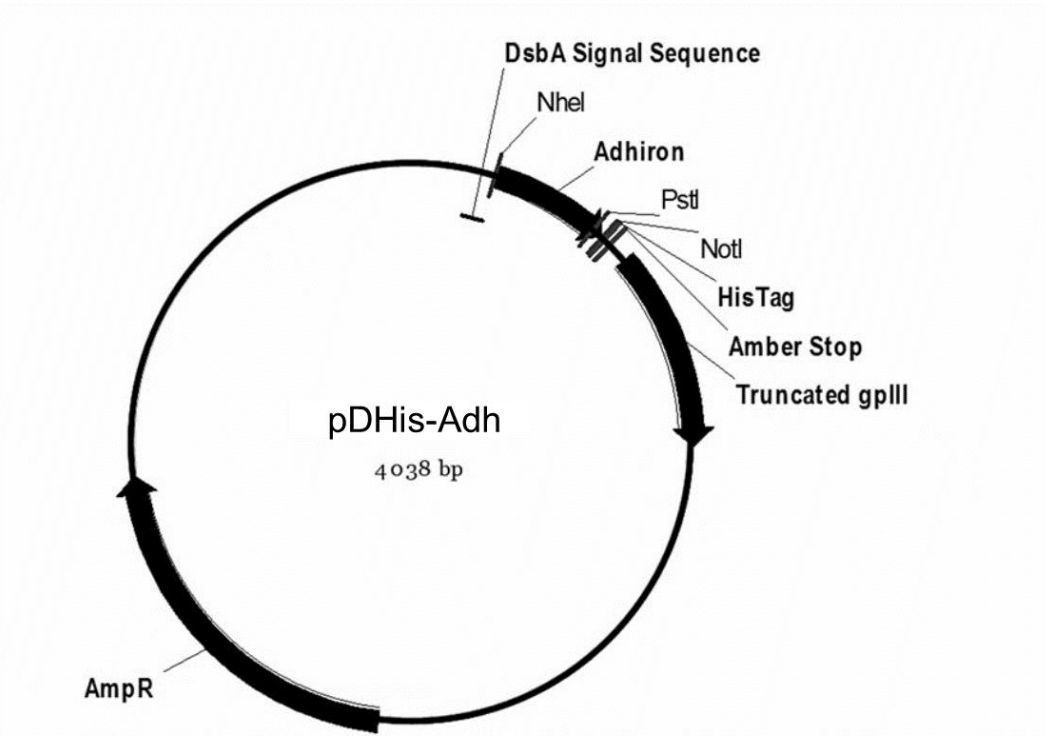

Figure 2.1: pDHis phagemid vector. The Affimer phagemid vector contains a fusion coding sequence encoding a DsbA secretion signal peptide, Affimer flanked between NheI and NotI restriction site, a hexa-histidine tag, Amber stop (TAG) codon and C-terminal half of gene III of bacteriophage M13. It contains an amp resistant gene for selection. (Adapted from Tiede *et al*., 2014).

2.2.2 pET Vectors

In this work, pET11a (Novagen) and pET28c (Novagen) were used as vectors for recombinant protein expression due to the presence of the T7 promoter upstream of the coding sequence. The *E. coli* strain BL21 star (DE3) was used for protein expression as it inducibly produces T7 RNA polymerase which has a high selectivity

for the T7 promoter leading to enhanced transcription of the gene of interest (Studier and Moffatt, 1986). The pET vectors also carry a copy of the *lacI* gene which codes for the lac repressor. When expressed, Lac repressor binds to the *lac* operator inhibiting the transcription of the gene of interest. Therefore, expression in pET vectors is regulated by the lac regulatory system.

2.2.2.1 pET11a

Source: Novagen

Backbone: 5677 bp ds-DNA plasmid

pET11a expression vector contains a T7 promoter and T7 termination site, multiple cloning site, a Lac I repressor coding sequence, and an ampicillin resistance gene (*amp*) for selection. In this project, all Affimer binders identified after phage display screening were sub-cloned from pDHis II phagemid vector into the pET11a vector for protein production.

2.2.2.2 pET28c

Source: Novagen

Back bone: 5369 bp ds-DNA plasmid

This vector has a pBR322 and an f1 origin of replication, the latter allowing the production of single stranded plasmid DNA when infected with helper phage. pET28c contains a kanamycin resistance gene, T7 promoter and T7 termination site, a N-terminal and C-terminal His. Tag, and a multiple cloning site. In this project, all synthetic coding regions ordered from GenScript were sub-cloned form pUC57 vector into the pET28c vector for protein production.

2.3 Growth Media

2.3.1 2TY medium

Tryptone (16 g/L), yeast extract (10 g/L) and NaCl (5 g/L) were dissolved in deionised water and the solution was autoclaved at 121 °C, 15 psi for 20 min.

2.3.2 SOB medium

Tryptone (20 g/L), yeast extract (5 g/L) and NaCl (0.5 g/L) were dissolved in deionised water and autoclaved at 121 °C, 15 psi for 20 min

2.3.3 SOC medium

Tryptone (20 g/L), yeast extract (5 g/L) and NaCl (0.5 g/L) were dissolved in deionised water and autoclaved at 121 °C, 15 psi for 20 min. The following sterile solutions were added to 79 mL before use (final concentrations are shown in brackets): 10 mL 1 M $MgCl_2$ (0.1 M), 10 mL $MgSO_4$ (0.1 M), 1 mL 2 M D-glucose (20 mM).

2.3.4 LB medium

Tryptone (16 g/L), yeast extract (10 g/L) and NaCl (5 g/L) were dissolved in deionised water, and autoclaved at 121 °C, 15 psi for 20 min.

2.3.5 LB Agar plates

Agar (12 g/L) was added to LB medium and the solution was autoclaved at 121 °C, 15 psi for 20 min. After autoclaving, the solution was cooled in a 50 °C water bath for 30 min before addition of antibiotic to the appropriate concentration (Section 2.4.3), followed by dispensing of approximately 25 mL into petri dishes under aseptic conditions.

2.4 Bacterial Transformation

2.4.1 Preparation of competent cells

Three strains of *E. coli* cells (XL1-Blue, XL10-Gold and BL21 Star (DE3)) were made competent by using rubidium chloride. Cells were streaked from glycerol stocks onto LB-agar plates containing no antibiotics, and incubated overnight in a static incubator at 37 ^{o}C. A single colony was picked from the agar plate into 5 mL of SOB and incubated overnight in a shaking incubator at 37 ^{o}C with shaking at 200 rpm. 50 µL aliquot of the overnight culture was used to inoculate 50 mL of pre-warmed SOB media which was then incubated in a shaking incubator at 37 °C and 200 rpm until OD_{600} is 0.4-0.6 (2-4 h). The culture was transferred into a 50 mL falcon tube and chilled on ice for 5 min. The cells were harvested by centrifugation in a Swing-out rotor at 3,000 rpm and 4 ^{o}C for 10 min, and the supernatant was discarded. Cells were gently resuspended in 20 mL of ice-cold TFB1 buffer (100 mM $RbCl_2$, 50 mM $MnCl_2$, 10 mM $CaCl_2$, 3 mM CH_3COOK, 15 % (v/v) glycerol, pH 5.8) and incubated on ice for 5 min, harvested by centrifugation in a swing-out rotor at 3,000 rpm and 4^{o}C

for 10 min. The supernatant was discarded and the tube wiped dry, then cells pellets were gently resuspended in 2 mL of ice-cold TFB2 buffer (10 mM $RbCl_2$, 75 mM $CaCl_2$, 10 mM MOPS, 15 % (v/v) glycerol, pH 6.5), and incubated on ice for 15 min. 250 µL aliquots of competent cells were dispensed into sterile microcentrifuge tubes, frozen on dry ice and stored at –80 °C.

2.4.2 *E. coli* transformation

Competent cells were thawed on ice and sterile microfuge tubes were cooled on ice. 25 µL of competent cells was gently mixed with 1 µL (40 ng) of plasmid DNA and incubated on ice for 30 min. The cells were then heat-shocked in a water bath at 42 ^{o}C for 45 s and immediately returned to chill on ice for 2 min. Pre-warmed LB (250 µL) was then added to the tube and the culture was transferred to a shaking incubator (37 ^{o}C, 230 rpm) for 1 h, allowing cell recovery and expression of the antibiotic resistance protein. Then, 50 µL of culture were transferred to labelled agar plates containing appropriate antibiotics and spread out until all liquid was absorbed. The plates were inverted and incubated overnight at 37 ^{o}C in a static incubator.

2.4.3 Antibiotics

Antibiotics used in this work were carbenicillin, kanamycin and tetracycline. A 1000 x stock solution of each antibiotic was made up in deionised water, filter sterilised through a 0.2 µm syringe-end filter and stored in 1 mL aliquots at -20 °C. The final concentration used in cultures was 60 µg/mL of carbenicillin or 50 µg/mL kanamycin (Sambrook *et al*., 1989). Carbenicillin was used in place of ampicillin because it demonstrates improved stability over ampicillin in growth media, and can reduce the growth of satellite colonies during long-term incubation. Also, the by-products generated upon its degradation are less toxic to cells, permitting denser cell growth.

2.5 Plasmid purification from *E. coli*

2.5.1 Mini-preparation of plasmid DNA

Routinely, the QIAprep® spin miniprep kit (Qiagen) was used to purify plasmid carrying the gene of interest (insert) from *E. coli* cells. A single colony containing the desired plasmid was used to inoculate 5 mL of LB media supplemented with the

appropriate antibiotic. The culture was incubated at 37 °C in a shaking incubator (230 rpm) and allowed to grow overnight for 16 h. The cells were harvested by centrifugation in a 50 mL falcon tube for 15 min at 4,700 rpm and the supernatant was drained by inverting the tube. The pellet was then completely resuspended in 250 µL of buffer P1 (50 mM Tris-HCl, pH 8.0, 10 mM EDTA, 100 µg/mL RNase A, 1 µL/mL lyse blue reagent) and transferred into a 1.5 mL microcentrifuge tube. Lysis was initiated by the addition of 250 µL of buffer P2 (200 mM NaOH, 1 % (w/v) SDS) and mixing was carried out by inversion until the blue colour was homogeneous. 350 µL of buffer N3 (4.2 M guanidium chloride, 0.9 M potassium acetate, pH 4.8) was added and immediately mixed by inversion until all the blue colour had disappeared, resulting in a white precipitant indicating neutralisation of lysis by precipitation of SDS. The sample was centrifuged at 13,000 rpm in a bench top microcentrifuge for 10 min to pellet all the cell debris. The supernatant was applied to a QIAprep column, containing a silica membrane which selectively adsorbs plasmid DNA in high salt buffer and binds up to 20 µg of DNA. The QIAprep column was centrifuged for 1 min. The flow-through was discarded and the column was washed with 750 µL of buffer PE (10 mM Tris-HCl pH 7.5, 80 % (v/v) ethanol) to efficiently remove the salts and centrifuged for 1 min. The flow-through was discarded and centrifuged for additional 1 min to remove any residual ethanol which could prevent loading of sample onto an agarose gel and inhibit any future enzymatic reactions. The column was transferred to a sterile 1.5 mL microcentrifuge tube and 30–50 µL of deionised water (depending on the desired final concentration) was carefully pipetted directly onto the membrane. After 1 min, the column was centrifuged for 1 min at 13,000 rpm in a bench top microcentrifuge to elute the DNA. The column was discarded and the plasmid DNA was stored at -20 °C.

2.5.2 Midi-preparation and maxi-preparation of plasmid DNA

For the purification of plasmids (pET11a and pET28c parent plasmid) from larger culture volumes of *E. coli* cells, the QIAprep® spin midiprep (plasmid purification from 50 mL culture) or the maxiprep kit (plasmid purification from 150 mL culture) was used according to the manufacturer's protocol.

2.5.3 Determination of DNA concentration

The concentration of the plasmid DNA was measured using a NanoDrop Lite spectrophotometer (Thermo Scientific^{TM}), which measures the nucleic acid concentration at 260 nm and assesses sample purity using the 260/280 nm ratio. From the home tab on the screen dsDNA assay was selected, following the on-screen instructions, a blank was established by pipetting 1.5 µL of deionised water onto the bottom pedestal. Once the blank measurement was confirmed, the sample holder was wiped clean using a dry laboratory wipe. A 1.5 µL aliquot of DNA sample was pipetted onto the sample holder and the concentration determined. As a rule of thumb, samples with A260/A280 ratio between 1.8 and 2.0 are considered pure. The purified plasmid DNA were stored at -20 ^{o}C or sequenced.

2.5.4 DNA sequencing

DNA sequencing was carried out using Beckman Coulter Genomics, and the sequencing primers are listed in Table 2.1. Plasmid DNA samples were prepared at 100 ng/µL and a 15 µL aliquot was sent for DNA sequence determination. Data were returned as Fasta files and .ab1 files. Results were analysed using the BioEdit Sequence Alignment Editor v. 7.0.9.1 to confirm the chromatogram, ExPASy translate tool to translate nucleotide sequences into protein sequences and ClustalW alignment tool for sequence alignments.

2.6 Molecular biology and DNA manipulation

2.6.1 Polymerase Chain Reaction (PCR) protocols

For the amplification of Affimer insert in cloning vectors, standard PCR protocol was employed using Phusion High-Fidelity DNA Polymerase (NEB) which offers high fidelity and robust performance. The component of the standard PCR protocol for a 25 µL reaction volume is given in Table 2.1, while the amplification was carried out using the conditions outlined in Table 2.2.

Table 2.1: Components of the PCR reaction

Component	Volume (µL)	Final Concentration
Sterile Water	13.8	
5X Phusion HF Buffer	5	1X
dNTP Mix, 25 mM	0.2	200 µM each
DMSO	0.75	3 %
Forward Primer, 10 µM	2	0.8 µM
Reverse Primer, 10 µM	2	0.8 µM
Phusion DNA Polymerase	0.25	0.02 units/µL
Template DNA (phagemid vector)	1	

Table 2.2: Thermocycling condition for PCR reaction

Cycle Step	Temperature (°C)	Time (s)	Cycles
Initial Denaturation	98	30	1
Denaturation Annealing Extension	98 54 72	20 20 20	30
Final Extension Hold	72 4	10 min Hold	1

The PCR products were analysed by electrophoresis of a 5 µL aliquot through an agarose gel of the appropriate pore size (Table 2.5). This confirmed the yield and size of the PCR product.

2.6.2 Oligonucleotide primers

All oligonucleotides were ordered from Sigma. All primary stocks were diluted to 100 µM and working stocks to 10 µM. Table 2.3 gives a list of the primers used in this study for insert amplification, mutagenesis and for DNA sequencing.

Table 2.3: List of primers used in the study

	Primer name	Sequences
Affimer insert Amplification	pDHisIID-final-for	5′TTCTGGCGTTTTCTGCGTCTGC 3′
	Affimer Short	5′ATGGCTAGCGGTAACGAAAACTCCCTG 3′
	forward shorter	5′ATGGCTAGCAACTCCCTGGAAATCGAAG 3′
	pDHisIID-final-rev	5′TACCCTAGTGGTGATGATGGTGATGC 3′
	pDHIS-C-rev	5′TTACTAATGCGGCCGCACAAGCGTCACCAACCGGTTTG 3′
	Adh R8C - for	5′AAATCTGCTAGCGCCGCTACCGGTGTTTGTGCAGTTCCGGGTAACGAAAAC 3′
Colony PCR	T7P	5′TAATACGACTCACTATAGGG 3′
	T7R	5′CCGCTGAGCAATAACTAG 3′
Site-directed mutagenesis	N16D For	5′GCAGTTCCGGGTAACGAAGACTCCCTGGAAATCGAAGAACTGGC 3′
	N16D Rev	5′GCCAGTTCTTCGATTTCCAGGGAGTCTTCGTTACCCGGAACTGC 3′
	Q50E For	5′CGTTCGTGTTGTTAAAGCTAAAGAAGAAGAAGTTGTTGTTCAGCG 3′
	Q50E Rev	5′CGCTGAACAACAACTTCTTCTTCTTTAGCTTTAACAACACGAACG 3′
	N94D For	5′CGCTGCTAAAATCATGTCTGACTTCAAAGAACTGCAG 3′
	N94D Rev	5′CTGCAGTTCTTTGAAGTCAGACATGATTTTAGCAGCG 3′
	D16N For	5′GTTCCGGGTAACGAAAACTCCCTGGAAATC 3′
	D16N Rev	5′GATTTCCAGGGAGTTTTCGTTACCCGGAAC 3′
	E50Q For	5′CGTTCGTGTTGTTAAAGCTAAAGAACAGGAAGTTGTTGTTCAGCG 3′
	E50Q Rev	5′CGCTGAACAACAACTTCCTGTTCTTTAGCTTTAACAACACGAACG 3′
	N94D For-2	5′CTGCTAAAATCATGTCTGACTTCAAAGAACTGCAG 3′
	N94D Rev-2	5′CTGCAGTTCTTTGAAGTCAGACATGATTTTAGCAG 3′
DNA sequencing	M13-26REV	5′CAGGAAACAGCTATGAC 3′
	T7 P	5′TAATACGACTCACTATAGGG 3′
	T7 R	5′CCGCTGAGCAATAACTAG 3′

2.6.3 Restriction digestion

Restriction endonucleases cut plasmid DNA at specific sequences. All restriction endonucleases used were purchased from New England Biolabs®, (NEB) as High-Fidelity (HF) endonucleases with the added benefit of reduced star activity, rapid digestion (5-15 min) and 100 % activity in CutSmart® Buffer. Briefly, 1-5 units (U) of restriction enzyme were used to digest 20 ng-2 µg of DNA in a buffered volume of 50 µL. According to NEB, 1 U is defined as the amount of enzyme required to digest 1 µg of DNA in an hour at optimum temperature in a reaction volume of 50 µL.

Unless otherwise stated, double digestion was carried out with NheI-HF™ and NotI-HF™ restriction enzymes. Following PCR clean-up of amplified Affimer insert, a

typical double digestion reaction contains 3 µL sterile water, 6 µL CutSmart® buffer, 50 µL of amplified Affimer insert, and 0.5 µL each NheI-HF and NotI-HF restriction enzymes, making a total of 60 µL reaction volume in a microcentrifuge tube. The reaction is mixed and incubated for a minimum of 6 h or overnight at 37 ^{o}C in a static incubator.

2.6.4 Ligation

Ligation of linearised plasmid and insert was carried out using T4 DNA ligase from NEB. The appropriate amounts of the digested, dephosphorylated plasmid (75 ng) and the digested insert (25 ng) were combined with 2 µL of 10 x T4 DNA ligase reaction buffer, 1 µL of T4 DNA ligase and made up to a total reaction volume of 20 µL with deionised water. Incubations were carried out in 200 µL PCR tubes overnight at room temperature.

2.6.5 Colony PCR

Colony PCR is a quick screening method for determining the presence or absence of inserts DNA in plasmid constructs directly from transformed *E. coli* colonies. A 200 µL pipette tip was used to collect a single colony and was swirled gently in 100 µL sterile deionised water before being used to inoculate 3 mL 2TY broth containing the appropriate antibiotic. This culture was incubated overnight at 37 °C with shaking at 220 rpm to enable purification of the DNA by miniprep (Section 2.5.1). Meanwhile, the inoculated water was heated to 99 °C for 5 min in a G-Storm GS2 thermal cycler, cooled to room temperature and centrifuged at 13,000 rpm in a microcentrifuge to pellet cell debris leaving the DNA in suspension. Colony PCR was performed by adding 1 µL of this suspension to 24 µL of PCR master-mix (containing 0.2 mM dNTPs, 0.1 µM T7P primer; 0.1 µM T7R primer, 1 x GoTaq Hot start Green Master mix and sterile water to make up the reaction volume to 25 µL- see Table 2.1 for T7P and T7R primer sequence). Positive and negative controls were included and the amplification was performed as outlined in Table 2.4. The PCR products were analysed by agarose gel electrophoresis alongside a 5 µL aliquot of 2 log DNA marker to confirm the presence or absence of the desired product.

Table 2.4: The reaction conditions for colony PCR

Stage	Temperature (˚C)	Time (s)
Hot start	95	60
30 cycles:		
Denature	94	60
Anneal	55	60
Extend	75	Depends on expected product
Final extension	72	300
Store	4	∞

2.6.6 Agarose gel electrophoresis

Agarose gels were prepared and run using a HU6 Mini (small gel) or HU10 Mini-Plus (large gel) horizontal gel unit (Scie-Plas, Harvard Bioscience). Agarose gels of the desired percentage were made by combining the appropriate volume of Tris-acetate ethylenediaminetetraacetic acid (TAE) buffer (40 mM Tris-acetate, 1 mM ethylenediaminetetraacetic acid (EDTA), made up as a 50 x stock, pH 8.0) with agarose in a 250 mL Duran bottle and heated in the microwave for approximately 2 min until the agarose completely dissolved and the solution was bubbling. The agarose solution was cooled in a 50 °C water bath for 30 min before adding the appropriate volume of SYBRsafe DNA gel stain (Invitrogen). The molten agarose was then poured into the casting tray in a casting unit, a comb added and the gel left to set at room temperature.

Table 2.5: Recommended agarose gel percentages for the resolution of linearised DNA

Agarose gel percentage	DNA size range
0.5 %	1,000-30,000 bp
0.7 %	800-12,000 bp
1.0 %	500-10,000 bp
1.2 %	400-7,000 bp
1.5 %	200-3,000 bp
2.0 %	50-2,000 bp

To run the gel, the casting tray containing the agarose gel was removed from the casting unit and placed into the running chamber. The comb was removed and TAE buffer was added until the gel was submerged. DNA samples were prepared by

addition of 6 x gel loading dye (NEB) and then loaded into the wells of the agarose gel. A 1 µL aliquot of the appropriate DNA size ladder was also combined with 1 µL 6 x gel loading dye and added to a well: either 1 kb DNA size ladder or 100 bp DNA size ladder (NEB) were used (Figure 2.2).

Once samples were loaded, the running chamber was connected to the power unit and a voltage of 100 V wasapplied for 40 min or longer if better resolution was required. DNA was either visualised under UV light and photographed using an Alpha Imager system (Alpha Innotech) or if it was to be used for downstream applications, was visualised using a Safe Imager (Invitrogen) which is a blue light trans illuminator and does not lead to DNA damage as does UV light.

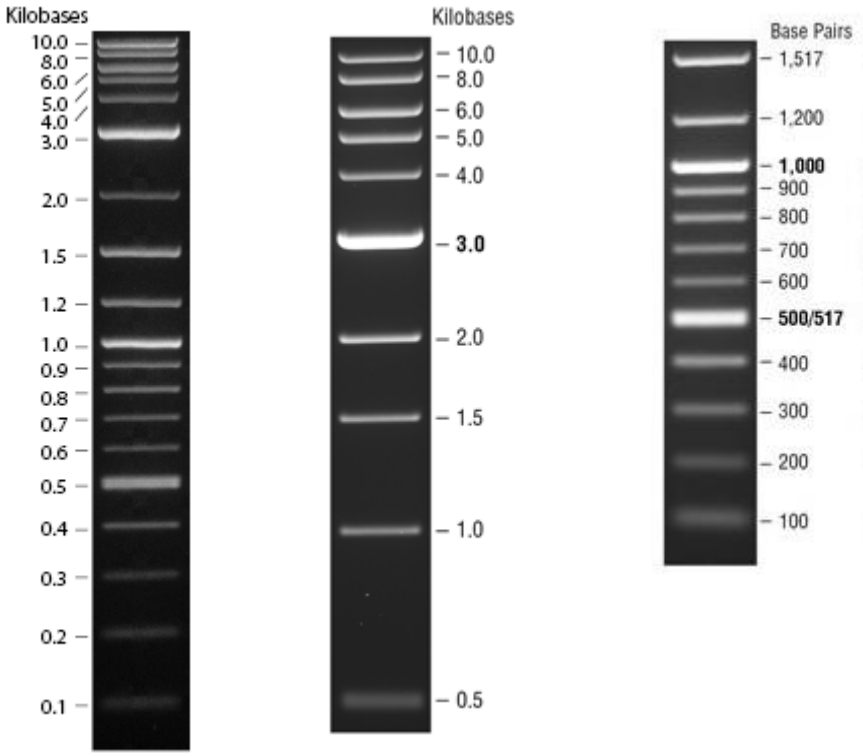

Figure 2.2: DNA size ladders used in agarose gel electrophoresis. The 2-log, 1 kb and 100 bp DNA size ladders (NEB) were used to estimate the size of DNA analysed by agarose gel electrophoresis.

2.6.7 Dephosphorylation of DNA

By dephosphorylating the digested plasmid, the 5' phosphate groups are removed and self-ligation is prevented (Sambrook *et al.*, 1989). Dephosphorylation was carried out by adding 0.1 U/µL Antarctic Phosphatase and 1 x Antarctic

Phosphatase reaction buffer (NEB) to the completed restriction digestion reaction (Section 2.6.4) and incubating at 37 °C for 15 min. The phosphatase enzyme was heat-inactivated by incubation at 65 °C for 5 min in a G-Storm GS2 thermal cycler.

2.6.8 Purification of DNA from an agarose gel

The QIAquick® Gel Extraction kit (Qiagen) was used to purify DNA from agarose gels. The DNA sample was first separated by agarose gel electrophoresis and visualised using a Safe Imager (Invitrogen) (Section 2.6.6). DNA was not visualised by UV light as this can cause damage which significantly reduces the efficiency of downstream applications such as overlap extension, and ligation. The band of interest was excised using a clean, sharp scalpel and placed in a weighed 1.5 mL microcentrifuge tube. The agarose gel was solubilised by addition of 3 gel volumes (v/w) of buffer QG (5.5 M guanidine thiocyanate, 20 mM Tris-HCl, pH 6.6) at 50 ˚C; the chaotropic salt guanidine thiocyanate ensures binding of DNA to the QIAquick membrane. To ensure the highest efficiency binding, the pH of the solution was adjusted to below pH 7.5 by addition of 10 µL of 3 M sodium acetate, pH 5.0 and 1 gel volume of isopropanol was added. The sample was then applied to the QIAquick column and centrifuged for 1 min at 13,000 rpm in a microcentrifuge. The flow-through was discarded and the column was washed to remove impurities by addition of 750 µL of buffer PE (10 mM Tris-HCl, pH 7.5, 80 % (v/ v) ethanol) and centrifugation for 1 min at 13,000 rpm. To elute the DNA the column was placed in a clean 1.5 mL microcentrifuge tube and 30 µL deionised water added to the centre of the membrane. After 1 min at room temperature this was centrifuged for 1 min at 13,000 rpm, the spin column discarded and the DNA solution stored at -20 ˚C.

2.6.9 Purification of PCR products

The QIAquick® PCR Purification kit (Qiagen) was used to purify DNA products following PCR, overlap extension or ligation where separation from other DNA species was not necessary but removal of reaction components was required for the highest efficiency of downstream processes, such as restriction digestion or transformation. The protocol was the same as that of the QIAquick® Gel Extraction kit except that the PCR reaction was mixed with 5 volumes of buffer PB (5 M

guanidinium chloride, 30 % (v/v) isopropanol) containing pH indicator, rather than buffer QG, before being applied to the QIAquick column.

2.7 Protein expression and purification

2.7.1 Expression by IPTG induction

Transformation of BL21 (DE3) Star cells with recombinant vectors was carried out and incubated overnight at 37 ^{o}C on LB-agar plate with the appropriate antibiotics (cab/kan). A single colony was picked from the agar plate and used to inoculate 7 mL Lb-(cab/kan) +1% Glucose, the starter culture. The inoculated starter culture was incubated overnight at 230 rpm and 37 ^{o}C. 2 mL overnight culture was used to inoculate pre-warmed autoclaved 50 mL LB-(cab/kan) in 250 mL baffled flasks, and then incubated at 37 ^{o}C, 230 rpm until the OD_{600nm} reaches 0.8, then induction of protein expression at $OD_{600\ nm}$ = 0.8 was carried out by addition of IPTG to a final concentration of 0.1 mM. The culture was incubated for 6 h at 25 ^{o}C at 150 rpm. Cells were harvested by centrifugation at 4,000 rpm, 4^{o}C for 15 min, and pellets were stored at -20^{o}C.

2.7.2 Expression by autoinduction

Single colonies of BL21 (DE3) Star cells containing the appropriate plasmids were used to inoculate 2 mL of autoinducing media (Terrific Broth - TB) containing the appropriate antibiotic and grown at 37 °C with shaking at 230 rpm for 6 h. Following this, 200 µL of the starter culture was used to inoculate 400 mL of TB supplemented with LAC and the appropriate antibiotic in 2 L baffled flasks. The cultures were then incubated at 25 °C with shaking at 250 rpm for 48 h.

2.7.3 Cell lysis

Protein-expressing cells were harvested by centrifugation at 4,700 rpm, 4 ^{o}C for 20 min and the pellets were stored at -20 ^{o}C. Buffers used for protein purification are provided in Table 2.6, they were filter sterilized and stored at room temperature.

Table 2.6: Buffers used during protein purification

Buffer	components
Lysis Buffer	50mM NaH_2PO_4, 300 mM NaCl, 20 mM Imidazole, pH 7.4
Wash Buffer	50mM NaH_2PO_4, 500 mM NaCl, 20 mM Imidazole, pH 7.4
Elution Buffer	50mM NaH_2PO_4, 500 mM NaCl, 300 mM Imidazole, pH 7.4
1 x PBS	137 mM NaCl, 2.7 mM KCl, 10 mM Na_2HPO_4, 2.0 mM KH_2PO_4, pH 7.4

Immediately before use, 1 mL of lysis buffer was supplemented with 100 µL BugBuster® 10X Protein Extraction Reagent (Novagen), 0.4 µL of Benzonase® Nuclease (Novagen), and 10 µL of Halt Protease Inhibitor cocktail EDTA-Free (100X) (Thermo Scientific). BugBuster® was used for the gentle disruption of the *E. coli* cell resulting in the liberation of the soluble proteins, Benzonase® Nuclease was used for the degradation of DNA and RNA impurities in the lysate, while the Halt Protease Inhibitor cocktail protects the expressed recombinant protein from degradation by inhibiting endogenous proteases. Cell pellet obtained from the 50 mL expression culture was lysed by resuspending the pellet in supplemented 1 mL lysis buffer centrifuged for 20 min at 13,000 rpm on a bench top centrifuge to separate the insoluble fraction from the soluble fraction (the supernatant). Expressed protein was purified usually from the soluble fraction.

2.7.4 Protein Purification using Ni-NTA affinity chromatography

His-tagged Affimer binders were purified from the soluble samples using affinity chromatography. The principle of purification using Ni-NTA affinity chromatography is that the hexahistidine tag present in the expressed protein exhibits very strong affinity and interaction for immobilized metal ion matrices. The electron donor group on the histidine imidazole forms coordination bond with the immobilized Ni^{2+}, therefore hexahistidine proteins are selectively retained on the column matrices while impurities are washed off. Bound his-tagged proteins can be easily eluted by adding higher concentration of free imidazole to the column which

displaces the protein from the matrix. The method outlined below was used as a one-step purification method for all Affimer binders.

300 µL of Ni-NTA resin slurry (Qiagen) was resuspended in 1 mL wash buffer in a 2 mL microcentrifuge tube, centrifuged at 1,000 x g for 1 mn to sediment the resin and the supernatant was carefully aspirate off with a pipette. The resin was washed 3 times and then resuspended in 150 µL wash buffer to make a 300 µL of Ni-NTA slurry.

The clear supernatant containing the soluble protein was mixed with 300 µL of Ni-NTA resin slurry for 1.5 h with mild agitation on a rotor at room temperature, then centrifuged at 1,000 x g for 1 min. The supernatant was carefully collected into a fresh tube as it contained all unbound protein and can be analysed on a SDS-PAGE. In the meantime, a 5 mL Pierce centrifuge column was equilibrated with 5 mL of wash buffer. The resin was resuspended in 1 mL wash buffer and transferred into the equilibrated column, and allowed to empty by gravity flow. The resin was washed extensively with wash buffer until the $A_{280\,nm}$ reading of the collected wash buffer fraction is consistently < 0.01. To elute the bound protein, the column was closed, and the resin resuspended in 1 mL elution buffer, incubated for 5 min and fractions collected into labelled 1.5 mL microcentrifuge tubes. Further elutions were collected with 500 µL elution buffer until the $A_{280\,nm}$ of the eluted fractions drops to < 0.5 g/mL.

2.7.5 Determination of protein concentration

The concentration of purified proteins was measured using a NanoDrop Lite spectrophotometer. Since the purified proteins contains tryptophan, tyrosine, phenylalanine or cysteine-cysteine disulphide bonds which absorbs at A_{280nm}, the absorbance at $A_{280\,nm}$ in combination with the molar extinction coefficient, can be used to calculate the concentration of the purified protein as described below.

From the home tab on the screen, Protein $A_{280\,nm}$ was selected, and the default setting in which 1 abs = 1 mg/mL was used. Following the on-screen instructions, a blank was established by pipetting 1.5 µL of elution buffer onto the bottom pedestal. Once blank measurement has been confirmed, the sample holder was

wiped clean using a dry laboratory wipe. The elution fraction was flicked to mix the sample, then 1.5 µL aliquot of protein was pipetted onto the sample holder and the absorbance determined. The protein concentration was determined by absorbance measurements at 280 nm using theoretical molecular mass and extinction coefficients calculated with the ExPASy ProtParam Tool (Pace *et al*., 1995).

2.7.6 Analysis by SDS-PAGE

Protein samples were separated according to their motility through a SDS-polyacrylamide gel by electrophoresis following the commonly used protocol developed by LaemmLi (1970). This was used to assess the purity of the protein samples.

2.7.6.1 Preparation of soluble samples

To ensure visualisation, denaturation and easy loading, samples were mixed with 4 x loading buffer (200 mM Tris-HCl, pH 6.8, 20 % (v/v) glycerol, 8 % (w/v) SDS, 0.4 % (w/v) bromophenol blue, 20 % (v/v) β-mercaptoethanol) and heated at 95 °C for 5 min.

2.7.6.2 Preparation of insoluble samples

The insoluble fraction obtained from the lysis of the cell pellet in 1 mL lysis buffer (Section 2.7.3) was resuspended in 1 mL 10 % (v/v) lysis buffer and centrifuged at 13,000 rpm in a microcentrifuge for 5 min. The supernatant was discarded and the pellet resuspended once more in 10 % (v/v) lysis buffer. This was repeated three more times to wash the insoluble pellet and remove any soluble proteins before the pellet was resuspended in enough 4 x loading buffer (Section 2.7.6.1) to make the total volume up to 1 mL. The resuspended pellet was then heated at 95 ˚C for 5 min.

2.7.6.3 Preparing and running the gel

Using a Bio-Rad PROTEAN casting system a 15 % resolving gel (15 % (v/v) acrylamide (Severn Biotech Ltd.), 375 mM Tris-HCl, pH 8.8, 0.1 % (w/ v) SDS, 0.1 % (w/v) ammonium persulfate (APS), 0.04 % (v/v) N,N,N’,N’,-tetramethylethylenediamine (TEMED)) was poured between casting plates using a Pasteur pipette and allowed to polymerise overlaid with ethanol to ensure a flat

interface. The ethanol was then removed by rinsing with deionised water and a stacking gel (5 % (v/v) acrylamide, 125 mM Tris-HCl, pH 6.8, 0.1 % (w/ v) SDS, 0.1 % (w/v) APS, 0.1 % (v/v) TEMED) poured using a Pasteur pipette before the addition of a 10- or 15-well comb to create sample wells. Protein samples were loaded along with PageRuler™ Unstained Protein Size Ladder (Fermentas) (Figure 2.3) to permit estimation of the size of the protein bands. Gels were electrophoresed at 150 V in SDS-PAGE running buffer (25 mM Tris, 250 mM glycine, 0.1 % (w/v) SDS, pH 8.3) until the dye front had just run off the bottom of the gel (approximately 60 min). The gel was stained with InstantBlue (Expedeon); bands were visible within about 10 min and the gel was photographed after 1 h using an AlphaImager system (Alpha Innotech).

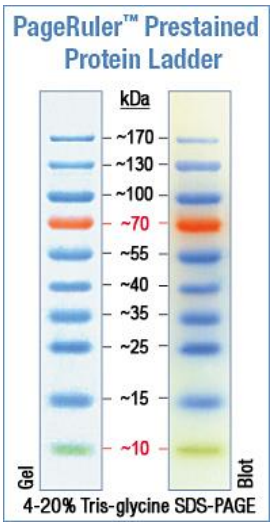

Figure 2.3: PageRuler™ prestained protein size ladder used in SDS-PAGE

2.7.7 Glutamate dehydrogenase enzyme assay

The assay for GDH activity was performed at 25 ^{o}C in a reaction mixture containing 300 mM potassium phosphate buffer, pH 8, 300 mM Glutamic Acid, pH 7.5, 1 mM NAD and 0.5 µg GDH. The initial velocity was determined by measuring NADH production spectrophotometrically at 340 nm. Cell lysate prepared from *E. coli* BL21 (DE3) Star cell containing pET11a carrying an unrelated gene was used as a negative control.

2.8 Biotinylation

2.8.1 Toxin A and Toxin B target protein

Purified native *C. diff* toxin A and B, and the recombinant fragment of toxin B (rTcdB) corresponding to the C-terminal domain of the toxin were kindly provided by Dr Cliff Shone, the Public Health England (PHE), United Kingdom. The purity of the toxins was analysed on an SDS-PAGE.

2.8.2 Biotinylation of targets

To prepare targets for phage display screening, targets were immobilised via Biotin-streptavidin interactions. Toxins A and B proteins were biotinylated using EZ-link NHS-SS-biotin (Pierce), according to the manufacturer's instructions, while $rGDH_{C.\ diff}$ was biotinylated using TCEP reduced EZ-HPDP-biotin since biotinylating with EZ-link NHS-SS-biotin led to the biotinylation of lysine residues present in the active site of GDH thereby rendering the enzyme inactive. Biotinylation of the *C. diff* targets was confirmed by ELISA using streptavidin conjugated to HRP (Invitrogen). Similarly, purified Affimers were also biotinylated using the EZ-link Maleimide Biotin kit from Pierce for use in protein and sandwich ELISA.

2.8.2.1 Biotinylation using EZ-Link® NHS-SS-Biotin

The EZ-Link® NHS-SS-Biotin were used to label the primary amines and free lysine residues in proteins. The vial of EZ-Link® NHS-SS-Biotin was equilibrated at room temperature before opening. Immediately before use, a 5 mg/mL solution of NHS-SS-Biotin was prepared in DMSO and appropriate volumes of NHS-SS-Biotin solution were added to the protein. For a 12 kDa Affimer protein, 10 µL of a 1 mg/mL solution was added to 0.8 µL of NHS-SS-Biotin in a total volume of 100 µL PBS. The solution was incubated for 1 h at room temperature. Excess biotin was desalted using the Zeba Spin Desalting Columns, 7K MWCO according to the manufacturer's instructions. Equal volume of 80 % glycerol was mixed with the biotinylated protein before storage at -20 ^{o}C.

2.8.2.2 Reduction of disulphide bonds using immobilized TCEP reducing gel

To label cysteines containing protein, the disulphide bonds were reduced to make the sulfhydryl groups (-SH) available for labelling. A 112.5 µL of immobilized TCEP disulphide Reducing Gel was placed in a microcentrifuge tube and centrifuged at 1,000 x g for 1 min, supernatant was removed by pipetting and was discarded. The gel was carefully washed by adding 300 µL of PBS containing 1 mM EDTA, vortexed gently to resuspend the gel, centrifuged at 1,000 x g for 1 min, and supernatant discarded. This washing step was repeated twice. A 3.75 µL aliquot of PBS containing 50 mM EDTA was added to the gel, and then 75 µL of a 1 mg/mL solution of the peptide to be reduced was added. The tube was vortexed briefly and incubated for 1 h at room temperature on a Stuart SB2 fixed speed rotator (20 rpm) to keep the gel in suspension. Immediately before biotinylation, the microcentrifuge tube was centrifuged at 1000 xg for 1 min to recover the supernatant containing the reduced peptide.

2.8.2.3 Biotinylation using EZ-Link® HPDP-Biotin

The EZ-Link® HPDP-Biotin (Thermo Scientific) is a membrane permeable biotin labelling reagent. It reacts with sulfhydryl (-SH) groups in the protein to form a reversible and cleavable disulphide bond between the target sulfhydryl molecule and the biotin group. The $rGDH_{C.\ diff}$ target protein was biotinylated using the EZ-Link® HPDP-Biotin protocol which is outlined below. A 4 mM HPDP-Biotin stock solution was prepared by adding 2.2 mg of EZ-Link® HPDP-Biotin to 1 mL of DMSO. The mixture was gently warmed to 37 ^{o}C and vortexed to ensure complete dissolution of the reagent. The stock was aliquoted and stored at –20 ^{o}C. 2 µL of HPDP-Biotin stock solution was added to 50 µL of the reduced peptide and the solution was incubated either at room temperature for 2 h or incubated overnight at 4 ^{o}C. The reaction mixture was desalted using a Zeba Spin desalting column equilibrated with PBS. Equal volume of 80 % glycerol was mixed with the biotinylated protein before storage at -20 ^{o}C.

2.8.3 ELISA to check biotinylation

Biotinylation of target was confirmed by ELISA using the protocol described below. 50 µL per well of PBS was added into 4 wells of a Nunc-Immuno™ MaxiSorp™ strip. 1, 0.1 and 0.01 µL of biotinylated target was added to the first 3 wells, while the 4th well was used as a negative control. The strip was incubated overnight at 4 ^{o}C to allow immobilization of the target onto the strip, then washed three times with 300 µL per well of the wash buffer (PBST) to remove excess sample. Each well was blocked with 250 µL of 10 x blocking buffer, incubated at 37 ^{o}C for 3 h without shaking and washed 3 x with 300 µL per well of the wash buffer. 1:1000 dilution of high sensitivity streptavidin-HRP was prepared in 2 x blocking buffer and 50 µL of the dilution was added to the wells then incubated at room temperature for 1 h on a vibrating platform shaker. Excess streptavidin-HRP was extensively washed off with 300 µL wash buffer 6 times and then 50 µL per well of TMB substrate was added and allowed to develop, noting the time taken for a blue colour to develop. The absorbance at 620 nm was measured using an ELISA plate reader.

2.9 Phage Display Screening.

An Affimer phage Library has been generated and used to identify high affinity binders to >350 targets. The stages involved in the isolation, identification and characterisation of binders are presented in Figure 2.4.

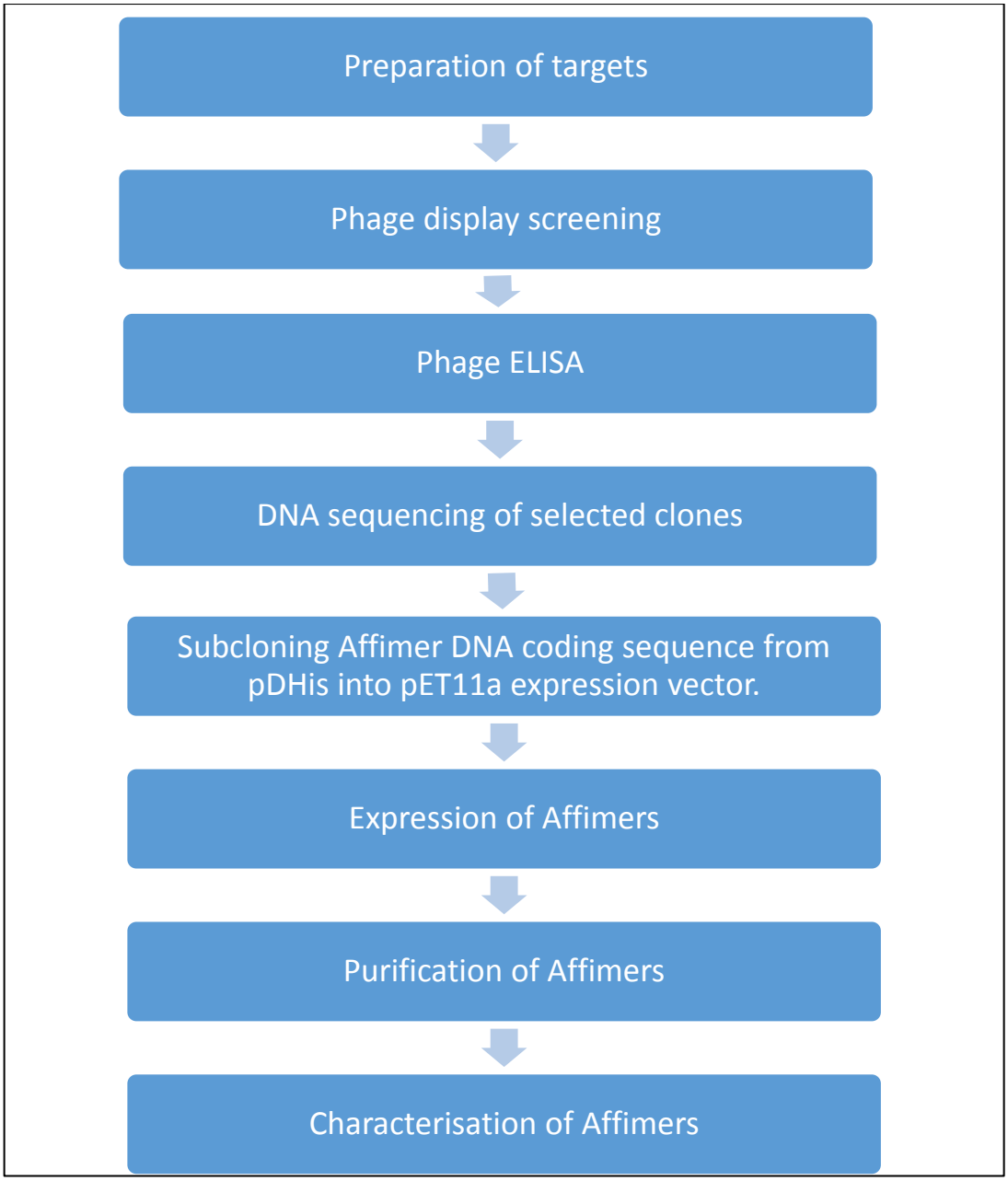

Figure 2.4: Overview of stages in the generation of Affimer to targets. Identification of Affimer binders to target of interest follows the stages outlined. The target of interest is immobilised and used in phage display screen, then phage ELISA to identify potential binders. DNA sequencing identifies unique binders and conserved binding motifs. The Affimer binder of interest is subsequently subcloned into an expression vector for expression, then purification and characterisation.

2.9.1 Preparation of ER cells.

E. coli host strain ER2738 cells were streaked onto LB agar plates containing tetracycline (12 µg/mL) and incubated at 37 ^{o}C overnight. A colony of ER2738 *E. coli* cells was picked into 5 mL of 2TY media supplemented with 12 µg/mL tetracycline and incubated overnight in an orbital incubator at 37 ^{o}C and 230 rpm.

2.9.2 Biopanning round 1

2.9.2.1 Preparation of streptavidin coated strips.

For each target, 4 wells of Streptavidin coated (HBC) 8-well strips (3 wells to be used for pre-panning the phage and 1 well to be used for binding the target and panning the phage) were blocked overnight with 300 µL per well of 2 x Blocking Buffer at 37 ^{o}C without agitation. The wells were washed 3 times with 300 µL PBST per well on a plate washer (TECAN HydroFlex), and a 100 µL aliquot of 2 x blocking buffer was added into all wells. 20 µL of the biotinylated target was added to the well to be used for panning, and incubated for 2 h at room temperature on the vibrating platform shaker (Heidolph VIBRAMAX 100; speed setting 3). During the incubation period, the phage was pre-panned.

2.9.2.2 Pre-panning the phage.

Extensive pre-panning steps were applied to reduce background binding of Affimer phage library to streptavidin coated strip surface, streptavidin and blocking buffer before panning of the Affimer library with the target protein. To the first pre-panning well containing 200 µL of 2 x blocking buffer, 5 µL of the phage was added, mixed and incubated on the shaker for 40 min. Blocking buffer was removed from the 2nd pre-panning wells, then the phage containing buffer from pre-panning well 1 was transferred into pre-panning well 2 and incubated for 40 min. This process was repeated for the 3rd pre-panning well.

2.9.2.3 Binding of pre-panned phage to target

The well containing the immobilised target was washed six times with 200 µL per well of PBST and then the phage from the 3rd pre-panning well was added. This was incubated for 2 h at room temperature on a vibrator platform shaker. Meanwhile, a

fresh 8 mL culture of ER2738 cells was prepared by adding 500 µL of the overnight culture, and incubated for about 1 h at 37 ^{o}C and 230 rpm to give an A_{600nm} of ~0.6.

2.9.2.4 Washing

Unbound phages were removed by washing the panning well 27 times with 300 µL per well of PBST on the plate washer.

2.9.2.5 Elution

Bound phages were eluted by adding 100 µL of Glycine elution buffer (0.2 M Glycine, pH 2.2), and incubated for 10 min at room temperature. To avoid decrease in phage infectivity, the eluted phage was neutralized immediately by adding 15 µL of 1 M Tris-HCl, pH 9.1, and added to the 8 mL aliquot of ER2738 cells in a 50 mL falcon tube. 14 µL of Triethylamine was diluted with 986 µL of PBS and the remaining phages in the panning well were eluted by adding 100 µL of the diluted trimethylamine. This was incubated for 6 min at room temperature, neutralised immediately by adding 50 µL of 1 M Tris-HCl, pH7 and added immediately to the ER2738 cells.

2.9.2.6 Amplification and phage particle propagation

The ER2738 cells were incubated for 1 h at 37 ^{o}C and 90 rpm to allow the cells to be infected with the phage. 1 µL of the phage infected cells were plated onto LB plates (containing 100 µg/mL of carbenicillin) to titre the phage. The remaining cells were harvested by centrifuging at 3,000 x g for 5 min, resuspended in a smaller volume (50 µL) and spread onto LB-carb plate for overnight incubation at 37 ^{o}C. Next morning, colonies on the plates containing 1 µL of cells were counted and multiplied by 8,000 to determine the total number of cells per 8 mL culture while cells were scraped from the plate containing the remaining cells by adding 5 mL 2TY-carb (2TY media supplemented with 100 µg/mL carbenicillin) to the plate, scraped using a disposable plastic spreader and transferred to a clean 50 mL falcon tube, then cells remaining on plate were further scraped with 2 mL 2TY- carb. The absorbance at 600 nm of a 1:10 dilution of the cells were measured to determine the dilution required to obtain $A_{600\ nm}$ = 0.2 for an 8 mL culture (in 2TY media) in fresh 50 mL falcon tube. This culture was incubated at 37 ^{o}C and 230 rpm, for 1 h to

allow cells propagation, then infected with 0.32 µL of M13K07 helper phage and incubated at 37 ^{o}C and 90 rpm for 30 min. Phage infected cells were amplified by adding 16 µL Kanamycin (25 mg/mL) and incubated overnight at 25 ^{o}C, 170 rpm.

2.9.2.7 Phage precipitation

Phage-infected culture was centrifuged at 3,500 x g for 10 min and the phage-containing supernatant was transferred to a fresh 15 mL falcon tube. A 100 µL aliquot was removed for use in the second panning round, before proceeding to phage precipitation. For precipitation, 2 mL of PEG-NaCl precipitation solution (20 % (w/v) PEG 8000, 2.5M NaCl) was added to the remaining supernatant and incubated overnight at 4 ^{o}C. Phage cells were harvested by centrifugation at 4,816 x g for 30 min, the supernatant discarded and the pellet resuspended in 320 µL of TE, transferred into microcentrifuge tube and centrifuged at 16,000 x g for 10 min. The supernatant containing precipitated phage was transferred to a fresh microcentrifuge tube and stored at 4 ^{o}C for long term storage or mixed with 40 % glycerol and stored at -80 ^{o}C.

2.9.3 Biopanning round 2

A solution-phase panning with affinity bead capture was used in biopanning round 2. Here, the Affimer phage library was reacted with the biotinylated target conjugated to streptavidin magnetic bead in solution, followed by the magnetic separation of the target-phage complexes from the solution. After binding, the library sorting (binding, washing, and elution steps) was performed using a Kingfisher instrument (Thermo Scientific). Also during this panning round, the binders could be eluted directly (called the standard protocol) or the binders could be subjected to 24 h incubation with free target in solution to improve and identify high affinity binders (this is referred to as competitive elution protocol). Both protocols are described in this section.

2.9.3.1 ER2738 *E. coli* cells preparation

ER2738 *E. coli* cells were prepared as described in section 2.9.1

2.9.3.2 Pre-blocking steps and plates preparation

Before panning, the streptavidin beads and plates for the kingfisher Flex protocol were pre-blocked. (i) 20 µL of streptavidin beads (Dynabeads® MyOne™ Streptavidin T1) per target was blocked overnight with 100 µL 2 x blocking buffer at room temperature on a Stuart SB2 fixed speed rotator (20 rpm). The pre-blocked streptavidin beads were centrifuged at 800 x g for 1 min, immobilized on a magnet and the blocking buffer removed. The beads were resuspended in fresh 100 µL 2x blocking buffer per 20 µL of streptavidin beads. (ii) 1 well (per target) in a deep 96-well plate was pre-blocked with2x blocking buffer for 6 h at 37 ^{o}C. This deep well plate was used for panning. (iii) 1 well (per target) in either one (for competitive elution protocol) or two (for standard panning protocol) kingfisher 96 well plate with 300 µL per well of 2 x blocking buffer for 6 h at 37 ^{o}C. These plates were used for the elution steps.

2.9.3.3 Pre-panning the phage

In Pan 2, negative selection was used to select background phage that bind specifically to the streptavidin bead. This was carried out by pre-incubating the amplified phage from pan 1 with the streptavidin bead in the absence of target. The supernatant containing the pre-panned phage was then reacted with the target in a positive selection. For the pre-panning protocol, 125 µL of phage-containing supernatant from the first panning round was mixed with 125 µL of 2x Blocking Buffer (or 5 µL of purified phage with 245 µL of 2 x Blocking Buffer), 25 µL of the pre-blocked Streptavidin beads was then added to the mixture in an eppendorf Protein LoBind Tube and incubated for 1 h at room temperature on the rotator. After this, the mixture was centrifuged at 800 x g for 1 min and placed on the magnet. The supernatant containing the phage was transferred to a fresh tube and pre-panned the second time by adding fresh 25 µL of the pre-blocked streptavidin beads, incubated for 1 h at room temperature on the rotor.

2.9.3.4 Target preparation and binding

The target was bound to the streptavidin beads by adding 15 µL of biotinylated target to 200 µL of 2 x blocking buffer and 50 µL of the pre-blocked streptavidin

beads, and incubated for 1 h at room temperature on a Stuart SB2 rotator. In the meantime, buffers were removed from the pre-blocked deep well 96 plate and the pre-blocked elution plates. For standard panning, 100 µL aliquot of 0.2 M Glycine, pH 2.2 was added into one well (per target) of the 96 well plate, while 100 µL aliquot of freshly diluted trimethylamine (14 µL of trimethylamine diluted with 986 µL of PBS) was added into one well (per target) of the other 96 well plate. After incubation, the tube containing the biotinylated target was centrifuged at 800 x g for 1 min, supernatant discarded and the beads containing the biotinylated target were washed 3 times in 500 µL of 2 x blocking buffer by repeating the resuspension, centrifugation and removal of supernatant cycle. To the beads-containing target, the supernatant containing the pre-panned phage was added and resuspended. This was then transferred to the pre-blocked deep 96 well plate. To complete binding, washing and elution of phage binders, either standard phage elution protocol or competitive phage elution protocol was followed on the KingFisher flex automated machine.

2.9.3.5 Standard phage elution protocol

For standard phage elution, the KingFisher Flex was setup to run the protocol "Phage display pH elution" as outlined in Table 2.7.

Table 2.7: KingFisher Flex automated phage elution protocol

Protocol Step	Plate	Volume (µL)	Duration	Standard panning	Competitive elution
Binding	Plate: Binding Microtiter DW 96 plate	300		✓	✓
Wash 1	Plate: Wash 1 Microtiter DW 96 plate	950		✓	✓
Wash 2	Plate: Wash 2 Microtiter DW 96 plate	950		✓	✓
Wash 3	Plate: Wash 3 Microtiter DW 96 plate	950		✓	✓
Wash 4	Plate: Wash 4 Microtiter DW 96 plate	950		✓	✓
pH Elution	Plate: pH elution KingFisher 96 KF plate	100		✓	-
Triethylamine Elution	Plate: Triethylamine KingFisher 96 KF plate	100		✓	-
Particle Release into PBS	Plate: pH elution KingFisher 96 KF plate	100		-	✓

In the meantime, a fresh 8 mL culture of ER2738 cells was prepared by making a 1:15 dilution of the overnight culture, and incubated for 1 h at 37 ^{o}C and 230 rpm. For the protocol, phage was first eluted into glycine elution buffer for 10 min, and immediately after elution, the solution was neutralized with 15 µL of 1 M Tris-HCl, pH 9.1, mixed and added to the 8 mL aliquot of ER2738 cells. Then the protocol will elute in trimethylamine for 6 min. After elution, the solution was neutralized immediately with 50 µL of 1 M Tris-HCl, pH 7, mixed and added to the ER2738 cells. Amplification and precipitation of phage particles were carried out as described in sections 2.9.2.6 and 2.9.2.7 respectively.

2.9.3.6 Competitive phage elution protocol

To isolate binders with higher affinity, the KingFisher Flex was set up to run the protocol "phage display particle release comp". As seen in Table 2.7, the protocol released the beads into the 100 µL PBS which was then transferred into an Eppendorf protein Lobind tube. To this tube, 60 µL of 10 x blocking buffer, 60 µL of 80 % glycerol, 3 µL of Halt protease inhibitor cocktail (100X), 2.5 µg of non-biotinylated target (for toxin A screen, non-biotinylated toxin B was used to improve specificity and get rid of cross-reactivity binders, while for toxin B screen, non-biotinylated toxin A was used), and PBS to bring the total volume to 300 µL. The tube was incubated at 4 ^{o}C on the rotor for 24 h to allow for competition and the retention of high affinity binders which are not displaced in the presence of non-biotinylated target protein. 5 mL of 2TY was inoculated in a 15 mL falcon tube with a single clone of ER2738 *E. coli* cell from an agar plate and grown shaking overnight at 37 ^{o}C and 230 rpm. A fresh 8 mL culture of ER2738 cells was prepared by adding 500 µL of the overnight culture, and incubated for about 1 h at 37 ^{o}C and 230 rpm to give an $A_{600\,nm}$ of 0.6. After the 24 h of competitive binding, the tube was centrifuged at 800 x g for 1 min and placed on a magnet to collect the beads while the supernatant was discarded. The beads were washed 6 times with 500 µL of 2 x blocking buffer per wash, then resuspended in 100 µL of 0.2 M Glycine elution buffer for 10 min for phage elution. The tube was placed on the magnet and the eluted phage was transferred to fresh tube containing 15 µL of 1 M Tris-HCl, pH 9.1 for neutralization. Remaining phage bound to the beads were eluted by

resuspending the beads in 100 µL of diluted trimethylamine and incubated for 6 min. The tube was again placed on the magnet and the eluted phage was transferred to fresh tube containing 50 µL of 1 M Tris-HCl, pH7 for neutralisation. Both sets of eluted phages were used to infect the 8 mL culture of ER2738 cells. The cells were incubated for 1 h at 37 ^{o}C and 90 rpm. Amplification and precipitation of phage particles were carried out as described in sections 2.9.2.6 and 2.9.2.7 respectively.

2.9.4 Biopanning round 3

2.9.4.1 Preparation of streptavidin coated strips.

For each target, 6 wells of NeutrAvidin coated (HBC) 8-well strips (4 wells to be used for pre-panning the phage, 1 well for panning against the target, and 1 well as a negative control panning against the blank well) were blocked overnight with 300 µL per well of 2x Blocking Buffer at 37 ^{o}C without agitation. The wells were washed three times with 300 µL PBST per well on a plate washer (TECAN HydroFlex), and a 200 µL aliquot of 2 x blocking buffer was added into all wells except the first pre-panning well.

2.9.4.2 Pre-panning the phage

Extensive pre-panning steps were applied to reduce background binding of Affimer phage library to streptavidin coated strip surface, streptavidin and blocking buffer before panning of the Affimer library with the target protein. To the first pre-panning well, a 20 µL aliquot of 10 x blocking buffer, and 200 µL of phage containing supernatant from the second panning round (or 8 µL of purified phage and 212 µL of 2 x blocking buffer) were added, mixed and incubated on the shaker for 1 h at room temperature. Blocking buffer was removed from the 2nd pre-panning wells, then the phage containing buffer from pre-panning well 1 was transfer into pre-panning well 2 and incubated for 1 h. This process was repeated for the 3rd and 4th pre-panning wells.

2.9.4.3 Target preparation and binding to pre-panned phage

During the 4th round of pre-panning the phage, buffers were removed from the well to be used for panning against the target, a 100 µL aliquot of 2 x blocking

buffer and a 20 µL aliquot of the biotinylated target was added to the well. This was incubated for 1 h at room temperature on the vibrating platform shaker. Well containing the target and the negative control blank well were washed three times with 300 µL PBST. For panning, 100 µL per well of pre-panned phage (from the 4th pre-panning well) was added to the well containing the target and the negative control blank well. This was incubated for 45 min at room temperature on a vibrating platform shaker.

2.9.4.4 Standard phage elution protocol

In the meantime, two 5 mL fresh cultures of ER2738 cells were setup by diluting the overnight culture (1:15 dilution) and incubated at 37 ^{o}C, 230 rpm for 1 h. After incubation period for panning, panning wells were washed 27 times with 300 µL per well of PBST on the plate washer. Bound phages were eluted and added to the ER2738 cells as described previously. The ER2738 cells were incubated for 1 h at 37 ^{o}C, 90 rpm, then a range of volumes such as 0.1, 1, 10 and 100 µL were spread onto LB-carb plates. For the negative control, only 10 µL was spread onto LB-carb plate. All plates were incubated overnight at 37 ^{o}C.

2.9.4.5 Competitive phage elution protocol

After incubation period for panning, panning wells were washed 27 times with 300 µL per well of PBST on the plate washer. To these wells, 80 µL of 2 x blocking buffer, 20 µL of 80 % glycerol, 1 µL of Halt protease inhibitor cocktail (100 X), 5 µg of non-biotinylated target (for toxin A screen, non-biotinylated toxin B was used to improve specificity and get rid of cross-reactivity binders, while for toxin B screen, non-biotinylated toxin A was used) was added. The tube was incubated at 4 ^{o}C on the vibrating platform shaker for 24 h to allow for competition and the retention of high affinity binders which are not displaced in the presence of non-biotinylated target protein. In the meantime, 5 mL of 2TY–Tet was inoculated in a 15 mL falcon tube with a single clone of ER2738 *E. coli* cell from an agar plate and grown shaking overnight at 37 ^{o}C and 230 rpm. The next day, two 5 mL fresh cultures of ER2738 cells was setup by diluting the overnight culture (1:15 dilution) and incubated at 37^{o}C and 230 rpm for 1 h. Following competitive binding, panning wells were washed 27 times with 300 µL per well of PBST on the plate washer. Bound phages

were eluted and added to the ER2738 cells as described previously. The ER2738 cells were incubated for 1 h at 37 ^{o}C and 90 rpm, then a range of volumes such as 0.1, 1, 10 and 100 µL were spread onto LB- carb plates. For the negative control, only 10 µL was spread onto LB carb plate. All plates were incubated overnight at 37 ^{o}C.

2.10 Identification of specific Affimer phage

After the 3rd panning round, individual clones from the target plates were randomly picked, amplified and tested for binding and specificity against the target of interest.

2.10.1 Propagation and preparation of individually selected binders

A 200 µL aliquot per well of 2TY carb was added into a 96-well V-bottom deep well plate using a multichannel pipette. 32 colonies were randomly picked from the 3rd panning round of phage display and used to inoculate the wells (one colony per well). The culture was incubated overnight at 37 ^{o}C and 1,050 rpm in an incubating microplate shaker (Heidolph Incubator 1000 and Titramax 1000). The following morning, a fresh culture was prepared by inoculating fresh 200 µL 2TY carb media with 25 µL of the overnight culture, and incubated for 1 h at 37 ^{o}C, in the incubating microplate shaker at 1050 rpm. Into this, a 10 µL aliquot per well of 1:1000 dilution of M13K07 helper phage (titre ca. 10^{14}/mL) in 2TY-carb was added and incubated for 30 min at room temperature, 450 rpm. Then, 10 µL aliquot per well of 1:20 dilution of kanamycin stock in 2TY-carb was added to the phage infected cultures and incubated overnight at room temperature, 750 rpm in the incubating microplate shaker. A streptavidin coated plate to be used for the phage ELISA was prepared as explained in section 2.10.2. Next morning, the phage-infected culture was centrifuged at 3,500 x g for 10 min and the phage-containing supernatant was used directly for phage ELISA (as described in section 2.10.3).

2.10.2 Preparation of streptavidin-coated 96-well plates

5 mg of Lyophilized streptavidin (in 10 mM phosphate buffered saline, pH 7.4) was reconstituted with 1 mL of deionized water and aliquots were stored at -20 ^{o}C. A 1:2000 dilution of streptavidin at 5 mg/mL was prepared by adding 2.5 µL into 5 mL

of PBS and 50 µL per well was added to a F96 Maxisorp Nunc-Immuno Plate. The plate was covered with a sealable strip and incubated overnight at 4 ^{o}C or 2 h at room temperature. Streptavidin-coated plates could be stored at 4 ^{o}C for up to one week.

2.10.3 Phage ELISA

The binding affinities and specificity of each Affimer phage clones were characterised using the phage ELISA technique (Li *et al*., 1995). The streptavidin coated plate was blocked overnight with 200 µL per well of 2 x blocking buffer at 37 ^{o}C without agitation, after which the plate was washed once with 300 µL per well of PBST on the plate washer. Biotinylated targets were diluted 1: 1000 in 2 x blocking buffer, and 50 µL per well was added to the first 4 columns of the streptavidin coated 96 well plate, 50 µL of 2 x blocking buffer was added to well A5-A8 (blank wells) and 50 µL of diluted biotinylated cross-reactive controls were added to wells A9-A12. The layout for target immobilisation on the 96 well plate (well A1 to H12) is given below.

Table 2.8: Layout of target immobilisation for Phage ELISA

Target	A1-H4 (Biotinylated target)	A5-H8 (Blank control)	A9-H12 (Biotinylated cross-reactive control)	Phage
toxin A	toxin A	Blocking buffer	toxin B	toxin A Phage
toxin B	toxin B	Blocking buffer	toxin A	toxin B phage
rGDH *c. diff*	rGDH *C. diff*	Blocking buffer	BL21 (DE3) Star cell lysates	rGDH*C. diff* phage

The plate was incubated for 1 h at room temperature on a vibrating platform shaker to allow for immobilization, and then washed once with 300 µL of PBST on a plate washer. A 10 µL aliquot of 10 x blocking buffer was added to all wells then, 40 µL per well of phage containing supernatant phage was added so that each phage is tested against the target and the corresponding controls (e.g binder 1 was added to target well A1, blank well A5 and cross-reactive well A9). This was incubated for 1 h at room temperature on the shaker to allow binding to occur between the target and the phage. Unbound phage was washed off once with 300 µL per well

of PBST on a plate washer. HRP conjugated anti-Fd-Bacteriophage diluted 1:1000 in 2x blocking buffer was added (50 µL per well) and the plate incubated for 1 h at room temperature on the shaker. The plate was washed 10 x with the wash buffer, then 3.3'5.5'-tetramethylbenzidine (TMB) substrate (50 µL) was added and the plate was incubated at room temperature until a blue colour developed (at least for 3 min). The absorbance was read at 620 nm using an ELISA plate reader.

2.11 Identification of Affimer pair to target

2.11.1 Sandwich phage ELISA

Individual Affimer phagemid plasmid was transformed into competent ER2738 cells and single colonies from each transformation plate were grown in 100 µL of 2TY with 100 µg/mL of carbenicillin in a 96-deep well plate at 37 ^{o}C and 900 rpm for 6 h. A 25 µL aliquot of the culture was added to 200 µL of 2TY containing carbenicillin, then grown at 37 ^{o}C and 900 rpm for 1 h. Helper phage (10 µL of 10^{11}/mL) were added, followed by kanamycin to 25 µg/mL overnight and incubated at 25 ^{o}C and 450 rpm.

50 µL of the protein solution (1 µg/mL of biotinylated Affimer in 2 x Blocking Buffer) were incubated in streptavidin-coated wells (Pierce) for 1 h at room temperature with gentle agitation. The wells were blocked with 200 µL of 2 x blocking buffer overnight at 4 ^{o}C with gentle agitation. Wells were washed once with 300 µL PBST and 50 µL per well aliquot of targets (10 µg/mL) were added and incubated for 1 h at room temperature with gentle agitation. Then, wells were washed once with 300 µL PBST, 10 µL of 10 x blocking buffer and 40 µL of phage containing supernatant was added and incubated for 1 h. Following 12 x washing with 300 µL PBST, phage was detected by a 1:1000 dilution of HRP-conjugated anti-phage antibody (Seramun) for 1 h, visualised with 3,3´,5,5´-tetramethylbenzidine (TMB) (Seramun) and the absorbance measured at 620 nm.

2.11.2 Sandwich protein ELISA - using surface Adsorbed capture Affimer

50 µL of the protein solution (10 µg/mL of Affimer in 2 x Blocking Buffer) were incubated in Nunc Maxisorp wells overnight at 4 ^{o}C with gentle agitation. Next

morning, the wells were blocked with 200 µL of 2 x blocking buffer for 4 h at 37 ^{o}C with no agitation, wells were washed once with 300 µL PBST and 50 µL per well aliquot of targets (10 µg/mL) were added and incubated for 1 h at room temperature with gentle agitation. The wells were washed once with 300 µL PBST; Biotinylated binders at concentrations as high as 10 µg/mL in PBS-T containing 2 × blocking buffer were added to the wells and incubated for 1 h with shaking. Wells were washed three times in PBS-T, and streptavidin conjugated to HRP (Invitrogen) diluted 1:1000 in 50 µL PBS-T was added for 1 h. After washing, Affimer binding was visualised by addition of 50 µL TMB (Seramun) and the absorbance measured at 620 nm.

2.11.3 Sandwich protein ELISA - using double biotinylation

50 µL of the protein solution (1 µg/mL of biotinylated Affimer in 2 x Blocking Buffer) were incubated in streptavidin-coated wells (Pierce) for 1 h at room temperature with gentle agitation. The wells were blocked with 200 µL of 2 x blocking buffer containing 2 mM biotin for 6 h at 37 ^{o}C with no agitation, wells were washed once with 300 µL PBST and 50 µL per well aliquot of targets (10 µg/mL) were added and incubated for 1 h at room temperature with gentle agitation. The wells were washed once with 300 µL PBST; Biotinylated binders at concentrations as high as 10 µg/mL in PBS-T containing 2 × blocking buffer were added to the wells and incubated for 1 h with shaking. Wells were washed three times in PBS-T, and streptavidin conjugated to HRP (Invitrogen) diluted 1:1000 in 50 µL PBS-T was added for 1 h. After washing, Affimer binding was visualised by addition of 50 µL TMB (Seramun) and the absorbance measured at 620 nm.

2.11.4 Sandwich Phage display

50 µL of the capture Affimer protein (1 µg/mL of biotinylated Affimer in 2 x Blocking Buffer) were incubated in streptavidin- coated wells (Pierce) for 1 h at room temperature with gentle agitation. The wells were blocked with 200 µL of 2 x blocking buffer for 6 h at 37 ^{o}C with no agitation, then washed once with 300 µL PBST. 50 µL per well aliquot of targets (10 µg/mL) were added and incubated for 1 h at room temperature with gentle agitation. The wells were washed once with 300

µL PBST. Phage display screening is then carried out on captured target using protocols described in Section 2.9 and 2.10.

2.12 Characterisation of Affimers

2.12.1 ELISA analysis with purified Affimers

ELISA was initially used to determine whether the purified Affimer binders recognized native toxin A, toxin B and rGDH$_{C.\ diff}$. Equimolar concentrations of proteins (toxin A, toxin B, rGDH$_{C.\ diff}$) in PBS were absorbed onto Immuno 96 Microwell™ Nunc Maxisorp™ plate wells overnight at 4 °C. The next day, wells were blocked with 200 µL of 3 × blocking buffer at 37 °C for 4 h with no shaking. Biotinylated binders at concentrations of 10 µg/mL in PBS-T containing 2 × blocking buffer were added to the wells and incubated for 1 h with shaking. Wells were washed three times in PBS-T, and streptavidin conjugated to HRP (Invitrogen) diluted 1:1000 in 50 µL PBS-T was added for 1 h. After washing, Affimer binding was visualised by addition of 50 µL TMB (Seramun) and the absorbance measured at 620 nm.

2.12.2 Size exclusion chromatography

Size exclusion chromatography (SEC) also known as gel-filtration is a technique that can be used to measure the distribution of protein sizes such as aggregates, monomers and fragments in a sample (Synge and Tiselius, 1950, Hong *et al*., 2012). Seperation of molecules based on size is achieved using a porous resin stationary phase. Under isocratic flow, large molecules which cannot fit into the pores of the resin are eluted first, while small molecules retained for longer on the column are eluted last.

The AKTA Purifier system (GE Healthcare) was used to perform all gel exclusion experiments. Dialysed Affimers at 1 mg/mL were loaded on to a Superdex 200 10/300 GL column (GE Healthcare) with a flow rate of 0.5 mL min^{-1} using the dialysis buffer - PBS (pH 7.4), 150 mM NaCl. Absorbance of each Affimer was monitored at 220 nm (for peptide bond absorption), 260 nm (to probe for DNA contamination) and 280 nm (absorbance of aromatic amino acids). The molecular

mass of eluted proteins was estimated following calibration of the gel filtration column using protein standards (GE Healthcare).

2.12.3 Surface Plasmon Resonance

The binding kinetics for the interaction of Affimers and Toxin A or Toxin B was determined by surface plasmon resonance using a Biacore 2000 biosensor system (GE Healthcare). Affimers were biotinylated with the EZ-link Maleimide Biotin kit from Pierce and successfully immobilised on to the surface of streptavidin-coated CM5 sensor chips using an Affimer capture method. Briefly, a streptavidin-coated CM5 sensor chip was docked to the system and subjected to standard cleaning according to the manufacturer's recommendations. A total of 92 resonance units (RUs) of biotinylated toxin A or toxin B Affimers were immobilised. Affinity measurements were carried out in PBS, pH 7.4, 0.05 % Tween 20) at a flow rate of 25 µL/ min. A titration of toxin concentrations (1, 10, 100 nM) was injected in horizontal orientation. An empty flow cell served as control, and toxin A served as a cross-reactivity control for toxin B and vice versa. Association and dissociation were measured over time as changes in the refractive index. Data were analysed with BIAevaluation 4.1 software (GE Healthcare).

2.12.4 Thermostability and aggregation profile

The Avacta Optim® compatible micro-cuvette arrays (MCAs) were loaded with sixteen 10 µL samples of 1 mg/mL Affimer proteins, in PBS at pH 7.4. The Optim® 2000 was programmed to measure the intrinsic protein fluorescence which monitors protein tertiary structure and static light scattering is utilised to monitor protein aggregation at sample temperatures in the range 10 – 90 °C at steps of 1 °C. The Static light scattering (SLS) at 266nm absorbance and barycentric mean (BCM) of the spectra range 280 - 460 nm were measured. Data were collected, exported and analysed with OriginPro software.

2.12.5 Differential Scanning Calorimetry (DSC) analysis

DSC measurements were carried out on VP-DSC (Microcal). The Affimer scaffold mutants were dialysed into 1 x PBS at pH 7.4 and the dialysed Affimer proteins were prepared at a concentration of 1 mg/mL in 1 x PBS at pH 7.4. Protein samples

and buffer were degassed twice under vacuum for 10 min. The scanning was performed between 11 ^{o}C and 130 ^{o}C at a scan rate of 90 ^{o}C/h with a 15 min pre-scan equilibration. A buffer only scan was measured to calculate a baseline for integration. Aliquots of each sample were taken pre- and post DSC analysis.

2.12.6 Heat denaturation and centrifugation SDS-PAGE analysis

Affimer mutant variants samples were diluted to 0.5 mg/mL, heated to 50 ^{o}C for 5 min, and centrifuged for 15 min at 13,000 rpm on benched centrifuge prior. This was repeated four times with the temperature sequential increased by 10 ^{o}C ultimately reaching a final temperature of 90 ^{o}C. Samples were then analysed on a 15 % SDS Page gel as described in Section 2.7.6.

2.12.7 Biolayer Interferometry (BLitz)

The BLitz^{TM} (ForteBio) dip and read Streptavidin biosensors were used to as a quick yes/no binding interaction between purified Affimers and the target. Prior to use, streptavidin (SAX) biosensors were soaked in BLitz assay buffer (1 x PBS, pH 7.4) for at least 10 min. Biolayer interferometry assays using the advanced kinetics mode consisted of five steps, all performed in Blitz assay buffer: initial base line (30 s), loading (60 s), baseline (30 s), association (120 s) and dissociation (60 s). Neat Biotinylated Affimers were immobilized onto the streptavidin biosensor chip during the loading step, excess biotinylated Affimer were washed off during the baseline step. 10 µg/mL of non-biotinylated target was added to the sample holder during the association step. Controls used during the assay were: (i) empty streptavidin sensor (no biotinylated Affimer loaded), (ii) association with an unrelated protein (such as using toxin B as target for biotinylated toxin A Affimer to test for cross-reactivity), and (iii) association with BLitz assay buffer. These experiments indicated that empty sensors and sensors loaded with controls yielded similar values in binding experiments. Since this assay was for quick yes/no, the sensograms were not used to determine the binding kinetics of the binders.

2.12.8 Conjugation of Affimer to HRP

The Affimer binders were reduced on TCEP resin (as described in section 2.8.2.2) and buffer exchanged into the maleimide coupling buffer (100 mM sodium

phosphate, 5 mM EDTA, pH 7.2) on Zeba spin columns. The maleimide-HRP (Sigma) comes as a powder of 1:4 HRP: salt. Since the HRP contains 1-3 moles of maleimide per mole of HRP, therefore, from the molecular weights, a 1:1 mass ratio of HRP: Affimer gives a 3.5 x molar excess of Affimer. 0.25 mg of the Affimer in a 250 µL volume was mixed with ~1.25 mg of the maleimide–HRP powder and the reaction was incubated overnight at room temperature. A SuperDex 200 analytical SEC column was equilibrated in the coupling buffer (degassed, filtered) and the sample was loaded and flowed through the column at 0.5 mL/min. After 6 mL were flowed through, 0.5 mL fractions were collected over 30 mL, while absorbance was monitored at 280 nm and 403 nm. Fractions were analysed by SDS-PAGE and western blot with anti-His antibody.

2.13 Evaluation of Affimer for diagnostic purposes

2.13.1 Determination of the limit of detection

Individual Affimer phagemid plasmid was transformed into competent ER2738 cells. Single colonies from each transformation plate were grown in 100 µL of 2TY with 100 µg/mL of carbenicillin in a 96-deep well plate at 37 ^{o}C and 900 rpm for 6 h. A 25 µL aliquot of the culture was added to 200 µL of 2TY containing carbenicillin and grown at 37 ^{o}C and 900 rpm for 1 h. Helper phage (10 µL of 10^{11}/mL) were added, followed by kanamycin to 25 µg/mL overnight and incubated at 25 ^{o}C and 450 rpm.

50 µL of the protein solution (1 µg/mL of biotinylated Affimer in 2 x Blocking Buffer) were incubated in streptavidin-coated wells (Pierce) for 1 h at room temperature with gentle agitation. The wells were blocked with 200 µL of 2 x blocking buffer overnight at 4 ^{o}C with gentle agitation, then washed once with 300 µL PBST. A serial dilution of toxin A, toxin B full length, toxin B-fragment and Glutamate dehydrogenase was prepared from 2.5 µg/mL to 1.2 ng/mL in 2 x blocking buffer and 50 µL aliquot was added per well accordingly, and incubated for 1 h at room temperature with gentle agitation. The wells were washed once with 300 µL PBST, then 10 µL of 10 x blocking buffer and 40 µL of phage containing supernatant was added and incubated for 1 h. Following 12 times washing with 300 µL PBST, phages were detected by a 1:1000 dilution of HRP-conjugated anti-phage antibody

(Seramun) for 1 h, visualised with 3,3´,5,5´-tetramethylbenzidine (TMB) (Seramun) and measured at 620 nm.

2.13.2 Affimer-Antibody hybrid assay - Protocol 1

The protocols outlined in the Techlab's *C. diff*icile TOX A/B II (for toxin A and toxin B), and *C. diff* QUIK CHEK® (for GDH) package inserts were modified to use biotinylated Affimer immobilised on streptavidin coated Nunc Maxisorp plate as the capture.

Briefly, 50 µL of the protein solution (1 µg/mL of biotinylated Affimer in 2 x Blocking Buffer) were incubated in streptavidin-coated wells (Pierce) for 1 h at room temperature with gentle agitation. The wells were blocked with 200 µL of 2 x blocking buffer for 4 h at 37 ^{o}C with no agitation, wells were washed once with 300 µL PBST. A serial dilution of toxin A, toxin B or GDH was prepared at the desired concentration (from 50 ng/mL to 1.2 ng/mL) in 2 x blocking buffer and 50 µL aliquot was added per well and incubated for 1 h at room temperature with gentle agitation. The wells were washed once with 300 µL PBST, then the conjugate antibody (50 µL/well) was added and the reaction was incubated for 1 h at room temperature with gentle agitation. Wells were washed 6 times with 300 µL PBST, then 50 µL of TMB substrate was added and incubated for 10 min. The absorbance was measured at 620 nm.

2.13.3 Affimer-Antibody hybrid assay - Protocol 2

The only difference between protocol 1 and protocol 2 was that for protocol 2, the target and conjugate antibody are added to the wells simultaneously, and incubated 37 ^{o}C, 1,200 rpm for 20 min.

Chapter 3: Optimisation studies of the Affimer scaffold

3.1 Introduction

Scaffold proteins have been used in great applications such as diagnostics, imaging and therapeutics. Affimers are novel non-antibody binding proteins used for the selection of high affinity binders that are thermally stable and monomeric against various targets (section 1.6.4.5). Nevertheless, aggregation-prone binders such as Ataxin binders (JD-F12) have been selected which makes them less desirable in some applications. It was therefore necessary to develop an aggregation resistance scaffold, from which highly soluble, thermally stable binders would be selected.

There have been various studies on improving the solubility of aggregation-prone proteins. As early as 1994, Dale and his colleagues (Dale *et al*., 1994) were able to improve the solubility and achieved a 240-fold increased activity of trimethoprim resistant –type SI dihydrofolate reductase (DHFR) which had low expression level and >95 % of the protein accumulated in inclusion bodies. Improved solubility was achieved by mutating two neutral charge residues at the surface of the protein to negatively charged residues (N63E, N130D). Similarly, one of the notable differences between camelid antibodies and human antibodies is that camelid antibodies possess more hydrophilic and charged residues close to their CDR loops, which may explain why they are aggregation-resistant. Randomised loops and variable regions in proteins are usually solvent exposed. They contain hydrophobic residues for high affinity binding to targets, which have also affected the solubility and aggregation of such proteins. Perchiacca, *et al*. (2011) compared a wild-type (WT) antibody prone to aggregation upon unfolding with an aggregation resistant strain, HeL4. Comparison of the amino acid sequences highlighted the differences between the antibody strains in the CDR region. During experiments to substitute either WT CDR 1, 2 or 3 with the corresponding HeL4 CDR region, they subjected them to thermal denaturing and centrifugation. It was found that the WT variants existed only as soluble (non-aggregated) antibodies and were left in solution. Substitution of WT CDR1 with HeL4 CDR 1 was found to confer the aggregation resistance and further analysis of the amino acid sequence within the CDR loop 1 revealed that a negatively charged triad of DED in the middle of CDR loop 1 was responsible for conferring the aggregation resistance.

Based on these studies, A new variant of ataxin Affimer (JD-F12-DED) was constructed by the introduction of DED-4x residues before and after the VR1 and VR2 of the Affimer. Though it has been previously shown that this variant exists as a monomer in solution with improved solubility, the addition of the 12 new amino acid residues ((D-E-D)-4x) would extend the binder's length. Therefore, it was desirable to have a variant of JD-F12 that is highly soluble, aggregation-resistant without extending the length of the scaffold.

This chapter describes:

(i) The generation of mutants containing charged residues through point mutation, their expression, purification and characterisation in an attempt to develop an improved Affimer scaffold that is aggregation-resistant.

(ii) The design and optimisation of bacterial cystatin for potential library generation.

3.2 Selection of residues for mutations

To study the effect of introducing negatively charged amino acid (aspartate and glutamate) as point mutations within the scaffold, the following properties were desirable.

(i) The selected residues must be solvent exposed.

(ii) Mutation of residues flanking the variable loops should help to improve solubility by decreasing hydrophobic interactions.

(iii) Since the variable loops are usually rich in hydrophobic residues which mediate their high affinity binding to targets, the presence of charged residues close to the variable loops would help to break long stretches of potential hydrophobic interactions.

(iv) Residues selected should not be involved in target binding or crucial to maintain the conformational stability of the Affimer scaffold.

Based on the outlined features, careful analysis of the Affimer structure guided the selection of eight positions for point mutation rather than the addition of extra amino acids that extends the length of the protein.

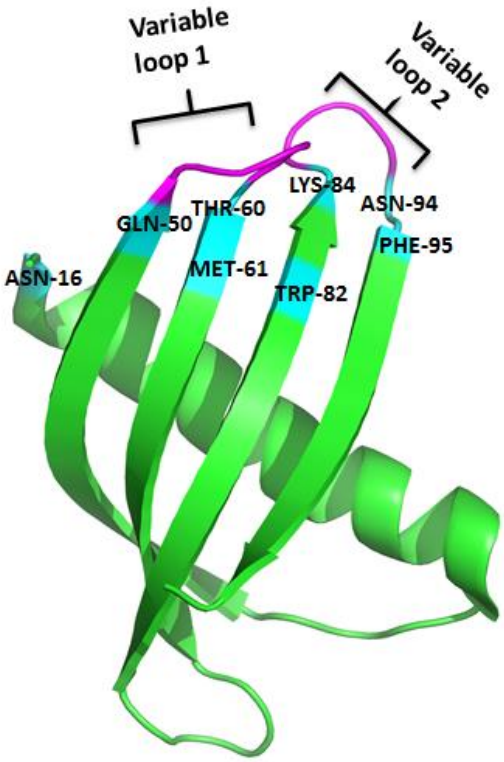

S/N	Mutation
1	N16D
2	Q50E
3	T60D
4	M61E
5	W82E
6	K84E
7	N94D
8	F95D

Figure 3.1: Structure of an Affimer. The eight residues selected for mutation are highlighted in cyan while variable loop 1 and 2 are shown in magenta. Drawn from PDB File ID no. 4N6U.

The eight residues selected for point mutation are shown in Figure 3.1. Asparagine 16 is located in the unstructured part of the scaffold at the N-terminal. Glutamine 50 is the amino acid before the variable loop 1; Threonine 60 and Methionine 61 are residues immediately after the variable loop 1. Tryptophan 82 and Lysine 84 are residues before variable loop 2, while Asparagine 94 and Phenylalanine 95 are residues after variable loop 2.

Effects of these mutations were studied using Ataxin binder (JD-F12) as the model protein, and three newly designed mutants containing varying amount of the mutation. JD-F12-3 contained 3 mutations - N16D, Q50E and N94D. JD-F12-5 contained 5 mutations N16D, Q50E, T60D, K84E and N94D. The last mutant, JD-F12-8 contained all 8 mutations N16D, Q50E, T60D, M61E, W82E, K84E, N94D and

F95D. Alongside these mutants, the previously tested variant JD-F12-(DED) 4x was studied.

3.3. Production of JD-F12 mutants

3.3.1 Cloning of JD-F12 Mutants.

The synthetic constructs of JD-F12 mutants (JD-F12-3, JD-F12-5 and JD-F12-8) ordered from GenScript, had their coding region cloned between NheI and PstI restriction sites in pUC57 cloning vector. The mutant genes were amplified by PCR using pUC57 forward and reverse primer (Table 2.3, Chapter 2). For subcloning, the fragments were ligated between the NheI and PstI restriction sites of linearised pDHis phagemid vector, amplified in pDHis vector using the pDHis forward and reverse primer. Then, the amplified fragments were digested using NheI/NotI endonucleases and then ligated into similarly digested pET11a expression vector.

Successful subcloning of Affimer mutants from pUC57 into pDHis phagemid vector was confirmed by DNA sequencing, as it can be seen in Figure 3.2a. The sequence contained pDHis DsbA signalling peptide sequence (shown in italics) and was ultimately subcloned into pET11a expression vector successfully (Figure 3.2b).

A. Sequence alignment after subcloning from pUC57 into pDHis vector

```
JD-F12      -----------------MASAATGVRAVPGNENSLEIEELARFAVDEHNKKENALLEFVR
JD-F12-3    MKKIWLALAGLVLAFSASASAATGVRAVPGNEDSLEIEELARFAVDEHNKKENALLEFVR
JD-F12-5    MKKIWLALAGLVLAFSASASAATGVRAVPGNEDSLEIEELARFAVDEHNKKENALLEFVR
JD-F12-8    MKKIWLALAGLVLAFSASASAATGVRAVPGNEDSLEIEELARFAVDEHNKKENALLEFVR
                            **************:**************************
JD-F12      VVKAKEQEVVVQRKMYTMYYLTLEAKDGGKKKLYEAKVWVKYKIAAKIMSNFKELQEFKP
JD-F12-3    VVKAKEEEVVVQRKMYTMYYLTLEAKDGGKKKLYEAKVWVKYKIAAKIMSDFKELQEFKP
JD-F12-5    VVKAKEEEVVVQRKMYDMYYLTLEAKDGGKKKLYEAKVWVEYKIAAKIMSDFKELQEFKP
JD-F12-8    VVKAKEEEVVVQRKMYDEYYLTLEAKDGGKKKLYEAKVEVEYKIAAKIMSDDKELQEFKP
            ******:*********  ******************** *:**********: ********
JD-F12      VGDAAAAHHH
JD-F12-3    VGDAAAAHHH
JD-F12-5    VGDAAAAHHH
JD-F12-8    VGDAAAAHHH
            **********
```

B. Sequence alignment after subcloning from pDHis into pet11a vector

```
ADHIRON-WT      MASAATGVRAVPGNENSLEIEELARFAVDEHNKKENALLEFVRVVKAKEQ-----VVAG--
JD-F12          MASAATGVRAVPGNENSLEIEELARFAVDEHNKKENALLEFVRVVKAKEQ---EVVVQRKM
JD-F12-DED      MASAATGVRAVPGNENSLEIEELARFAVDEHNKKENALLEFVRVVKAKEQDEDEVVVQRKM
JD-F12-3        MASAATGVRAVPGNEDSLEIEELARFAVDEHNKKENALLEFVRVVKAKEE---EVVVQRKM
JD-F12-5        MASAATGVRAVPGNEDSLEIEELARFAVDEHNKKENALLEFVRVVKAKEE---EVVVQRKM
JD-F12-8        MASAATGVRAVPGNEDSLEIEELARFAVDEHNKKENALLEFVRVVKAKEE---EVVVQRKM
                ***************:**********************************:   ********
ADHIRON-WT      ----TMYYLTLEAKDGGKKKLYEAKVWVK----PWE--------NFKELQEFKPVGDAAAAHHHH
JD-F12          Y---TMYYLTLEAKDGGKKKLYEAKVWVK---YKIAAKIMS---NFKELQEFKPVGDAAAAHHHH
JD-F12-DED      YDEDTMYYLTLEAKDGGKKKLYEAKVWVKDEDYKIAAKIMSDEDNFKELQEFKPVGDAAAAHHHH
JD-F12-3        Y---TMYYLTLEAKDGGKKKLYEAKVWVK---YKIAAKIMS---DFKELQEFKPVGDAAAAHHHH
JD-F12-5        Y---DMYYLTLEAKDGGKKKLYEAKVWVE---YKIAAKIMS---DFKELQEFKPVGDAAAAHHHH
JD-F12-8        Y---DEYYLTLEAKDGGKKKLYEAKVEVE---YKIAAKIMS---DDKELQEFKPVGDAAAAHHHH
```

C. Sequence Alignments of JD-F12 and its mutants

```
JD-F12          ASAATGVRAVPGNENSLEIEELARFAVDEHNKKENALLEFVRVVKAKEQ---EVVVQRKM
JD-F12-DED      ASAATGVRAVPGNENSLEIEELARFAVDEHNKKENALLEFVRVVKAKEQDEDEVVVQRKM
JD-F12-3        ASAATGVRAVPGNEDSLEIEELARFAVDEHNKKENALLEFVRVVKAKEE---EVVVQRKM
JD-F12-5        ASAATGVRAVPGNEDSLEIEELARFAVDEHNKKENALLEFVRVVKAKEE---EVVVQRKM
JD-F12-8        ASAATGVRAVPGNEDSLEIEELARFAVDEHNKKENALLEFVRVVKAKEE---EVVVQRKM
                **************:**********************************:   ********

JD-F12          Y---TMYYLTLEAKDGGKKKLYEAKVWVK---YKIAAKIMS---NFKELQ---
JD-F12-DED      YDEDTMYYLTLEAKDGGKKKLYEAKVWVKDEDYKIAAKIMSDEDNFKELQ---
JD-F12-3        Y---TMYYLTLEAKDGGKKKLYEAKVWVK---YKIAAKIMS---DFKELQ---
JD-F12-5        Y---DMYYLTLEAKDGGKKKLYEAKVWVE---YKIAAKIMS---DFKELQ---
JD-F12-8        Y---DEYYLTLEAKDGGKKKLYEAKVEVE---YKIAAKIMS---DDKELQ---
```

Figure 3.2: Sequence alignments of subcloned JD-F12 mutants. The DNA sequencing results for JD-F12 mutants (JD-F12-3, JD-F12-5 and JD-F12-8) are shown when subcloned into pDHis vector (a) pDHis vector with the DsbA signal peptide shown in italics, and (b) into pET11a expression vector, and aligned with the wild-type JD-F12 and the variant JD-F12-DED. Mutated residues are highlighted red.

3.3.2 Expression and purification of JD-F12 mutants

Once the sequence of mutants in pET11a expression vector had been confirmed, *E. coli* BL21 (DE3) Star cells were transformed with the recombinant pET11a expression vectors as described in Section 2.7.1. Recombinant JD-F12 and mutant proteins were produced in 50 mL LB cultures by IPTG induction under the control of the T7 lac promoter (Studier and Moffatt, 1986). After 6 h of induction, the cells

were harvested and pellets were lysed (Section 2.7.3) and aliquots of the total lysate, soluble fraction, column flow-through and elution obtained from the one-step Ni-NTA affinity chromatography, were analysed by 4-20 % SDS PAGE. The expression and purification profile of the empty Affimer scaffold (Affimer-WT) was used as the positive control. The results are shown in Figure 3.3.

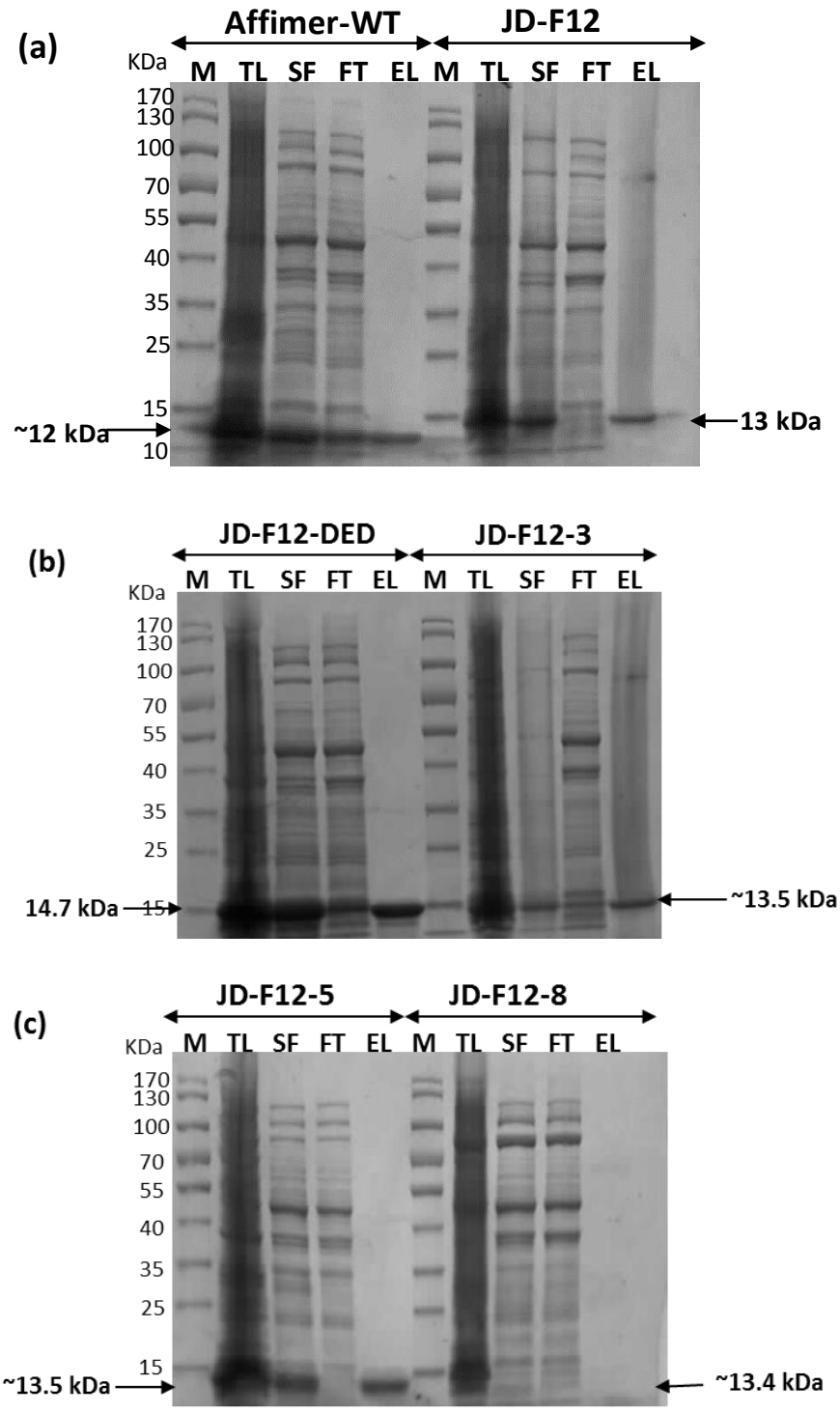

Figure 3.3: Purification profile of JD-F12 mutants analysed on 4-20% SDS-PAGE gels. Denaturing SDS-PAGE analysis of fractions obtained during purification steps for (a) Affimer wild-type and Ataxin binder JD-F12. (b) JD-F12-DED and JD-F12-3 (c) JD-F12-5 and JD-F12-8. The fractions analysed were total lysate - TL, soluble fraction - SF, flow-through - FT and the elution - EL. The expected protein bands are indicated with an arrow.

Lanes loaded with total lysate as expected have many bands but with the most prominent band migrating in the range of 10–15 kDa when compared to the protein markers. The prominent bands corresponded to the expected sizes of JD-F12 and mutant proteins, which confirmed their expression: JD-F12 (13. kDa); JD-F12-DED (14.7 kDa); JD-F12-3 (13.5 kDa); JD-F12-5 (13.5 kDa); JD-F12-8 (13.4 kDa). The mutation of W82E could account for the lower mass of JD-F12-8 compared to JD-F12-5. This prominent band was also observed in the lanes loaded with the solution fraction (SF) obtained after centrifugation of the cell lysate for all expressed protein except JD-F12-8. This suggest that the expressed JD-F12-8 was unstable and not properly folded and therefore accumulated in inclusion bodies.

The flow-through fraction (FT) obtained after incubating the soluble fraction with the Ni-NTA resin showed that most of the recombinant proteins were captured by the affinity resin. For Affimer WT and JD-F12-DED, the presence of a band corresponding to the expected molecular mass of recombinant protein in the flow through fraction indicated that the columns were saturated and some unbound recombinant proteins were eluted in the flow through. Specifically bound recombinant proteins were purified to homogeneity as seen as a single band on lanes loaded with the elution fraction (EL).

From the purification profile of the mutants, Figure 3.3 (b&c) showed that mutants and the controls were expressed and purified from the soluble fraction except JD-F12-8 which was therefore eliminated from further studies. The protein concentration of purified Affimer mutants that was calculated from their extinction coefficients are given in Table 3.1. JD-F12-8 does not contain any tryptophan residue. According to the ExPASy computational site, no tryptophan in the protein to be analysed could result in more than 10 % error in the computed extinction coefficient. This could explain why the extinction coefficient of JD-F12-8 was different from the other mutants.

Table 3.1: Biophysical properties of purified proteins from JD-F12 mutants. The isoelectric point pI, molecular masses, and the protein concentration of the mutants are given.

sample	pI	Molecular mass (Da)	Extinction coefficient	Abs 0.1% (=1g/l)	Elution $OD_{(280nm)}$	Protein concentration (mg/ml)
ADH-WT	6.75	12108.74	15470	1.278	2.212	1.69
JD-F12	9.05	13509.54	12950	0.959	2.019	2.06
JD-F12-DED	5.24	14672.43	12950	0.883	2.690	3.05
JD-F12-3	7.14	13512.50	12950	0.958	3.105	3.24
JD-F12-5	6.30	13527.42	12950	0.957	1.562	1.63
JD-F12-8	5.83	13436.16	7450	0.554	-0.09	-

3.4 Characterisation of Affimer mutants

The effect of the point mutations on the biophysical properties of JD-F12 was elucidated using several techniques such as size exclusion chromatography, differential Scanning calorimetry (DSC), Optim and gel electrophoresis. The results obtained from each technique is described below.

3.4.1 Effect of mutations on aggregation state of Affimers using size exclusion chromatography

Size exclusion chromatography is a useful technique that can be used to identify and characterise the oligomeric state of protein aggregates. In this study, it was important to determine the effect of the mutations introduced to JD-F12-3 and JD-F12-5 on the dimerisation of the JD-F12-wild-type.

From the results shown in Figure 3.4, the two dimeric peaks observed in JD-F12 (c) have been replaced by a single peak in JD-F12-3 (d) and JD-F12-5 (e). Comparing the chromatogram obtained from the mutants to the chromatogram for the wild-type Affimer scaffold (a) and JD-F12-DED (b) which are monomeric proteins and were used as controls in the experiment, the single peak observed in JD-F12-3 and JD-F12-5 are monomeric.

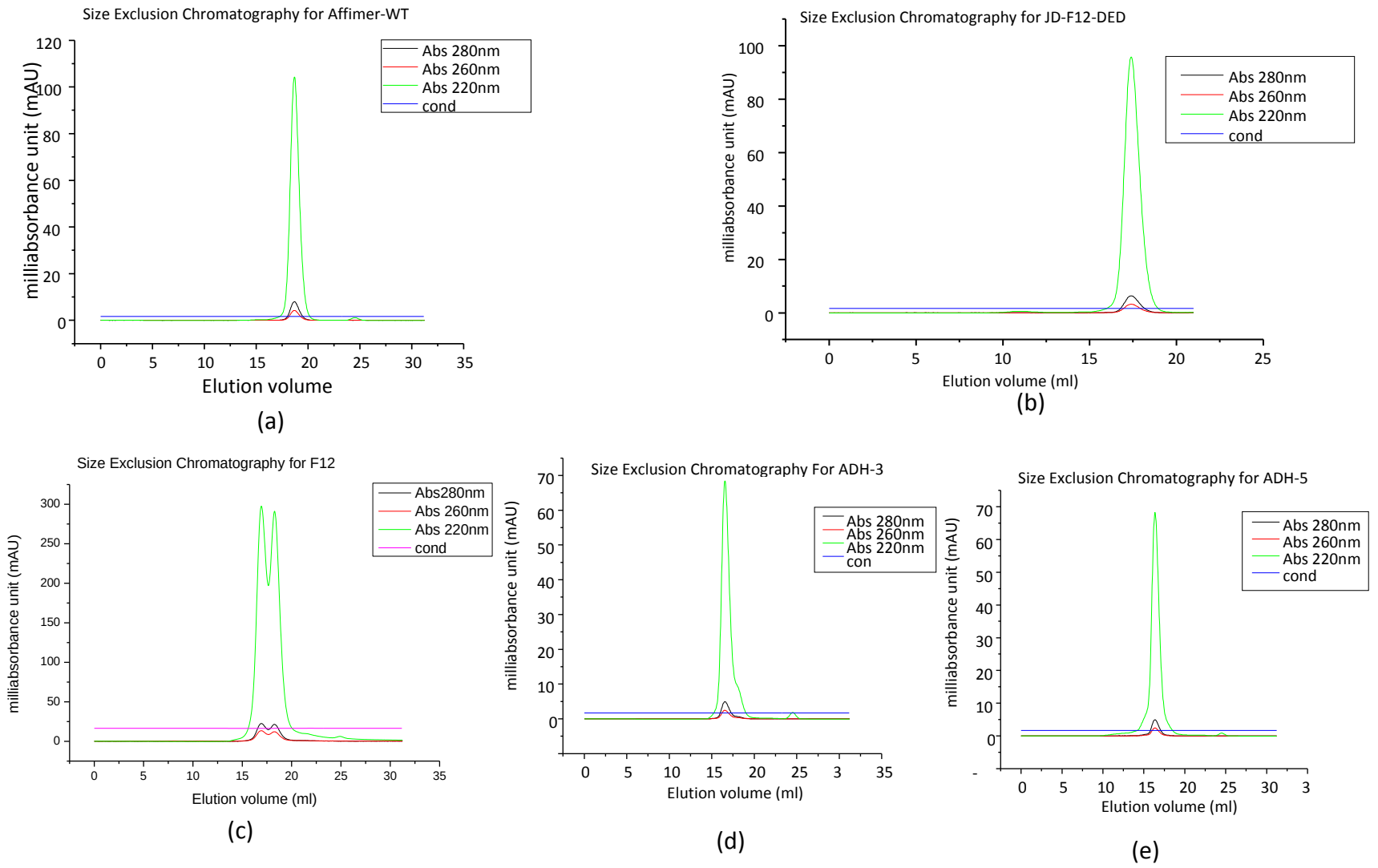

Figure 3.4: JD-F12 exist as a dimer. The Chromatograms of JD-F12 and its mutants (a-e) resolved in a Superdex 200 10/300 column.

3.4.2 SDS-PAGE used to determine thermostability

To study the influence of the mutants on the thermostability of the protein, SDS-PAGE was used as the first analytical technique to understand the effect of heat-induced denaturation of the protein in solution. As described in section 2.7.6.4, 9 aliquots of each mutant were prepared, heated at the desired temperature for 20 min, sedimented at 13,000 rpm for 5 min to remove aggregates while the soluble proteins were analysed on SDS-PAGE (Figure 3.5 (a-e)).

The Affimer scaffold which has been characterised as monomeric, thermally stable (up to 101 ^{o}C) with good expression yield (Tiede *et al*., 2012) was used as the positive control. From this experiment, Affimer-WT and JD-F12-DED were shown to be thermally stable up to 99 ^{o}C which is the highest heating temperature that could be obtained by the heating block. Figure 3.5a shows that JD-F12, JD-F12-3 and JD-F12-5 were thermally stable up to 70 ^{o}C, 70 ^{o}C and 60 ^{o}C respectively before reduction in soluble protein was observed.

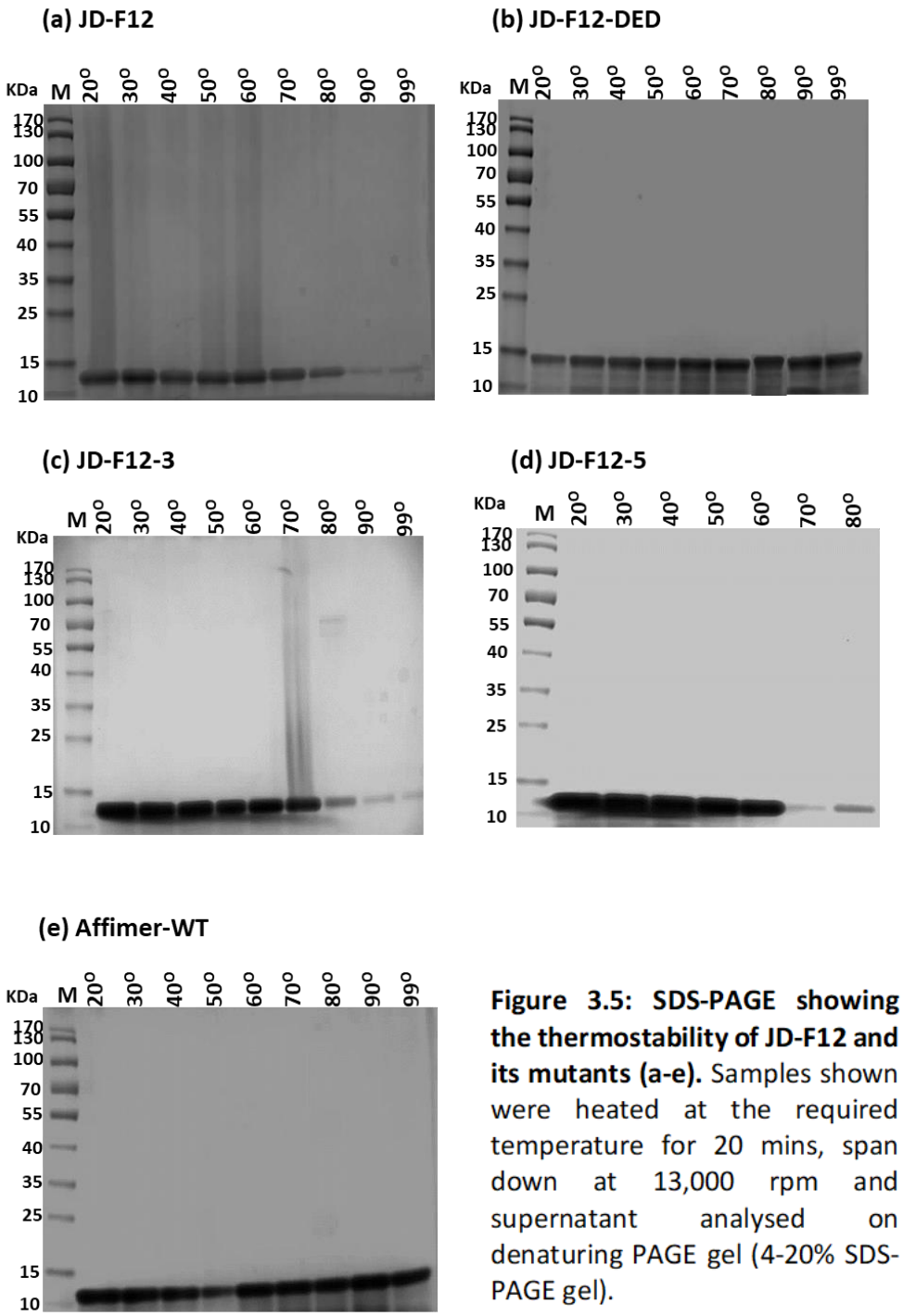

Figure 3.5: SDS-PAGE showing the thermostability of JD-F12 and its mutants (a-e). Samples shown were heated at the required temperature for 20 mins, span down at 13,000 rpm and supernatant analysed on denaturing PAGE gel (4-20% SDS-PAGE gel).

3.4.3 Effect of mutation on thermal stability of mutants using Differential Scanning Calorimetry (DSC)

Differential Scanning Calorimetry was used as a technique to understand the thermal unfolding properties of JD-F12 and its mutants. The Affimer-WT scaffold with a published Tm of 101^{o}C was used as the positive control to test instrument

performance. As shown in Figure 3.6a, the thermal stability of the Affimer scaffold gave a profile with a melting temperature of 101 °C as expected (Tiede *et al*., 2014).

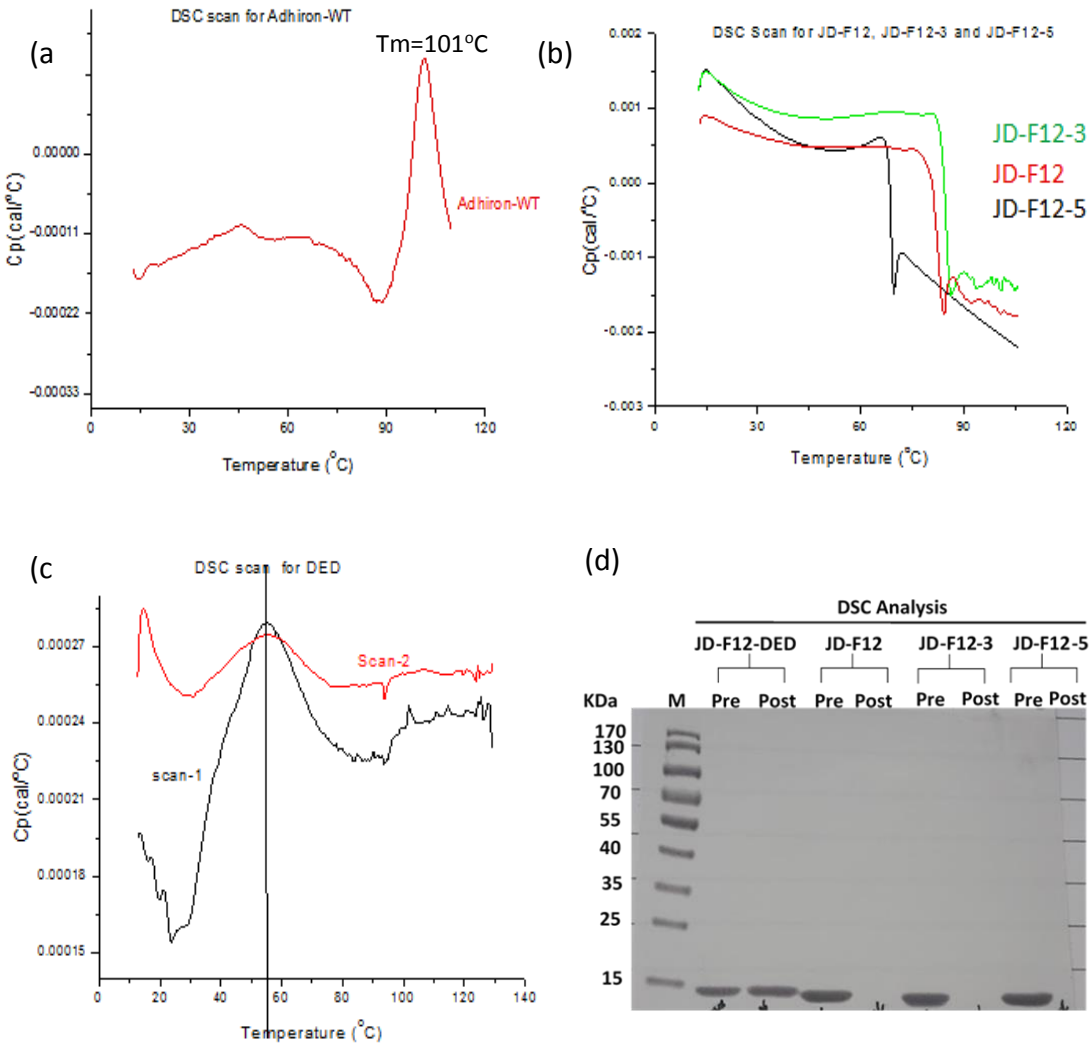

Figure 3.6: DSC results of JD-F12 mutants. 1 mg/mL of each sample was analysed using Microcal VPS DSC. (a) Determination of the melting temperature of Affimer scaffold (Tm= 101°C), (b) DSC scans for JD-F12 compared with the mutants JD-F12-3 and JD-F12-5. (c) DSC scans for JD-F12-DED (d) SDS-PAGE gel showing Pre- and Post DSC analysis of the mutants.

DSC thermogram confirmed that JD-F12, JD-F12-3 and JD-F12-5 (Figure 3.6b) aggregates upon thermal denaturation, which started to unfold at 75 °C, 83 °C and 66 °C respectively. The unfolding of these proteins was followed immediately by an irreversible exothermic aggregation step as indicated by the noisy data observed as unfolding starts. On the SDS PAGE gel (Figure 3.6d), the single protein band for JD-F12, JD-F12-3 and JD-F12-5 seen in the pre-DSC lane has aggregated and

precipitated out of solution in the post-DSC lane. Though the mutants aggregated, it is noteworthy that JD-F12-3 improves the thermal stability of JD-F12 by 8^{o}C before the onset of aggregation, while JD-F12-5 was less thermally stable by 9^{o}C.

The DSC scan for JD-F12-DED which is the variant with DED triad before/ after each variable loop has a Tm at 55 ^{o}C, the protein sample was soluble pre- and post DSC analysis (from the gel analysis). Scan 2 for JD-F12-DED was performed to test the reversibility of the DSC transitions of intact JD-F12-DED by consecutive heating of the same sample in the calorimeter. Although no aggregation was observed for scan 2, addition of 12 acidic residues have drastically reduced the transition temperature of JD-F12 by 20 ^{o}C.

3.4.4 Thermostability and aggregation profile of JD-F12 and its mutants

The Optim 2000® (Avacta) is a high throughput protein characterisation system that uses intrinsic fluorescence and the static light scattering technique simultaneously to measure the structural integrity of the proteins in solution. The results obtained from Optim analysis of JD-F12 and its mutants are given in Figure 3.7. This technique uses intrinsic fluorescence technology and static light scattering to test more than one parameter of a protein simultaneously including protein stability, unfolding transition temperature, and aggregation onset temperature (T_{agg}).

For protein unfolding characterisation, tryptophans were excited at 266 nm and its intrinsic fluorescence was measured at a range from 300 to 400 nm as the sample unfolds. The Barycentric mean (BCM) is the fluorescence intensity at a given wavelength (λ). Analysis of the BCM was performed using the Optim Analysis Software (Avacta Analytical). As seen in Figure 3.7a, JD-F12, JD-F12-3 and JD-F12-5 remained folded up to 78 ^{o}C, 74.5 ^{o}C, and 63 ^{o}C respectively. This shows that JD-F12 has the highest conformational stability, while JD-F12-3 is the most stable of the mutants. On the other hand, the melting temperature of JD-F12-DED showed an unfolding pattern from as early as 50 ^{o}C and increases with rise in temperature.

This indicates that of the mutants, JD-F12-DED has the lowest conformation stability.

The static light scattering (SLS) of the JD-F12 and its mutants was recorded as the samples were heated from 10 ^{o}C to 90 ^{o}C to detect the presence of aggregates. Importantly, the aggregation onset temperature (T_{agg}), which is the temperature at which a protein begins to aggregate, was identified for each sample. T_{agg} is usually accompanied by a significant increase in the static light scattering (SLS) intensity count. Figure 3.7b gives the thermogram for JD-F12 and its mutants. Data from the static light scattering generated automatically by the Optim software, showed that JD-F12-DED has the highest colloidal stability which means it does not aggregate when subjected to thermal denaturation up to 90 ^{o}C. For JD-F12, JD-F12-3 and JD-F12-5, the temperature for the onset of aggregation (T_{agg}) was calculated to be 58 ^{o}C, 62 ^{o}C, and 55 ^{o}C respectively. Comparison of the effects of JD-F12-3 and JD-F12-5 on the unfolding and aggregation profile of JD-F12 showed that JD-F12-3 delayed the onset of aggregation temperature and decreased the aggregation level of JD-F12. On the other hand, JD-F12-5 only decreased the aggregation level but has a lower T_{agg}.

Based on the results obtained so far on the biophysical characterisation of the effect of adding acidic residues at selected position by point mutation, the following were inferred and used as a guide for the next step of the study.

(i) JD-F12-3 containing the three mutations reduces the aggregation propensity of JD-F12. Therefore, it was used for subsequent studies.

(ii) JD-F12-DED has high colloidal stability, with no aggregation up to 90 ^{o}C, however from DSC data and protein unfolding data (Optim analysis), it unfolds at 55 ^{o}C.

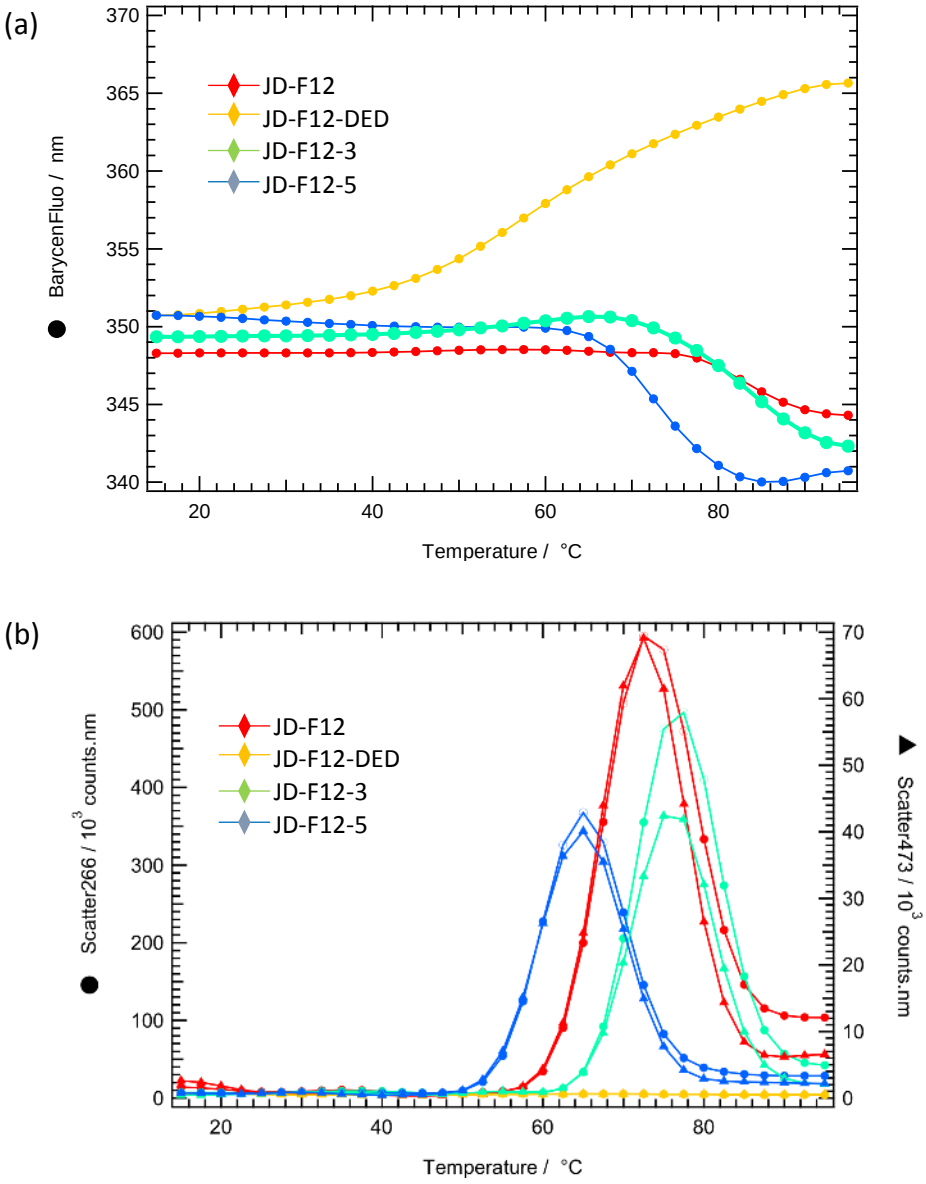

Figure 3.7: Thermal denaturation and aggregation analysis of JD-F12 and mutants. (a) Unfolding profile of the samples while (b) provides their thermal aggregation profile.

3.5 Mutational studies on other Affimer binders

This section describes the work carried out to understand the effect of each of the mutations introduced in JD-F12-3 and the impact of the three mutations on two other previously characterised aggregation-prone binders. Similarly, the impact of having one (D) or two acidic residues (either DD, or DE, or ED) before and after each loop was investigated.

3.5.1 Impact of each point mutation and their combination on aggregation resistance of JD-F12-3

The three mutations in JD-F12-3 (N16D, Q50E and N94D) were individually studied to determine if just one of the mutations was sufficient to improve aggregation resistance in JD-F12, or whether two or all three mutations are required.

Samuel Rhoden, as part of his undergraduate research project carried out mutagenesis, cloning, expression, purification and characterisation of the single and double mutants (Rhoden, 2015). The table below gives a comparison of the data for the single and double mutants to JD-F12-3 and JD-F12.

Table 3.2: Characterisation of Affimer and mutants for thermostability and aggregation profile. The the aggregation profile (T_{agg}) and the aggregation intensity count obtained from Optim analysis.

Mutants	SLS (T_{agg}) °C	Peak SLS intensity count
JD-F12	58	590 x 10^3
JD-F12 (N16D)	51	580 x 10^3
JD-F12 (Q50E)	49	582 x 10^3
JD-F12 (N16D, Q50E)	48	585 x 10^3
JD-F12-3 (N16D, Q50E, N94D)	62	350 x 10^3

The results obtained from DSC and SLS analysis of the mutant variants (Table 3.2) revealed that neither single mutations in JD-F12 (N16D or Q50E), nor the double mutations (N16D and Q50E) increased the aggregation resistance of the binder. So far, the mutant with all three mutations (JD-F12-3) was the best mutant that improves the melting temperature of the JD-F12 by 8 °C and delayed the onset of aggregation by 4 °C with 40.7 % reduction in aggregation intensity count.

3.5.2 mGFP21 and EGFR-H9-N

Based on these results, the next question in mind was “can N16D, Q50E, N94D mutations increase the aggregation-resistance in other binders?” Therefore, to answer this, the ability of three point mutations to decrease aggregation was

further studied using two more aggregation-prone binders, MGFP 21 and EGFR-H9-N and on the Affimer-WT scaffold.

3.5.2.1 Cloning of mGFP-21, EGFR-H9-N and Affimer-WT mutants

The mutant gene of MGFP-21, EGFR-H9-N and the Affimer-WT scaffold was designed to carry the N16D, Q50E and N94D mutations. These synthetic constructs were ordered from GenScript with their coding region cloned between NheI and NotI restriction sites in pUC57 cloning vector. The mutant genes were amplified by PCR using pUC57 forward and reverse primer (Table 2.3, Chapter 2) then treated with DpnI enzyme to get rid of methylated plasmid template. The amplified fragments were digested using NheI/NotI endonucleases then ligated into similarly digested pET11a expression vector.

Successful subcloning of Affimer mutants from pUC57 into pET11a vector was confirmed by DNA sequencing, as it can be seen in Figure 3.8.

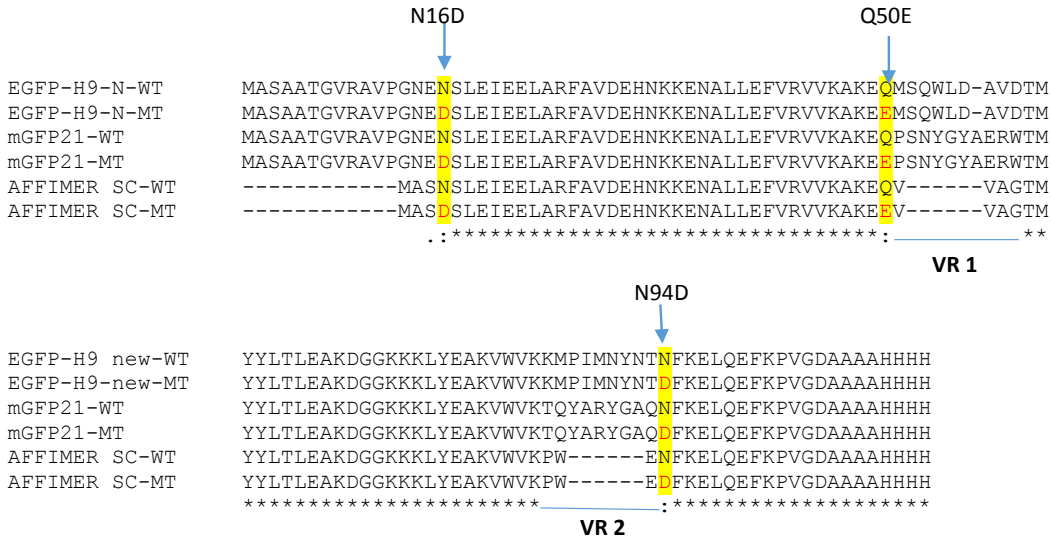

Figure 3.8: Sequence alignment for EGFR-H9-N, mGFP-21 and Affimer-scaffold. The alignment of the wild-type (WT) and the mutant (MT) is shown, with the mutated residues highlighted and the variable region 1 (VR1) and 2 (VR2) underlined.

3.5.2.2 Purification and characterisation of mGFP-21, EGFR-H9-N and Affimer-WT mutants

Expression by IPTG induction of the wild-type and mutant variants of mGFP-21, EGFR-H9-N and Affimer scaffold called (MG, EG, and SC respectively) were carried

out as previously described in Section 3.3.2. Cell pellets obtained from the 50 mL culture samples were lysed and the His-tagged variants were purified using Ni-NTA affinity chromatography. Analysis of the purity of the eluted proteins is given in Figure 3.9a which shows >99 % purity. Purified protein samples from JD-F12 variants (DE, DD, ED, and D) described in Section 3.5.3 were analysed alongside on the gel, and the proteins were used without further purification step in other experiments.

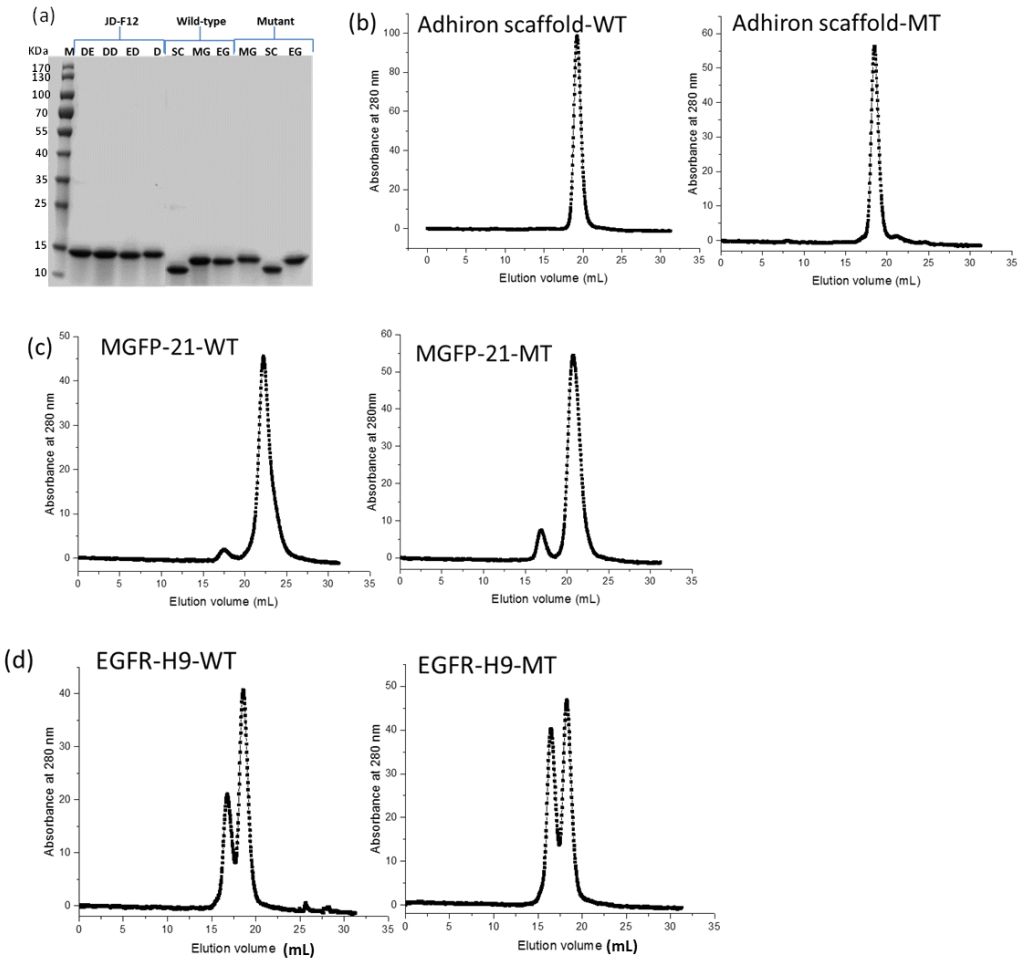

Figure 3.9: Analysis of purified variants. (a) The purified proteins of the wild-type and the mutants were analysed on 4-20% SDS-PAGE. SC, MG and EG are the short forms for Affimer-scaffold, MGFP-21 and EGFR-H9-N respectively. The size exclusion analysis of each protein WT and mutant is shown in (b,c,d) respectively.

Size exclusion chromatography: 1 mg/mL of dialysed Affimer-scaffold, EGFR-H9-N, mGFP21 wild-type binders and their corresponding mutants were analysed on sepharose 200 10/300 column to investigate if the presence of N16D, Q50E and

N94D mutations has effectively decreased aggregation. The results are presented in Figure 3.9(b-d). Mutant of the Affimer scaffold possessed only a major peak corresponding to the monomeric peak of the wild-type as expected. For mGFP21 (3.9c) and EGFR-H9-N (3.9d), the chromatogram of the mutants indicated the presence of two peaks which corresponds to the monomeric and dimeric peaks. This suggested that the mutations in mGFP21 and EGFR-H9-N did not eliminate aggregation.

Thermal unfolding properties of the binders: To further characterise the impact of the mutations, the intrinsic flourescence properties of each protein was used to probe its unfolding and light scattering properties during thermal denaturation. From Figure 3.10a, 3.11, and 3.12a, a common trend was observed across all the mutants as their thermograms followed the same pattern as the wild-types. These results suggest that the presence of more acidic residue made the buried tryptophan become more exposed in the mutants.

Aggregation profile of the binders: A more pronounced effect of the mutants was observed when static light scattering was used to detect the aggregation intensity of each protein. For EGFR-H9-N, the aggregation intensity count was reduced from 75 x 10^3 in the wild-type to 28 x 10^3 in the mutant which gives a 63 % reduction in aggregation. Similarly, the aggregation intensity count for mGFP21 was reduced from 62 x 10^3 (wild-type) to 35 x 10^3 (mutant), resulting in a 44 % reduction in aggregation. For both Affimer scaffold wild-type and mutant, no aggregation was observed as the intensity count across the temperture gradient was < 1 x 10^3.

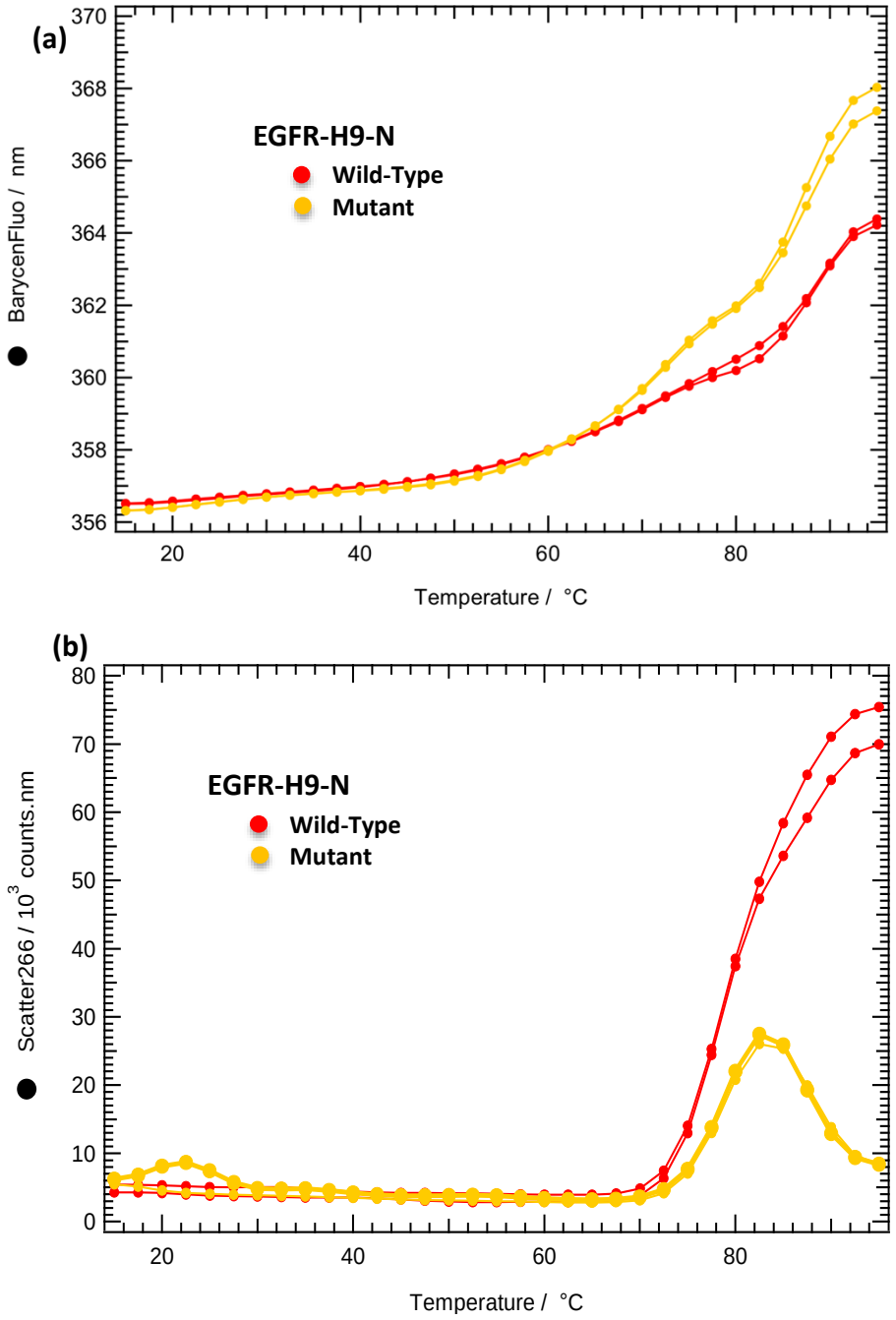

Figure 3.10: Optim Analysis for EGFR-H9-N. The effect of mutation N16D, Q50E and N94D on the thermal unfolding properties and aggregation profile of EGFR-H9-N is given in (a) and (b) respectively. Wild-type plot given is in (red) while mutant in (orange).

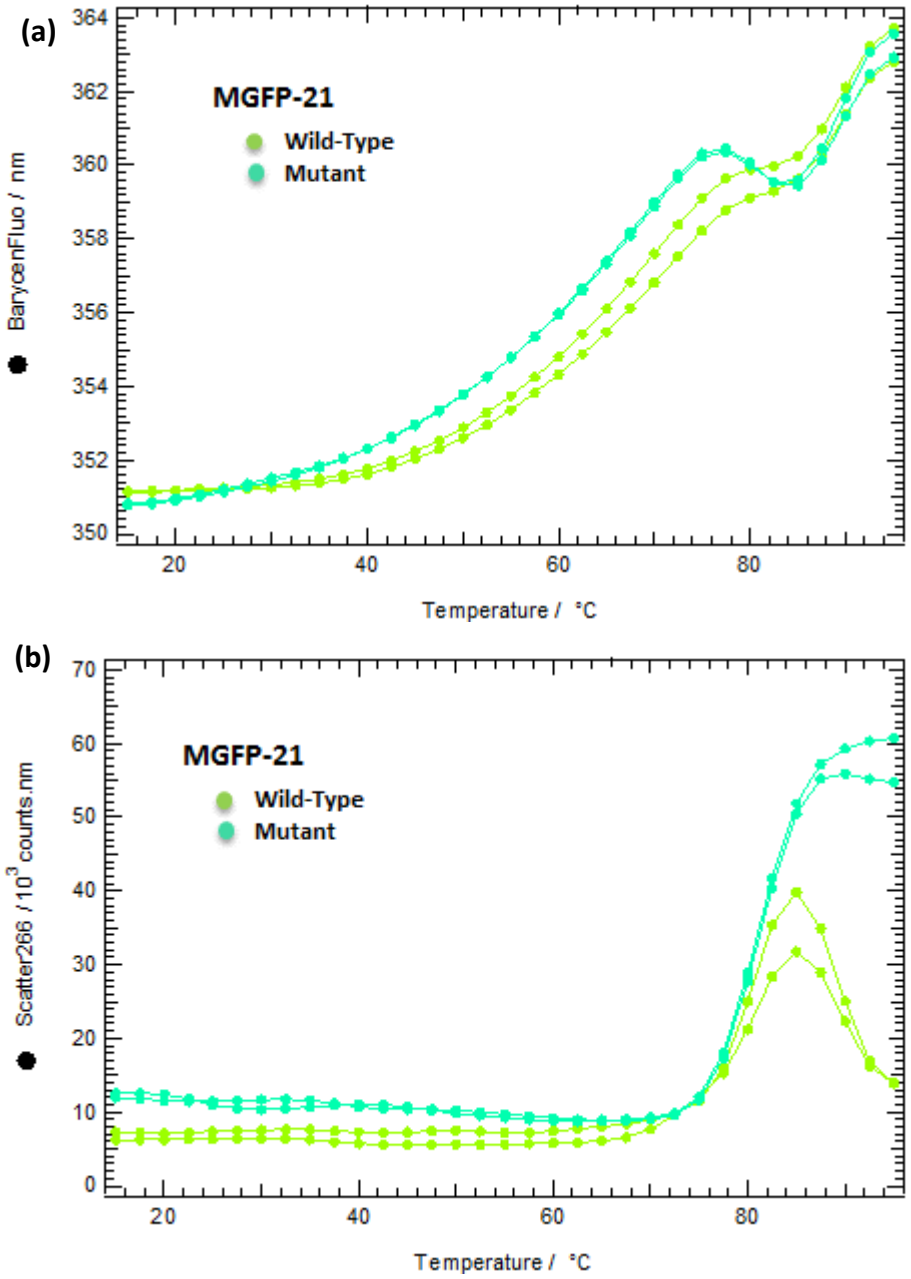

Figure 3.11: Optim Analysis for mGFP-21. The effect of mutation N16D, Q50E and N94D on the thermal unfolding properties and aggregation profile of mGFP-21 is given in (a) and (b) respectively. Wild-type plot is given in (light green) while mutant in (cyan).

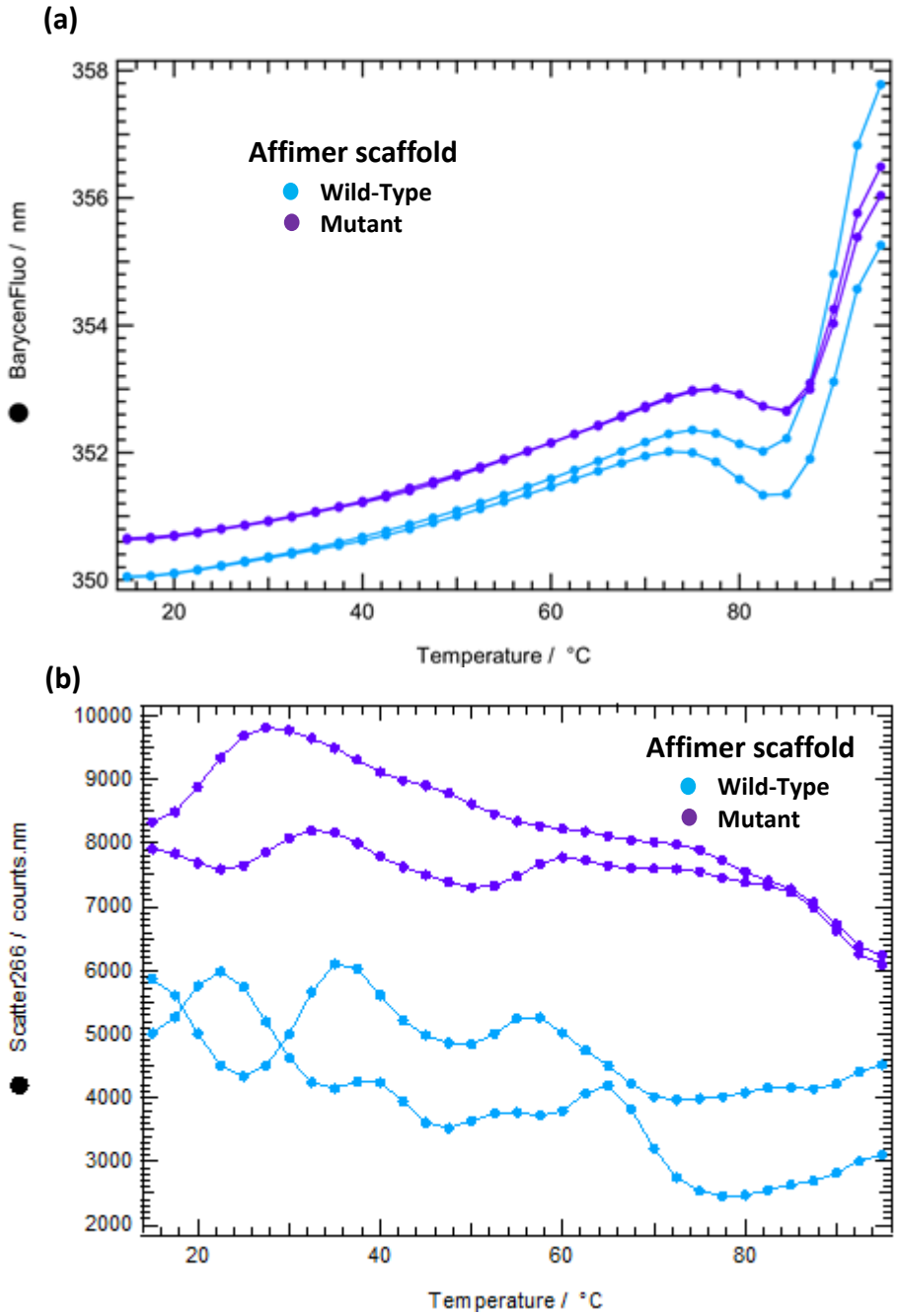

Figure 3.12: Optim Analysis for Affimer scaffold. The effect of mutation N16D, Q50E and N94D on the thermal unfolding properties and aggregation profile of Affimer scaffold is given in (a) and (b) respectively. Wildtype plot is given in (blue) while mutant in (purple).

3.5.3 Effect of adding D/DD/ ED/ E residues before each loop

From section 3.4 and 3.5 above, the data presented showed that the three point mutations N16D, Q50E and N16D, have the potential of decreasing but not eliminating aggregation propensity in the binders. Therefore, it is not a generic approach to stability enhancement. However, addition of DED residues before and after VR1 and VR2 showed complete elimination of aggregation in JD-F12. Taking these together, this section describes the characterisation of new JD-F12 variants with either D or DD or ED or DE, before and after VR1 and VR2.

The cloning, expression and purification of JD-F12-D, JD-F12-DD, JD-F12-ED and JD-F12-DE was carried out just as described in section 3.5.2.1 and 3.5.2.2 respectively. The alignment of the variants is given below with the added residues highlighted in red (Figure 3.13). All variants were easily expressed, purified and the analysis of the purified proteins is presented in Figure 3.9a.

```
JD-F12-D      --NENSLEIEELARFAVDEHNKKENALLEFVRVVKAKEQD--EVVVQRKMYD--TMYYLT
JD-F12-DD     --NENSLEIEELARFAVDEHNKKENALLEFVRVVKAKEQDD-EVVVQRKMYDD-TMYYLT
JD-F12-ED     --NENSLEIEELARFAVDEHNKKENALLEFVRVVKAKEQED-EVVVQRKMYED-TMYYLT
JD-F12-DE     --NENSLEIEELARFAVDEHNKKENALLEFVRVVKAKEQDE-EVVVQRKMYDE-TMYYLT
JD-F12-DED    --NENSLEIEELARFAVDEHNKKENALLEFVRVVKAKEQDEDEVVVQRKMYDEDTMYYLT
                ************************************   *********   ******

JD-F12-D      LEAKDGGKKKLYEAKVWVKD--YKIAAKIMSD--NFKELQ---
JD-F12-DD     LEAKDGGKKKLYEAKVWVKDD-YKIAAKIMSDD-NFKELQ---
JD-F12-ED     LEAKDGGKKKLYEAKVWVKED-YKIAAKIMSED-NFKELQ---
JD-F12-DE     LEAKDGGKKKLYEAKVWVKDE-YKIAAKIMSDE-NFKELQ---
JD-F12-DED    LEAKDGGKKKLYEAKVWVKDEDYKIAAKIMSDEDNFKELQ---
              ******************   *********   ******
```

Figure 3.13: Sequence alignments of JD-F12 variants. The variants of JD-F12 were successfully subcloned into pET11 expression vector. The added residues for each variant are highlighted in red.

Optim static light scattering analysis was used to probe the aggregation profile of each variant. As described in section 3.4.4, samples used for analysis were dialysed into PBS (pH7.4) and prepared to a final concentration of 1 mg/mL. For comparison, fresh aliquot of Affimer scaffold, JD-F12, JD-F12-3, JD-F12-DED, JD-F12-D, JD-F12-DD, JD-F12-ED and JD-F12-DE were analysed at the same time. Figure 3.14 and Table 3.3 presents the results obtained.

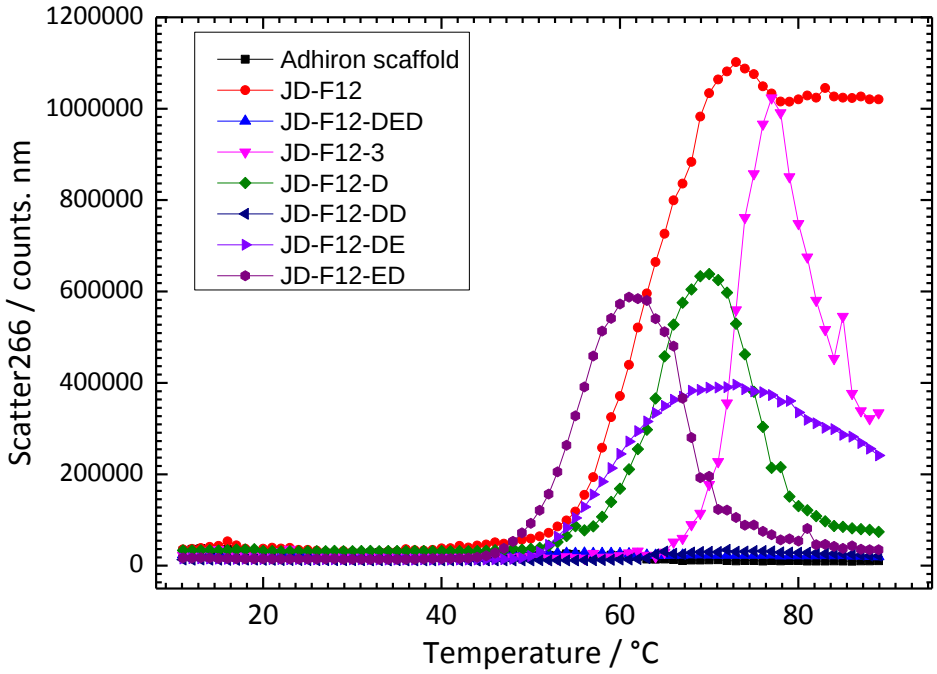

Figure 3.14: Analysis of the aggregation profile of all JD-F12 variants. The effect of adding residues D/ DD/ DE / ED were monitored on the aggregation profile of the variants alongside DED, JD-F12-3, JD-F12 and the Affimer scaffold as controls.

Table 3.3: Aggregation parameters for JD-F12 variants

Mutants	SLS (Tagg) °C	Aggregation intensity count (counts. nm)
Affimer scaffold	No aggregation	Negligible
JD-F12	58	$1.12x10^6$
JD-F12-3	62	$1.0x10^6$
JD-F12 -D	56	$6.38x\ 10^5$
JD-F12- DD	No aggregation	Negligible
JD-F12- ED	48	$5.88x10^5$
JD-F12- DE	54	$3.96x10^5$
JD-F12-DED	No aggregation	Negligible

This result gives a complete analysis of the effect of each variant. JD-F12 which is the wildtype has the highest aggregation count as expected. The presence of the three-point mutation D-E-D in JD-F12-3 delayed the onset of aggregation of JD-F12 by >10°C but did not eliminate the aggregation intensity observed in JD-F12. Addition of aspartic acid residue before and after each loop for JD-F12-D reduced

the aggregation of JD-F12 by 50 %. Interestingly, two aspartic acid before and after each loop in JD-F12-DD completely eliminated aggregation as seen in JD-F12-DED and the Affimer scaffold, which remained monomeric across the temperature gradient. Overall, JD-F12-DD looks promising and could be taken forward for future work.

3.6 Bacterial cystatin

The Cystatin superfamily comprises cysteine protease inhibitors such as stefins, cystatin and kininogens that play key roles in regulating protein degradation processes (Kordiš *et al*., 2009). Structural analysis of stefin and cystatin revealed three conserved regions that are important for their inhibitory properties. These are the N-terminal sequences, the highly conserved QXVXG motif, which forms the VR1, and the PW motif, which formed the VR2 (Kordiš *et al*., 2009). Besides its inhibitory properties, characterisation of human Stefin A showed it is a monomeric, single-domain protein of 98 amino acid residues, which made it a potential candidate for developing a scaffold protein (Woodman *et al*., 2005). In 2011, an engineered protein scaffold from Stefin A was developed (Stadler *et al*., 2011). Similarly, the novel non-antibody binding protein called Affimer used in this thesis was engineered and developed from the consensus sequences of plant cystatins (Tiede *et al*., 2014). To date, little is known about microbial cystatin in (Kordiš *et al*., 2009). Therefore, it was of interest to examine the extent to which bacterial cystatins exist and whether these might also provide a useful scaffold protein for potential library generation. This section describes the design and the expression optimization steps for bacteria cystatin.

3.6.1 Consensus sequence framework for bacterial cystatin protein design

To design the consensus bacterial cystatin gene, a tblastn search of the GenBank database was performed using PCA-1 (*Pectobacterium carotovorum*; CP009678.1) and VCO (Vibrio cholera; AJFN02000019.1) protein sequences as the search probes which yielded 66 sequences. 58 sequences (>80 %) were from bacteria while the remaining 8 sequences have origins other than bacteria such as from fungi,

parasitic flatworm, pacific oyster, orchard grass, sheep and western clawed frog. No definite function has been attributed or known about bacterial cystatin, thus it is mainly a hypothetical protein. Each of the sequences identified was in turn used as an input query sequence to ensure all potential bacterial cystatin was retrieved. The coding sequences obtained were translated and aligned using the program MultAlin (Corpet, 1988). The output of the multiple alignment is shown in LOGOS (Crooks *et al*., 2004) in Figure 3.15.

The final bacterial cystatin consensus called BacCysCon 9.4 was manually checked to ensure that each residue in the consensus was the most frequent residue for that position. Alignment of the bacterial csytatin consensus sequence with the Affimer revealed only 16 % sequence similarity. Using ExpaSy protoparam, the physical parameters of Bacterial cystatin (BacCysCon) was computed. Bacterial cystatin contained 87 residues and a pI of 9.4 which was high compared to Affimer scaffold (92 residues) with a pI of 5.84. The high pI of BacCysCon was due to the high number of lysines but relative low abundance of acidic residues. Essentially Affimer has more lysines, but also a greater number of acidic residues than of lysines and so have a lower pI. Therefore, seven residues coloured red as outlined in Figure 3.16 were substituted in the Bacterial cystatin (pI-9.4) to obtain Bacterial cystatin (pI-6.0), by increasing the number of acidic residues at positions where there is significant variation in residue. Four threonine residues were substituted with two uncharged polar residue serine and two negatively charged glutamate. Two lysines were replaced, one with alanine and the other with glutamate. One leucine was replaced with glycine.

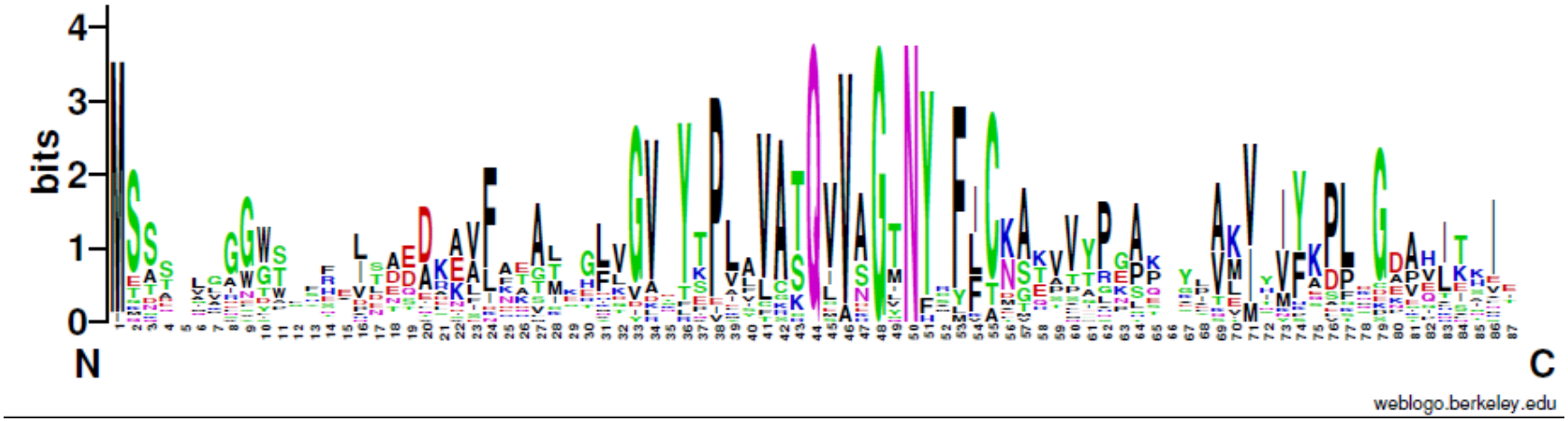

Figure 3.15 Weblogo showing the conserved sequences in bacterial cystatin (Crooks *et al*., 2004**).** The percentage abundance of each amino acid in the sequences is represented by the height of each residue. Negatively charged residues are represented in red, each logo consists of stacks of symbols, one stack for each position in the sequence. The overall height of the stack indicates the sequence conservation at that position, while the height of symbols within the stack indicates the relative frequency of each amino or nucleic acid at that position. Polar amino acids (G, S, T, Y, C, Q, N) show as green, basic (K, R, H) blue, acidic (D, E) red, and hydrophobic (A, V, L, I, P, W, F, M) amino acids as black.

```
BacCysCon9.4 MASTQLLGG WTAFHELTAE DKAVFKTALK GLVGVTYTPL AVAT-QVVAG TNYSFITKAT VVYPGAKVYL AKVYIYKPLK GDAHITKIE
BacCysCon6.0 MASTQLGGG WSAFHELSAE DKAVFAEALK GLVGVEYTPL AVAT-QVVAG TNYSFITKAT VVYPGAKVYL AKVYIYKPLE GDAHITKIE
```

Figure 3.16: Sequences of Bacterial cystatin consensus. The amino acid residues in the consensus sequence with a description of the effect of amino acid mutations on the pI of Bacterial Cystatin. The substituted residues in bacterial cystatin consensus 9.4 and 6.0 are shown in red.

The synthetic bacterial cystatin construct was designed to contain a NcoI restriction site at the N terminal, the coding sequence of the protein, a linker sequence, StrepTagII sequence for purification, two stop codons and XhoI restriction site at the C terminal. An *E. coli* codon optimised gene was synthesized by GenScript in pUC57 plasmid DNA cloning vector.

3.6.2 Subcloning of Bacterial cystatin from pUC57 into pET28c expression vector

The bacterial cystatin construct from GenScript (BCc9.4 and BCc6.0) arrived in the cloning vector pUC57. For further studies and characterisation of bacterial cystatin to be carried out, the bacterial cystatin was subcloned into pET28c expression vector.

Aliquots from purified cloning vector (pUC57) containing the bacterial cystatin coding regions (BCc9.4 and BCc6.0) alongside purified expression vector pET28c and 1 kb DNA ladder were analysed on 1 % (w/v) agarose gel (Figure 3.17a). The bands show purified plasmids migrating at the expected positions of 2.3Kbp. Analysis of double restriction digestion of pUC57-BCc9.4 and BCc6.0 on a 2 % (w/v) agarose gel electrophoresis is given in Figure 3.17b. Digestion of pUC57-BCc with NcoI and XhoI restriction enzymes gave two clear bands on the gel. The top bands correspond to the cleaved pUC57 vector (2 kbp), while the lower bands migrating at 317 bp correspond to the BCc insert (BCc9.4 and BCc6.0 respectively). These inserts were successfully ligated between the NcoI and XhoI restriction site of linearised pET28c expression vector. Colony PCR was performed for 3 different colonies from pET28c-BCc9.4 and pET28c-6.0 plates respectively using T7P and T7F primers to amplify the region between T7 promoter and T7 terminator to identify clones with insert. The analysis of the colony PCR products of transformed XL-10 Gold *E. coli* cells with pET28c-BCc9.4/BCc6.0 on 1 % (w/v) agarose gel electrophoresis is presented in (Figure 3.17c). Positive control (undigested vector) migrated at 309 bp, no band was seen on the negative control (pUC57) because it has no T7 promoter and terminator site. Successful ligations have band size of 517 bp while vectors without insert have 244 bp band size.

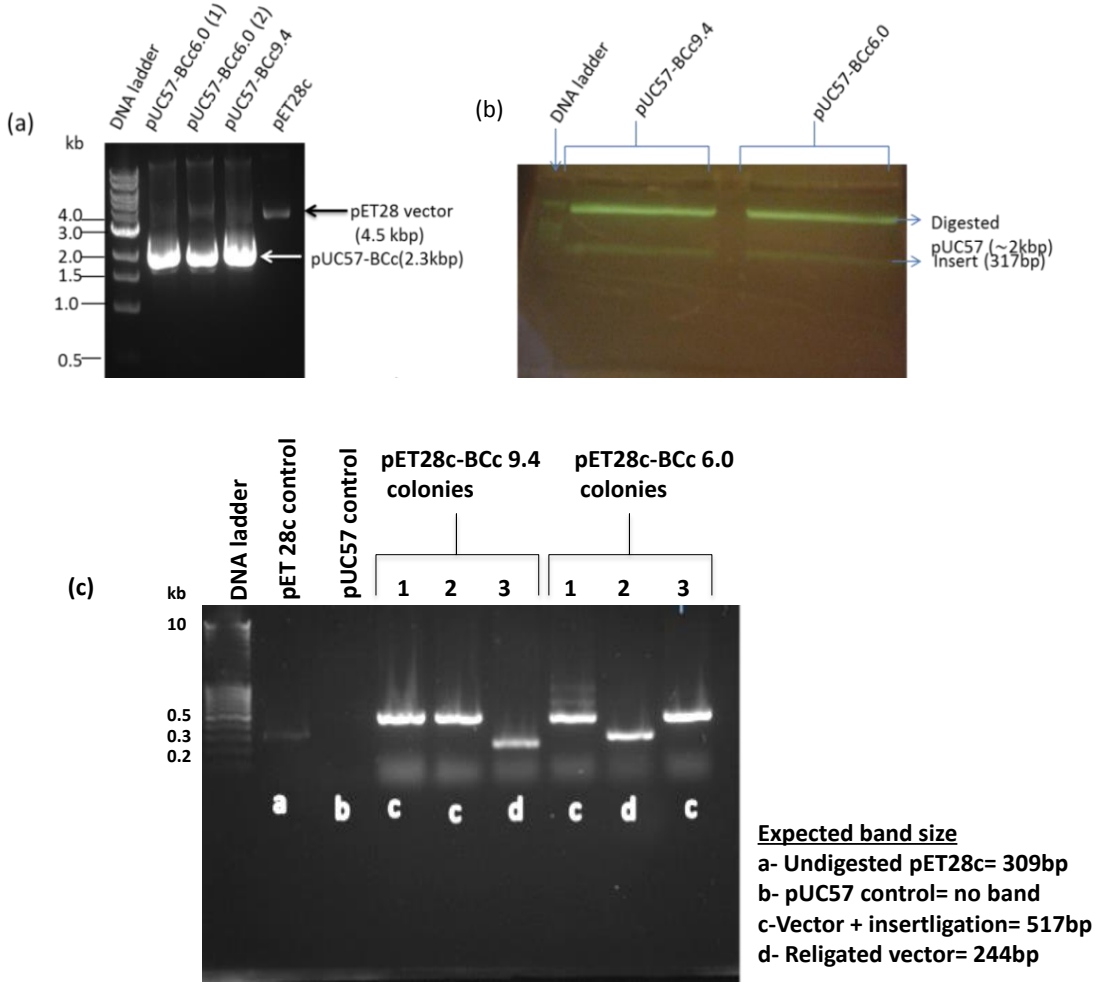

Figure 3.17: Subcloning of Bacterial cystatin from pUC57 into pET28c vector. (a) 1 % (w/v) agarose gel showing eluted plasmid DNA. (b). Analysis of double restriction digestion (NcoI /XhoI) of pUC57-BCc9.4 and BCc6.0 with on a 2 % (w/v) agarose gel electrophoresis. (c) PCR analysis of transformed colonies with ligation products for pET28-BCc inserts.

The plasmid DNA of the positive clones from colony PCR was sequenced. All colonies identified as having insert by colony PCR was confirmed as correct through DNA sequencing as shown in Figure 3.18. This indicated that colony PCR is a reliable analytic method of screening for positive ligation clones before sequencing.

```
GenScript9.4    MASTQLLGGWTAFHELTAEDKAVFKTALKGLVGVTYTPLAVATQVVAGTNYSFITKATVV 60
BCc9.4.         MASTQLLGGWTAFHELTAEDKAVFKTALKGLVGVTYTPLAVATQVVAGTNYSFITKATVV 60
                ************************************************************

GenScript       YPGAKVYLAKVYIYKPLKGDAHITKIEAAASSAWSHPQFEK 101
BCc9.4          YPGAKVYLAKVYIYKPLKGDAHITKIEAAASSAWSHPQFEK 101
                ****************************************


Genscript6.0     MASTQLGGGWSAFHELSAEDKAVFAEALKGLVGVEYTPLAVATQVVAGTNYSFITKATVV 60
Bac6.0.2        MASTQLGGGWSAFHELSAEDKAVFAEALKGLVGVEYTPLAVATQVVAGTNYSFITKATVV 60
                ************************************************************

Genscript6.0    YPGAKVYLAKVYIYKPLEGDAHITKIEAAASSAWSHPQFEK 101
Bac6.0.2        YPGAKVYLAKVYIYKPLEGDAHITKIEAAASSAWSHPQFEK 101
               ****************************************
```

Figure 3.18: Multiple sequence alignment to show successful subcloning. DNA sequencing data for pET28c-BCc9.4 and pET28c-BCc6.0 cloning regions were aligned with the original sequences provided for the synthesised genes GenScript for BCc9.4 and BCc6.0 respectively. The astrices show the presence of same residue at each position. Thus, the bacterial cystatin with correct sequence has been successfully cloned into the expression vector (pET28c).

3.6.3 Protein expression of Bacterial Cystatin

A pET-28c-BCc9.4 or pET28c-BCc6.0 plasmid was transformed into BL21 (DE3) Star cells for expression. 3 colonies were picked from each plate and grown overnight as a starter culture which was used to inoculate 50 mL of media. 1 mM IPTG was used for protein induction and cells were harvested after 6 h. To investigate the expression levels of the six bacterial cystatin proteins expressed before purification, 1 mL samples were taken after the 6 hours expression culture and lysed. The total lysate and soluble fractions from each sample were analysed on a SDS-PAGE gel alongside the Affimer-WT control and is given in Figure 3.19. In the lane loaded with total lysate and soluble fractions from Affimer wild-type, a prominent band was seen at the expected size, this indicated that the Affimer wild type expressed well and can be purified from the soluble fraction. However, no protein band corresponding to the expected size (BCc9.4 = 10.8 kDa; BCc6.0 = 10.7 kDa) was observed on the total lysate and soluble fraction lane for BCc9.4 and BCc6.0. Therefore, the protein purification of BCc9.4 and BCc6.0 was not done.

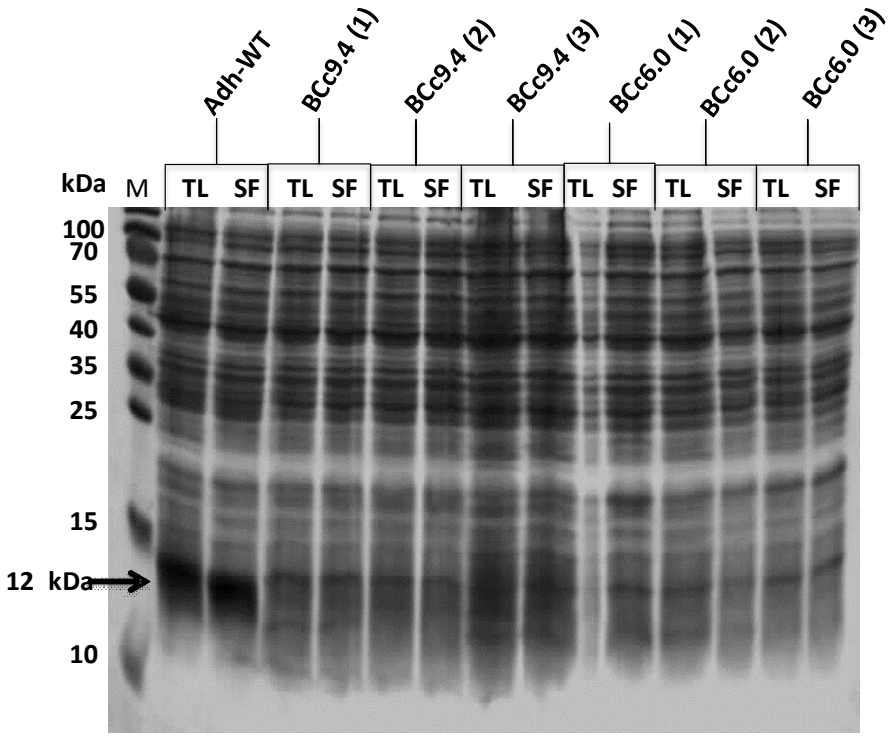

Figure 3.19: Analysis of IPTG-induced protein expression of bacterial cystatin on 15 % SDS-PAGE. A 1 mL sample for each protein expression trial was lysed with Bugbuster TM (Novagen). Total lysate and soluble fraction from Affimer wild-type (Adh-WT); three different colonies for bacterial cystatin 9.4 (BCc9.4); and three different colonies for bacterial cystatin 6.0 (BCc6.0), were analysed alongside a molecular weight ladder. Proteins were viewed on Coomassie blue stained 15 % SDS-PAGE. Expressed Adh-WT protein in total lysate and soluble fraction lane is marked by the arrow at 12 kDa.

To improve expression for BCc9.4 and BCc6.0, different strategies were used. First, the bacterial cystatin was sub-cloned from pET28c into pET11a, since the Affimer-WT used for positive control is expressed in pET11a. Secondly, aside IPTG induction, the bacterial cystatin was also expressed by auto-induction since greater cell mass will often result in greater soluble protein yield. Third, two different negative controls (undigested pET28c expression vector, BL21 (DE3) Star expression host cells were included, and lastly, dot blot analysis was carried out on the total lysate obtained during the 96 h autoinduction. The results obtained are given in Figure 3.20 and 3.21. As seen in Figure 3.20a, only Affimer-WT gave significant expression level in the soluble fraction after 24 h of incubation, with increased intensity after 72 h, a small band was also observed in its insoluble fraction at 72 h incubation. No

band was seen for BCc9.4 in either soluble or insoluble fractions and the change in expression vector did not improve its expression level at 24 h and 72 h. For BCc6.0, It appears that the protein pET28-BCc6.0 is poorly expressed at both 24 h and 72 h. No improvement in expression level was observed with the change in expression vector. These observations led to the decision of performing dot blot analysis on the total lysate obtained from the autoinduction experiment.

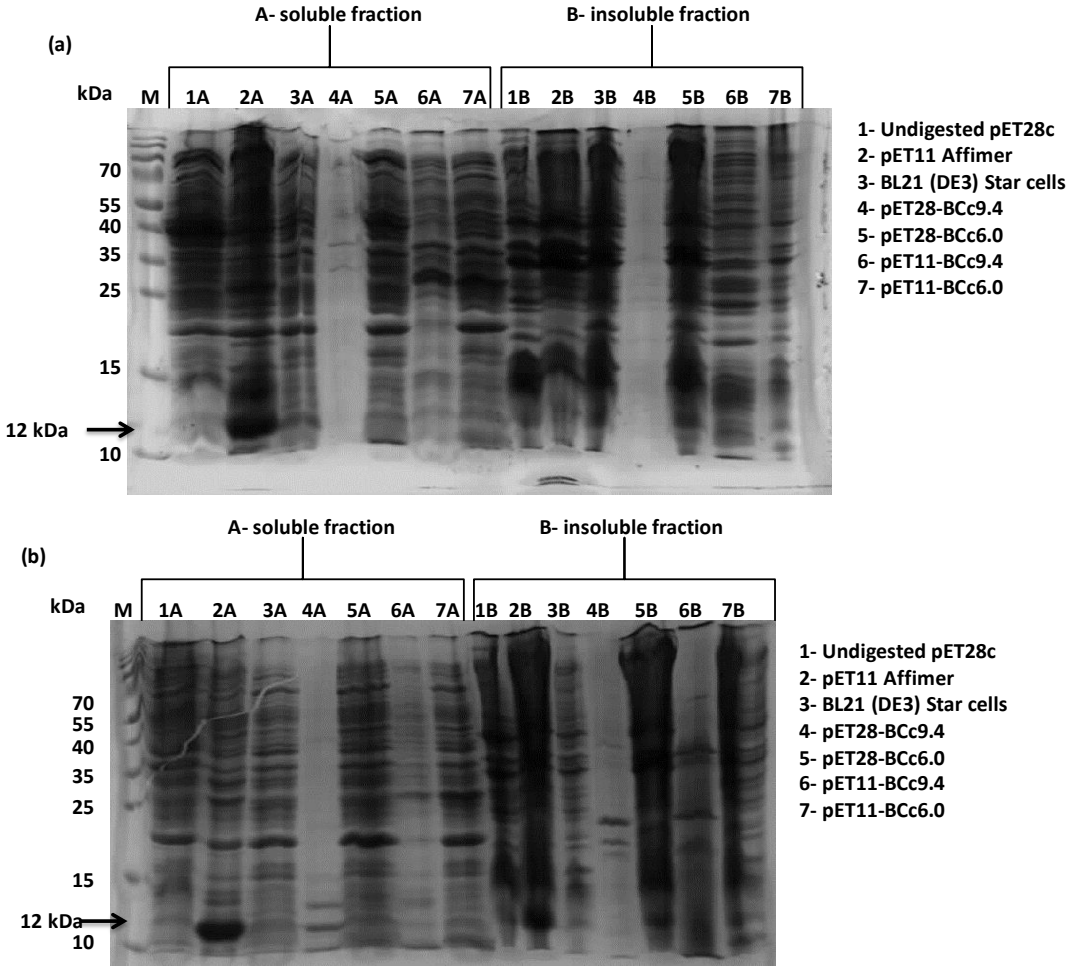

Figure 3.20: Analysis of auto-induction of bacterial cystatin protein expression on 15 % SDS-PAGE. A 1 mL sample for each expression culture was lysed with Bugbuster. Soluble and insoluble fractions alongside effect of change of expression vector (from pET28c to pET11a) on the expression level of bacterial cystatin was analysed on the 15 % SDS-PAGE. (a) The expression profile of proteins after 24 h of autoinduction. (b) The expression of proteins after 72 h of autoinduction. The expressed protein samples are from negative controls (undigested pET28c and BL21(DE3) Star cells), positive control (pET11-Affimer)and test samples (pET28-BCc9.4, pET28-BCc6.0, pET11-BCc9.4 and pET11-BCc6.0)

3.6.4 Dot blot analysis of Bacterial cystatin

The dot blot analysis was carried out on the total lysate obtained from 96 h auto-induction expression culture at specific time intervals is shown in the Figure 3.21, to detect strep-tagged protein. Using strep-tag GO as the positive control, signals were visualised on the lane dotted with pET28c-BCc6.0, and the highest signal intensity was observed for BCc6.0 at 48 h. Expression level decreased after 48 h of auto induction for BCc6.0 as signified by decrease signal intensity. On the other hand, no signal was observed in the lane dotted with pET28c-BCc9.4 from 15 h until 96 h. This confirmed the results obtained from the expression trials. No signals were seen on lane dotted with the negative controls as expected; undigested pET28c vector, since it has no insert and BL21 (DE3) Star cells which was the untransformed expression host. No expression was found on pET11-BCc9.4/ BCc6.0, which confirms the previous result, that the change of vector has no effect on the expression level of bacterial cystatin.

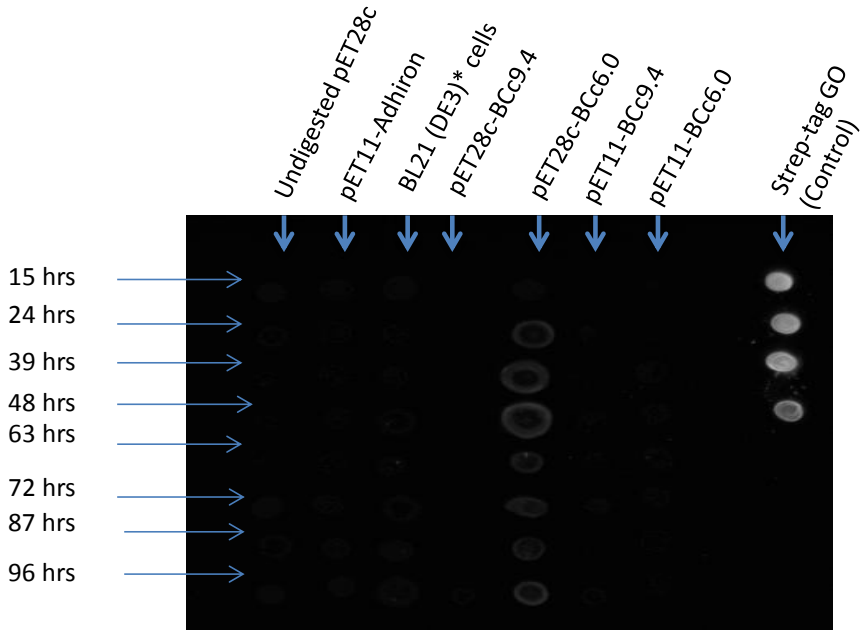

Figure 3.21: Dot blot analysis for the detection of strep-tagged protein. Total lysate from 1 mL samples of expression cultures taken at the indicated hours during 96 h autoinduction were analysed on a dot blot using Streptactin for detection, only pET28-BCc6.0 and the galactose oxidase (GO) control gave signal on the dot blot. pET11a-Affimer which is his-tagged (not strep-tagged) was used as the negative control and gave no signal on the dot blot.

From this experiment, Bacterial cystatin (BCc6.0) was chosen for further analysis. To further improve the expression of BCc6.0 even more, a second version called BCc6.0v2 was designed to exclude rho dependent termination factor, which may cause early termination of transcription and disrupt protein synthesis of BCc6.0. The results for the cloning of the improved version (BCc6.0v2) is explained in the section below.

3.6.5 Cloning of Bacterial cystatin version 2 - BCc6.0v2

The improved version BCc6.0v2 was subcloned from pUC57 and cloned successfully into pET28c as described for BCc6.0. The DNA sequencing results in Figure 3.22 showed that pET28c-BCc6.0v2 has the expected sequence.

```
1.1.C           MASTQLGGGWSAFHELSAEDKAVFAEALKGLVGVEYTPLAVATQVVAGTNYSFITKATVV 60
BCc6.0v2        MASTQLGGGWSAFHELSAEDKAVFAEALKGLVGVEYTPLAVATQVVAGTNYSFITKATVV 60
                ************************************************************

1.1.C           YPGAKVYLAKVYIYKPLEGDAHITKIEAAASSAWSHPQFEK 101
BCc6.0v2        YPGAKVYLAKVYIYKPLEGDAHITKIEAAASSAWSHPQFEK 101
                *****************************************
```

Figure 3.22: Multiple sequence alignment to show successful subcloning. DNA sequencing result for pET28c-BCc6.0v2 was aligned with the original sequence provided by GenScript for BCc6.0v2. The asterisks show the presence of same residue at each position. Thus, the bacterial cystatin version 2 with the expected sequence has been successfully cloned into the expression vector (pET28c).

3.6.6 Protein expression and time course analysis for BCc6.0v2

Expression of BCc6.0v2 was carried out alongside BCc6.0 (previous version) to enhance comparative studies, while Affimer scaffold expressed in pET11a was used as the positive control. The time course analysis obtained showed a similar growth trend for the cells in all flasks (Figure 3.23).

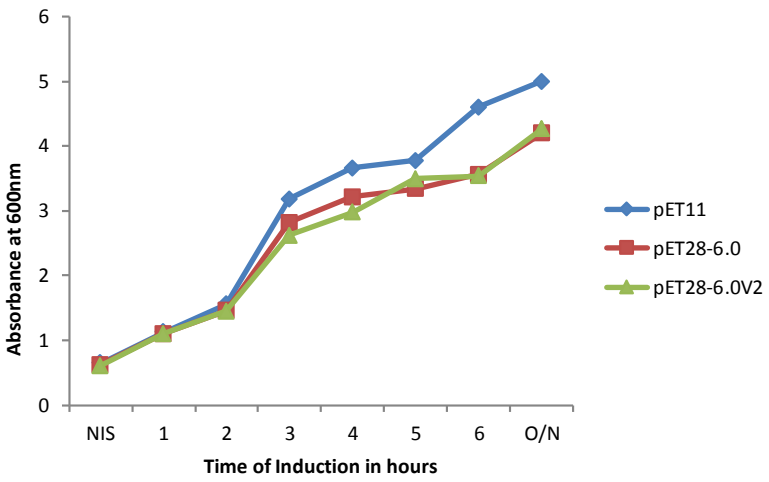

Figure 3.23. Time course analysis for BCc6.0v2 expression: The absorbance measured at 600 nm at one-hour intervals for each sample are presented. NIS (Non-Induced Sample) represents absorbance taken before IPTG induction. The absorbances were measured each hour after induction for 6 h then overnight (O/N) respectively.

3.6.7 SDS-PAGE Analysis of protein expression

Fractions obtained from a 1 mL sample taken at intervals during protein expression were prepared and 10 µL aliquot of the total lysate, soluble fraction and insoluble fraction were analysed on a 4-20 % SDS-PAGE gel. Figure 3.24 gives the result obtained.

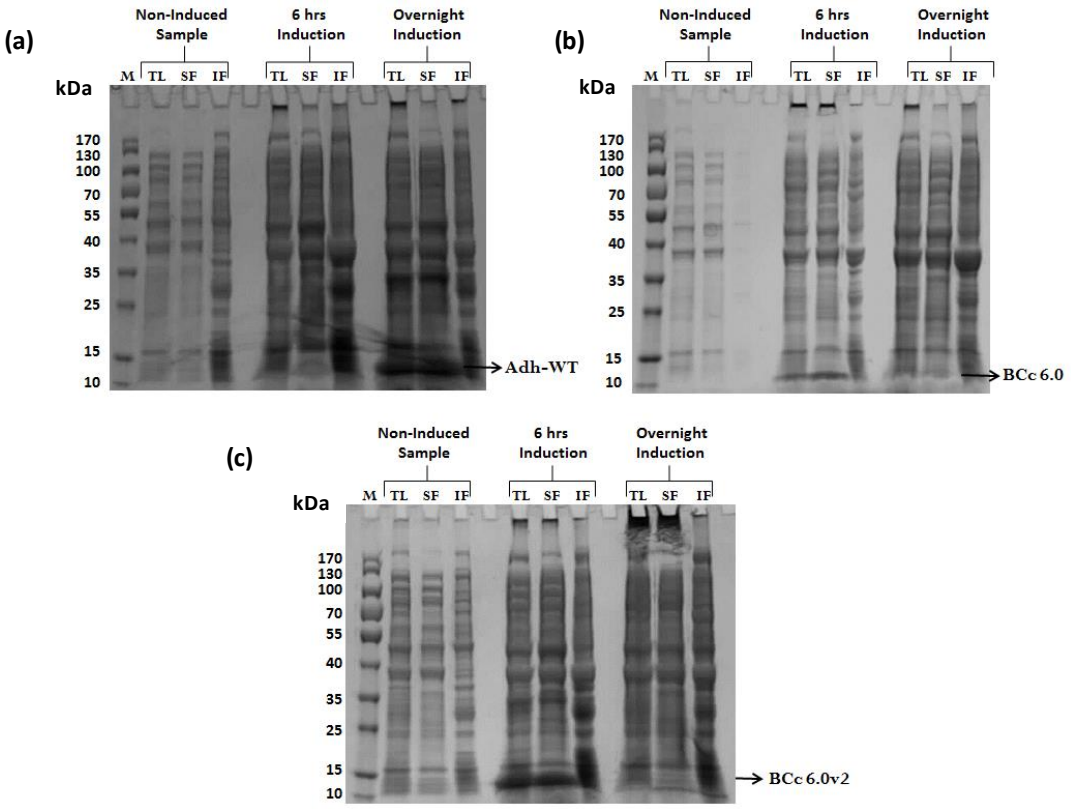

Figure 3.24: Comparative SDS-PAGE analysis for the expression level for Adh-WT, BCc6.0 and BCc6.0v2 (a-c). A 1 mL sample for each protein expression trial was lysed with Bugbuster ^{TM} (Novagen) and total lysate, soluble and insoluble fraction were loaded on the gel. (a) gives the SDS-Page analysis for Adh-WT which was used as positive expression control. (b) gives the SDS-PAGE analysis for BCc6.0 which is the previous version of bacterial cystatin with very low expression level. While (c) gives the SDS-PAGE analysis for the new version of bacterial cystatin (BCc6.0v2).

The intensity of the band obtained for BCc6.0v2 at 6 h after IPTG induction shows that the new version (BCc6.0v2) (Figure 3.24c) is better expressed compared to BCc6.0 (Figure 3.24b). It is noteworthy that BCc6.0 showed some level of expression, this could have been because of a change in the expression conditions. Previously, BCc6.0 have been expressed at 30 ^{o}C and 150 rpm but the expression condition used here included reduced temperature 25^{o}C and 150 rpm).

3.7 Discussion

3.7.1 JD-F12 and its mutants

Interactions between polypeptides in quaternary structure cause them to aggregate and form complexes. These interactions are usually stabilised by interfacial contacts between residues (Mino *et al*., 2013). When such residues are

mutated, the observed stability and aggregation are altered. According to Trevino *et al*., (2007) the approach generally used to increase the solubility of a protein is to replace the most hydrophobic residue on the surface with a charged or polar residue. Bertone *et al*., (2001) analysed 562 proteins from *Methanobacterium thermoautotrophicum* and confirmed that high content of negative residues (DE >18 %) and absence of hydrophobic patches are associated with improved solubility (Smialowski *et al*., 2007).

Studies carried out in this chapter have shown that no generalised scaffold optimisation strategy has been achieved through selected point mutation for eliminating aggregation propensity in aggregation-prone binders. Nevertheless, introduction of DD residues before and after VR1 and VR2 eliminated aggregation in JD-F12. This result presents a potential binder-specific approach for engineering aggregation-resistant Affimer binders.

3.7.2 Bacterial cystatin

The bacterial cystatin scaffold was engineered using the consensus design concept, an approach that has been used to develop novel Affimer scaffold (from plant cystatin). The gene construct for the bacterial cystatin consensus sequence BCc9.4 and BCc6.0 was successfully cloned in frame between the NcoI/XhoI site of pET28c. It is noteworthy that results from colony PCR results identified colonies with the correct insert, therefore increasing positive results obtained from the DNA sequencing data. The time course analysis for the IPTG induction of bacterial cystatin expression shows that the absorbance of BCc6.0 is similar in trend to that observed in the control while BCc9.4 shows minimal increase in its absorbance compared to control. Analysis of the 1 mL sample taken from each flask on 15 % SDS-PAGE gel respectively shows that only the control ADH-WT was expressed well in the soluble fraction. Though a faint band about the MW of BCc9.4 and BCc6.0 was observed on the gel, it is hard to conclude it was expressed since lysozyme, which is similar in size, was used for the cell lysis. According to Boettner *et al*., (2007), a high isoelectric point has been associated with no detectable protein expression. Hence, BCc6.0 (pI=6.0) was expected to express better than BCc9.4 (pI=9.4). It has been shown that change of expression vector could enhance the

expression of synthetic proteins (Deacon and McPherson, 2011, Terpe, 2006), thus BCc9.4 and BCc6.0 were subcloned respectively into pET11a to allow for expression comparison with the control ADH-WT. SDS-PAGE and dot blot analysis of the total lysate of the samples (Fig 3.20 and 3.21) eliminates the possibility of contamination of the expression vector or the expression strain BL21 (DE3) Star cells with foreign protein. However, no significant improvement was observed in the soluble expression of BCc9.4 with a vector change. For BCc6.0, change in vector improved the expression, but was accumulated in the insoluble fraction. Further steps taken to improve the expression of bacterial cystatin was to ensure that no rho factor binding sequence was present upstream the gene. Rho factor when present upstream or within the gene to be expressed could cause abrupt termination of gene expression. Thus, BCc6.0 version 2 was synthesised. IPTG induction of BCc6.0v2 shows improved level of expression compared to BCc6.0. As protein solubility is an important pre-requisite for structural, biophysical studies, and applications (Smialowski *et al*., 2007), the difficulty encountered with the expression of bacterial cystatin has limited further analysis initially planned to be carried out. Analysis done so far in comparing plant cystatin (Affimer) to bacterial cystatin revealed that much optimisation is required before bacterial cystatin could be considered for the generation of new libraries.

Chapter 4: Identification and characterisation of Affimer binders against GDH*C. diff*

4.1 Introduction

Glutamate dehydrogenases (GDH) are a class of enzymes that are involved in the oxidative deamination of glutamate to α-ketoglutarate and vice versa. The metabolic role of GDH is determined by its coenzyme specificity (NAD or NADH, NADP or NADPH). GDHs involved in glutamate catabolism are NAD^+-dependent and those involved in ammonia assimilation are $NADP^+$-dependent. Glutamate dehydrogenases found in *E. coli* and certain yeasts are $NADP^+$-dependent, that consist of six subunits (McPherson and Wootton, 1983), while GDH enzymes from several anaerobes such as *C. difficile*, *Peptostreptococcus assacharolyticus* are NAD^+-dependent (Anderson *et al*., 1993). NAD^+-dependent GDH can either be hexameric (six subunits that are 48 kDa each) or tetrameric (four subunits that are about 115 kDa each) (Baker *et al*, 1992), while mammalian form of glutamate dehydrogenase can utilise either NAD(H) or NADP(H) as coenzymes.

For GDH produced by *C. difficile*, it has a hexameric structure with each of the GDH subunits assembling to form an oligomer (Baker *et al*, 1992). Each GDH subunit comprises of two domains separated by a cleft and the enzyme active site is located in the cleft between the two domains (Pasquo *et al*, 1996). *C. difficile* GDH is NAD^+-dependent and is encoded by the gene gluD (Lyerly, 1991). It catalyses the deamination of glutamate to α-ketoglutarate using NAD^+ as the coenzyme.

$$\text{L-glutamate} + H_2O + NAD^+ \longrightarrow \text{2-oxoglutarate} + NH_3 + NADH + H^+$$

GDH produced by *C. difficile* can be detected in both intracellular and extracellular culture supernatants. Intracellular GDH is an important metabolic enzyme for the fermentation of amino acids. while the role of extracellular GDH in *C. diff* is unclear, it was suggested that it could be used for generating extracellular NADH to create a reducing environment for the anaerobe. Glutamate in the host acts as an important signalling molecule to regulate gut function and modulate the immune response. Therefore, it was also suggested that *C. difficile* may affect its host functions by scavenging the host glutamate (Bartlett *et al*, 2008). Most recently, Girinathan *et al*., (2016), provided the first evidence that *C. difficile* utilises glutamate to establish itself in the human gut, thereby promoting colonisation and disease progression.

Glutamate dehydrogenase (GDH) was discovered as a potential biomarker for *Clostridium difficile* infection when the latex agglutination test that was developed to identify *C. diff* toxin A was reported to be cross-reactive to an unknown protein (Lyerly and Wilkins, 1986, Lyerly *et al*., 1988). A few years later, Lyerly and his colleagues completed the DNA sequencing of the gluD gene that codes for the glutamate dehydrogenase in *Clostridium difficile*, and did a comparative sequence analysis with glutamate dehydrogenases from other bacteria (Lyerly *et al*., 1991). It was confirmed that the cross-reactive protein produced by *C. difficile* is glutamate dehydrogenase. It is produced by both toxigenic and non-toxigenic strains of *C. difficile*, therefore it has been used as a screening biomarker for the detection of the presence of *C. difficile* (Eastwood *et al*., 2009).

This chapter describes how a codon optimised gene for *C. difficile* glutamate dehydrogenase was generated and used for production and purification of active GDH. Then, the recombinant GDH was used as a target for the identification of potential Affimer binders by screening an Affimer phage display library. Finally, characterised binders were tested for use as a diagnostic tool for CDI.

4.2 Design and production of GDH

The complete coding sequence for *Clostridium difficile* GDH was obtained from GenBank using accession number: M65250 (Anderson *et al*., 1993) and was codon optimised for *E. coli* expression using JCAT. The construct for production of recombinant GDH (rGDH$_{C.\ diff}$) was designed to contain the following: a NcoI site at the N-terminal end of the coding sequence and a HindIII site, His$_6$-tag to facilitate purification and a stop codon at the C-terminal end (Figure 4.1).

Figure 4.1: Schematic of of the synthetic gene construct for *C. difficile* glutamate dehydrogenase (GDH). The features of the construct are presented.

4.2.1 Subcloning of the rGDH$_{C.\ diff}$ coding region

The synthetic construct for rGDH$_{C.\ diff}$ was ordered from GenScript cloned between the NcoI and HindIII restriction sites in the cloning vector pUC57. PCR (Section 2.6.1) was carried out to amplify the coding sequence for rGDH$_{C.\ diff}$ using pUC57 forward

and reverse primer (Table 2.3, Chapter 2). The thermal cycling was carried out for 30 cycles: denaturation at 98 ^{o}C for 30 s, annealing at 54 ^{o}C for 20 s, extension at 72 ^{o}C for 1 min 20 s, with a final extension at 72 ^{o}C for 20 min to allow complete extension of rGDH$_{C.\ diff}$ (1306 bp). Following purification of the products using a QIAquick PCR purification kit (Section 2.6.9), the amplicon was digested with NcoI and HindIII and ligated into similarly digested pET28c expression vector. Chemically competent XL10-Gold cells (Section 2.1.1) were transformed with recombinant pET28c-rGDH$_{C.\ diff}$ plasmid and plated onto LB-agar plates containing kanamycin. Following overnight incubation, several colonies were analysed by colony PCR and agarose gel electrophoresis, and the products corresponded to a ca. 1310 bp DNA fragment corresponding to the calculated size of expected PCR product of pET28c-rGDH$_{C.\ diff}$. Plasmids were purified from two positive clones using a QIAgen miniprep kit (Section 2.5.1) and DNA sequencing confirmed the correct incorporation of the insert (Figure 4.2). Translation of the DNA sequencing results showed the subunit, with the addition of the 6xHis tag comprises 440 amino acids with a deduced molecular mass of 47.907 kDa which was calculated using ExPASy Protparam tool (Gasteiger *et al*., 2003).

```
T7F-GDH1        MGSGKDVNVFEMAQSQVKNACDKLGMEPAVYELLKEPMRVIEVSIPVKMDDGSIKTFKGF 60
GenScript       MGSGKDVNVFEMAQSQVKNACDKLGMEPAVYELLKEPMRVIEVSIPVKMDDGSIKTFKGF 60
                ************************************************************
T7F-GDH1        RSQHNDAVGPTKGGIRFHQNVSRDEVKALSIWMTFKCSVTGIPYGGGKGGIIVDPSTLSQ 120
GenScript       RSQHNDAVGPTKGGIRFHQNVSRDEVKALSIWMTFKCSVTGIPYGGGKGGIIVDPSTLSQ 120
                ************************************************************
T7F-GDH1        GELERLSRGYIDGIYKLIGEKVDVPAPDVNTNGQIMSWMVDEYNKLTGQSSIGVITGKPV 180
GenScript       GELERLSRGYIDGIYKLIGEKVDVPAPDVNTNGQIMSWMVDEYNKLTGQSSIGVITGKPV 180
                ************************************************************
T7F-GDH1        EFGGSLGRTAATGFGVAVTAREAAAKLGIDMKKAKIAVQGIGNVGSYTVLNCEKLGGTVV 240
GenScript       EFGGSLGRTAATGFGVAVTAREAAAKLGIDMKKAKIAVQGIGNVGSYTVLNCEKLGGTVV 240
                ************************************************************
T7F-GDH1        AMAEWCKSEGSYAIYNENGLDGQAMLDYMKEHGNLLNFPGAKRISLEEFWASDVDIVIPA 300
GenScript       AMAEWCKSEGSYAIYNENGLDGQAMLDYMKEHGNLLNFPGAKRISLEEFWASDVDIVIPA 300
                ************************************************************
T7F-GDH1        ALENSITKEVAESIKAKLVCEAANGPTTPEADEVFAERGIVLTPDILTNAGGVTVSYFEW 360
GenScript       ALENSITKEVAESIKAKLVCEAANGPTTPEADEVFAERGIVLTPDILTNAGGVTVSYFEW 360
                ************************************************************
T7R-GDH1        VQNLYGYYWSEEEVEQKEEIAMVKAFESIWKIKEEYNVTMREAAYMHSIKKVAEAMKLRG 420
GenScript       VQNLYGYYWSEEEVEQKEEIAMVKAFESIWKIKEEYNVTMREAAYMHSIKKVAEAMKLRG 420
                ************************************************************
T7R-GDH1        WYGGGGSKLAAALEHHHHHH 440
GenScript       WYGGGGSKLAAALEHHHHHH 440
                ********************
```

Figure 4.2: Sequence analysis for rGDH*C. diff*. The pET28-rGDH*C. diff* was sequenced using T7F and T7R primers and the sequence obtained was aligned with the sequence data provided by GenScript for the pUC57 construct. This shows that rGDH*C. diff* was successfully subcloned into pET28c.

4.2.2 Expression and purification

The pET28c-rGDH*C. diff* expression vector was used to transform BL21 (DE3) Star cells and the expression of rGDH*C. diff* protein was induced with 0.1 mM IPTG, then the time course was followed for 6 h. Total lysates obtained from each time point were analysed on a 4-20 % SDS-PAGE and by Coomassie blue staining. Even though more protein was loaded for the 6 h sample, as shown in Figure 4.3a, the highest expression level was obtained 6 h post-induction - the level of GDH protein is substantially greater than in the preceding fraction. While later induction times were not analysed, the level of GDH production at 6 h was considered sufficient for the current experiments, as indicated by the yield of protein. Therefore, cells were harvested after 6 h induction and lysed (Section 2.7) and the recombinant GDH protein was purified from the soluble fraction using Ni-NTA affinity chromatography.

For assess the protein purity, aliquots of the unbound fraction, final wash and the elution fractions were analysed on a 4-20 % SDS-PAGE. As shown in Figure 4.3b, a faint band migrating at around 48 kDa corresponding to the expected size of a GDH subunit was observed in the flow-through, showing that the column was saturated with the target protein. Bound rGDH*C. diff* was eluted with a single band migrating at

~48 kDa corresponding to the expected size of a GDH subunit. The purification profile shows the recombinant protein was 90 % pure.

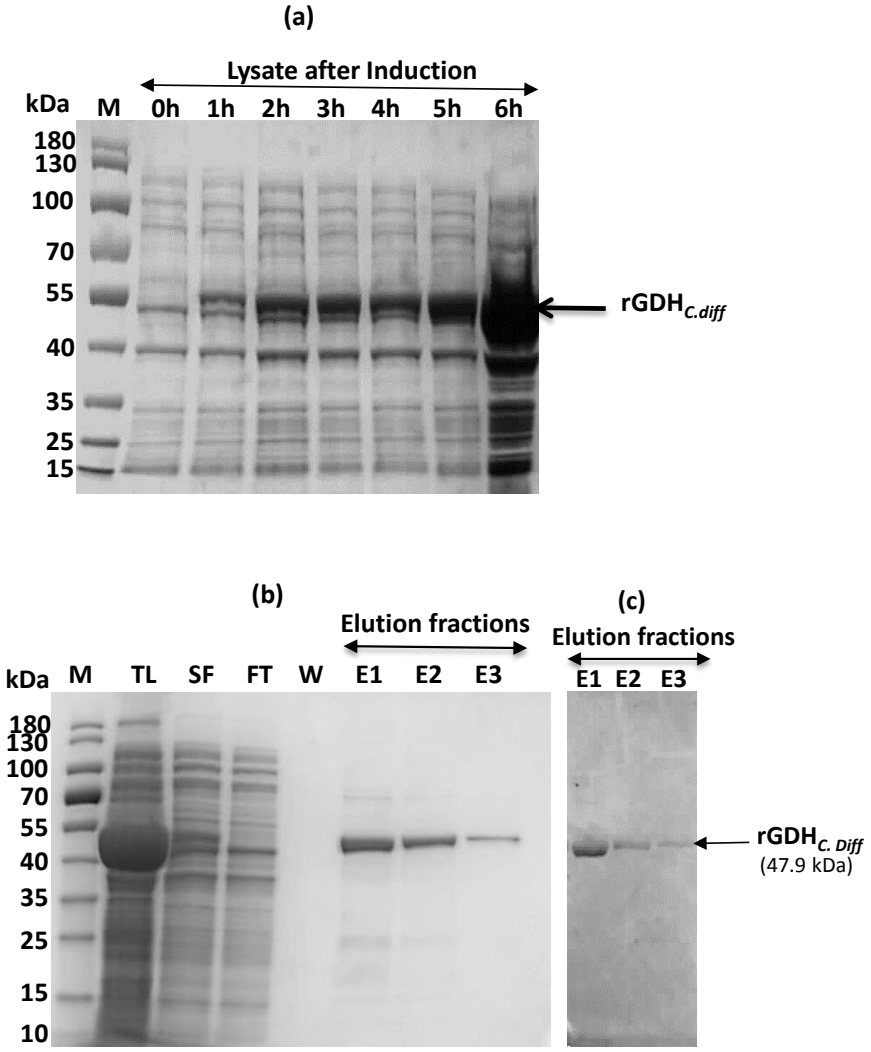

Figure. 4.3: Production of rGDH*C. diff*. (a) SDS-PAGE analysis of the expression profile of rGDH*C. diff* showing product at 6 h induction. (b) SDS-PAGE analysis of the fractions obtained during purification. Only a single band corresponding to rGDH$_{C. diff}$ was observed on the elution fraction lane indicating the purity of the protein. (c) Western blot analysis of the eluted fractions showed only a prominent band in each lane corresponding to rGDH$_{C. diff}$ (47.9 kDa). M - Molecular weight marker; TL - total lysate; FT - flow-through; W - final wash.

Using an anti-His tag antibody, the western blot analysis confirmed the presence of His-tagged GDH protein in the elution fractions (Figure 4.3c) as a single prominent band in all the elution fractions. The protein concentration of the purified protein was determined by nanodrop, using the theoretical molecular weight and extinction coefficient calculated with the ExPASy ProtParam tool (Gasteiger *et al*., 2005). rGDH$_{C. diff}$ has a pI of 5.52 and it was well expressed in *E. coli* with a protein

concentration of 21 mg obtained from a 50 mL expression culture (= 427.69 mg/L). This agrees with previous studies (Anderson *et al*., 1993, Girinathan *et al*., 2014) who reported a high yield of GDH in *E. coli*. Purified GDH was then dialysed into PBS (pH 7.2) for use in further experiments or stored at -80 ^{o}C.

4.3 Characterisation of recombinant GDH

4.3.1 Determination of the molecular mass of rGDH$_{C. diff}$

Glutamate dehydrogenase from *C. difficile* is a hexameric protein containing six identical subunits with calculated native molecular weight of ~300 kDa (Anderson *et al*., 1993). Under denaturing conditions, the molecular mass of a glutamate dehydrogenase subunit as determined by SDS-PAGE (Figure 4.3b) is consistent with the calculated theoretical MW (47.9 kDa).

4.3.2 Enzyme activity

GDH$_{C. diff}$ catalyses the deamination of glutamate to alpha-ketoglutarate using NAD as the coenzyme. Purified recombinant protein was analysed for glutamate dehydrogenase activity (Section 2.7.7). Enzymatic activity of glutamate dehydrogenase was measured spectrophotometrically in the direction of oxidative deamination of glutamate by following the increase in absorbance at 340 nm. The reaction assay contained 300 mM potassium phosphate buffer, pH 8, 300 mM Glutamic Acid, pH 7.5, 1 mM NAD and 0.5 µg GDH in a final volume of 1 mL. The reaction was started with the addition of enzyme into the reaction mixture at room temperature. Since the cell lysate from BL21 (DE3) Star not expressing rGDH$_{C. diff}$ would be used for pre-panning the phage during the phage display screening, the GDH enzyme activity of the lysate was examined to serve as a negative control. As expected, Figure 4.4 shows that only recombinant glutamate dehydrogenase displayed enzyme activity while no activity was found in the BL21 (DE3) Star cell lysate (negative control).

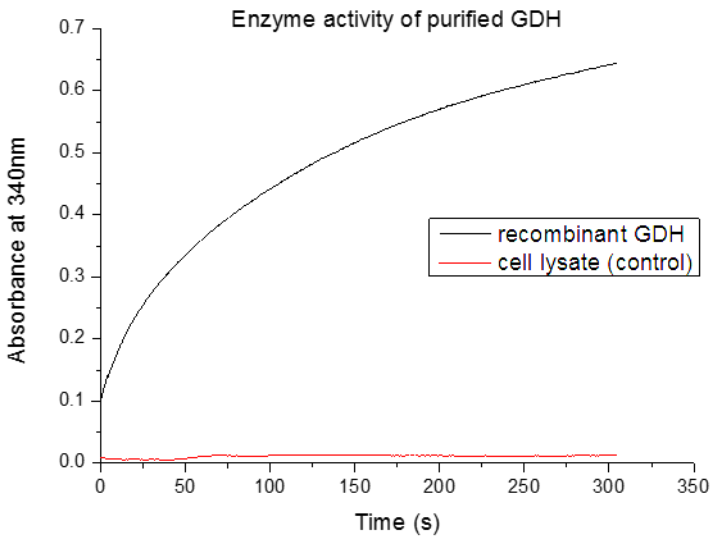

Figure 4.4: Glutamate dehydrogenase enzyme activity at 340 nm. The enzyme activity of purified rGDH$_{C.\ diff}$ and BL21 (DE3) Star cell lysate (negative control) was monitored. Enzyme activity was only seen in the purified enzyme sample.

Summarily, a synthetic gene for GDH$_{C.\ diff}$ was constructed. It was expressed in *E. coli* and purified from the soluble fraction using Ni-NTA chromatography, and displayed glutamate dehydrogenase enzyme activity as expected.

4.4 Identification of Affimer binders to rGDH$_{C.\ diff}$ through phage display

The next phase of the project was to identify high affinity binders against glutamate dehydrogenase from *Clostridium difficile*, for diagnostic purposes. This was achieved by screening the Affimer phage display library against the target (rGDH$_{C.\ diff}$), as outlined below.

4.4.1 Biotinylation of rGDH$_{C.\ diff}$

Direct surface immobilisation of targets can lead to partial denaturation, or result in inaccessible binding sites during phage display screening. Hence, recombinantly produced glutamate dehydrogenase was immobilised onto streptavidin-coated Nunc Maxisorp plate via biotin-streptavidin interaction. For diagnostic purposes, a high affinity binder is sufficient and it does not matter where it binds. However, selecting inhibitory binders for other applications requires that the enzyme maintain its activity during the selection process. As an example, the active site of

glutamate dehydrogenase contains residues (including lysine 125) that are critical for its catalytic activity, (Baker *et al*., 1992).

In preparation for the phage display screening, rGDH$_{C.\ diff}$ was biotinylated using EZ-link® NHS-SS-Biotin and EZ-link®HPDP-Biotin (see Section 2.8.2.1 and 2.8.2.2). EZ-link® NHS-SS-Biotin labels lysine ε-amino groups and N-terminal amine groups while EZ- link® HPDP-Biotin labels reduced cysteine residues. Lysate from BL21 (DE3) Star cells was also biotinylated since it would be used in pre-panning steps in order to reduce non-specific binding during phage display, while non-biotinylated GDH was used as negative control (blank). Biotinylation was confirmed by ELISA and the absorbance read at 620 nm within 3 min of incubation with the TMB substrate (Section 2.8.3). The results presented in Fig 4.5 show successful biotinylation of the three samples.

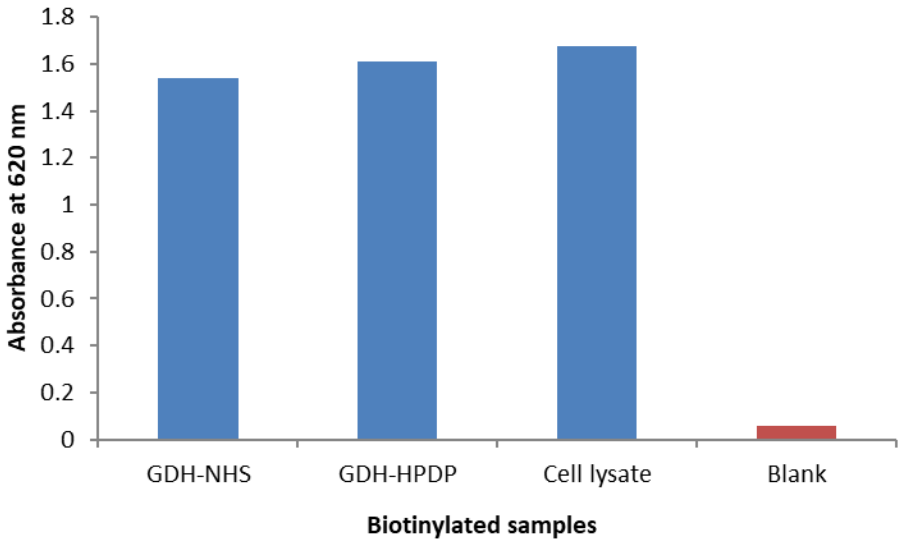

Figure 4.5: ELISA to show biotinylation of GDH. The binding of adsorbed biotinylated GDH-NHS, GDH-HPDP and the cell lysate to strep-HRP was detected using TMB substrate. The absorbance reading at 620 nm shows that were successfully biotinylated while no signal was observed with the blank.

4.4.2 Effect of biotinylation on enzyme activity

To evaluate the impact of the two biotinylation methods used on the enzyme activity of glutamate dehydrogenase, samples of GDH-NHS (glutamate dehydrogenase biotinylated with EZ-link® NHS-SS-Biotin), GDH-HPDP (glutamate dehydrogenase biotinylated with EZ-link® HPDP-Biotin), biotinylated cell lysate

(negative control) and non-biotinylated GDH (positive control) were examined for GDH enzyme activity. GDH activity for biotinylated enzyme was measured spectrophotometrically in the direction of oxidative deamination of glutamate by following the increase in absorbance at 340 nm. As stated in Section 4.4.1, biotinylating free lysine (using EZ-link® NHS-SS-Biotin kit) randomly labels lysine residues, which may include those in the active site of an enzyme that are important for its catalytic activity. The results obtained revealed that GDH became inactivated upon biotinylation with EZ-link® NHS-SS-Biotin (magenta trendline) while GDH biotinylated with EZ- link® HPDP Biotin maintained its enzyme activity (blue trendline) which overlays the activity observed for the non-biotinylated purified GDH (black trendline). Therefore, it is vital to consider the effect of biotinylation method when designing phage display screen for various targets especially enzymes. No enzyme activity was observed with the negative control which is biotinylated cell lysate (green).

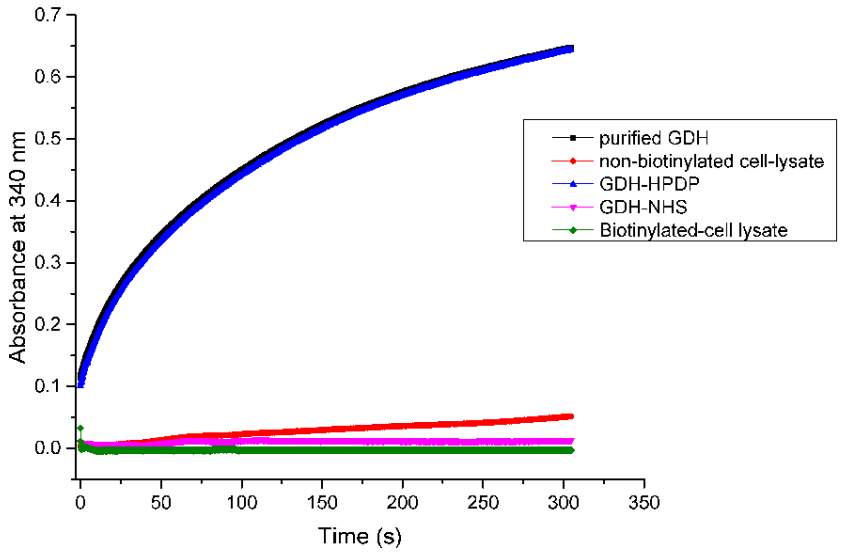

Figure 4.6: Effect of biotinylation with HPDP-Biotin and NHS-SS-Biotin on GDH enzyme activity: Enzyme activity of freshly biotinylated GDH with either HPDP-Biotin (Blue trendline) or NHS-SS-Biotin (Magenta- trendline) and biotinylated cell lysate was monitored at 340 nm wavelength. Purified GDH and non-biotinylated cell-lysate was used as positive and negative control respectively.

4.4.3 Phage display screening

Affimer-displaying phage that bound to rGDH*C. diff* were selected from the Affimer phage library by three successive biopanning rounds. In the first panning round,

wells of streptavidin-coated Nunc Maxisorp strip were incubated with biotinylated rGDH$_{C.\ diff}$ as target (panning well) or biotinylated cell lysate (pre-panning wells). The input phage was pre-panned against biotinylated cell lysate before addition to the panning well, to minimise the non-specific cross-reactivity with bacterial proteins. (Section 2.9.2.2). Bound phage particles were eluted with 0.2 M glycine pH 2.2 followed by neutralisation with 1 M Tris-HCl, pH 9.1 and then an alkali elution step (trimethylamine) followed by neutralisation with 1 M Tris-HCl, pH 7. The eluted phages were used to infect ER2738 cells and the resulting colonies collected, resuspended in growth medium and infected with M13K07 helper phage to generate a fresh enriched phage pool, which was used as input for the second panning round. To exert selective pressure to ensure affinity and specificity, the second and third panning rounds for GDH included a 24 h incubation in the presence of free, non-biotinylated GDH target. Over 500-fold amplification in colony recovery was observed after the third panning round compared to control samples, which gave signal of a successful screening for target-specific Affimers and not just background phage. Then, 32 clones were randomly picked and assessed for specific binding to GDH.

4.4.4 Phage ELISA

Phage ELISA was carried out to assess whether the selected clones showed specificity towards GDH protein. As described in Section 2.10.3, the biotinylated GDH was captured onto streptavidin coated plates, then individual phage produced from the selected clones were tested for specific binding to immobilised GDH using immobilised cell lysate as negative control. Binding was confirmed using HRP-conjugated anti-phage antibody then visualised using TMB substrate. Absorbance was read within 6 min of incubation with the substrate (Figure 4.7).

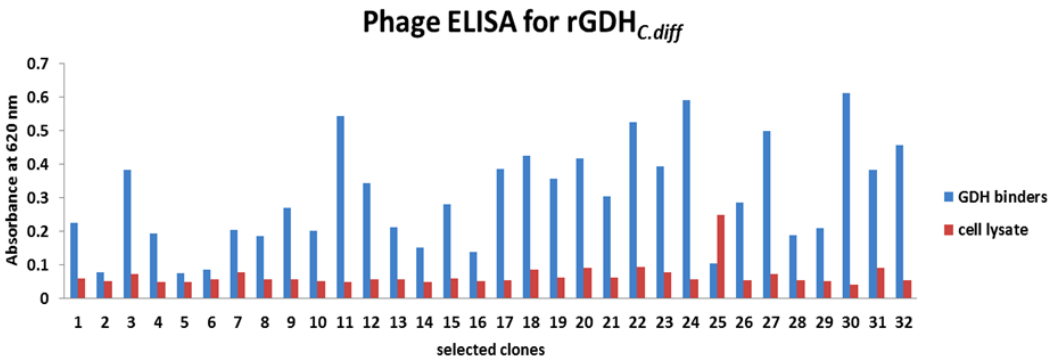

Figure 4.7: Evaluation of binding ability of screened phages by phage ELISA. GDH phage ELISA of randomly selected clones after the 3rd panning round including 24 h incubation with free non-biotinylated GDH. Signals for GDH (blue bar) and cell lysate control (red bar) are presented.

From the phage ELISA result, clones were selected based on the signal intensity obtained in the sample well compared to their corresponding control wells. Clones with absorbance >0.2 (more than 2-fold increase in signal intensity in the control well) were selected as positive clones. Based on this, 25 of the 32 analysed clones were positive clones showing specific binding to immobilised $rGDH_{C.\ diff}$. On the other hand, clone 2, 5 and 6, 14, 16 and 25 gave A_{620} values ≤ 0.1, are non-specific background binders therefore were not selected. This indicates that 25 of the randomly selected $rGDH_{C.\ diff}$ phage express Affimers that bind specifically to glutamate dehydrogenase from *C. difficile* with no cross-reactivity to the cell lysate, representing a 78 % success rate in Affimer binders selection for the sample screened.

4.4.5 DNA sequencing and identification of unique binders

In total, phagemid DNA was prepared from 25 clones that were judged positive in the phage ELISA, with the DNA concentrations ranging from 400-550 ng/µL. A 15 µL aliquot of each phagemid DNA was prepared at 100 ng/µL and submitted for DNA sequencing from the M13-26REV primer (Table 2.3). Sequencing results were analysed using the ExPASy translate tool (Gasteiger *et al.*, 2003) to ensure the integrity of the Affimer coding region and to determine their amino acid diversity in the variable region 1 and 2. As an example, an annotated version of the sequencing data obtained for the GDH-HPDP-4 binder is presented in Figure 4.8.

As expected, the DNA sequence contained the DsbA signal peptide required for periplasmic secretion, NheI and NotI restriction sites which can be used for cloning, sequence in the variable region 1 and 2 which gives the unique binding properties to each Affimer, and a Hexa-His tag sequence for affinity purification. The in-frame amber (TAG) stop codon allows translational read-through to create an Affimer-truncated-gpIII fusion protein in a suppressor *E. coli* strains such as ER2738 but Affimer alone in non-suppressor strains such as JM83.

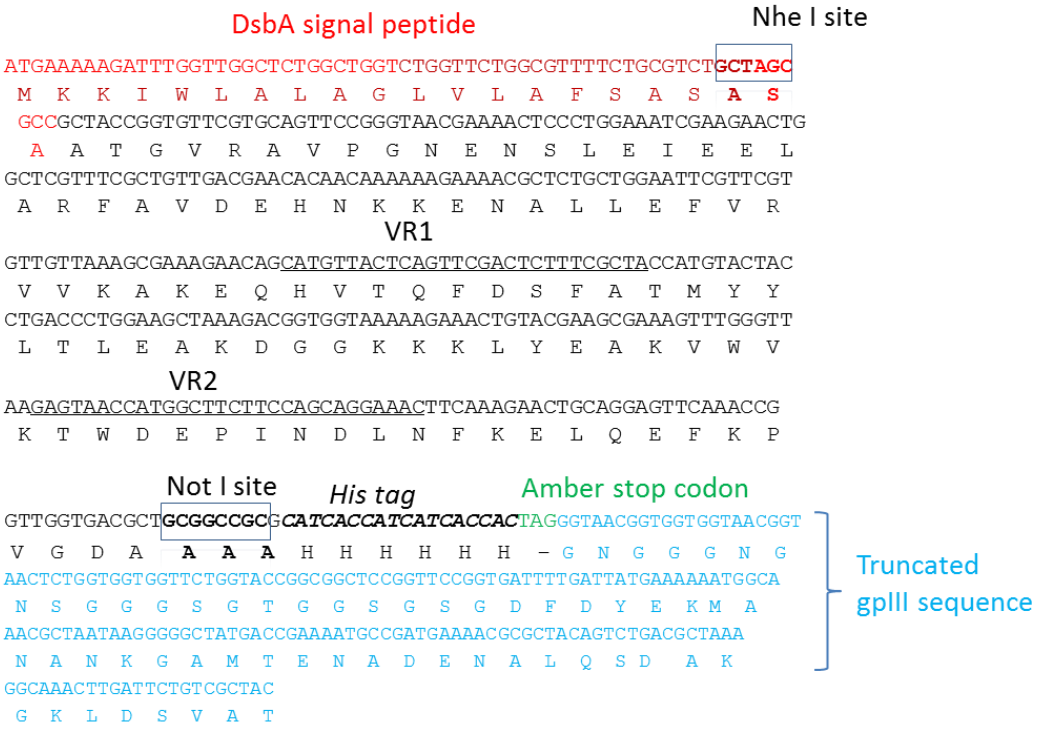

Figure 4.8: Annotation of DNA sequence of Affimer phagemid vector. The analysis of the sequencing result obtained with M13-26 REV primer for GDH-HPDP-4 clone is shown, with important features highlighted.

4.4.6 Sequence alignment for GDH$_{C.\ diff}$ Affimer binders.

To determine the sequence diversity of the clones, protein sequence alignment of the GDH$_{C.\ diff}$ Affimer binders was performed using the ClustalW alignment tool, and nine distinct Affimers were identified with the amino acid sequences in the VRs given in Table 4.1. For binders occurring more than once, one binder was selected as representative of the group.

Table 4.1: Sequences of variable regions in GDH Affimer binders. The frequency of each sequence is presented, and the conserved residues among the sequences in variable region 1 and 2 (VR1 and VR2) are highlighted.

Representative binder	VR1	VR2	Frequency	Affimer clone ID
GDH-HPDP-19	QQAYYPFQE	VNHWTDAYF	2x	19, 29
GDH-HPDP-18	TLWSYMAAS	HNHGYWDAM	3x	7, 18, 20
GDH-HPDP-28	VEIYIWDYP	AVHGFHMDA	1x	28
GDH-HPDP-23	TQNNLYTPA	AHGFWLDQ	6x	23, 32, 13,8, 8, 21
GDH-HPDP-26	PHISIDYYD	PQHEFWTEE	1x	26
GDH-HPDP-31	VPPLLWDYN	PGHGFFTND	4x	10, 17, 27, 31,
GDH-HPDP-4	HVTQFDSFA	SNHGFFQQE	1x	4
GDH-HPDP-24	HSNGIHGYS	AEMGFFVTR	4x	11, 22, 24, 30,
GDH-HPDP-15	RHPNLWQQY	QSFQMPQYG	3x	1, 12, 15

Analysis of the sequence alignment of the distinct binders for rGDH$_{C.\ diff}$ shows that there are conserved residues in VR2 (shown in red) and potential similarities in VR1 (shown in blue). Only GDH-HPDP-15 has no conserved sequences in VR1 or VR2. The conserved residues in VR2 are presented graphically in Figure 4.9. In VR2, seven out of the nine selected Affimers (77 %) have a histidine residue conserved at position 3, six out of nine (67 %) have glycine at position 4, phenylalanine at position 5, phenylalanine or tryptophan at position 6, while no conserved sequence was found at position 1,2,7,8 and 9. Conserved sequences within the variable loop gives an indication that the binders could be binding to the same epitope on the target.

Figure 4.9. Weblogo analysis of conserved residues of unique GDH binders: The sequence alignment showing conserved residues in the VR2.

4.5 Protein production of rGDH*C. diff* Affimer binders

Once binding of individual clones to GDH had been confirmed by phage ELISA, nine Affimer binders with unique sequences in VR1 and VR2 were identified from the sequencing result. As described in Section 2.2.1, the Affimer coding region was fused to coding region for the C-terminal D2 domain of pIII in the phagemid vector which could obstruct the study of interactions of the binders to GDH. Thus, for expression and further characterisation, the coding sequences of each Affimer binder was subcloned from the phagemid into an expression vector. Once expressed and purified, each Affimer binder was characterised for their biophysical properties and utility in applications such as enzyme-linked binding assays.

4.5.1 Subcloning of selected clones into expression vector

A schematic diagram of the subcloning experiment is provided in Figure 4.10.

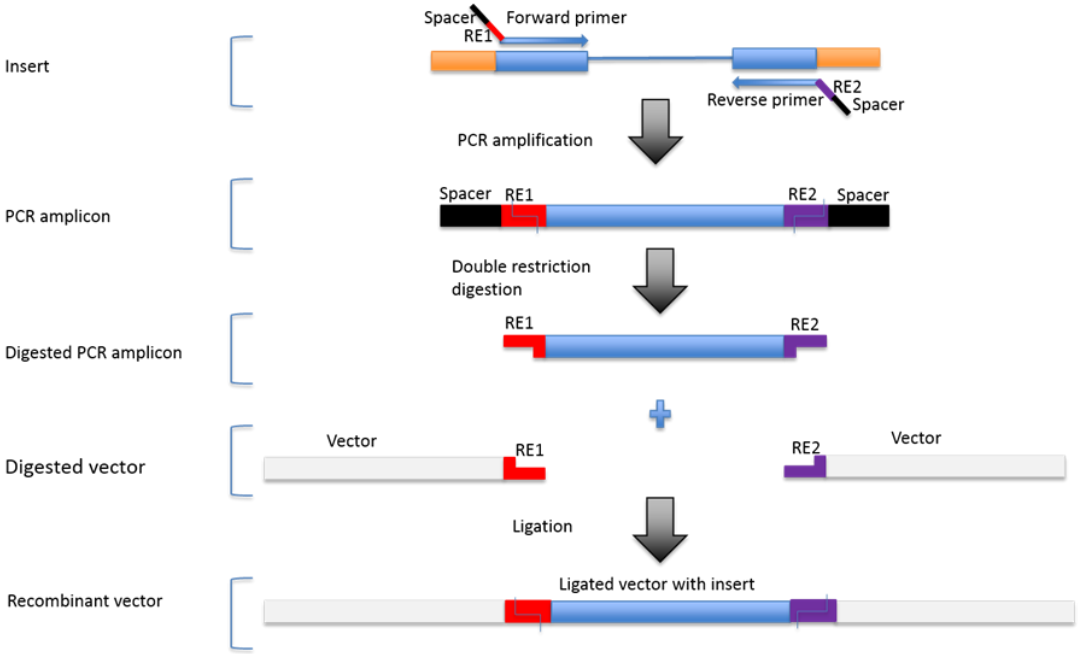

Figure 4.10: Schematic diagram of the subcloning experiment. The steps involved in the subcloning steps are provided which includes amplification, digestion with restriction enzymes 1 and 2 (RE1, RE2), and ligation.

First, the coding region of Affimer binder (insert) is amplified from the phagemid vector by PCR using Phusion DNA polymerase. Since the Affimer library was generated without any cysteine residues, a cysteine codon could be introduced by PCR into the C-terminal region upstream of the His-tag to enable site-specific

coupling of biotin, fluorescent labels or enzymes to facilitate analysis and subsequent use on assays. Thus, the coding DNA sequence for each Affimer binder was amplified as versions with and without a cysteine codon using forward primer and alternative reverse PCR primers (Section 2.6.1). The amplicon is then cleaned up using QiAgen PCR purification kit according to the manufacturer's protocol. Next, both the destination vector (pET11a) and the amplicon was digested with restriction enzyme 1 (RE1) and restriction enzyme 2 (RE2) - NheI/NotI generating cohesive ends. Digested vector and inserts are then ligated to generate a recombinant vector. Transformation of *E. coli* cells with the ligation products and then DNA sequencing is used to confirm the DNA sequence of the insert and insert orientation in the recombinant vector.

The PCR products obtained were initially digested with DpnI to destroy any of the template plasmid DNA, which would be methylated and thus susceptible to this enzyme, and purified using a QIAquick PCR purification kit according to the manufacturer's protocol (Section 2.6.10). The purified PCR products were digested using NheI-HF and NotI-HF restriction enzymes before a further QIAquick PCR purification step and quantification using a Nanodrop spectrophotometer. Figure 4.11 shows the DNA samples of the double digested PCR fragments separated on a 2 % (w/v) agarose gel. These corresponded to the theoretical size of the Affimer binder inserts (370 bp).

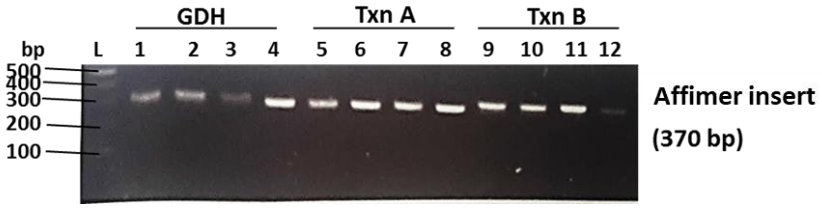

Figure 4.11: Agarose gel analysis of GDH-Affimer binder inserts. After restriction digestion of the PCR products, twelve samples were randomly selected for GDH, toxin A and toxin B and were analysed by 2 % agarose gel electrophoresis to show that the digestion was successful.

4.5.1.1 Ligation and preparation of Affimer coding regions in pET11a for DNA sequencing

Affimer binder inserts were ligated into linearised pET11a expression vector similarly digested with NheI-HF/NotI-HF restriction enzymes, while a ligation control reaction was carried out for the linearised pET11a vector containing no insert. The ligation products were used to transform *E. coli* XL1-Blue competent cells (Section 2.1.2) and the ligation control reaction was used as the negative control for re-ligated plasmids. Over 50-fold increase in colony counts were seen on the ligation plate compared to the negative control plate. For each sample, two clones were selected from the positive plate, then plasmid DNA was prepared from each colony. The DNA concentration of purified plasmid DNA was quantified using a Nanodrop spectrophotometer.

4.5.1.2 DNA sequence analysis of Affimer clones.

As stated in Section 4.5.1, each Affimer coding region was subcloned with or without a cysteine codon at the C-terminal (C96). Plasmid DNA was prepared for two clones per subcloning experiment, therefore, a total of 32 clones were submitted for DNA sequencing using the T7P primer (Table 2.2).

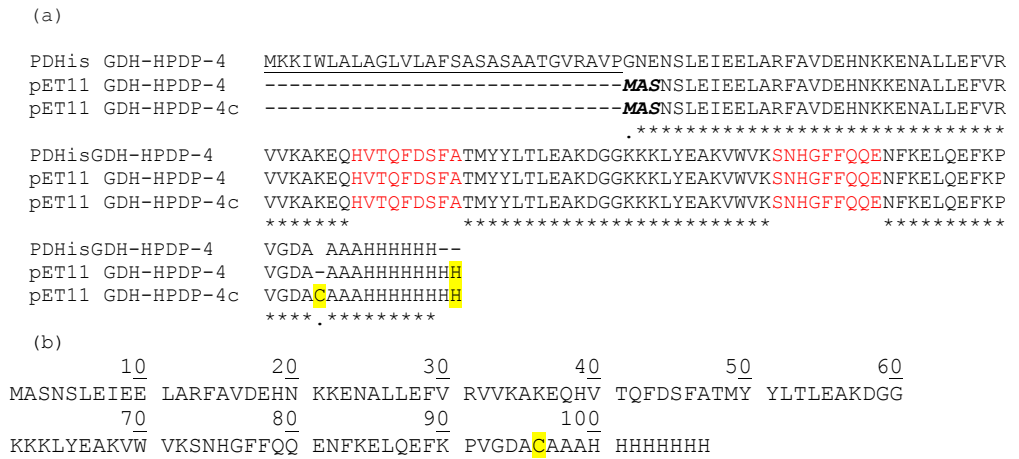

Figure 4.12: Alignment of ExPASy translated sequences of pDHis and pET11a-GDH-HPDP-4 clones. (a) The DNA sequencing analysis shows successful subcloning of Affimer coding region from pDHis into pET11a expression vector and confirms that the pET11a GDH-HPDP-4 clones have the same insert sequence (VR1 and VR2 are shown in red) and that pET11a GDH-HPDP-4C contains the additional cysteine residue (yellow). **(b)** The single C-terminal cysteine was successfully introduced at position 96 of the Affimer coding region.

Subcloning of GDH-HPDP-19C was not successful after three attempts, therefore it was not taken further. DNA sequencing results were translated using the ExPASy translate tool (Gasteiger *et al*., 2003) to ensure the integrity of the Affimer coding region. Each sequence was aligned to the sequence of its corresponding pDHis plasmid and overall, 95 % of the clones had the correct insert sequence. Figure 4.12 showed an annotated version of the sequencing data obtained for GDH-HPDP-4 binder which was used as a representative binder.

These results confirm the successful subcloning of binder coding sequences from pDHis phagemid vector into pET11a expression vector. It confirms that the final-reverse-c primer introduced a cysteine codon into pET11a-GDH-HPDP-4C, positioned as C96 (12 residues from the C-terminal). Also, pET11a vector carried a His_8-tag at its C-terminal rather than His_6-tag in pDHis. Except for GDH-HPDP-19C, the Affimer coding regions were successfully subcloned both with and without a cysteine codon. Table 4.2 gives the subcloning profile of each binder with and without a cysteine codon.

Table 4.2: Subcloning profile for GDH Affimers.

Representative binder	VR1	VR2	Subcloning	
			Without C96	With C96
GDH-HPDP-19	QQAYYPFQE	VNHWTDAYF	✓	X
GDH-HPDP-18	TLWSYMAAS	HNHGYWDAM	✓	✓
GDH-HPDP-28	VEIYIWDYP	AVHGFHMDA	✓	✓
GDH-HPDP-23	TQNNLYTPA	AHGFWLDQ	✓	✓
GDH-HPDP-26	PHISIDYYD	PQHEFWTEE	✓	✓
GDH-HPDP-31	VPPLLWDYN	PGHGFFTND	✓	✓
GDH-HPDP-4	HVTQFDSFA	SNHGFFQQE	✓	✓
GDH-HPDP-24	HSNGIHGYS	AEMGFFVTR	✓	✓

4.5.2 Expression and purification of GDH Affimer binders

E. coli BL21 (DE3) Star competent cells were transformed with the recombinant pET11a expression vectors as described in Section 2.7.1. Recombinant proteins were induced with 0.1 mM IPTG to facilitate transcription from the T7 lac promoter (Studier and Moffatt, 1986). After 6 h induction, the cells were harvested and lysed (Section 2.7.3). To assess the expression profile of each Affimer, the soluble

fraction (SF) and the insoluble fraction (IF) were analysed on a precast 4-20 % SDS-PAGE gel. Figure 4.14 presents only the expression analysis for 12 clones. Seven of these twelve Affimer binders were produced as predominantly soluble proteins. GDH-HPDP-28 Affimer protein was predominantly in the insoluble fraction. On the other hand, GDH-HPDP- (23C, 23, 26C and 26) had very low levels in both soluble and insoluble fractions.

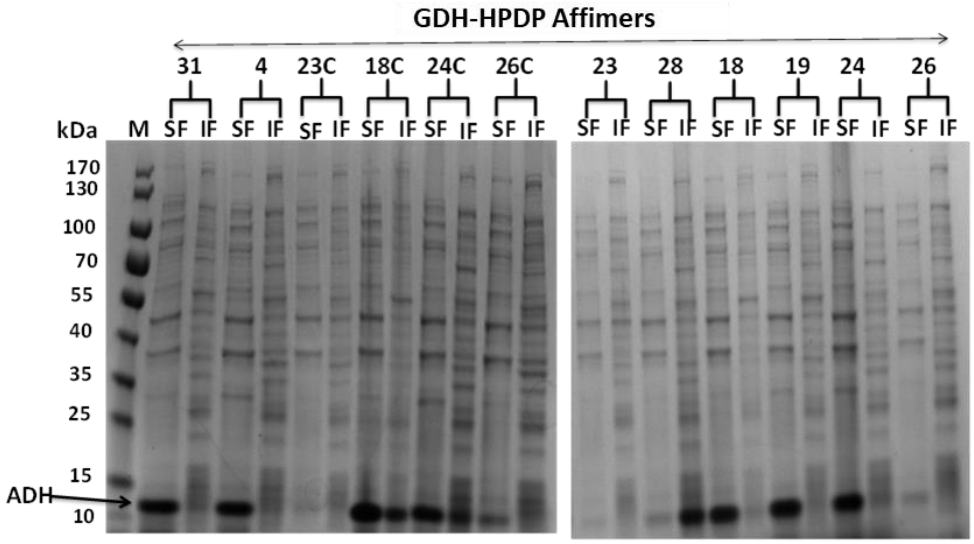

Figure 4.14: Expression analysis of Affimer binders. The soluble and insoluble fraction of each protein sample was resolved on a 4-20 % SDS-PAGE. The Affimer (ADH) is indicated by an arrow; M- Molecular weight markers; SF- soluble fraction; IF- insoluble fraction.

To purify GDH-HPDP Affimers from the soluble fraction, samples were loaded onto Ni-NTA affinity resin slurry. The resin was washed extensively with 20 mM imidazole until the A_{280nm} of the washed fraction is <0.01 which signifies the removal of unbound proteins from the resin, bound protein is then eluted with 300 mM imidazole including 500 mM NaCl. During purification, 300 µL of Ni-NTA slurry was used to capture recombinantly expressed His-tagged protein from a 50 mL culture, since the binding capacity of the resin used is 50 mg his-tagged recombinant protein/ mL resin (Amintra, Expedeon Ltd, Cambridgeshire, UK).

To analyse the fractions obtained during purification, the flow-through (FT) collected after loading the soluble fraction onto the column, the fraction collected after washing the column extensively (fraction OD_{280nm} <0.01), and up to five elution fractions were analysed on 4-20 % SDS-PAGE. The result obtained from the

analysis of these fractions shows that Ni-NTA affinity chromatography is sufficient to effect one-step purification sufficiently pure for our purposes. Since the purification of GDH binders as well as the toxin A and B binders were carried out simultaneously (35 proteins purified), the result for the gel electrophoresis for an example binder toxin B-18 is presented in Figure 4.15a while the purified proteins for GDH Affimers are shown in Figure 4.15b. Purity estimated to be of >99 % was achieved for all GDH Affimer binders as shown in Figure 4.15b.

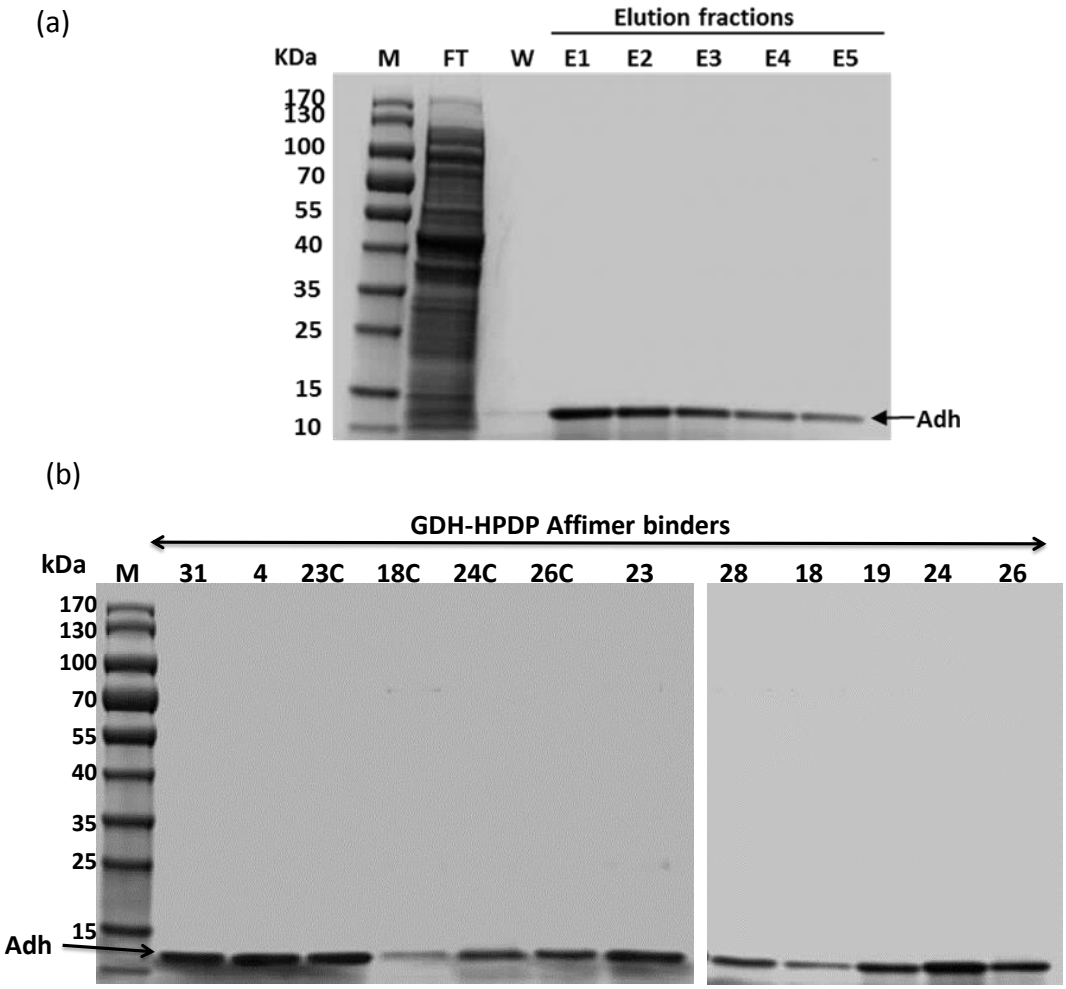

Figure 4.15: SDS-PAGE analysis of the purification of Affimers. Analysis on 4-20 % SDS-PAGE gel of purified Affimers after one-step Ni-NTA affinity chromatography. Gel (a) gives the analysis of fractions obtained during purification of Affimer binders. A 5 µg aliquot of each GDH binder was loaded on the gel (b). Affimers produced a single band of ca. 12 kDa as expected. M- Molecular weight markers; FT- flow-through; W- last wash; E1- E5- elution fractions; ADH- Affimer.

The SDS-PAGE gel analysis of the fractions obtained during purification as presented in Figure 4.15a shows that the flow-through and the wash elution

fraction contained a faint band present at 12.5 kDa, corresponding to the expected size of expressed Affimer. This showed that all other soluble proteins were successfully washed off, while the expressed His-tagged Affimer remained complexed with the resin during the washing step. Bound Affimer were eluted with a single band migrating at ~12 kDa corresponding to the expected size of Affimer in the eluted fractions. The theoretical molecular mass and pI for each Affimer binder was calculated using the ExPASy protparam tool and is presented in Table 4.3 alongside the calculated protein yield in mg/L for cysteine and no cysteine-containing Affimer.

Table 4.3: Properties and yields of purified Affimer proteins. Calculated molecular mass (MM), pI and the concentration of protein obtained from purification.

Affimers	MM (kDa)	pI	Yield (mg/L)	
			No cys	With cys
GDH-HPDP-31	12.3	6.54	213.0	Not expressed
GDH-HPDP-28	12.4	6.4	11.1	0.8
GDH-HPDP-24	12.2	7.21	249.7	169.6
GDH-HPDP-18	12.4	6.83	232.2	42.8
GDH-HPDP-23	12.3	6.83	8.0	5.5
GDH-HPDP-4	12.4	6.59	306.2	148.1
GDH-HPDP-26	12.5	6.24	37.0	36.6
GDH-HPDP-15	12.5	8.03	99.8	54.9
GDH-HPDP-19	12.5	6.54	313.6	Not expressed

As seen in Table 4.3, the protein yield for Affimer proteins ranged from 0.8 mg/L to 313.6 mg/L. These data are consistent with the expression profile obtained for the Affimers as shown in Figure 4.14. GDH-HPDP-28, 28C, 23, 23C, 26 and 26C, with very low protein expression profile gave the poorest protein yields, while Affimer binders such as GDH-HPDP-31, 19 and 4, with very high expression levels, gave similarly high protein yield with GDH-HPDP-4 having the highest protein yield. The pattern of protein yield obtained from Affimer proteins without cysteine were higher than those of the corresponding protein containing the cysteine. For example, GDH-HPDP-4 had a yield of 306.2 mg/L while GDH-HPDP- 4C had a yield of 148.1 mg/L. This represents a 52 % decrease in the protein yield. Overall, 4 of the 7 binders had at least a 40 % decrease in protein yield when expressed as a cysteine-containing protein.

The reason for the reduced yield is unclear, and is not due to reduced expression levels as shown in Figure 4.14. One possible explanation is that the proteins aggregated during purification steps and could not be purified to the same level as those Affimers without cysteine residue. Addition of reducing agents in buffers used for lysis and elution may enhance future yields. Nevertheless, the yield obtained from the cysteine-containing Affimers was sufficient for further analysis.

4.6 Biophysical characterisation of binders

Purified Affimer proteins were characterised to determine their biophysical properties using two techniques. First, size exclusion chromatography was used to analyse the oligomeric state of the proteins. Second, Optim® 2000 (Avacta) was used to determine the thermostability profile of each protein using the intrinsic florescence properties while the static light scattering function of Optim was used to decipher the aggregation profile of each protein. For this biophysical characterisation, 4 of the 7 GDH Affimer binders were selected as representatives. These are GDH-HPDP-4, -15, -19, and -24. The results obtained from each analysis are presented below.

4.6.1 GDH Affimer proteins are monomeric

Size exclusion chromatography was used as an analytical technique to identify the oligomeric state of purified GDH Affimer proteins (non-cysteine Affimers). Each binder was buffer exchanged into 1 x PBS (pH 7.4) and prepared to a concentration of 1 mg/ml before loading onto a Superdex 200 10/300 column. Absorbance of each sample was monitored at 220 nm, 260 nm and 280 nm, also conductivity was monitored to detect changes in salt concentration during the chromatographic run. Chromatograms obtained for the binders are presented in Figure 4.16. Comparing the absorbance of each Affimer at the three different wavelengths used, a general trend is seen, $A_{260\ nm}$ showed the least absorbance which indicated minimal contamination of the sample with nucleic acids. At $A_{280\ nm}$, a low absorption reading was obtained, this is because the Affimer scaffold contained only a few aromatic amino acid residues in its backbone. This signal was amplified at $A_{220\ nm}$ where peptide bonds absorb light. A stable signal obtained from monitoring conductivity

throughout the chromatographic run shows equilibration of the salt concentration in the column buffer.

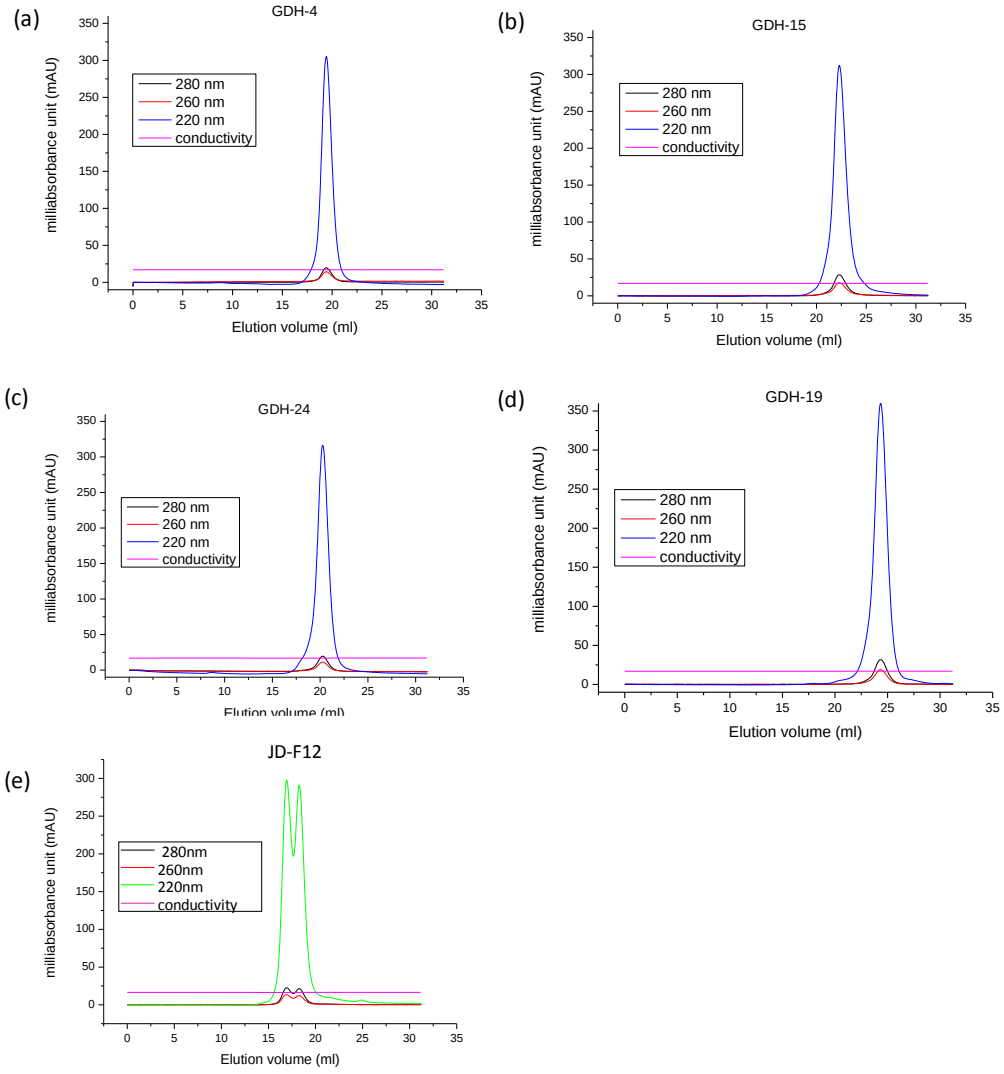

Figure 4.16: Size exclusion chromatography for GDH Affimer binders: Purified protein samples of GDH Affimers were analysed using Superdex 200 10/300 column. The chromatograms of the GDH Affimers showed single monomeric peaks compared to JD-F12 Affimer which is an oligomeric Affimer (showing two peaks) and used as a negative control.

As shown above, all four GDH Affimer binders show a monomeric peak as expected. This result is consistent with the literature that wild-type Affimer, and >90 % of binders selected from the Affimer phage library are monomeric (Tiede *et al.*, 2014).

4.6.2 Thermostability and aggregation profile of GDH Affimer proteins

Thermostability and aggregation profile of GDH binders were characterised using the Avacta OpTim® 2000 analytical instrument (see Section 2.12.4 and 3.4.4). When compared with Differential scanning calorimetry (DSC) which is a standard technique for measuring the thermostability of protein samples, Avacta OpTim® 2000 provides useful advantages. First, only 4 µL of sample at a concentration as low as 0.5 mg/mL is needed compared with Differential scanning calorimetry (DSC) which requires 2 ml of 1 mg/mL per sample. Second, 48 samples can be analysed at once using the multi cuvette array (MCA) in Optim while only one sample can be analysed by DSC. Third, there is no need for a buffer control in Optim and finally, it uses intrinsic fluorescence technology and static light scattering to test more than one parameter including protein stability, unfolding transition temperature, aggregation onset temperature (T_{agg}), simultaneously of a protein. The only limitation in using an Optim in this work is that the temperature ranges from 10-90 ^{o}C while DSC can analyse over a temperature range from 0 to 130 ^{o}C. Nevertheless, Optim was the preferred technique since the binders would not be used in any application that requires a temperature greater than 90 ^{o}C.

The static light scattering (SLS) of the Affimers was recorded as the samples were heated from 10 to 90 ^{o}C to detect the presence of aggregates. Importantly, the aggregation onset temperature (T_{agg}), which is the temperature at which a protein begins to aggregate, was identified for each Affimer. T_{agg} is usually accompanied by a significant increase in the static light scattering (SLS) intensity count. Figure 4.17 gives the thermogram for GDH binders. Analyses were performed in duplicate and the data presented are the average obtained.

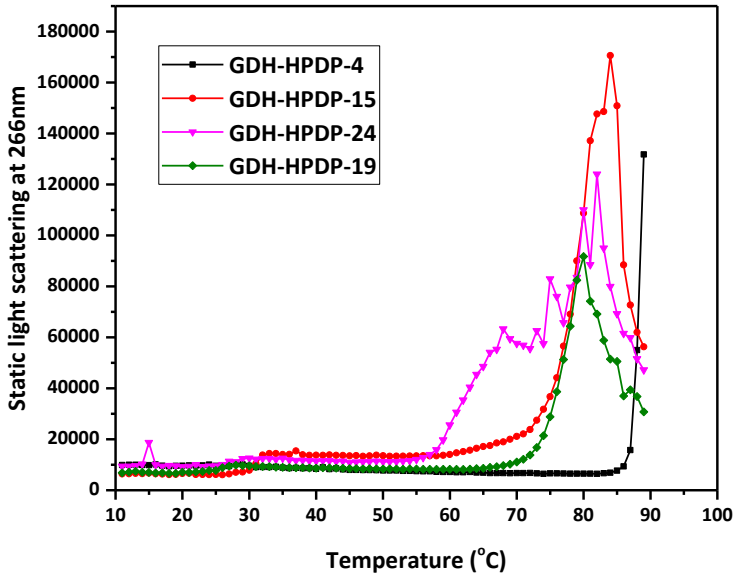

Figure 4.17: The static light scattering of the GDH Affimer binders at pH 7 upon thermal stress by Optim. Thermally induced aggregation of GDH Affimer samples were monitored with static light scattering. Duplicates were performed and the mean values were plotted.

The thermostability of each binder is shown in Figure 4.17 the four binders show a similar pattern of stability with <20,000 static light scattering (SLS) intensity count as they were heated from 0 to 60 °C. Then, as the temperature increases each binder displayed its distinct property. For comparison, the T_{agg} for each binder was set as the temperature at which the SLS intensity count is >25,000. Affimer GDH-HPDP-4 has the highest thermostability with T_{agg} of 88 °C (SLS intensity count 15,733.5 at 87 °C to 55,010.5 at 88 °C and 131,750.0 at 89 °C). GDH-HPDP-19 has a T_{agg} of 75 °C, with a SLS intensity count that peaks at 80 °C. GDH-HPDP-15 has a T_{agg} of 73 °C with a SLS intensity count which peaks at 85 °C while GDH-HPDP-24 has a T_{agg} of 60 °C, and a broad aggregation profile from 60 °C which peaks at 80 °C.

4.7 Characterisation of Affimer Binding to rGDH*C. diff*

4.7.1 Protein ELISA using purified GDH Affimer protein

Protein ELISA was carried out to test for the binding of purified Affimer binders to GDH. Each Affimer (without cysteine) at 10 µg/mL was adsorbed onto a separate microtitre plate well and incubated overnight. 1 µg/mL of biotinylated GDH was added to wells and detected with strep-HRP. Binding was confirmed with the

addition of TMB substrate and incubated for 6 min and the absorbance at 620 nm was then measured. As expected, all GDH binders showed binding to GDH. GDH-4 has the highest signal intensity ($OD_{620\ nm}$= 1.4) while GDH-28 has the lowest signal intensity ($OD_{620\ nm}$= 0.14). There was no binding in the control wells that contained the toxin B Affimer, which showed the specificity of the Affimer binders in the test wells to GDH. The protein ELISA results confirmed that Affimer phage binders, selected from the phage display library maintained binding to the target as purified Affimer protein. It is interesting that despite the small size of the Affimers and how they were randomly oriented during adsorption onto the wells, the Affimers bound specifically to GDH.

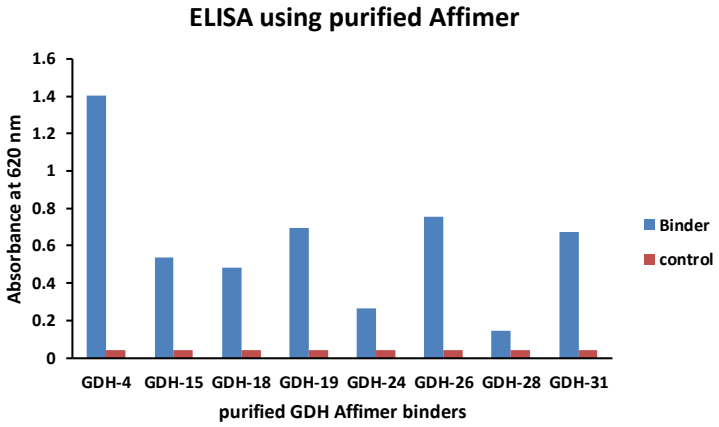

Figure 4.18: Protein ELISA for purified GDH Affimer binders. Biotinylated GDH was used to detect immobilised Affimers followed by the addition of strep-HRP. Binding was confirmed with the addition of TMB substrate and signal was measured at 620 nm. The blue bars represent the binding for each Affimer binder with biotinylated GDH while the red bar (control) showed no binding for biotinylated GDH in wells containing toxin B-Affimer.

4.7.2 Sandwich ELISA of GDH Affimers to Hexameric GDH

GDH from *Clostridium difficile* is a hexameric protein which implies that each subunit has a binding site for an Affimer. To test the binding of Affimers to hexameric GDH, a sandwich assay format was used as outlined in Section 2.11.2. As seen in Figure 4.18 GDH-4 has the highest signal intensity for binding to GDH, therefore it was selected to be used as capture Affimer. A 10 µg/mL solution of non-biotinylated GDH-4 was immobilised in each well and used to capture GDH. A panel of all biotinylated GDH–Affimer binders were prepared at 1 µg/mL and used

as detection Affimer. Therefore, each well has a sandwich of GDH-4 + GDH target + biotinylated detection Affimer. Binding was detected with Streptavidin-HRP and the $A_{620\ nm}$ was recorded at 6 min incubation with the TMB substrate. The results are presented in Figure 4.19.

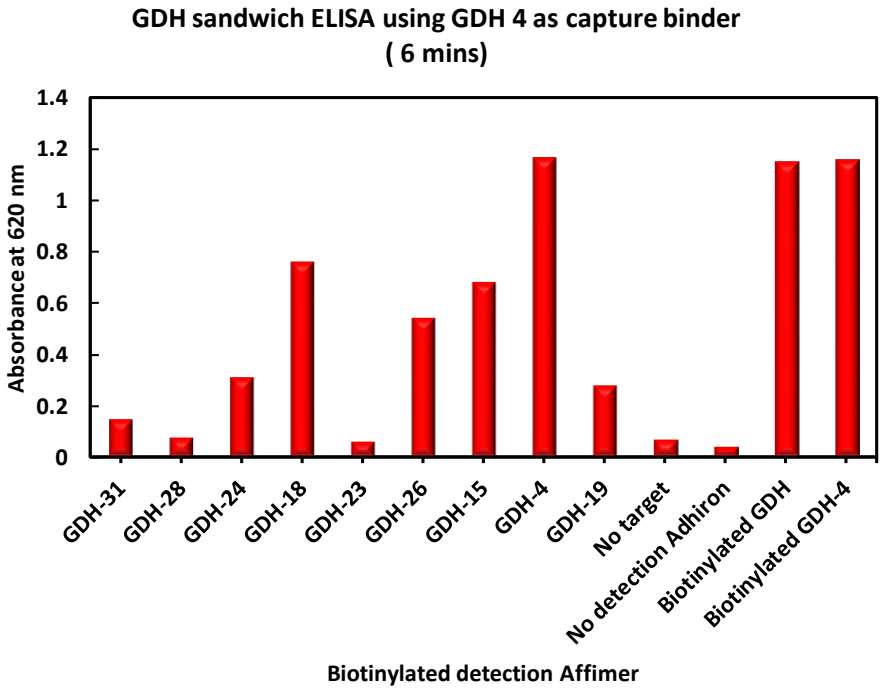

Figure 4.19. GDH-sandwich ELISA: Non-biotinylated GDH-HPDP was immobilised onto Nunc wells and was used to capture GDH. Biotinylated GDH-HPDP Affimer binders was used as detection binder. The binding of the sandwich assay was detected using Strep-HRP and TMB substrate.

From the sandwich ELISA, the detection binder that gave the strongest and highest signal is GDH-4. This shows that GDH-4 that gave the highest affinity binder for GDH, can serve as both a capture binder and detection binder and provides the most sensitive detection of all Affimer combinations tested.

4.8 Comparative studies of binders with commercially available kit.

Glutamate dehydrogenase is produced in large quantities in both toxigenic and non-toxigenic strains and has been found to be highly conserved between PCR ribotypes (Carman *et al.*, 2012). It is usually referred to as *C. difficile* common antigen. Glutamate dehydrogenase ELISA remains a sufficient screening test to

accurately rule out the presence of *Clostridium difficile* in faecal samples (Sharp, *et al*, 2010; Goldenberg *et al*., 2010). A GDH ELISA test has been recommended as a possible first step in a two-step diagnostic algorithm by current UK and USA guidelines (Novak-Weekley and Hollingsworth, 2008). One of the most widely used kits, the Techlab Quik CheK® can detect up to 0.8 ng/mL of GDH in clinical samples. Most researches confirm it has a specificity of 100 % and sensitivity of 99 %. According to the package insert, this sandwich ELISA consists of microwells coated with polyclonal antibodies against GDH and the conjugate solution containing highly specific monoclonal antibodies conjugated to horseradish peroxidase.

It was therefore necessary to test the sensitivity and specificity of identified Affimers against glutamate dehydrogenase from *Clostridium difficile* compared to Techlab Quik CheK® kit.

4.8.1 Determination of the Limit of Detection (LOD) for Affimers against rGDH *C. diff*

Sandwich phage ELISA was used to determine the limit of detection of Affimer binders using serial dilutions of PBS spiked with purified rGDH$_{C.\ diff}$ protein from 2500 ng/mL to 1.2 ng/mL). Following on from the result shown in Figure 4.19, GDH-4 was used as the capture while GDH-4 phage or GDH-18 was used for detection and their signal intensity compared. As described in Section 2.13.1, 50 µL of biotinylated capture at 1 µg/mL was immobilised onto streptavidin coated Nunc Maxisorp plate, and then 50 µL from the serial dilutions were added to their respective well. A 50 µL aliquot of the detection phage supernatant introduced to bind captured target. Binding was detected using anti-phage-HRP then TMB substrate.

4.8.1.1 Optimisation of incubation time

To monitor the effect of TMB incubation time on the ELISA signal intensity, the ELISA signal for the sandwich phage ELISA was measured at 3, 9, 15, 30 and 45 min as shown in Figure 4.20.

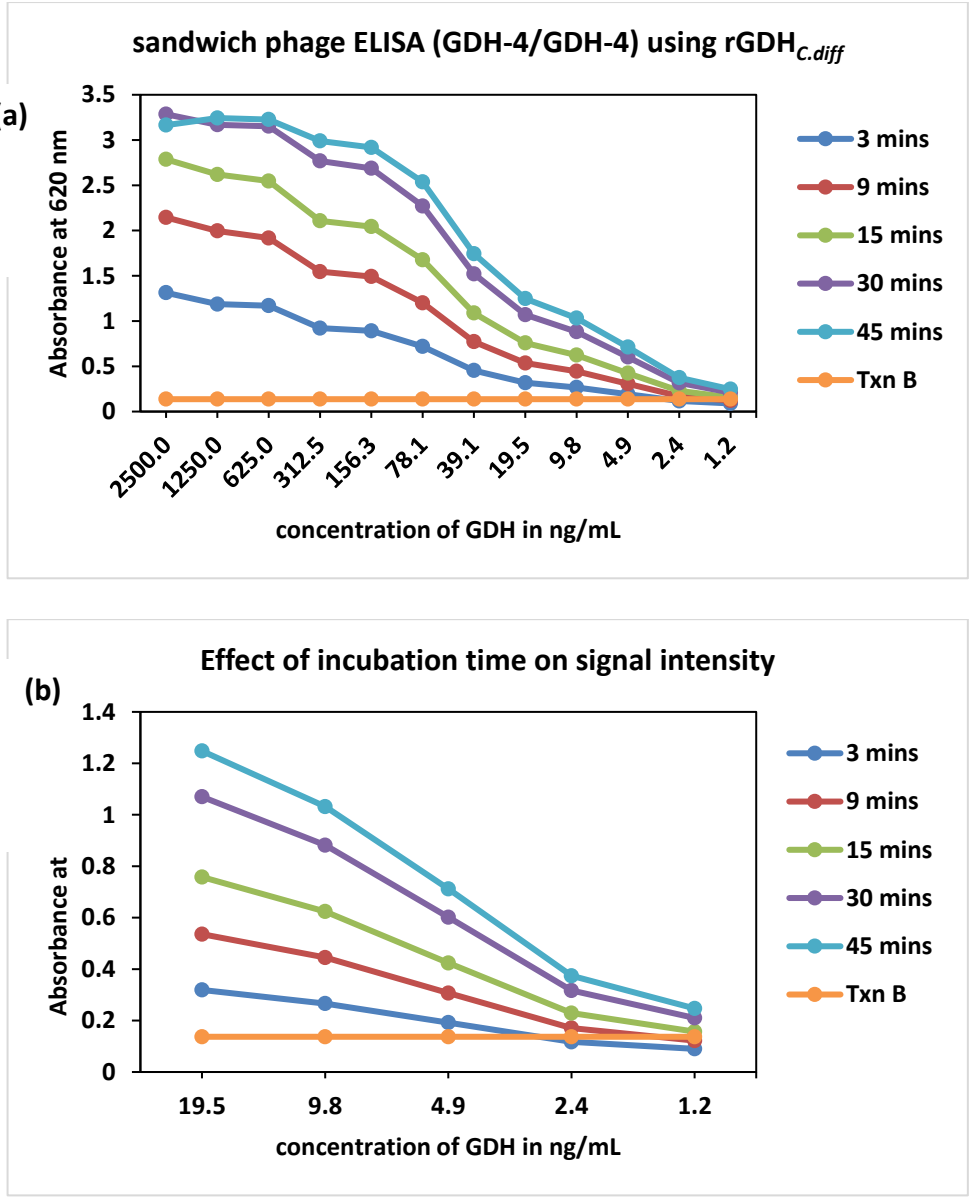

Figure 4.20. Optimisation of incubation time for GDH-4 phage ELISA. (a) Sandwich phage ELISA for GDH using GDH-4 as capture Affimer binder and GDH-4 phage as detection binder. A serial dilution of $rGDH_{C.\ diff}$ from 2500 ng/mL to 1.2 ng/mL was used to determine the limit of detection of the Affimer. (b) Expanded segment of part (a) showing the signal intensity obtained between 19.5 ng/mL to 1.2 ng/mL. Signals at 3, 9, 15, 30 and 45 min are represented as navy, red, green, purple and blue trend lines.

As a negative control, toxin B at 2500 ng/mL was used to replace the target and even at 45 min incubation (orange line) no signal was observed between the capture and detection binder in the absence of the target.

From Figure 4.20a, it was confirmed that GDH-4 can serve as both capture and detection molecule for hexameric GDH. Next, the signal intensity was observed at

regular time points for each target concentration to identify the best incubation time for the assay. This result shows that as the incubation time increases, the signal intensity also increases. However, the effect of longer incubation times could not be easily detected at lower toxin concentration. Therefore, for better assessment, the signal intensity from 19.5 ng/mL to 1.2 ng/ mL was expanded in Figure 4.20b. This shows that increasing the incubation from 3 min to 30 min, there was a 234 % increase in signal intensity (from at 19.5 ng/mL GDH concentration and a 133 % increase at 1.2 ng/mL GDH concentration. From this result, increasing the incubation to 30 min increases the limit of detection for GDH from 9.8 ng/mL to 1.2 ng/mL. As expected, no signal was observed when toxin B (negative control) was used as the target against biotinylated GDH-4 and GDH-4 phage with 45 min incubation time.

4.8.1.2 GDH-4 Affimer as best capture and detection molecule GDH.

Since GDH-4 could serve as both capture and detection Affimer, its limit of detection was compared with the GDH-4/GDH-18 pair in a sandwich phage ELISA. As shown in Figure 4.21, GDH-4/GDH-18 detects GDH up to 19.5 ng/mL while GDH-4/GDH-4 detects GDH at 1.2 ng/mL. This result shows that GDH-4 has higher affinity for GDH than GDH-18. Importantly, GDH-4 is sufficient to act as both capture and detection binder.

In *Clostridium difficile* infection, GDH would be present in faecal samples alongside the bacterial toxins. To test for the specificity of GDH-4/ GDH-4 pair, toxin A or toxin B at 2.5 µg/mL were used as target in place of GDH. The absorbance at 620 nm was measured after 30 min incubation with TMB. The result obtained is presented in Figure 4.21. It shows that there was no binding (no positive signal detected) with either toxin A or toxin B as the trendline for toxin A and B overlaps. This result indicates that the GDH Affimer is specific for the detection of GDH from *C. difficile*.

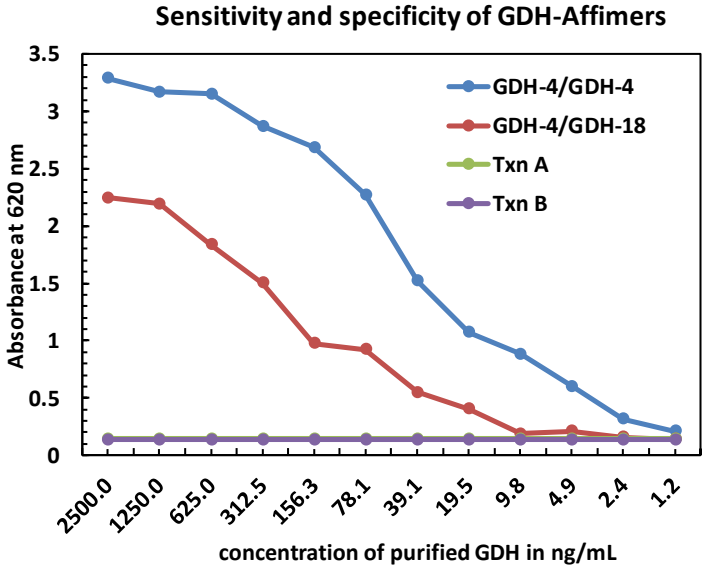

Figure 4.21: Evaluating the sensitivity and specificity for GDH Affimer pairs. The limit of detection was compared for GDH-4 (capture) / GDH-4 phage (detection)- blue trendline and GDH-4 (capture)/ GDH-18 (detection) - red trendline. Specificity was tested using toxin A (green trendline) or toxin B (purple trendline) as target, no binding occurred as expected in the absence of GDH.

4.8.2 Affimer has comparable sensitivity to GDH techlab kit

The ability of GDH-4 Affimer to serve as a capture molecule in an Affimer-antibody hybrid assay was tested. This was done by replacing the capturing antibody in the Techlab Quik CheK® with biotinylated GDH-4 Affimer immobilised onto streptavidin-coated plates.

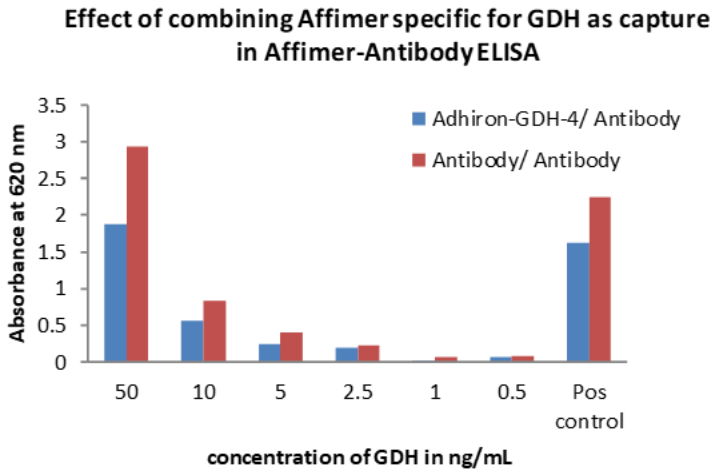

Figure 4.22: ELISA showing hybrid assay for GDH Affimer. The signal intensity for Antibody/Antibody sandwich assay was compared with those from Affimer/Antibody assay

As shown in Figure 4.22, GDH was detected in both the antibody-antibody assay and the Affimer-antibody assay at concentration of 2.5 ng/mL in spiked buffer. With further optimisation, this result suggests that Affimers against $GDH_{C.\ diff}$ can be used as alternative capturing molecule in diagnostic kit for CDI screening.

4.9 Summary

Identification of high affinity specific diagnostic reagents is essential for the development of affinity reagent for *C. diff* infection diagnosis. One of the validated biomarkers for *C. diff* is glutamate dehydrogenase. In this chapter, the design of a synthetic gene and the successful production of active recombinant *C. difficile* glutamate dehydrogenase were demonstrated. The enzyme activity was maintained after biotinylation. Using phage display technology, highly specific Affimers against $rGDH_{C.\ diff}$ have been selected. Nine Affimers were identified through DNA sequencing. These were subcloned successfully into the expression vector pET11a and were expressed and purified. Characterisation of GDH Affimer binders shows that the properties of these binders are consistent with those of toxin A and toxin B Affimer binders (see chapter 5) as well as published data (Raina *et al*., 2015; Tiede *et al*., 2012). GDH Affimer proteins were purified from the soluble fraction of cell lysates with yields as high as 300 mg/L. >98 % of the binders were monomeric and they can withstand thermal stress at 85^{o}C without forming aggregates. The binding of GDH Affimers to GDH has been confirmed using protein ELISA and sandwich ELISA. Using GDH-4 as capture Affimer and GDH-4 phage for detection, the limit of detection for GDH was determined to up to 1.2 ng/mL. Further studies are required to explore approaches to enhance the detection limits and considerations of possible future experiments will be discussed in Chapter 7.

Chapter 5: Identification and characterisation of Affimer binders against *C. difficile* Infection toxin A and toxin B

5.1 Introduction

The previous chapter discussed the identification and selection of specific Affimer binders for *Clostridium difficile* glutamate dehydrogenase, which is a common antigen found in both toxigenic and non-toxigenic strain of the bacteria. Glutamate dehydrogenase remains a key screening biomarker for *Clostridium difficile* infection, in addition to the two toxins (toxin A and toxin B) used as diagnostic biomarkers in CDI (Planche *et al*., 2013). During the infection, *C. difficile* produces one or both virulence factors toxin A and toxin B.

One of the readily available diagnostic test for the detection of toxin A and toxin B in clinical samples is enzyme immunoassay (see Section 1.3.2). As described in Section 1.4, enzyme immunoassays rely on the use of antibodies as molecular recognition elements because they bind their targets with high affinity and specificity. Nevertheless, their batch-to-batch variation, cost, production timeframe and modest thermostability, have been the major limitations of these assays. On the other hand, commercially available diagnostic ELISA kits for *Clostridium difficile* infection have displayed unacceptably low sensitivity, which makes them inadequate for them to be used as a standalone test (Eastwood *et al*., 2009, Crobach *et al*, 2010, Planche and Wilcox, 2011). Therefore, there remains a huge desire to develop an optimum diagnostic test, which is highly sensitive, specific, cheap, and could be incorporated into a point-of-care technology for CDI diagnosis.

This chapter describes the identification of highly specific and sensitive Affimer binders to toxin A and B by phage display. The identified Affimer proteins were expressed, purified and characterised to determine their biophysical properties and affinity profiles. Finally, pairs of Affimers that recognised different epitopes on toxin A and B were identified for use in sandwich-type of applications. Together with the Affimers identified against glutamate dehydrogenase from *C. difficile* in Chapter 4, a panel of Affimers was generated which could be tested for the development of a one-step diagnostic tool for *C. difficile* infection.

5.1.2 Toxin A and toxin B target

To isolate Affimer binders against toxins A and B, which are routinely used as diagnostic biomarkers for *Clostridium difficile* infection, purified native proteins of toxin A and toxin B (VPI 10463 strains) were kindly provided by Dr Cliff Shone, Public Health England (PHE), Porton Down.

5.2 Phage Display

5.2.1 Biotinylation of toxin A and toxin B

In preparation for the phage display screening, biotinylation of toxin A and toxin B was performed using EZ-Link® NHS-SS-biotin (Section 2.8.2) which labels lysine ε-amino groups and N-terminal amine groups exposed on toxin A and B. Then, ELISA was used to confirm biotinylation and the absorbance read at 620 nm within 3 min of incubation with the TMB substrate (Section 2.8.3). Biotinylated GDH protein (Chapter 4) was used as the positive control while blocking buffer was used as the negative control (blank). The result presented in Figure 5.1 shows that toxin A and B were successfully biotinylated.

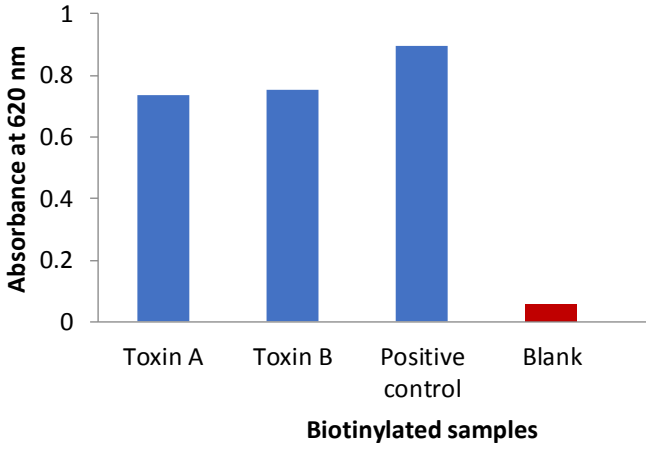

Figure 5.1: ELISA to show biotinylation of toxin A and B. The binding of immobilised biotinylated toxin A and toxin B to strep-HRP were detected using TMB substrate. The signal intensity of the binding was measured at 620 nm wavelength, which showed the successful biotinylation of toxin A and B when compared with the positive control (biotinylated GDH). No signal was observed in the negative control containing only blocking buffer (blank) as expected.

5.2.2 Screening of Affimer phage Library for specific and high affinity binders

Once biotinylated, toxin A and toxin B were immobilised on high affinity streptavidin-coated strips (Thermo Scientific). The Affimer phage display library was screened against the immobilised toxin A and B wells to identify specific and high affinity binders using three biopanning selection rounds as described in Chapter 2 (Section 2.9.2). After each biopanning round, phage particles were eluted with an acid and then an alkali elution step. They were then used to infect ER2738 cells, and the resulting colonies collected were infected with M13K07 helper phage to generate a fresh enriched phage pool. Three standard panning rounds were carried out for both toxin A and B, but only toxin A screen was successful from which 32 clones were randomly picked for phage ELISA. Due to the failure of toxin B screen, the phage display screening for toxin A and B was repeated. This time with a view to exerting selective pressure to ensure specificity, the third panning round for toxin B included a competitive incubation in the presence of free non-biotinylated toxin A. Similarly, free non-biotinylated toxin B was included in toxin A screen. Over 500-fold amplification in colony recovery was observed compared to control samples. As shown in Table 5.1, 48 clones were randomly picked from the toxin B screen while an additional 32 clones were randomly picked from the toxin A screen.

Table 5.1 Number of clones selected from toxin A and B screen

Target	Final panning round	Tested in phage ELISA	Positive clones sequenced
Toxin A	3rd standard panning round	32	21
	with 24h incubation of free toxin B	32	16
	Total	**64**	**37**
Toxin B	3rd standard panning round	-	-
	with 24h incubation of free toxin A	48	32
	Total	**48**	**32**

The individual selected clones were isolated, grown overnight and phage was produced in a 96-well format (section 2.10.1). Finally, phage clones were tested for their ability to bind their target by phage ELISA (section 2.10.3).

5.3 Identification of target-binding Affimer clones.

5.3.1 Phage ELISA

The phage ELISA was performed to investigate the binding and specificity of Affimers for toxin A and B. As an example, the 96 well plate layout for toxin A phage ELISA (from the standard panning round) is shown in Figure 5.2. On the streptavidin-coated plate, wells A1 to H4 (32 wells) were incubated with biotinylated toxin A, wells A5 to H8 (32 wells) contained the blocking buffer (negative control) and wells A9 to H12 (32 wells) incubated with biotinylated toxin B. Then, phage-containing suspension was added to all wells. Binding was confirmed by using HRP-conjugated anti-phage antibody, then visualised using TMB substrate.

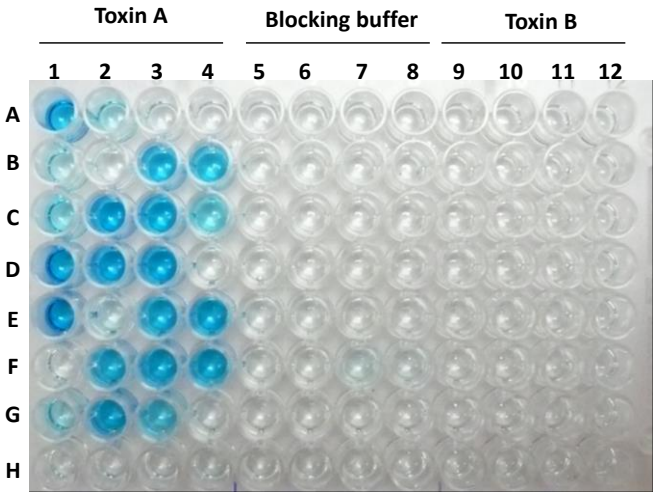

Figure 5.2 Plate layout for Phage ELISA. The 96 well plate layout for toxin A phage ELISA performed on 32 toxin A Affimer binder clones randomly selected after three rounds of panning of phage display library. A1-H4 wells were immobilised with biotinylated toxin A, A5-H8 contained blocking buffer (negative control), and A9 – H12 contained immobilised biotinylated toxin B (cross-reactivity test). Therefore, clone A1 has a negative control well A5 and a cross-reactivity test well A9 etc.

Binding of Affimer-displaying phage raised against toxin A was observed in 21 wells containing immobilised toxin A, while no binding occurred in the blank wells or in

the immobilised toxin B wells. This indicates that 21 of the randomly selected toxin A phage clones express Affimers that bind to toxin A and that they are specific for toxin A showing no cross-reactivity with toxin B. Similar ELISA analysis of random clones selected against toxin B was also performed. The absorbance readings of each ELISA well were measured after 6 min of incubation with TMB substrate. The data are presented graphically in Figure 5.3 for toxin A and Figure 5.4 for toxin B.

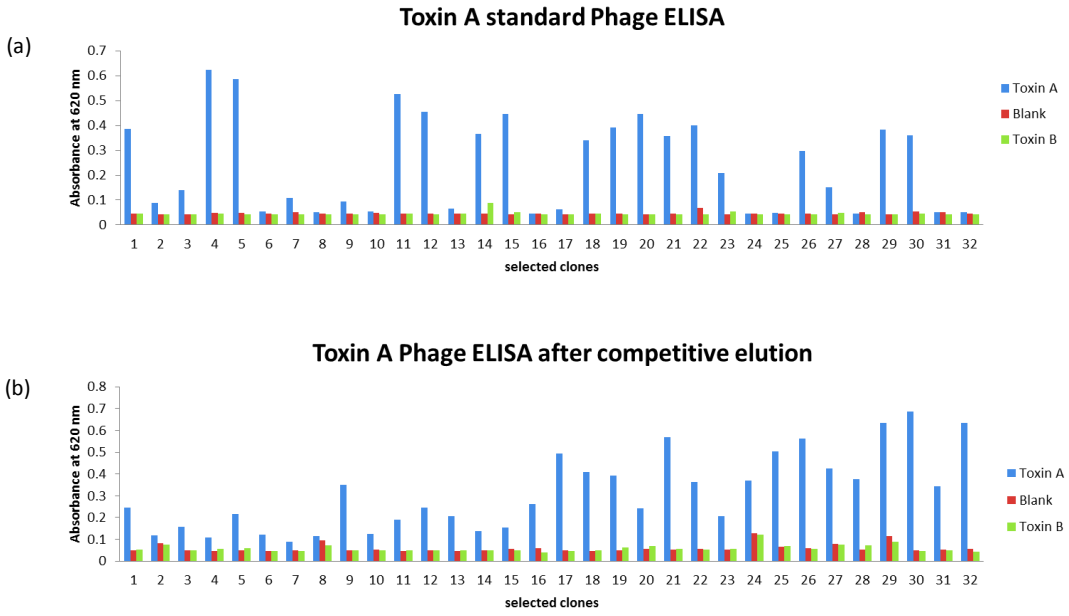

Figure 5.3. Toxin A phage ELISA. (a) toxin A phage ELISA after 3rd standard panning round. (b) toxin A phage ELISA after 3rd panning round with 24 h incubation with free toxin B. signals for toxin A (blue bar), blocking buffer control (red bar) and toxin B for cross-reactivity control (green bar) are presented.

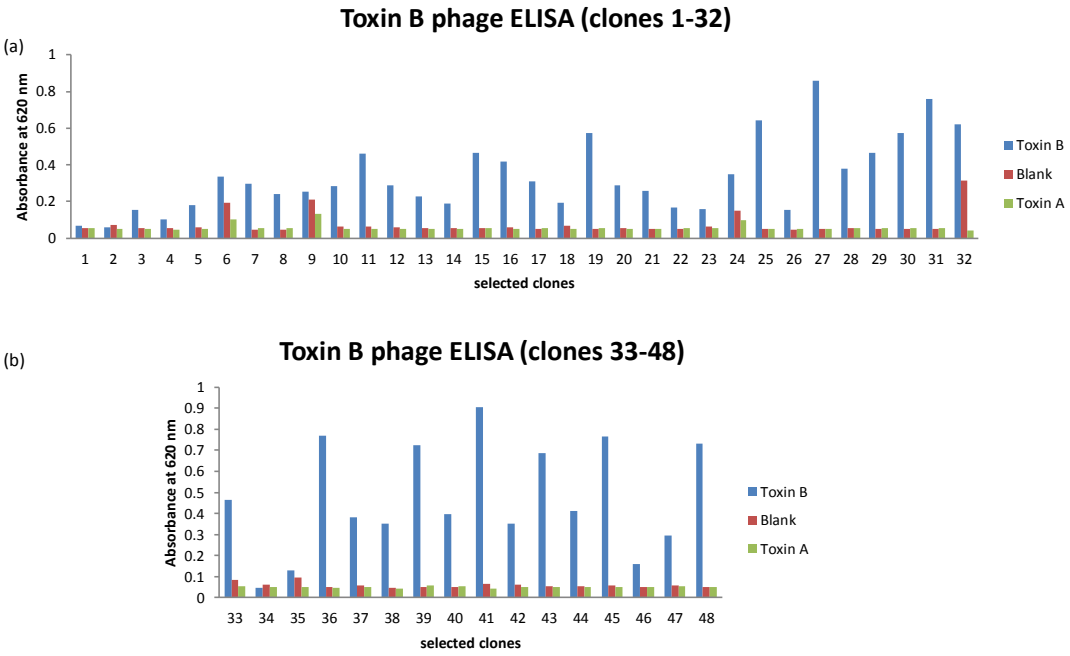

Figure 5.4. Toxin B phage ELISA. Toxin B phage ELISA of the selected clones 1-32 are presented in (a) and 33-48 in (b). Signals for toxin B (blue bar), blocking buffer control (red bar) and toxin A for cross-reactivity control (green bar) are presented.

Figure 5.3 and 5.4 gives the absorbance readings obtained from the toxin A and toxin B phage ELISAs. Clones with >2-fold increase in absorbance over their controls were selected for DNA sequencing. It is positive that binders are specific for the target against which they were screened, despite the fact that toxin A and B exhibit a high degree of overall sequence similarity of 66 % (Von Eichel-Streiber *et al*., 1992**,** Di Bella *et al*., 2016).

5.3.2 DNA Sequencing

In total, phagemid DNA was prepared from 37 clones for toxin A and 32 clones for toxin B (Table 5.1) that were judged to be positive in the phage ELISA, and submitted for DNA sequencing from the M13-26REV primer (Table 2.3). Sequencing results were analysed using ExPASy translate tool (Gasteiger *et al*., 2003) to ensure the integrity of the Affimer coding region and insertional junctions and to determine their amino acid diversity in the VR1 and VR2. Figure 5.5 shows an annotated version of the sequencing data obtained for Toxin A-1 binder.

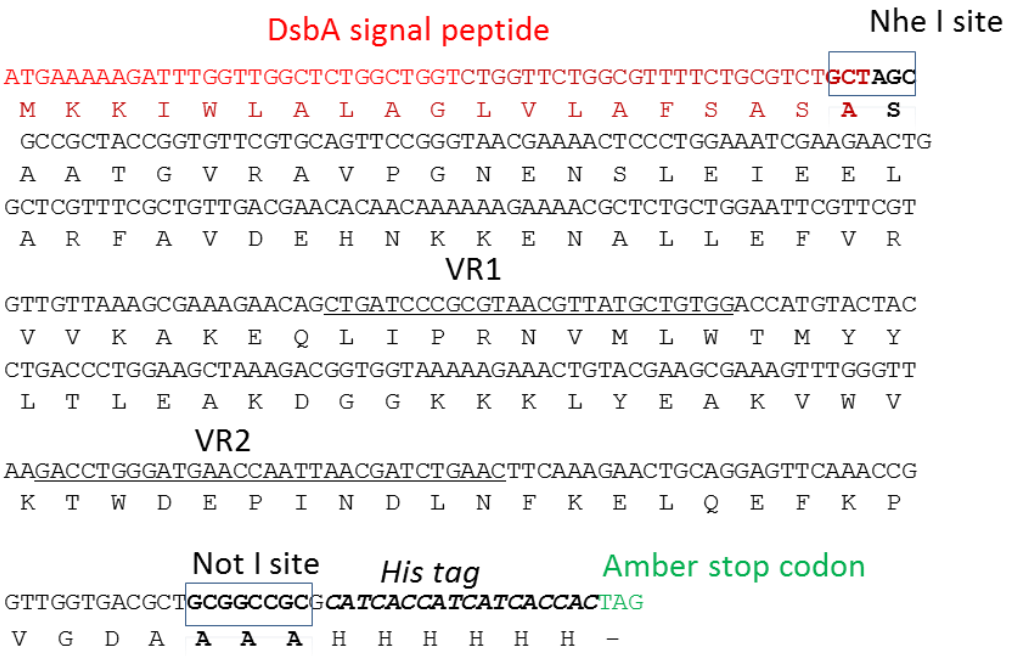

Figure 5.5: Description of the sequencing of Affimer phagemid vector. Analysis of the sequencing result obtained with M13-26 REV primer is shown, with important features highlighted.

As expected, the sequence contained the DsbA signal peptide required for periplasmic secretion, NheI and NotI restriction sites which are used for cloning, sequence diversity in the variable region (VR) 1 and 2 which gives unique binding properties to each Affimer, a hexa-His tag sequence for affinity purification and an amber stop codon for expression in suppressor bacterial strains.

5.3.3 Toxin A sequence alignment and selection of unique binders

The protein sequence alignment of toxin A Affimer binders was performed using the ClustalW alignment tool. The sequence alignments of binders from standard panning (labelled with Txn-A prefix) and the panning with competitive elution (labelled with TOXIN-A prefix) are shown in Table 5.2.

Table 5.2 Groups of toxin A binders: the 12 unique binders of toxin A were divided into three groups based on sequence similarities. The frequency of each binder is provided.

Group	Representative binder	VR1	VR2	Frequency	Affimer clone ID
1	Txn-A-1	LIPRNVMLW	TWDEPINDL	8x	1,3,4,9,12,15,19,21
	TOXIN-A-31	HVPRNVQMW	WSGAQDPWM	1x	31*
	TOXIN-A-25	PIPRNVYLW	KVKSNMFMN	1x	25*
2	Txn-A-22	WVPRNIFLG	QNEKHDDGQ	2x	22,26
	Txn-A-29	FVPKFIWLG	GEPADMPMG	3x	29,17*,30*
	Txn-A-30	AYPKFIWLG	SQRNLNQPM	3x	30, 24*,29*
	Txn-A-23	IVPRFIWVG	EDVVEPAWK	1x	23
	TOXIN-A-20	PYPKFVFLG	QYQSEFTGV	1x	20*
	TOXIN-A-23	IIPKLHWLG	HDPAAEQMT	1x	23*
3	Txn-A-14	VARSAYHWD	SPPKNRMLT	10x	14,5,20,27,18*,19*,21*,22*,26*,32*
	Txn-A-18	SYVDPWQQT	QSAGFHRLN	2x	18,27*
	Txn-A-7	VVIISSTFA	KKHMYPTWS	1x	7

For binders occurring more than once, a representative binder was selected for the group as shown in Table 5.2. In total, 12 unique Toxin A Affimer binders were selected after sequencing, their sequence alignment is provided in Figure 5.8. Analysis of the sequence alignment of the unique binders allowed the binders to be grouped into 3 based on the revealed conserved residues in Loop 1. Group 1-binders (Txn- A-1, Toxin A-25, and Toxin A-31) have P.R.N.V.X.L.W. Group 2-binders (Txn-A-22,29,30,23, Toxin A-20,23) have P.R/K.F/N.I.W.L.G conserved sequences while Group 3- binders have no conserved residues.

From the sequencing results: (i) four sequences came up in both standard and competitive elution round (ii), sequences with VARSAYHWD in VR1 and SPPKNRMLTN in VR2, occur as 21 % of the population from standard panning round, and 40 % in the competitive round. (iii) sequences with LIPRNVMLW in VR1 and TWDEPINDL in VR2 occurs as 42 % of the population in the standard panning only and not at all in the competitive panning. It is noteworthy that Toxin A-14 has the highest frequency 10x, but has no conserved residues with other binders. There are no conserved residues in the Loop 2 of all the 12 binders for Toxin A. Further characterisation of these binders would shed more light on their properties.

A graphical representation of conserved residues using Weblogo (Crook *et al.*, 2004) for group 1, group 2 and a combination of group 1 and 2 is given in Figure 5.6.

(a) VR1- Group 1

(b) VR1- Group 1

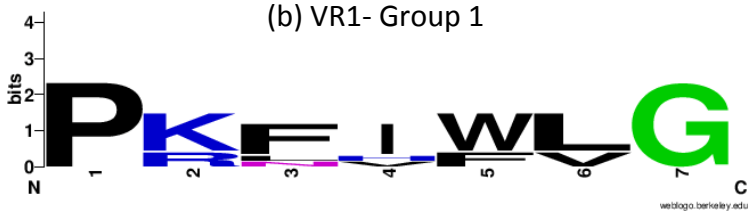

(c) VR1- Group 1 and 2

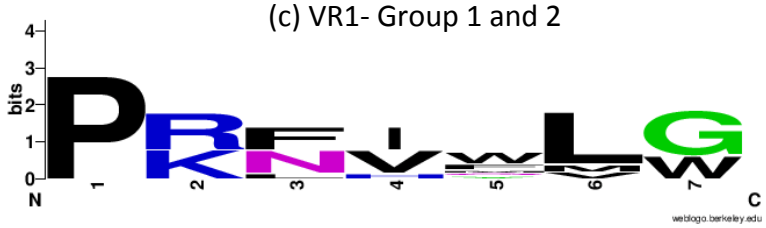

Figure 5.6. Analysis of conserved residues of unique Toxin A binders: The conserved residues in the variable region (VR1) of group 1 (a), group 2 (b) and combined group 1 and 2 (c) are shown in LOGOS (Crooks *et al*., 2004); the input to LOGOS was a ClustalW (Thompson *et al*., 1994) alignment of the VR1 of each group.

5.3.4 Sequence alignment and selection of unique toxin B Affimer binders

The sequence alignment of toxin B Affimer binders identified from the phage display screening is presented in table 5.3. The frequency of each unique sequence is also indicated.

Table 5.3: Alignment of sequences in the VR1 and VR2 of toxin B Affimer binders

Representative binder	VR1	VR2	Frequency	Affimer clone ID
1. TOXIN-B-45	EQRHKHATF	NNNRAMFMT	12x	17,19,20,25,27,31,36,30, 39, 43,44,45
2. TOXIN-B-18	EETNVYGKD	RFNRWPSNL	8x	18,21,22,29,37,38,40,46
3. TOXIN-B-28	QKEESAMFL	YIKRWPHNM	1x	28
4. TOXIN-B-33	AQEYQPAFTN	RIHRWPPEM	1x	33
5. TOXIN-B-35	NGRRAYIRN	GDYVMPGNR	1x	35
6. TOXIN-B-24	NMHSSRYST	KIGFWNAGN	1x	24
7. TOXIN-B-26	DIANSRFFI	EQVHALPLF	1x	26
8. TOXIN-B-47	VMPPHWTWK	SYRQQISLQ	1x	47
9. TOXIN-B-32	QTIPYPTTH	QFHYRHRGK	1x	32
10.TOXIN-B-23	ADTSPFALP	YYHPYIKHM	1x	23

Usually, Affimer binders have 9 randomised residues in VR1 and VR2, but occasionally, binders with 10 randomised residues in either VR are also recovered. An example of this is Toxin B-33 with 10 residues in VR1. For binders occurring more than once, one binder was selected as representative of the group. In total, 10 unique toxin B Affimer binders were selected after sequencing. There are no observable highly conserved sequences, nonetheless, Toxin B-18, Toxin B-33 and toxin B-28 have R.W.P conserved residues at position 4-6 in VR2. This might suggest they have similar binding properties. Toxin B-45 was selected as the representative binder with the highest frequency (12x) and Toxin B-18 for those with 8x frequency. In summary, 12 unique binders were identified from toxin A screen and 10 unique binders were identified from toxin B screen.

5.4 Production of Affimer Proteins

Once binding of individual clones to the targets of interest has been confirmed by phage ELISA, toxin A and B screening identified 22 unique Affimer binders. As described in section 2.2.1, the Affimer coding region was fused to the gene encoding C-terminal half of gene pIII of the phagemid vector which could obstruct the study of interactions of the binders to their target. Therefore, for expression and further characterisation, the Affimer insert coding sequences were subcloned from the phagemid vector into an expression vector to remove the phage coat particles. Once expressed and purified, each Affimer binder was characterised for their biophysical properties and utility in applications such as enzyme-linked binding assays.

5.4.1 Subcloning of Affimer binders into pET11a expression vector.

Subcloning of Affimer binders was carried out in five stages.

(i) Amplification of the coding region of Affimer binder from the phagemid vector by PCR using Phusion DNA polymerase. Since the Affimer library was generated to exclude cysteine, site-specific cysteine(s) was introduced by PCR into the C-terminal region before the His-tag of the expression vector to enable site specific coupling of biotin and fluorescent labels during

characterisation. Therefore, the coding DNA sequence for each Affimer binder was amplified using specific primers that either encoded a cysteine or no cysteine upstream of the octa-His tag (section 2.6.1).

(ii) Digestion of the Affimer PCR fragment using NheI/NotI restriction endonucleases

(iii) Ligation of inserts into similarly digestion pET11a expression vector already containing an Affimer coding region.

(iv) Transformation of *E. coli* competent cells with the ligation product

(v) DNA sequence analysis of recombinant plasmids to confirm the DNA sequence of the insert and insert orientation.

The results obtained from subcloning experiments are presented in below.

5.4.1.1 Amplification and digestion of Affimer binders

The PCR products obtained from the amplification of the Affimer coding regions from the phagemid vector were digested with DpnI to remove the methylated template plasmid DNA and purified using the Macherey-Nagel NucleoSpin® Gel and PCR Clean-up kit according to the manufacturer's protocol (Section 2.6). The purified PCR products were digested using NheI-HF® and NotI-HF® restriction enzymes to obtain the Affimer coding region which was further purified using the NucleoSpin® Gel and PCR Clean-up kit, then quantified by Nanodrop. An aliquot of the purified fragments obtained from the double digestion of toxin A and toxin B binders were analysed alongside GDH binders which was presented in Figure 4.11.

5.4.1.2 Ligation and preparation of Affimer binders for DNA sequencing

Affimer binder inserts were ligated into linearised pET11a expression vector (NheI-HF®/NotI-HF® digested) using T4 DNA Ligase. To check for religated vector, a ligation control reaction (negative control) was carried out for the linearised pET11a vector without the insert. The ligation products were used to transform *E. coli* XL-1 blue competent cells (Section 2.6.5 and 2.4.2). Over a 50-fold increase in colony counts was seen on the ligation plate compared to the negative control plate. Two clones were selected from the positive plate for each sample, then recombinant plasmid DNA was prepared from each colony. The DNA concentration

of purified plasmids was quantified by using the Nanodrop giving a range of 100 ng/µL- 250 ng/µL.

5.4.2 DNA sequence analysis of Affimer clones

As stated in Section 5.4.1.1, each Affimer coding region was subcloned with or without a cysteine residue. In total, plasmid DNA was prepared from the 46 clones for toxin A and 36 clones for toxin B, and was submitted for DNA sequencing from the T7P primer except Toxin A-23c, Toxin B-23 and Toxin B-23c which was not successfully subcloned. Sequencing results were analysed using ExPASy translate tool (Gasteiger *et al*., 2003) to ensure the integrity of the Affimer coding region. Each sequence was aligned to the sequence of its corresponding pDHis phagemid. Of the clones submitted for DNA sequencing, 95 % had the correct insert sequence. Figure 5.7 shows an annotated version of the sequencing data obtained for Toxin B-45 binder used as a representative binder. This result shows the successful subcloning of binders from pDHis phagemid vector into a pET11a expression vector. Using the final-reverse-C primer, a cysteine residue was successfully introduced into pET11a Toxin B-45c. The sequencing result also confirmed that the pET11a vector carried a His8 tag at its C-terminus rather than a hexa-His-tag as in pDHis vector. Table 5.4 gives the subcloning profile of each binder with and without cysteine residue (C96). From the sequencing result, all toxin A binders (except Toxin A-25 and Toxin A-23), and all toxin B binders (except Toxin B-23 and Toxin B-23c) were successfully subcloned with and without cysteine (C96).

```
CLUSTAL O(1.2.1) multiple sequence alignment

PDHis Toxin B-45    MKKIWLALAGLVLAFSASASAATGVRAVPGNENSLEIEELARFAVDEHNKKENALLEFVR
pET11 Toxin B-45    ----------------------------MASNSLEIEELARFAVDEHNKKENALLEFVR
pET11 Toxin B-45C   ----------------------------MASNSLEIEELARFAVDEHNKKENALLEFVR
                                                 .****************************

PDHisToxinB-45      VVKAKEQEQRHKHATFTMYYLTLEAKDGGKKKLYEAKVWVKNNNRAMFMTNFKELQ
pET11 Toxin B-45    VVKAKEQEQRHKHATFTMYYLTLEAKDGGKKKLYEAKVWVKNNNRAMFMTNFKELQ
pET11 Toxin B-45C   VVKAKEQEQRHKHATFTMYYLTLEAKDGGKKKLYEAKVWVKNNNRAMFMTNFKELQ
                    ****************************************.*********

PDHisToxinB-45      EFKPVGDA-AAAHHHHHH-
pET11 Toxin B-45    EFKPVGDA-AAAHHHHHHH
pET11 Toxin B-45C   EFKPVGDACAAAHHHHHHH
```

Figure 5.7: Sequencing alignment for subcloning experiment. The DNA sequencing analysis shows successful subcloning of binders from pDHis phagemid vector into pET11a expression vector and that the pET11a Toxin B-45 has the same insert sequence (VR1 and VR2 are shown in red) as contained in the pDHis vector.

Also, pET11a-Toxin B-45c was successfully sub-cloned with a cysteine residue C96 (highlighted in yellow).

Table 5.4: Subcloning profile for toxin A and toxin B Affimer binder.

	Representative binder	VR1	VR2	Subcloning	
				Without cys	With cys
1	TOXIN-A-25	PIPRNVYLW	KVKSNMFMN	✓	x
2	TOXIN-A-31	HVPRNVQMW	WSGAQDPWM	✓	✓
3	TOXIN-A-23	IIPKLHWLG	HDPAAEQMT	✓	x
4	TOXIN-A-20	PYPKFVFLG	QYQSEFTGV	✓	✓
5	Txn-A-1	LIPRNVMLW	TWDEPINDL	✓	✓
6	Txn-A-22	WVPRNIFLG	QNEKHDDGQ	✓	✓
7	Txn-A-29	FVPKFIWLG	GEPADMPMG	✓	✓
8	Txn-A-30	AYPKFIWLG	SQRNLNQPM	✓	✓
9	Txn-A-23	IVPRFIWVG	EDVVEPAWK	✓	✓
10	Txn-A-14	VARSAYHWD	SPPKNRMLT	✓	✓
11	Txn-A-18	SYVDPWQQT	QSAGFHRLN	✓	✓
12	Txn-A-7	VVIISSTFA	KKHMYPTWS	✓	✓
1	TOXIN-B-18	EETNVYGKD	RFNRWPSNL	✓	✓
2	TOXIN-B-35	NGRRAYIRN	GDYVMPGNR	✓	✓
3	TOXIN-B-45	EQRHKHATF	NNNRAMFMT	✓	✓
4	TOXIN-B-28	QKEESAMFL	YIKRWPHNM	✓	✓
5	TOXIN-B-33	AQEYQPAFTN	RIHRWPPEM	✓	✓
6	TOXIN-B-24	NMHSSRYST	KIGFWNAGN	✓	✓
7	TOXIN-B-26	DIANSRFFI	EQVHALPLF	✓	✓
8	TOXIN-B-47	VMPPHWTWK	SYRQQISLQ	✓	✓
9	TOXIN-B-32	QTIPYPTTH	QFHYRHRGK	✓	✓
10	TOXIN-B-23	ADTSPFALP	YYHPYIKHM	x	x

5.4.3 Expression and purification of toxin A and toxin B Affimer binders

Once the sequence of each binder in pET11a expression vector had been confirmed, *E. coli* BL21 (DE3) Star competent cells were transformed with the recombinant pET11a expression vectors as described in Section 2.4.2. Recombinant Affimer proteins were produced in 50 mL LB cultures by IPTG induction (0.1 mM) under the control of the T7 lac promoter (Studier and Moffatt, 1986). After 6 h of induction, the cells were harvested and pellets were lysed (Section 2.7.3). To assess the expression profile of each Affimer, the soluble fraction (SF) and the insoluble fraction (IF) were analysed on a 4-20 % SDS-PAGE gel. Figure 5.8 presents a representative set of the expression analysis for 21 protein samples. This shows

that the Affimer proteins were expressed mostly as soluble protein except for B-26c which had very low expression level in both soluble and insoluble fraction. Based on the analysis of protein expression, all toxin A and B Affimer binder protein were purified from the soluble fraction of the lysate using Ni-NTA affinity chromatography. To analyse the fractions obtained during purification, the flow through (FT) collected after loading the soluble fraction onto the column, the last wash with $OD_{280\,nm}$ (<0.01), and five elutions were analysed by 4-20 % SDS-PAGE. The result of the gel electrophoresis for a sample binder is presented in Figure 5.9a.

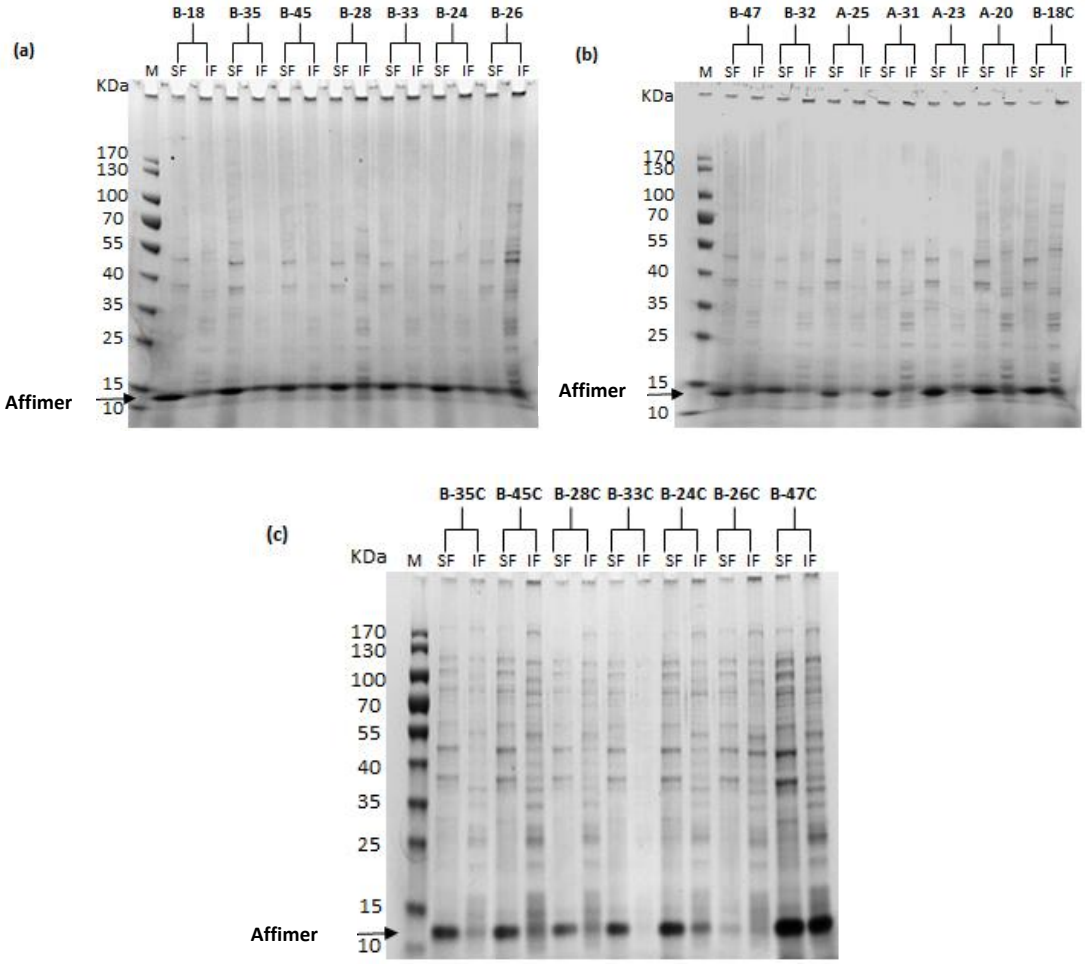

Figure 5.8: Expression analysis of Affimer proteins by 4-20 % SDS-PAGE: The soluble (SF) and insoluble (IF) fraction of each protein sample were analysed alongside the protein marker(M). The over-expressed Affimer protein is indicated by an arrow.

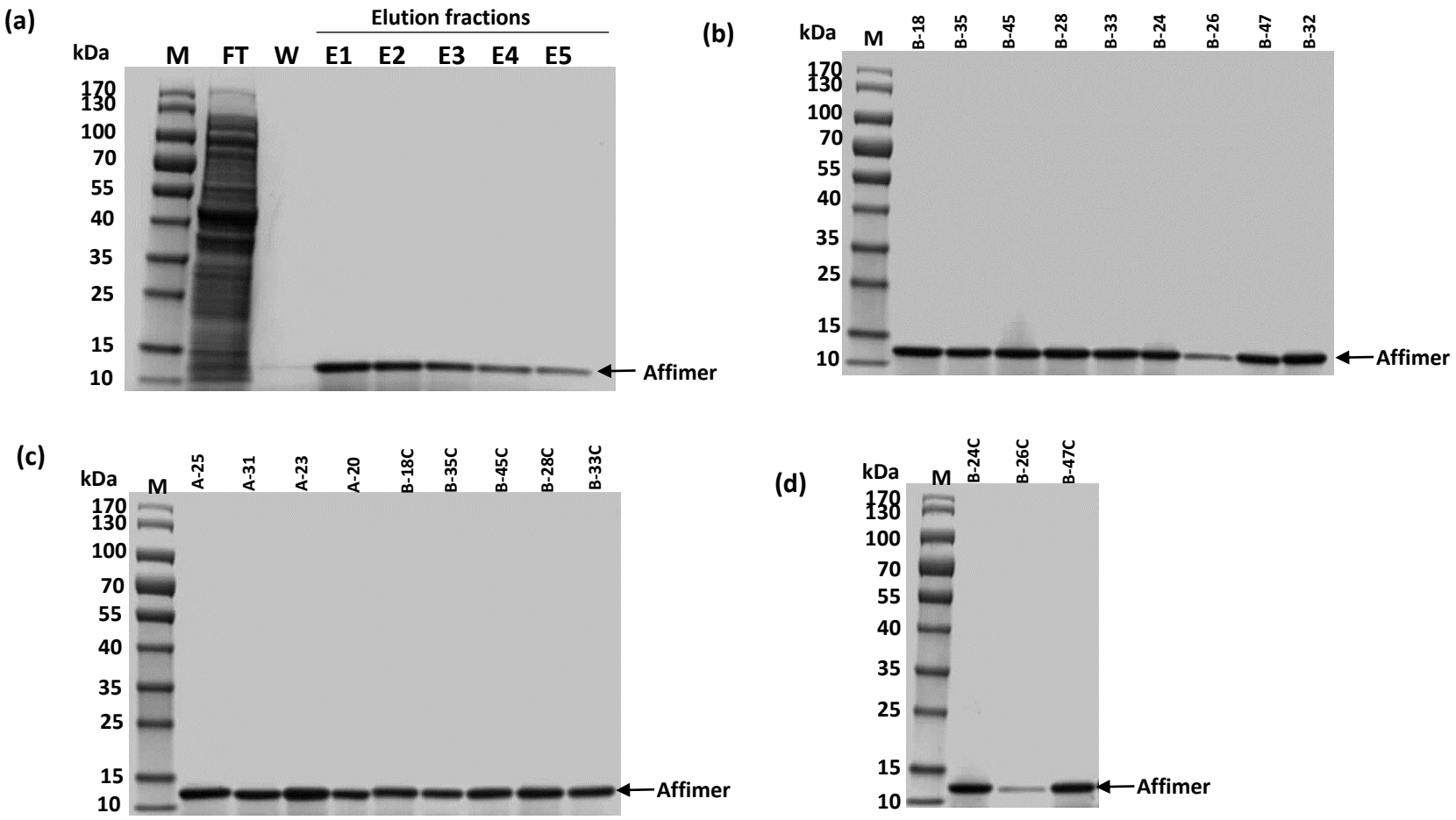

Figure 5.9: SDS-PAGE analysis of the purification of Affimers. Analysis on 4-20 % SDS-PAGE gel of purified Affimers after one-step Ni-NTA affinity chromatography. (a) Analysis of fractions obtained during purification for Toxin B-18: FT- Flow-through, W- Wash, E- Elutions. 5 µg of each toxin A and toxin B binders, and protein marker (M) were loaded on gels shown in (b)-(d). Affimers produced a single band of ~ 12 kDa as expected.

During purification, the 300 µL of Ni-NTA slurry used was sufficient to capture most His-tagged recombinant protein prepared from 50 mL cultures. This agrees with the binding capacity of resin used (50 mg his-tagged recombinant protein/mL resin) (Amintra, Expedeon Ltd, Cambridgeshire, UK).

After binding, proteins were washed and eluted from Ni-NTA affinity matrix with elution buffer containing 300 mM imidazole. The result obtained from the analysis of fractions collected during the affinity purification of Affimer proteins shows that Ni-NTA affinity chromatography is sufficient to obtain a one-step purification. Purity estimated to be of >99 % was achieved for all toxin A and toxin B Affimer binders as shown in Figure 5.10 (b-d).

The theoretical molecular mass and pI for each Affimer binder was calculated using the ExPASy protparam tool. This is presented in Table 5.5 alongside the calculated protein yield in mg/L for cysteine and no cysteine-containing Affimer.

Table 5.5 Properties of purified Affimer proteins. Calculated molecular mass from the extinction coefficientof each Affimer, pI and the concentration of protein obtained from purification. NA (Not applicable) was used for Affimers that were not expressed.

Affimers	Calculated Molecular mass (kDa)	pI	Yield (mg/L)	
			No cysteine	With cysteine
TOXIN-A-25	12.5	9.1	108	66
TOXIN-A-31	12.5	7.18	204	50
TOXIN-A-23	12.3	6.83	227	**NA**
TOXIN-A-20	12.3	7.14	148	94
Txn-A-1	12.5	6.49	114	66
Txn-A-22	12.4	6.79	160	**NA**
Txn-A-29	12.2	6.75	106	86
Txn-A-30	12.4	8.81	116	111
Txn-A-23	12.4	6.75	152	55
Txn-A-14	12.4	8.81	86	87
Txn-A-18	12.4	7.18	100	35
Txn-A-7	12.3	8.78	100	46
TOXIN-B-18	12.5	7.14	131	79
TOXIN-B-35	12.3	9.13	124	111
TOXIN-B-45	12.5	8.84	76	57
TOXIN-B-28	12.5	8.01	97	118
TOXIN-B-33	12.6	7.18	97	90
TOXIN-B-24	12.3	8.81	154	119
TOXIN-B-26	12.3	6.79	4	6
TOXIN-B-47	12.5	8.81	66	95
TOXIN-B-32	12.5	9.1	70	100

As seen in Table 5.5, the protein yield for Affimer proteins ranged from 4 mg/L to 227 mg/L. Toxin B-26 had the lowest protein yield. This agrees with the expression profile result for Toxin B-26 shown in Figure 5.11. In addition, the pattern of protein yield obtained from Affimer proteins without cysteine were higher than those of the corresponding protein containing the cysteine. For example, Toxin A-31 had a yield of 204 mg/L while Toxin A-31c had a yield of 50 mg/L. This represents a 75 % decrease in the protein yield. Overall, 11 of the 19 binders had at least a 40 % decrease in protein yield when expressed as a cysteine-containing protein. A similar pattern was observed for GDH binders as discussed in Chapter 4.

5.5 Biophysical characterisation of Affimer binders

5.5.1 Toxin A and B Affimer proteins are monomeric

Size exclusion chromatography was used as an analytic technique to identify the oligomeric state of purified toxin A and B Affimer proteins. For aggregation studies, purified binders without cysteine residues were analysed. Each binder was buffer exchanged into 1 x PBS (pH 7.4) and prepared to a concentration of 1 mg/mL before loading onto a Superdex 200 10/300 column. As shown in Figure 5.10, all toxin A binders except Txn-A-23 show a monomeric peak. Similarly, Figure 5.11 shows that all toxin B binders are monomeric.

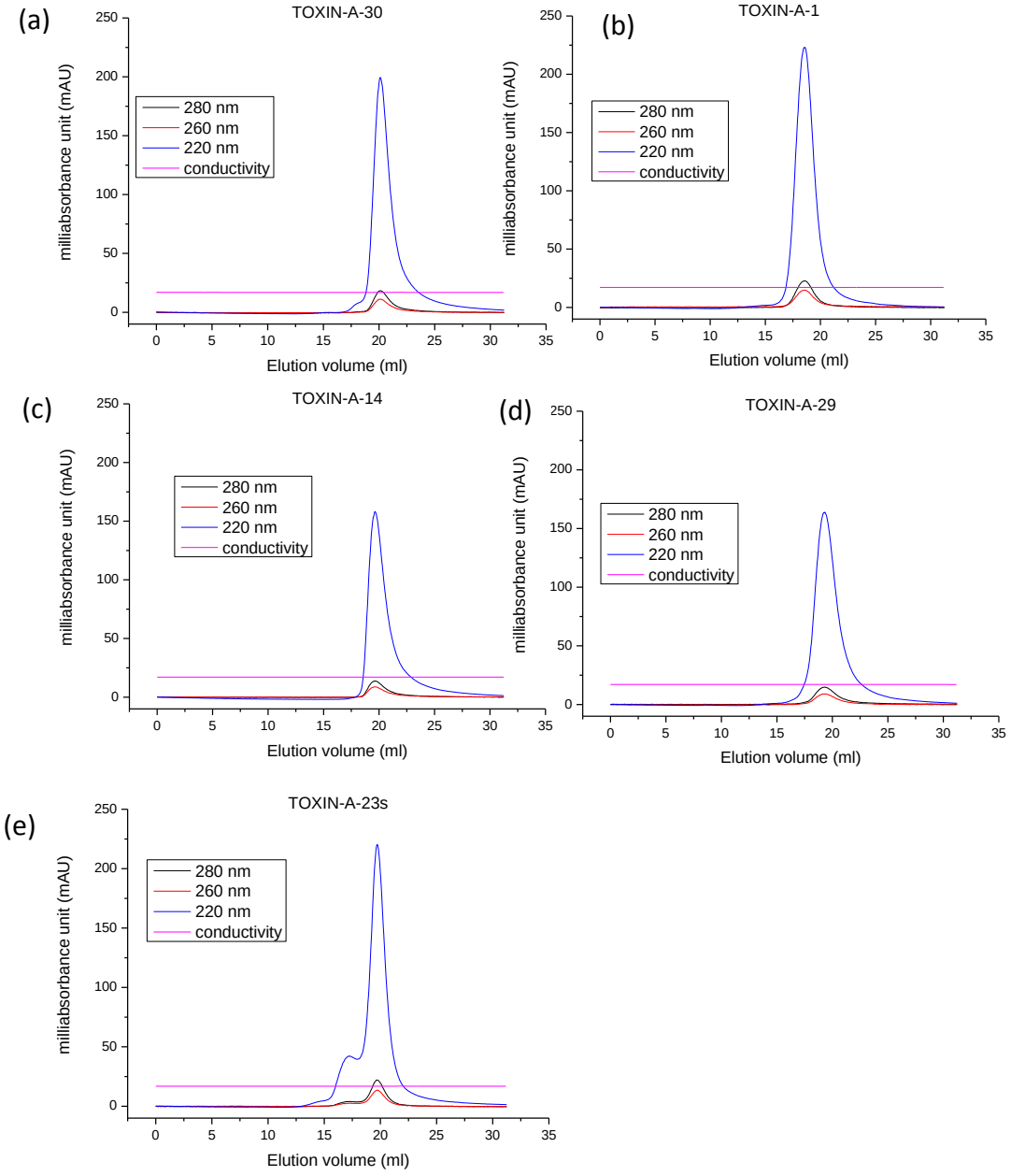

Figure 5.10: Size exclusion chromatography for toxin A binders. Toxin A binders analysed using Superdex 200 10/300 column. Chromatograms for binders (a)-(d) showed a single monomeric peak while chromatogram for (e) shows Toxin A-23s with a major monomeric peak and two mutimeric shoulders.

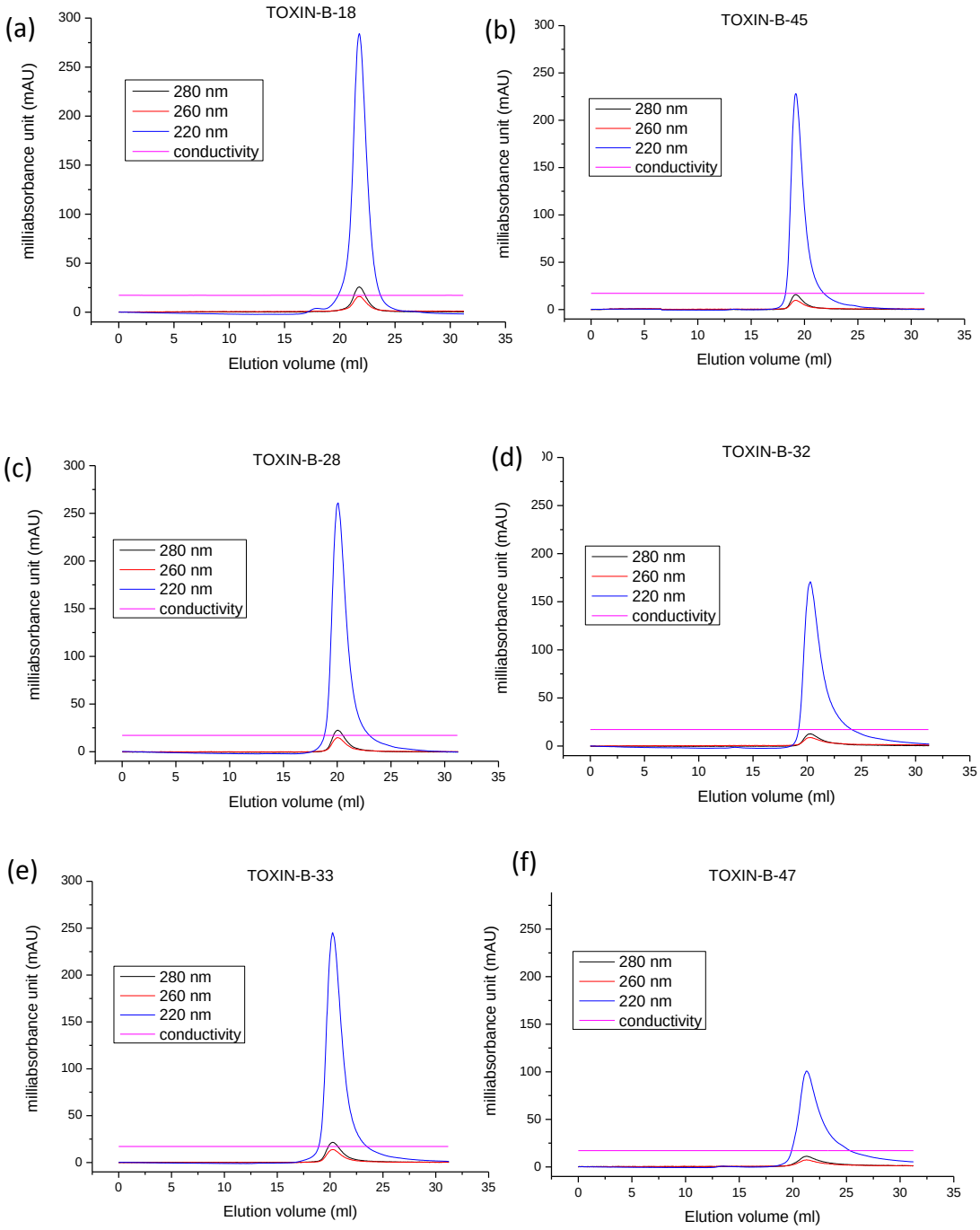

Figure 5.11: Size exclusion chromatography for toxin B binder. Toxin B binders analysed using Superdex 200 10/300 column. Chromatograms for binders (a)-(f) showed a single monomeric peak.

5.5.2 Thermostability and aggregation profile of toxin A and B Affimer proteins.

The thermostability of toxin A and B binders was characterised using the Optim 2000® (Avacta) (Section 2.12.4) and as described for GDH binders in Chapter 4 (Section 4.6.2). The Optim 2000® was programmed to monitor the static light scattering (SLS) using a 266 nm laser source. Increase in size of the species in solution and of aggregation is reported by an increase in the scattered light intensity. The static light scattering (SLS) of the binders was recorded in 1 ^{o}C steps to detect the presence of aggregates as the samples are been heated from 10 to 90 ^{o}C. The Optim software analysed the data set to obtain the integrated scattered light intensity as a measure of the amount of aggregation. These primary results were further analysed automatically in the software to yield a temperature for the onset of aggregation for each binder.

The aggregation onset temperature (T_{agg}) is the temperature at which protein begins to aggregate. This is usually accompanied by a significant increase in the static light scattering intensity count. Figure 5.12 and 5.13 gives the thermogram for toxin A binders and toxin B binders, respectively. Duplicate analyses were performed and the data presented is the average obtained. An assessment of the T_{agg} for all toxin A binders reveals that Toxin A-22 was the most thermally stable as it remained thermally stable up to 90 ^{o}C and had the lowest scattered light intensity (41,000 intensity count) compared to other toxin A binders. The complete T_{agg} and the SLS intensity count for all toxin A binders analysed are given in Table 5.6.

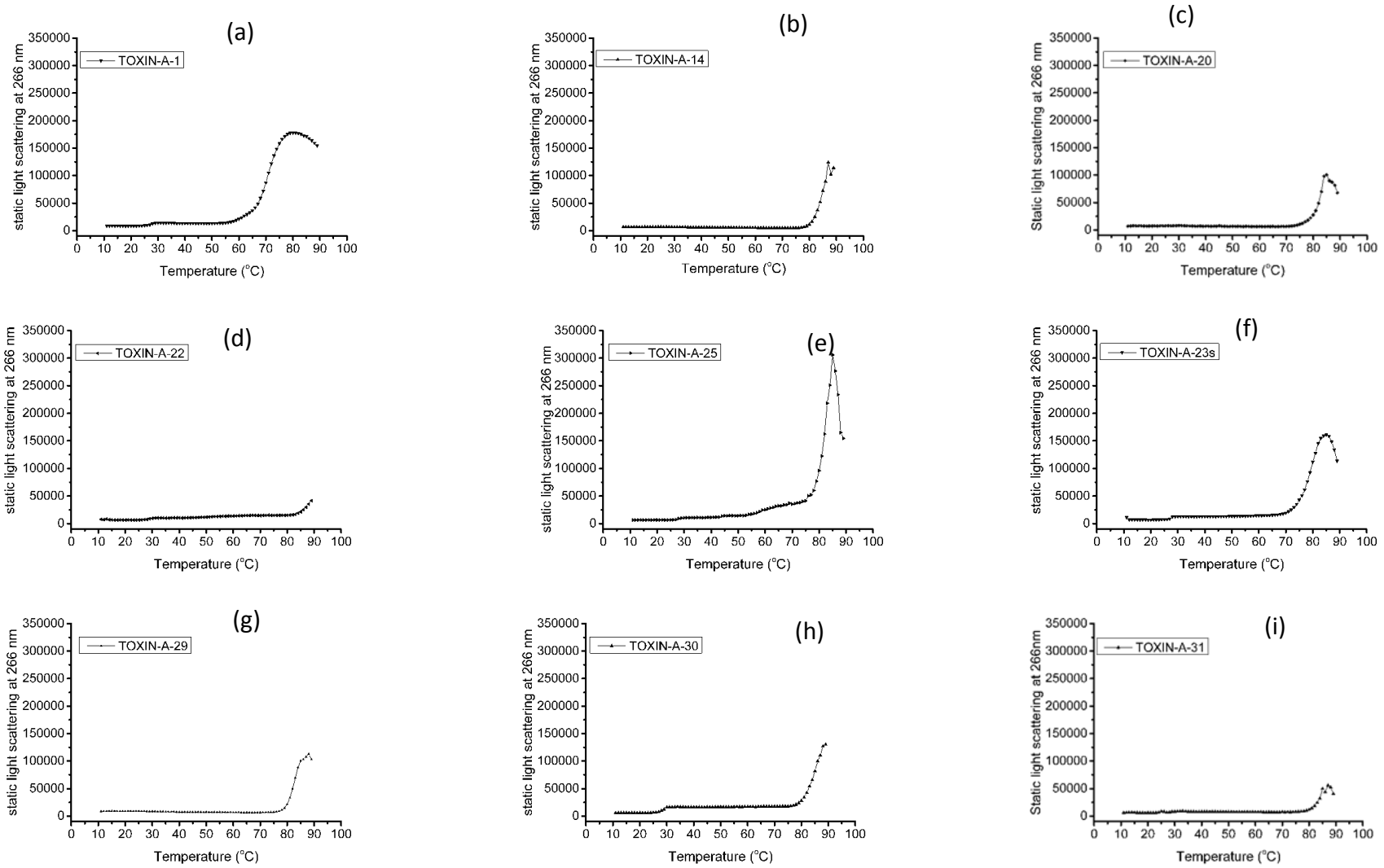

Figure 5.12: The static light scattering of the toxin A Affimer binders at pH 7 upon thermal stress. Duplicates were performed and the average values were plotted.

Table 5.6. Ranking of toxin A and B binders: (a) and toxin B binders (b) based on aggregation profile from the most aggregation-prone binder (having the highest peak SLS intensity count) to the least.

(a)

Binder	T_{agg} (^oC)	Peak SLS intensity count
Toxin A-25	76	306, 000
Toxin A-1	68	178, 000
Toxin A-23s	76	161, 000
Toxin-A-30	83	130, 000
Toxin A-14	84	124, 000
Toxin A-29	82	113, 000
Toxin A-20	82	100, 000
Toxin A-31	82	50, 000
ToxinA-22	90	41, 000

(b)

Binder	T_{agg} (^oC)	Peak SLS intensity count
Toxin B-28	70	480,000
Toxin B-32	75	369,000
Toxin B-47	71	241,000
Toxin B-24	82	95,000
Toxin B-33	83	84,000
Toxin B-45	90	15,355
Toxin B-18	90	13,000

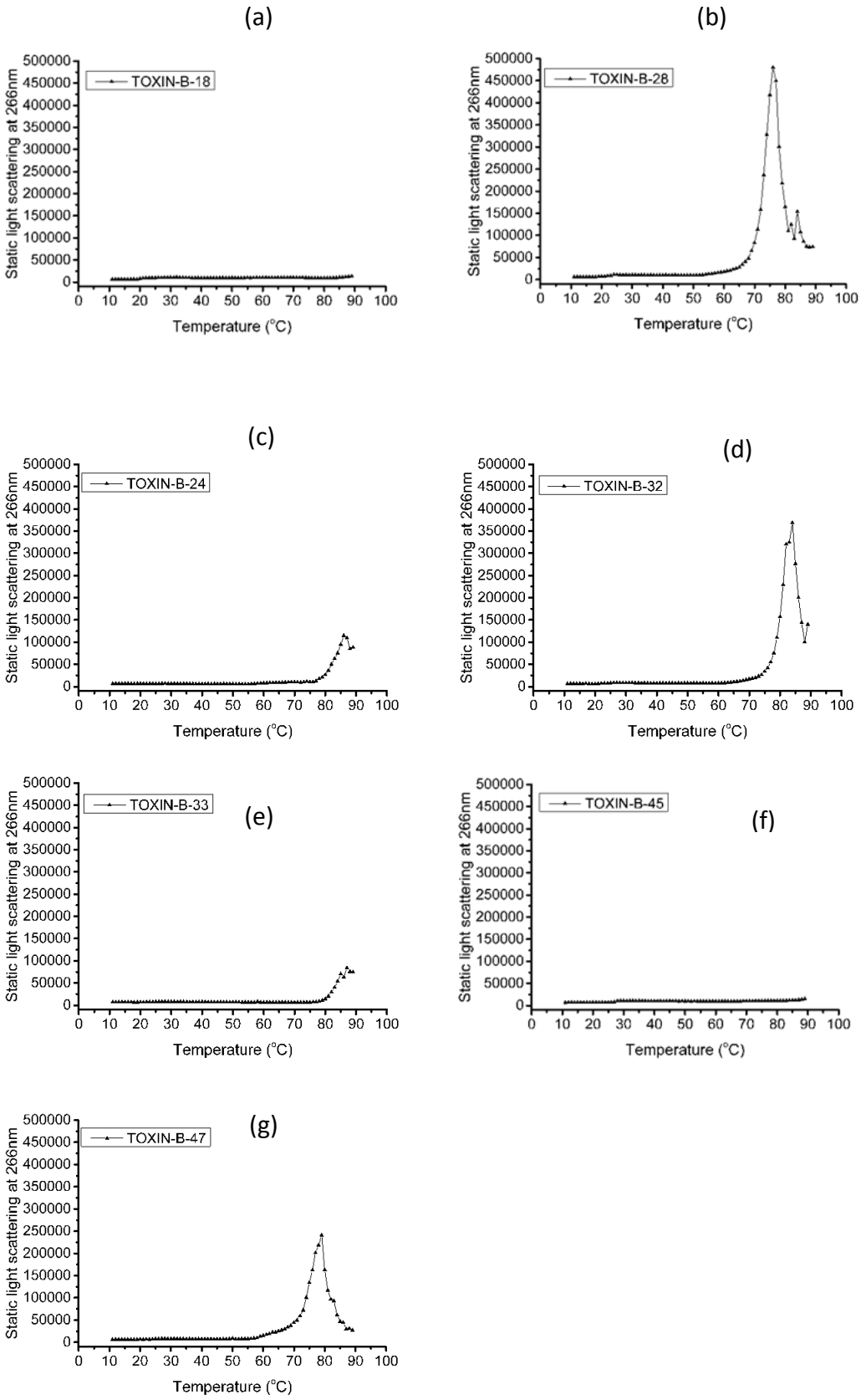

Figure 5.13: The static light scattering of the toxin B Affimer binders at pH 7 upon thermal stress. Duplicates were performed and the mean values were plotted.

5.6 Binding characterisation of Affimers to toxin A and B

The binding characterisation of purified Affimers selected against toxin A and B was carried out, and the results are described in this section. Using Enzyme linked immunosorbent assay (ELISA), purified Affimers were characterised for their ability to bind to immobilised targets or targets in solution. They were tested in different formats to identify pairs of Affimer capable of binding to non-overlapping epitopes on the targets, which would be useful in a sandwich assay format.

5.6.1 ELISA analysis with purified Affimer

Once the selected Affimer from phage display were purified, it was important to test if the purified Affimer protein binds the target as seen in the phage ELISA results using two formats (i) purified Affimers directly coated onto Nunc-plate and detected with biotinylated targets (ii) target protein directly coated onto Nunc-plate and detected with biotinylated Affimers.

5.6.1.1 Direct immobilisation of Affimer onto Nunc plates

The purified Affimer proteins were directly coated onto Nunc Maxisorp plates, biotinylated targets (toxin A or toxin B) were introduced and binding was detected with Streptavidin–HRP. From the ELISA analysis with purified Affimers, Figure 5.14a shows that for toxin A, 10 out of the 12 Affimers tested bind to toxin A while two binders (Toxin-A 18 and A-23) showed a poor binding signal. For toxin B (Figure 5.14b), 5 out of 9 Affimers showed binding to toxin B while Toxin B-32 showed poor binding signal and B-47, B-45 and B-35 showed no signal. These results show that only 71 % of the binders tested bound to the target when they were directly immobilised onto a plate surfaces. This led to the question of whether the remaining Affimer proteins were poor binders or simply affected by their direct immobilisation onto the plate surface?

(a)

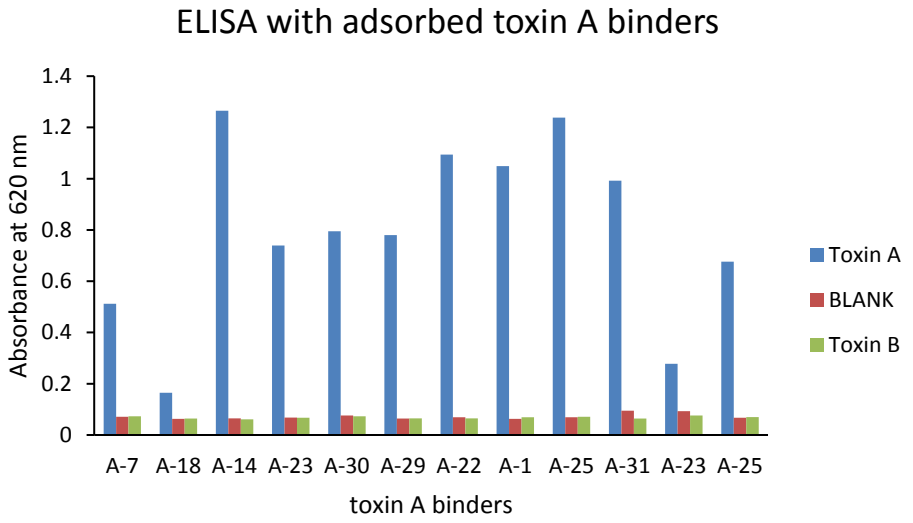

(b)

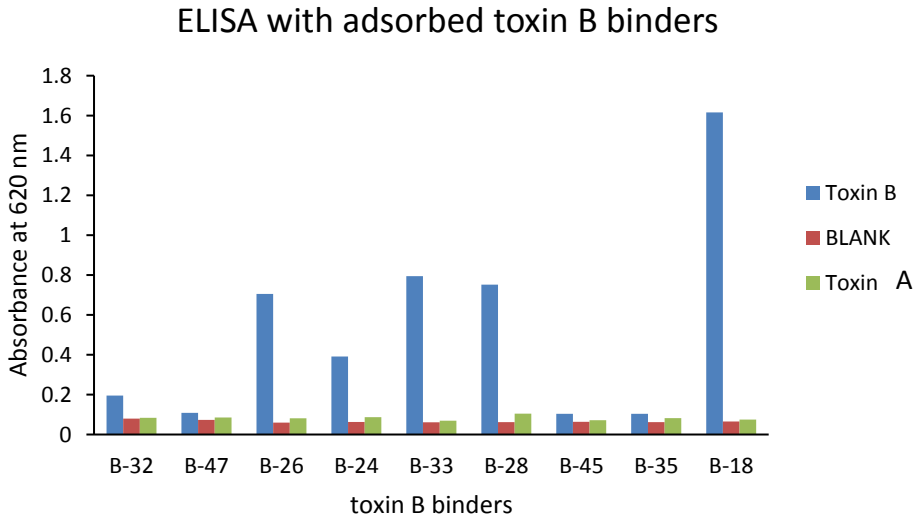

Figure 5.14: ELISA result using binders coated directly onto Nunc plate. (a) Binding of adsorbed toxin A binders to toxin A (blue bar), blocking buffer blank serving as negative control (red bar) and toxin B (green bar) for test for cross-reactivity. (b) Binding of adsorbed toxin B binders to toxin B (blue bar), blocking buffer blank serving as negative control (red bar) and toxin A (green bar) for test for cross-reactivity.

Passive adsorption of proteins onto the surface of plates offers a simple approach for immobilisation. However, proteins could denature at interfaces, undergo conformational changes due to random immobilisation, which would affect their binding abilities.

5.6.1.2 Direct immobilisation of target onto Nunc plates.

For the second format of protein ELISA, toxin A and B were directly immobilised onto the surface of Nunc Maxisorp plate by passive adsorption and detected with biotinylated Affimers. To ensure site-specific biotinylation of the Affimers, all cysteine-containing binders were biotinylated with BMCC-biotin via the single cysteine-residue and biotinylation was confirmed with ELISA as shown in Figure 5.15, before used in the protein ELISA.

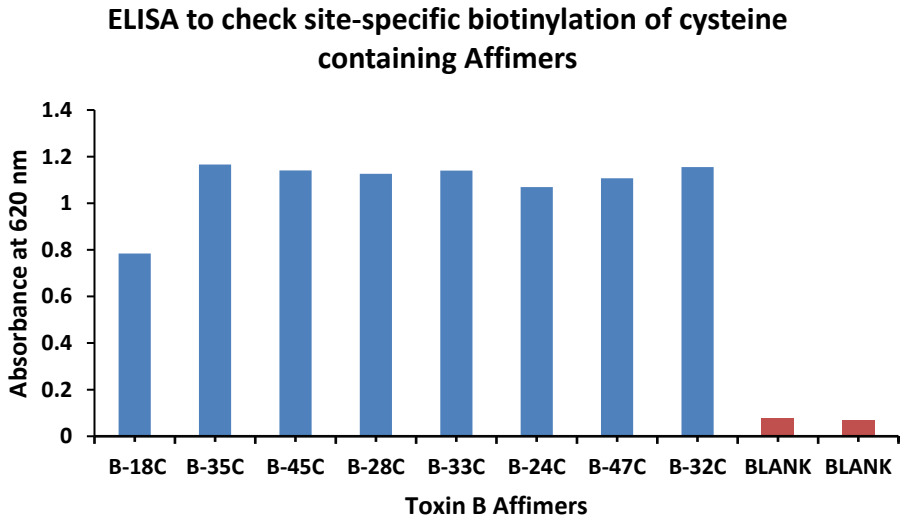

Figure 5.15. ELISA showing successful biotinylation of Affimer with single-cysteine

For the protein ELISA, toxin B was immobilised onto the plates by surface adsorption and then detected with biotinylated Affimers. Figure 5.16 shows the ELISA results from using immobilised Affimers (format one) and immobilised target (format two).

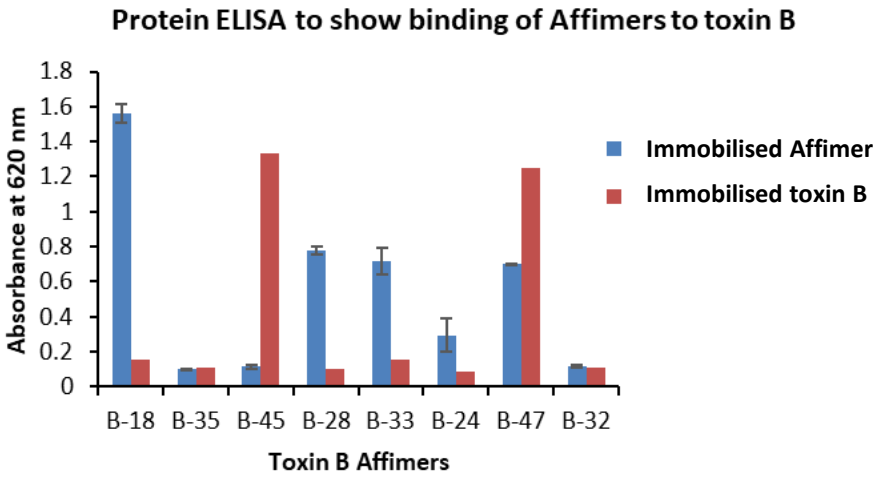

Figure 5.16: ELISA showing binding of Affimer to immobilised or free toxin B. Each binder was tested when it was adsorbed onto the microwell as capturing molecule and biotinylated toxin B was added (blue bar). Each was also tested with adsorbed toxin B and biotinylated Affimer used for detection (red bar).

It was clear from this experiment that the immobilisation strategy used during ELISA places a crucial role in binding events. Toxin B-18, B-28, B-33 and B-24 gave better signal intensity ($OD_{620\,nm}$ = 1.56, 0.78, 0.72, 0.29 respectively) when they were passively immobilised onto the surface of Nunc Maxisorp plates as capturing molecule compared to when used as detection molecule against passively adsorbed toxin B ($OD_{620\,nm}$ = 0.16, 0.10, 0.15, 0.09 respectively). On the other hand, this result shows that passive immobilisation of toxin B-45 Affimer negatively affected its binding to toxin B ($OD_{620\,nm}$ = 0.11). However, high signal intensity was observed when the target was adsorbed and biotinylated toxin B-45 was used for detection ($OD_{620\,nm}$ = 1.33). Toxin B-47 gave good signals in the two panels, but a 50 % increase in signal intensity when used for detection ($OD_{620\,nm}$ = 1.25). The signal obtained from Toxin B-35 and toxin B-32 in either panels show that they are weak binders.

5.6.1.4 BLItz analysis

Biolayer interferometry technology was used as a technique to measure the interactions between biotinylated Affimers (ligand) immobilized onto streptavidin biosensor tip and the targets - toxin A or toxin B (analytes) in solution. This is particularly useful because for diagnostic applications the targets would be free in solution, not biotinylated. Interactions were measured in real time, providing the

ability to monitor binding specificity, rates of association and dissociation, with precision and accuracy.

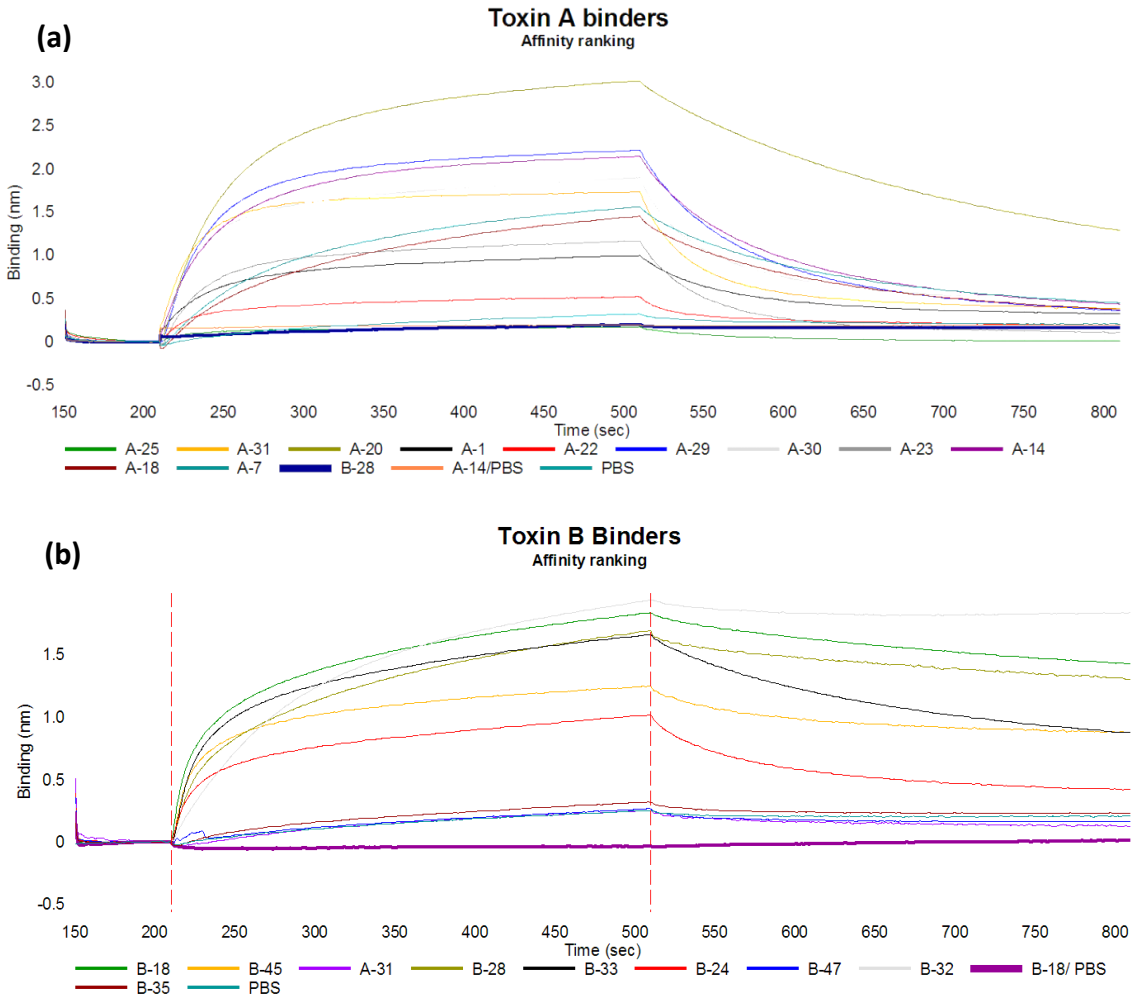

Figure 5.17. BLItz analysis showing the binding of biotinylated Affimers to target in solution. Biotinylated toxin A Affimers (a) and toxin B Affimers (b) were immobilised on streptavidin coated biosensor chip. The binding association and dissociation is presented.

All toxin A binders showed binding to toxin A but with varying affinity. A PBS negative control was included to test for background binding of immobilized Affimer binder, as shown in Figure 5.17a, no binding to PBS was observed. Similarly, to test for specificity or cross-reactivity, biotinylated Toxin B-28 binder was immobilized on to a streptavidin biosensor tip and tested for binding to toxin A, the sensogram line labelled B-28 shows that there was no binding interaction of Toxin B-28 to toxin A. This shows that toxin A truly binds specifically to toxin A binders. The toxin A sensogram shows that toxin A binders have a high on-rate as well as a

high off-rate which gives an indication about the affinity of the binders, though BLItz was not used to determine the binding kinetics of the Affimer binders, it could be hypothesised that Toxin A binders were not very high affinity binders. No binding was observed in the negative control when PBS was used as the analyte.

For toxin B, the sensogram shown in Fig 5.17b shows that all toxin B binders bind to toxin B but with varying affinity, with Toxin B-35 showing the least binding. No binding was observed when one of the toxin A binders (A-31) was immobilized onto a streptavidin biosensor chip and interacted with toxin B in solution, this shows the specificity of Toxin B binders to Toxin B. No background binding of binders was observed when PBS was used in place of toxin B (B-18/PBS), similarly, toxin B did not bind to streptavidin chip (in PBS) in the absence of biotinylated Affimer.

Comparing the result obtained from the protein ELISA and BLItz assay for toxin B, it was clear that the method used for immobilising the binders play a crucial role in their binding to the target. A summary of the binding characteristics of each toxin B Affimer binders is presented in Table 5.7 this shows that Toxin B-18, B-28 and B-33 are best suited as a capturing molecule while Toxin B-45 is best suited as a detection molecule. On the other hand, Toxin B-35 and B-24 should not be taken forward because of their very weak binding signal with toxin B.

Table 5.7. Summary of binding characteristics of toxin B Affimers. Binding ability of binders with different C-capturing molecule and D- detection molecule. High binding ability= $OD_{620\ nm} > 0.7$; weak = $OD_{620\ nm}=0.3$; low= $OD_{620\ nm}$- <0.1

	Binding characteristics		
Binder	**ELISA data** C: Adsorbed binder D: Biotinylated toxin B	**BLItz data** C: Biotinylated binder D: Free toxin in solution	**ELISA data** C: Adsorbed toxin B D: Biotinylated binder
Toxin B-18	High	High	Low
Toxin B-35	Low	Low	Low
Toxin B-45	Low	High	High
Toxin B-28	High	High	Low
Toxin B-33	High	High	Low
Toxin B-24	weak	weak	Low
Toxin B-47	High	High	High
Toxin B-32	Low	High	Low

5.6.2 Identification of pairs of Affimers for toxin A and B

The treatment and control of CDI is critically dependent on accurate laboratory diagnosis which relies on sensitive and quantitative measurement of validated biomarkers in patient samples. Sandwich-type immunoassays is a highly sensitive and specific analytical technique that has been widely employed for diagnostic purposes. To develop a sandwich ELISA, a pair of binders (capture and detection binder) recognising non-overlapping epitopes on the targets should be selected.

As described for hexameric glutamate dehydrogenase (Chapter 4), one Affimer binder was sufficient to act as both capture and detection molecule since GDH has six binding sites. Thus, pairs against multimeric proteins were less important. However, selection of pairs against monomeric toxin A and B are necessary for sandwich type assays that require optimisation to identify the best capture and detection binder and the best orientation. This section describes the selection of Affimer pairs against toxin A and toxin B, and the characterisation of the selected pairs.

5.6.2.1 Sandwich ELISA by adsorption of capture Affimer

Since the binding of the Affimers was confirmed to their respective targets using protein ELISA and BLItz, the Affimers identified for toxin A and B were evaluated through sandwich ELISA to identify Affimer pairs that could recognise distinct epitopes of Toxin A and Toxin B respectively. The first approach used for potential pair identification was to immobilise two binders that showed the highest signal in protein ELISA (see Figure 5.18) as the capture Affimer by direct surface adsorption, while a panel of the remaining binders were tested for potential binding to different epitopes. Toxin A-1 and Toxin A-14 were capture Affimers for toxin A while Toxin B-18 and Toxin B-28 were capture Affimers for toxin B. The results obtained are shown in Figure 5.18.

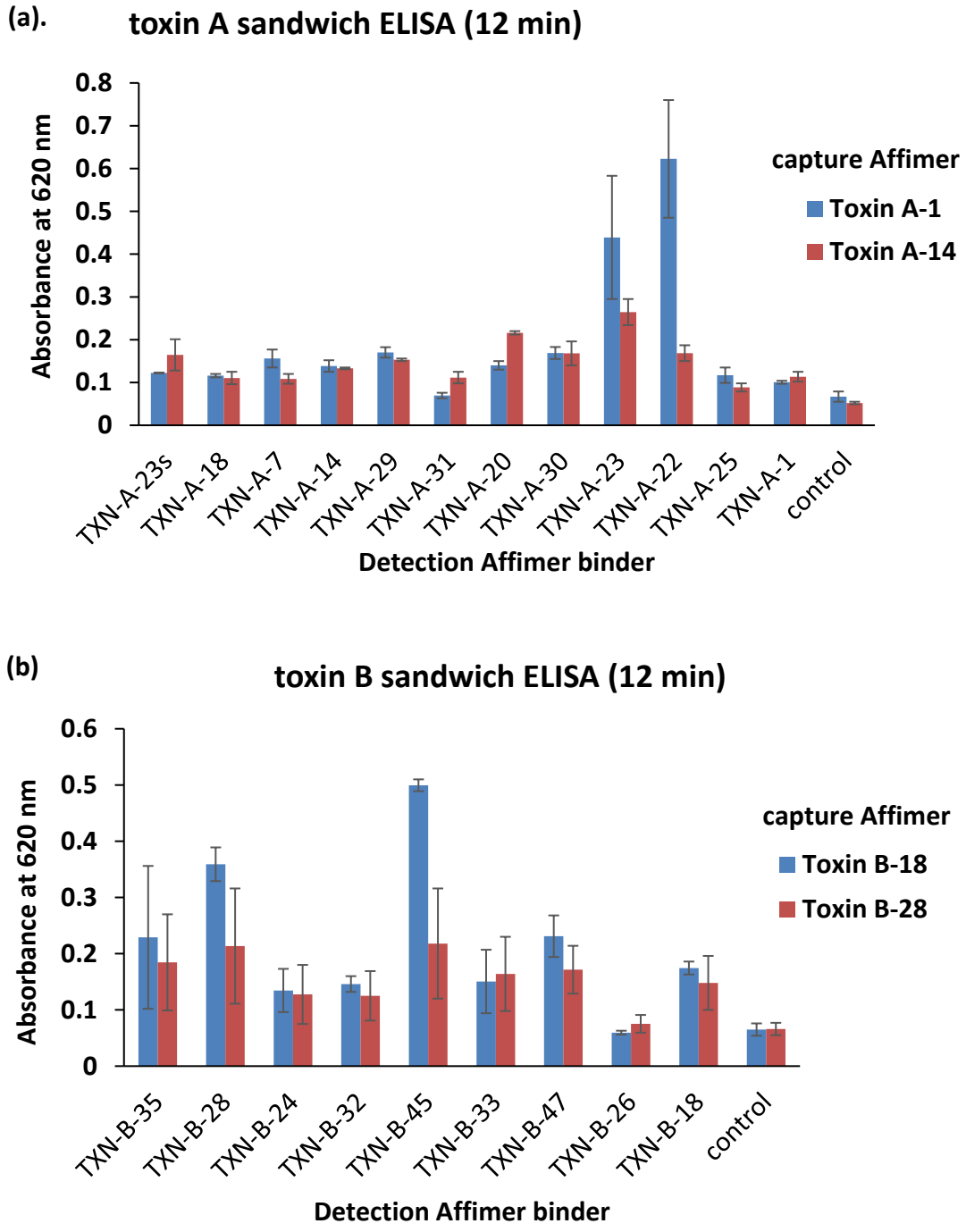

Figure 5.18: ELISA analysis to identify Affimer pairs. (a) toxin A binders were tested in sandwich ELISA format using toxin A-1 (blue bar) or toxin A-14 (red bar) as capture Affimers. **(b)** toxin B binders were also tested using toxin B-18 (blue bar) or and toxin B-28 (red bar) as capture Affimers. The data represents mean absorbance value ($OD_{620\ nm}$). The error bars indicate standard deviation of averaged data ($OD_{620\ nm}$) from duplicate microtitre wells.

With Toxin A-1 as the capture Affimer (blue bars in Figure 5.18a), two potential pairs were identified. These are Toxin A-1/Toxin A-23 ($OD_{620\ nm}$ = 0.44) and Toxin A-1/Toxin A-22 ($OD_{620\ nm}$ = 0.63). On the other hand, when Toxin A-14 was

immobilised as the capture Affimer (red bars in Figure 5.21a), Toxin A-14/ Toxin A-23 pair gave the highest signal ($OD_{620\,nm}$ = 0.26). Comparing the two capture toxin A binders, toxin A-23 would pair with either toxin A-1 or toxin A-14, however Toxin A-1 acts as a better capture molecule for toxin A-23 with a 2-fold increase in signal intensity when immobilised directly onto Nunc Maxisorp plates than Toxin A-14.

For toxin B, direct immobilisation of Toxin B-18 (blue bar in Figure 5.18b) showed that of all the binders, Toxin B-45 with an $OD_{620\ nm}$ of 0.5 could be the best potential detection binder to make a pair, though B-18/B-28 also gave a signal intensity 0.36. With the direct immobilisation of Toxin B-28, no potential detection binder was identified. This suggested that Toxin B-18 is a better capture Affimer molecule for Toxin B when immobilised directly onto Nunc Maxisorp plates.

The results from Sandwich ELISA by direct immobilisation (adsorption) of capture Affimer indicates that it is possible to identify potential binder pairs, but due to the lower sensitivity observed with longer incubation times (12 min incubation of bound streptavidin-HRP to TMB substrate), inconsistent ELISA values for controls in different wells and plates, further optimization was therefore required.

5.6.2.2 Oriented immobilisation of capture for Sandwich ELISA

As an alternative method to surface adsorption of the capturing Affimer, oriented immobilisation of the capturing Affimer was tested for Affimer pair identification to achieve higher sensitivity, reduced non-specific binding, providing consistent and reproducible results.

Three methods where explored for this purpose, for the identification of Affimer pairs using streptavidin-biotin based directional immobilisation of capture Affimer.

5.6.2.2.1 Sandwich ELISA with biotinylated capture and detection Affimer

It has been reported that when a biotinylated capture molecule is used in sandwich assays, a biotinylated detection can be introduced once the available biotin sites on the plates are blocked with excess free biotin (Sherwood and Hayhurst, 2012, Zhu *et al*., 2014). An overview of this method is given in Figure 5.19 while the protocol used is described in section 2.11.3 and the result obtained from this experiment is shown in Figure 5.20.

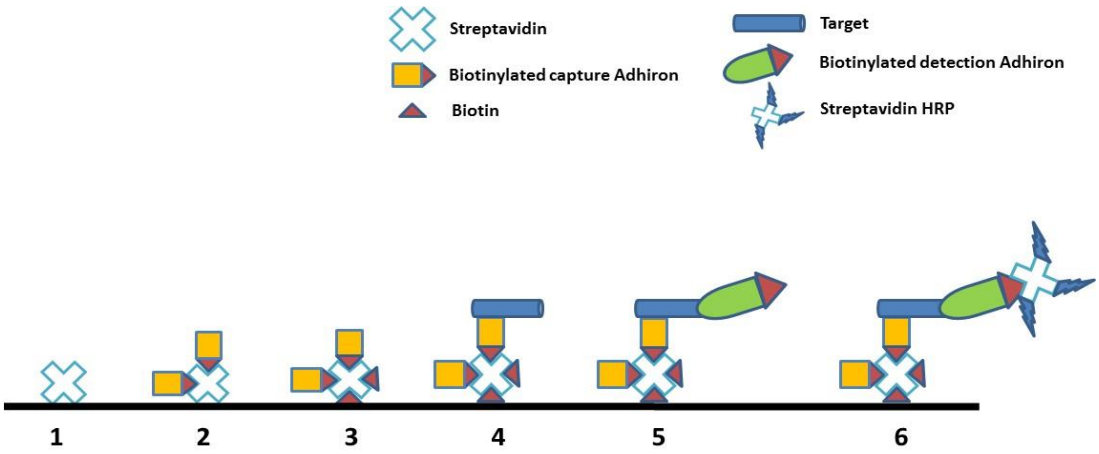

Figure 5.19: Schematic diagram for double-biotinylation sandwich assay (adapted from Sherwood and Hayhurst, 2012). 1. Streptravidin is coated on a surface, by passive adsorption onto wells of an ELISA plate; 2. Immobilisation of biotinylated capture Affimer via the single biotin molecule; 3. Unoccupied biotin binding sites are blocked with free biotin; 4. Target is added and is captured by the immobilised Affimer; 5. Biotinylated detection Affimer is added and binds to a different epitope on the target; 6. Streptavidin conjugated to HRP is added which can only bind to the biotinylated detection Affimer, and TMB substate is added for signal development.

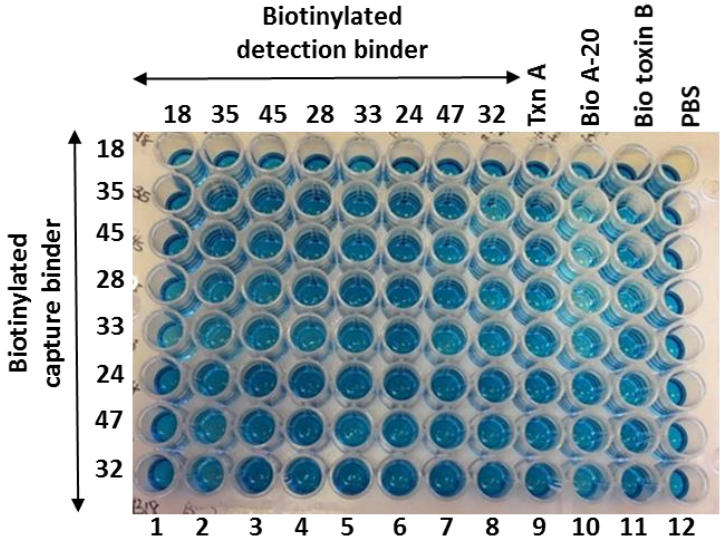

Figure 5.20: Double biotinylation sandwich ELISA. The plate layout obtained from the sandwich ELISA for toxin B using biotinylated capture toxin B Affimer and biotinylated detection Affimer is given. In Lane 1-8 each biotinylated capture is tested with different biotinylated detection Affimer. Lane 9 -12 were used for controls. In lane 9, toxin A was used as the target in place of toxin B when the same binder was capture and detection. In lane 10, a biotinylated toxin A binder (Bio A-20) was used as capture against toxin B. Lane 11 contained immobilised capture detected with biotinylated toxin B. Lastly, Lane 12, contained a buffer blank control using PBS in place of toxin B.

When biotinylated capture Affimers were immobilised onto a streptavidin coated Nunc plate, free biotin was introduced to block remaining biotin sites on the plates, followed by the target molecule, then biotinylated detection binder was added. As seen in figure 5.20, the whole plate shows positive signals (blue colour) including the controls which indicated that the added free biotin was not an efficient method to block the remaining biotin-binding sites on the streptavidin coated plate. Therefore, the control wells were able to produce a signal in the absence of the target because the biotinylated Affimer (capture/detection) remained in the well and was detected by the streptavidin-HRP conjugate. Sherwood and Hayhurst (2012), gave an explanation why this might occur - when capture molecules are chemically biotinylated, multiple biotins are randomly distributed over the surface of the protein, which is unlikely to allow for single-biotinylated capture molecule. Therefore, devising a sandwich ELISA requires that the detection molecule is made distinct to the capture molecule either by fusion to a different enzyme or tag (Sherwood and Hayhurst, 2012).

5.6.2.2.2 Sandwich Phage Display

Sandwich phage display (capture sandwich panning) is a technique that can be used as a selection strategy to identify pair of binders against a single target. Ki *et al*. (2010) described the selection of EGFR-specific antibody using the capture sandwich panning. The selected single-chain variable fragment (scFv) antibodies yielded sandwich ELISA reagent that could be used for capturing or detection, and also paired with commercial cetuximab.

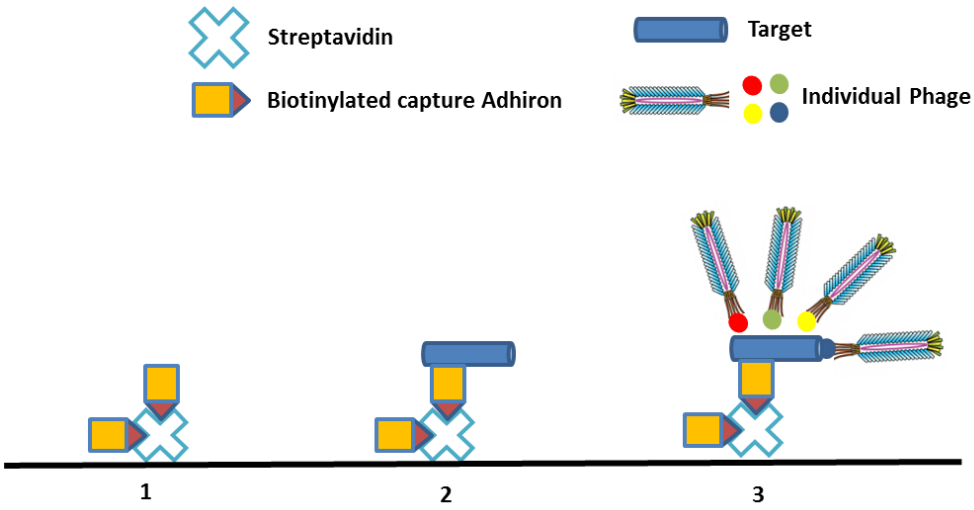

Figure 5.21: Schematic diagram for sandwich phage display. Biotinylated capture Affimer is immobilised onto the surface of streptavidin coated Nunc plate. Streptravidin. 2. Target is added and is captured by the immobilised Affimer; 3. Phage display screening is carried out on the captured target to identify detection Affimer that identifies non-overlapping epitope on the target. The phage display screening involves four steps (bind; wash; amplify; elute).

To test this approach, Toxin A-1 and Toxin B-18 were used as the capture Affimer in toxin A and toxin B sandwich capture panning respectively. After immobilisation of the target on the capture Affimer, phage obtained from the second panning round of the target is used as the input phage, and the phage display screening is carried out as previously described (section 2.9). However, this sandwich capture panning failed for toxin A and B (colony count on control plate and panning plate were similar: 20/25). Therefore, rather than repeating it which is time consuming, It was decided to analyse the panels of binders already selected against toxin A and B in a sandwich assay before searching for new pairs.

5.6.3 Sandwich Phage ELISA

Having tried two methods for the selection of Affimer pairs described in section (5.6.2.1 and 5.6.2.2) which failed, sandwich phage ELISA was explored. Here, the capture Affimer is immobilised onto streptavidin coated plate using biotin-streptavidin interation. Once the target is added and captured, individually prepared phage of the Affimer binder is tested for binding (section 2.11.4). The main advantages of the sandwich phage ELISA is that it provides oriented immobilisation of the capture Affimer, enables the capture and detection Affimer

are differently labelled, and enjoys the amplification provided by the use phage in detection.

5.6.3.1 Sandwich phage ELISA for toxin A

Sandwich phage ELISA was carried out for toxin A using biotinylated Affimers immobilised in lane 1-9 as the capture Affimer on a streptavidin coated plate. Biotinylated toxin A was immobilised in lane 10 to test the binding of the capture Affimer phage to Toxin A, serving as the positive control. Biotinylated toxin B in lane 11 was used for cross-reativity testing for each of the Affimer phage , while PBS was added to lane 12 to serve as a negative control to ensure there is no background binding. The result obtained from the sandwich phage ELISA is presented in Figure 5.22.

This result shows that Toxin A-14 is the best capture Affimer for Toxin A and it could pair with a panel of other binders (Figure 5.22a and c). Although no other binder showed binding in a sandwich format, the individual Affimer phage bound to toxin A when biotinylated toxin A was immobilized in lane 10 (positive control). This confirms that all the selected Affimer binders bind toxin A. A graph showing the signal intensity obtained for each Affimer phage when tested against toxin A, toxin B or PBS is given in Figure 5.22b. As expected, toxin A Affimers are highly specific for toxin A.

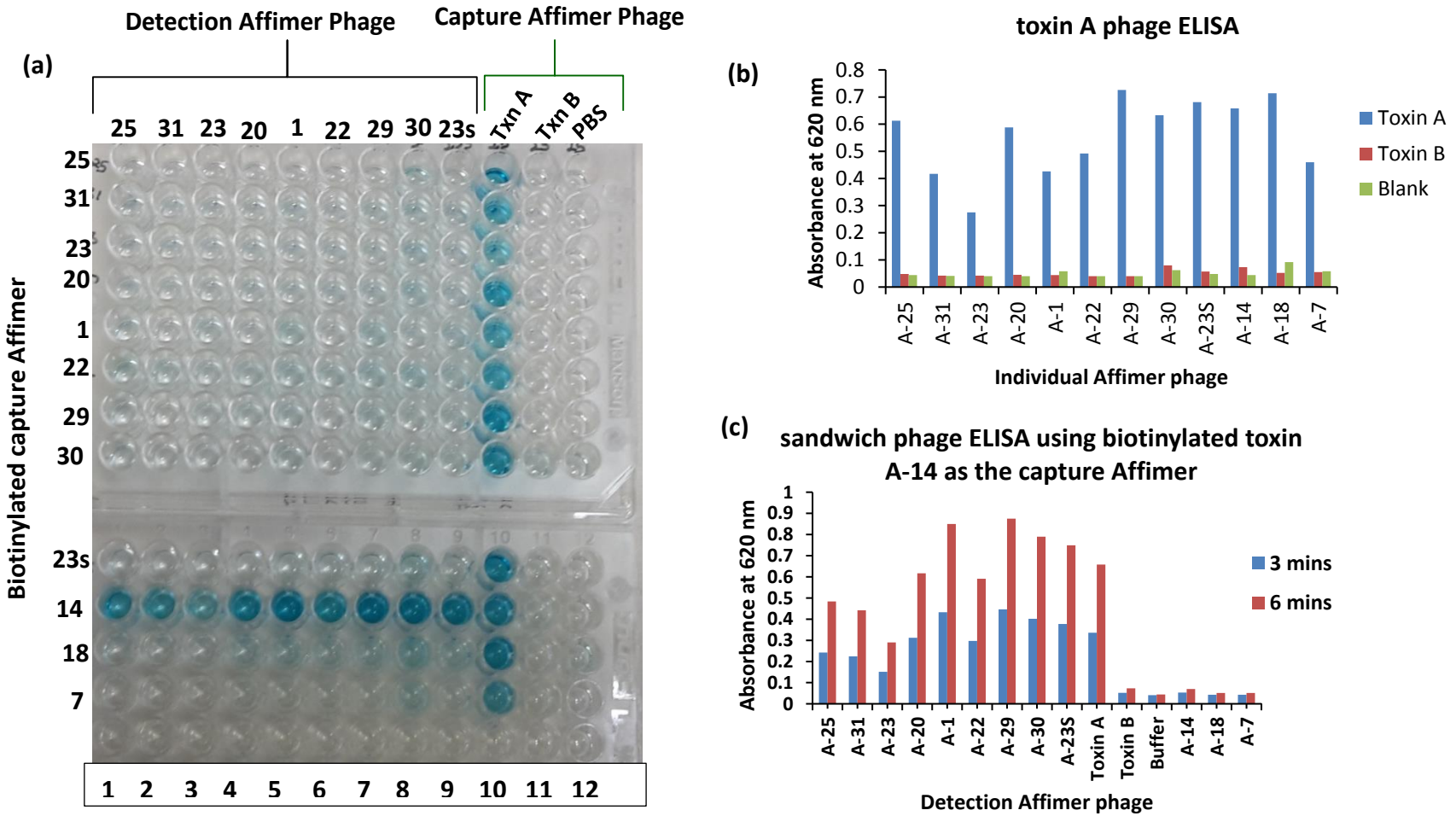

Figure 5.22. Toxin A sandwich phage ELISA. (a) The sandwich phage ELISA for toxin A is shown. Lane 1-9 contains toxin A sandwiched between biotinylated capture and the detection Affimer phage; lane 10 is a positive control containing immobilised biotinylated toxin A detected with the capture Affimer phage; lane 11 is a negative control containing immobilised biotinylated toxin B tested against each capture Affimer phage, while lane 12 is the buffer (PBS) control. (b) The signal intensity obtained from the phage ELISA shown in lane 10, 11, 12 from (a). (c) The sandwich phage ELISA using biotinylated toxin A-14 as the capture.

5.6.3.2 Sandwich phage ELISA for toxin B

Sandwich phage ELISA was also carried out for toxin B using biotinylated Affimers immobilised in lane 1-9 as the capture Affimer on a streptavidin coated plate, biotinylated toxin B immobilised in lane 10 to test the binding of the capture Affimer phage to toxin B, serving as the positive control. In lane 11, biotinylated toxin A was used for cross-reativity testing for each of the Affimer phage , while PBS was added to lane 12 to serve as a negative control to ensure there is no background binding. The results obtained from the sandwich phage ELISA is presented in Figure 5.23. Figure 5.23a gives an image of the sandwich phage ELISA plate after 6 min incubation with TMB substrate. An overview of this result shows that for toxin B, an array of potential pairs have been identified for use in a sandwich-type of assay. Analysis of the binding patterns obtained for each capture binder reveals that the binders can be grouped into three groups based on the similarities observed.

Group 1 binders – Toxin B-18, Toxin B-28 and Toxin B-33: These are capture binders that form pairs with the same detection binders (Toxin B-45 and Toxin B-47) with highly similar signal intensity. On the other hand, weak signals were observed when Toxin B-18, Toxin B-28 and Toxin B-33 detection phage was added to wells containing immobilised Toxin B-45, while no binding of these binders were observed in wells containing immobilised Toxin B-47. This suggests that for the right orientation of the Group 1 binder pairs, Toxin B-18, B-28, and B-33 would serve best as capturing Affimer with Toxin B-45 and Toxin B-47 serving as detection Affimer. It is noteworthy that the group 1 binders consist of RWP motif in the variable loop 2 (see Table 5.3) which might be an indication that they bind the same epitope.

Group 2 binders- Toxin B-45 and Toxin B-24: This binder pair shows binding to each other when used either as capture or detection binder.

Group 3 binders- **Toxin B-47 and Toxin B-32**: These binders when used as capturing Affimer did not pair with any binder except a mimimal binding observed for Toxin B-32 with immobilised Toxin B-32. Nonetheless, the two binders could serve as

good binders for toxin B in single-binder applications. The toxin B-35 result shows that it is not a good binder because no binding was observed when it was used as either a capturing Affimer or detection Affimer. This is not surprising since no binding signal was observed with immobilised toxin B.

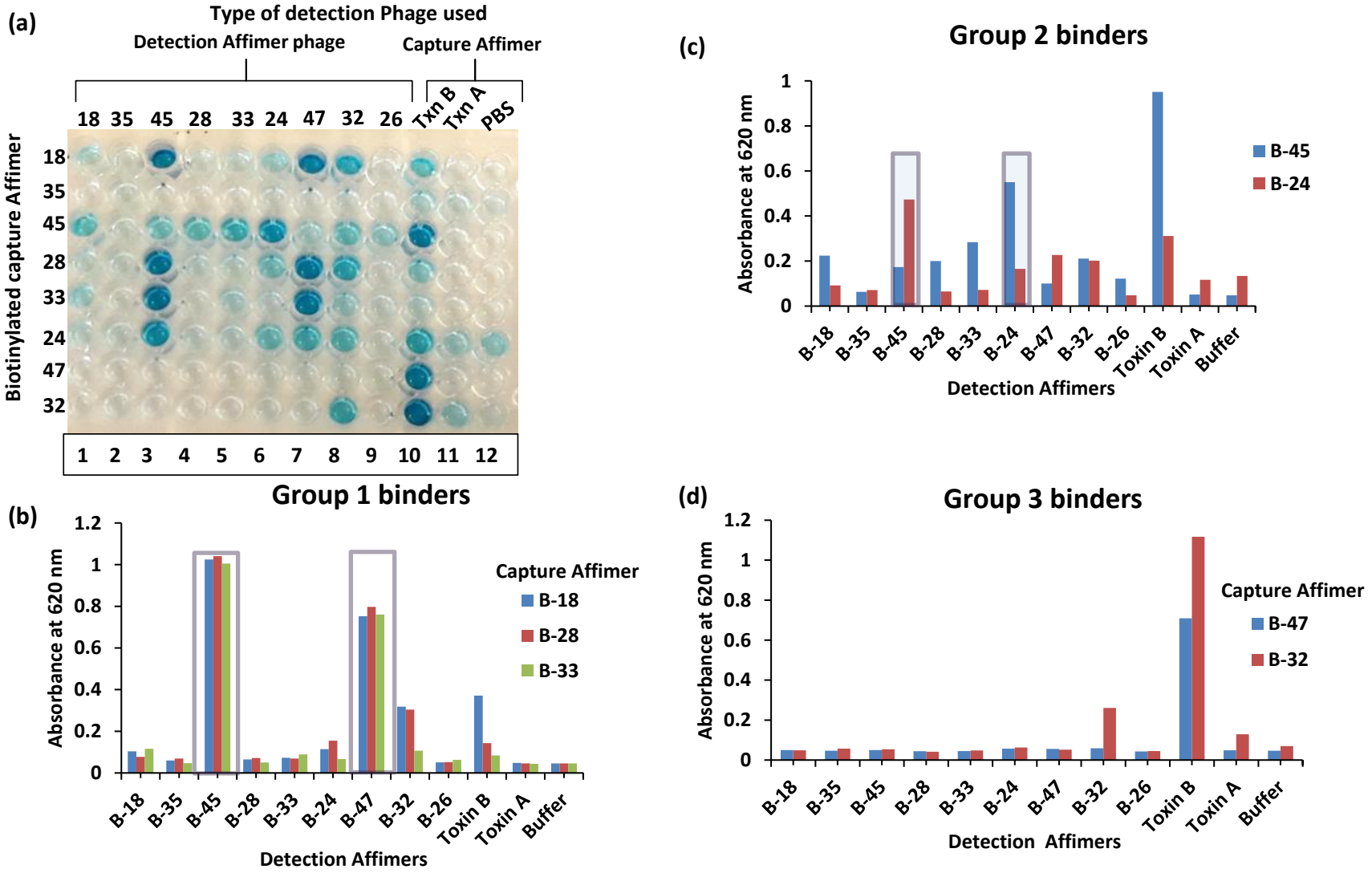

Figure 5.23. Toxin B sandwich phage ELISA. (a) The sandwich phage ELISA for toxin B is shown. Based on the binding pattern, the binders were grouped into three which are presented in (b) – (d).

Analysis of the signal intensity of each Affimer phage against immobilised toxin B showed that Affimers B-32, B-45 and B-47 gave the highest binding signal (A_{620nm} = 0.4-0.7) to immobilised toxin B in Lane 10, Toxin B-18 and B-24 gave signal intensities of 0.24 and 0.18 respectively, while Toxin B-35, B-28 and B-33 showed no binding signal. With biotinylated toxin A immobilised in Lane 11 or PBS in lane 12, no signal was observed across the binders showing their specificity to toxin B.

5.6.4 Selection of the best toxin B binder pairs.

In total, 8 potential pairs were identified from toxin B sandwich ELISA. To select the best binder pair, sandwich ELISA was repeated, and the result obtained is shown in Figure 5.24.

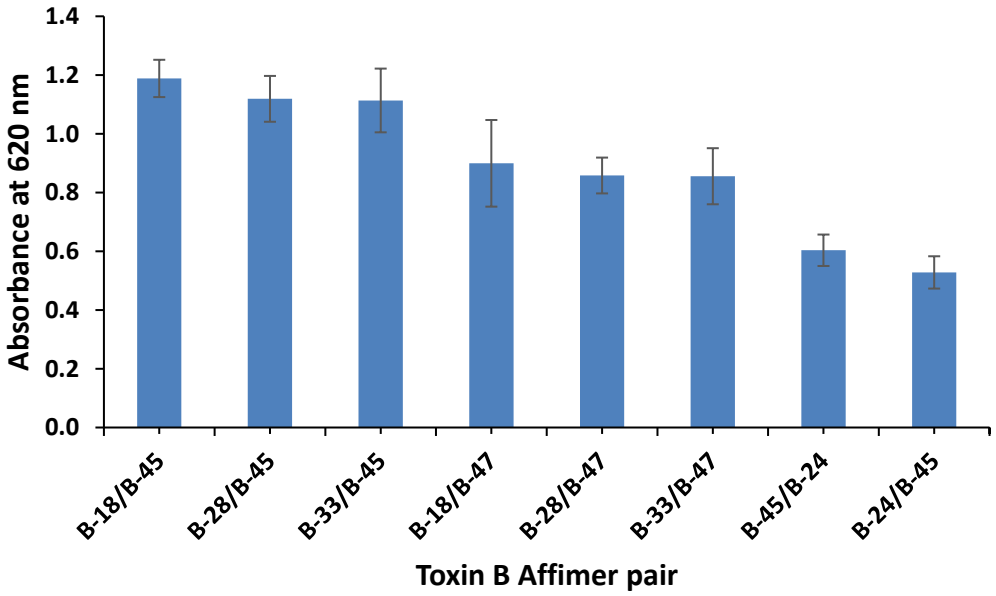

Figure 5.24: Sandwich ELISA for the selection of the best pair. The signal intensities obtained from the sandwich phage ELISA of each pair is presented as average of two independent repeats and the error bar indicate standard deviation of averaged data ($A_{620\,nm}$) from the two independent repeats.

Toxin B-18 has consistently shown higher binding signal intensity to toxin B compared to Toxin B-28 and Toxin B-33, therefore was taken forward as the best capturing Affimer. For detection Affimer, Toxin B-45 has also given consistently higher binding signal intensity in Group 1 binders compared to Toxin B-47, therefore was taken forward as the best detection binder. Although Toxin B-45 and Toxin B-24 would pair with each other in any direction, the signal intensity

obtained from this pair made it less optimal for developing a highly sensitive rapid diagnostic tool for toxin B.

Overall, Toxin B-18/ B-45 Affimer pair has the highest signal intensity and was therefore taken forward as the best toxin B Affimer pair.

5.7 Surface plasmon resonance (SPR)

SPR was used to assess the interaction of toxin A and B binders with toxin A and B. The SPR biosensor chip was streptavidin-coated to allow for immobilisation of biotinylated Affimers through streptavidin-biotin interactions, and toxin A or B were used as analytes. Each biosensor chip has four flow cells (called channel 1, 2, 3 and 4) to allow the running of parallel experiments.

To investigate the Toxin B-18 kinetics, channel 1 was used to check the change in the SPR angle due to the refractive index of the buffer control. For channel 2, 3 and 4, they were functionalised with Toxin B-18 dilutions (0.1 nM, 10 nM and 100 nM respectively). The SPR sensograms for the binding of Toxin B-18 to toxin B, and for the evaluating the cross-reactivity of the binders are shown in Fig 5.25a and 5.25b respectively.

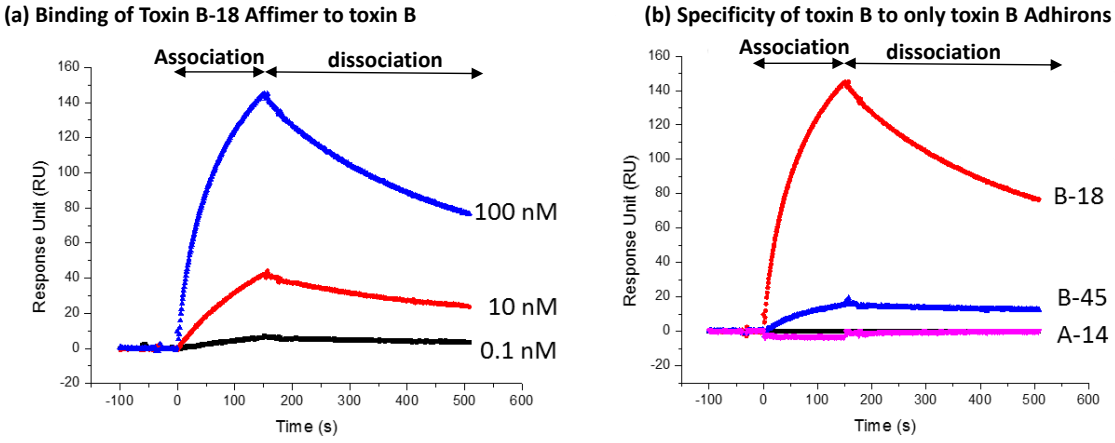

Figure 5.25. SPR analysis of the binding of toxin A and B to Affimers. Biotinylated Affimers were immobilised on streptavidin chips, and toxin A or toxin B was flowed through as analyte. The SPR sensograms were recorded with 10-fold serial dilutions, starting at the lowest concentration of 0.1 nM. (a), Sensogram for biotinylated Toxin B-18 against Toxin, (b). Sensogram showing the specificity of toxin B Affimers for toxin B. There was no cross-reactivity observed on the flow cell on which Toxin A-14 Affimer was immobilised.

Figure 5.25(a) shows the binding curve obtained for toxin B-18 after subtracting the response due to the change in refractive index of 10 mM PBS, pH 7.2. Based on the association and dissociation curve, the data were analysed with BIAevaluation 4.1 software (GE Healthcare). Toxin B-18 and B-45 Affimers bind to toxin B with equilibrium dissociation constant (K_D) of 4.04 nM and 4.68 nM respectively, while Toxin A-14 Affimer binds to toxin A with a K_D of 81.5 nM. Investigating the cross-reactivity of toxin B Affimers to toxin A reveals the specificity of the Affimers identified. Toxin B Affimers do not cross-react with toxin A and vice versa. The SPR data confirms the specificity results obtained from phage ELISA (see Figure 5.4), sandwich phage ELISA (Figure 5.23) and BLItz data (Figure 5.17).

5.8 Summary

This chapter describes the use of the Affimer phage display library as a robust technique for the identification of highly specific and sensitive binders to the two exotoxins toxin A and toxin B, which are used as biomarkers for the diagnosis of *Clostridium difficile* infection CDI. Twelve binders were selected for further characterisation for toxin A while 10 binders were selected for toxin B. The Affimers were easily expressed in *E. coli* and purified from the soluble fraction of lysed cells using one-step Ni-NTA affinity chromatography with the highest yield of 227 mg/L. Biophysical characterisation of toxin A and B binders revealed that most binders were monomeric, thermally stable with no evidence of aggregation at 90 ^{O}C. The Affimers were then tested for use in direct and sandwich ELISA format, toxin B-18 was identified as the best capturing Affimer for toxin B while toxin B-45 was the best detection Affimer, and both binders serving as the best identified pair for toxin B. Toxin A-14 was identified as the best capturing Affimer for toxin A. The K_D of these three binders was determined by surface plasmon resonance.

Chapter 6: Development of a hybrid Affimer-based assay for CDI diagnosis

6.1 Introduction

Following the identification and biophysical characterisation of unique Affimers against toxin A and B as described in chapter 5, the next objective was to develop an Affimer-based diagnostic assay referred to here as Affimer-sorbent assay (AFFISA) and then compare its sensitivity and specificity to commercially available kit.

6.2 Determination of the Limit of Detection (LOD)

Most commercially available ELISA kits for toxin detection can detect 1 to 2 ng/mL of toxin in clinical samples (Novak-Weekley and Hollingsworth, 2008). Therefore, sandwich phage ELISA was used to determine the limit of detection of toxin A and B pairs identified using serial dilution of PBS spiked with purified native toxin A and B. The molar concentration of toxin A and B used for the serial dilution (from 2500 ng/mL to 1.2 ng/mL) is given in Table 6.1. For the determination of the limit of detection for toxin A, Toxin A-14, which has been identified as the best capture in Section 5.6.3 was paired with Toxin A-20 phage as the detection Affimer. For the determination of the limit of detection for toxin B, the best pair identified for toxin B (Toxin B-18: Toxin B-45) were tested with Toxin B-18 as the capture and Toxin B-45 phage as the detection Affimer.

Table 6.1. Molar concentration of Toxin A and B used for the serial dilution.

concentration (ng/mL)	Molar concentration	
	toxin A	toxin B
2500.0	8.12 nM	9.26 nM
1250.0	4.06 nM	4.63 nM
625.0	2.03 nM	2.31 nM
312.5	1.01 nM	1.16 nM
156.3	0.51 nM	0.58 nM
78.1	0.25 nM	.29 nM
39.1	0.13 nM	.15 nM
19.5	63 pM	72 pM
9.8	32 pM	36 pM
4.9	16 pM	18 pM
2.4	8 pM	9.04 pM
1.2	4 pM	4.5 pM

As described in Section 2.11.1, 1 µg/mL of biotinylated capture was immobilised, and then 50 µL from the serial dilutions were added to their respective wells. Following incubation and washing step, a 50 µL aliquot of the detection phage supernatant introduced to bind the captured target. Binding was detected using Anti-phage-HRP then TMB substrate. To monitor the effect of TMB incubation time the ELISA signal intensity was measured at 3 min, 9 min, 15 min, 30 min and 45 min. Results obtained from the toxin B sandwich phage ELISA are presented in Figure 6.1 while that of toxin A is provided in Figure 6.2.

(a)

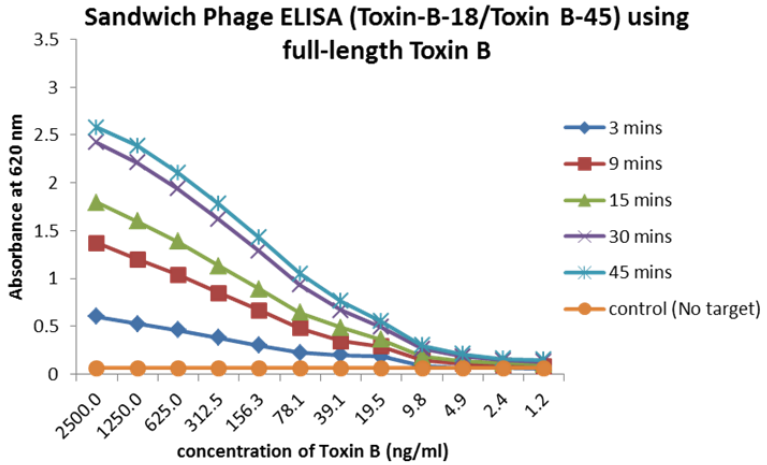

(b)

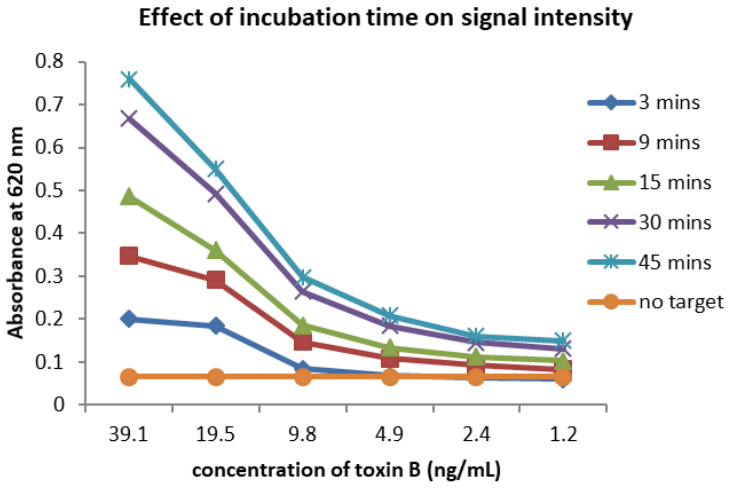

Figure 6.1: Optimisation of incubation time for Toxin B-18/Toxin B-45 phage ELISA. (a) Sandwich phage ELISA using Toxin B-18 as capture Affimer and Toxin B-45 phage as detection binder. A serial dilution of toxin B from 1500 ng/mL to 1.2 ng/mL was used to determine the limit of detection of the Affimer pair. (b) Expanded region of (a) showing effect of incubation time on the signal intensity obtained between 39.1 ng/mL to 1.2 ng/mL. Signals at 3, 9, 15, 30 and 45 min are represented as navy, red, green, purple and blue trend lines respectively.

As a negative control, GDH was used to replace the target to show that no signal was observed between the capture and detection binder in the absence of the target. The signal intensity after 45 min incubation was represented as the orange trend line.

Figure 6.1a, confirmed that Toxin B-18 is a binding partner to Toxin B-45. The result shows that as the incubation time increases, the signal intensity also increases. The effects of increasing the incubation time were seen more clearly at lower concentrations from 39.1 ng/mL, to 1.2 ng/ mL Toxin B in the expanded region shown in Figure 6.1b. Increasing the incubation time from 3 min to 30 min, showed a 58 % rise in signal intensity at 39.1 ng/mL toxin B concentration and a 30 % rise at 1.2 ng/mL toxin B concentration. From this result, it is clear that increasing the incubation to 30 min increases the limit of detection for toxin B, making it possible to detect the toxin even at 1.2 ng/mL concentration. In the negative control well, that contained biotinylated Toxin-B-18 and Toxin-B-45 phage but no target, there was no signal observed up to 45 min incubation time.

For toxin A, the sandwich phage ELISA result is presented in Figure 6.2. Toxin A binder-pair (Toxin A-14/Toxin A-20) detects toxin A in a sandwich format only in the presence of the target. No signal was observed in wells with no toxin A. Like results for toxin B, increasing the incubation to 30 min increases the limit of detection for toxin A.

The Sandwich Phage ELISA for toxin B Affimers demonstrated high sensitivity and specificity toward toxin B, and no positive results were obtained from using toxin A as the target or from the control (Figure 6.3). A sample was considered positive if the $OD_{620\,nm}$ was twice the average of the negative controls from three replicates. Therefore, toxin B assay detected toxin B down to 1.2 ng/mL and for toxin A assay detected toxin A down to 312 ng/mL.

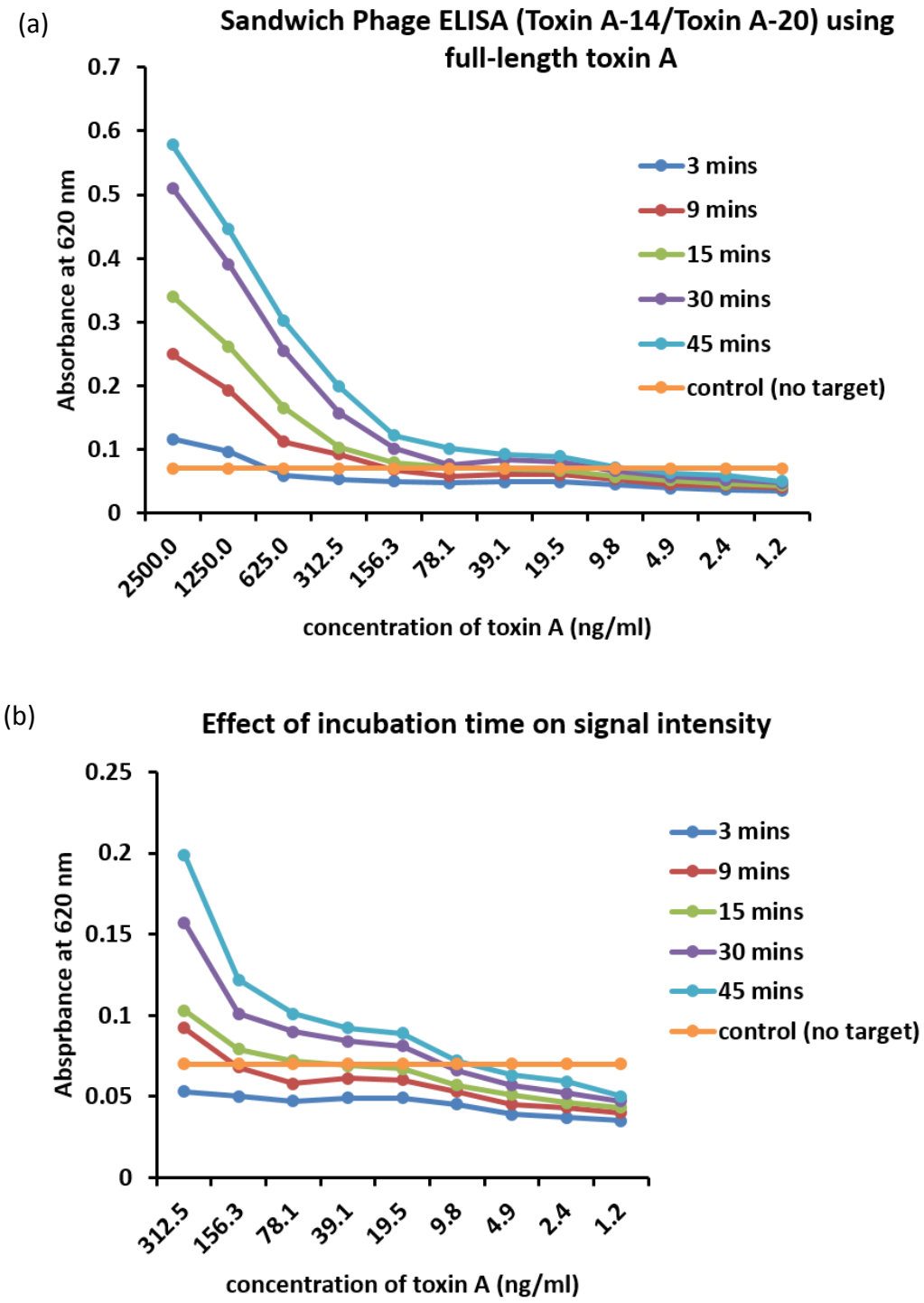

Figure 6.2: Optimisation of incubation time for Toxin A-14/Toxin A-20 sandwich phage ELISA. (a) The sandwich phage ELISA for toxin using Toxin A-14 as capture Affimer binder and Toxin A-20 phage as detection binder is presented. A serial dilution of toxin A from 2500 ng/mL to 1.2 ng/mL was used to determine the limit of detection of the Affimer pair. (b) Effect of incubation time on the signal intensity obtained between 312.5 ng/mL to 1.2 ng/mL. Signals at 3, 9, 15, 30 and 45 min are represented as navy, red, green, purple and blue trend lines respectively.

6.3 Evaluating the specificity of Affimer pair

Despite the sequence similarity between toxin A and B, toxin-specific antibodies have been reported for toxin A. However, identification of monoclonal antibodies against toxin B are difficult to generate (Humphrey *et al*., 2013). By contrast, the selection of toxin specific Affimers was quite straightforward. To test for the specificity of the toxin A Affimer pair therefore, toxin B at 2.5 µg/mL was used. Similarly, toxin A at 2.5 µg/mL was used to test the specificity of the toxin B Affimer pair. Toxin A Affimers showed no positive signal for toxin B as the target (Figure 6.3a), and similarly for toxin B Affimers, no positive signal was detected for toxin A as the target (Figure 6.3b).

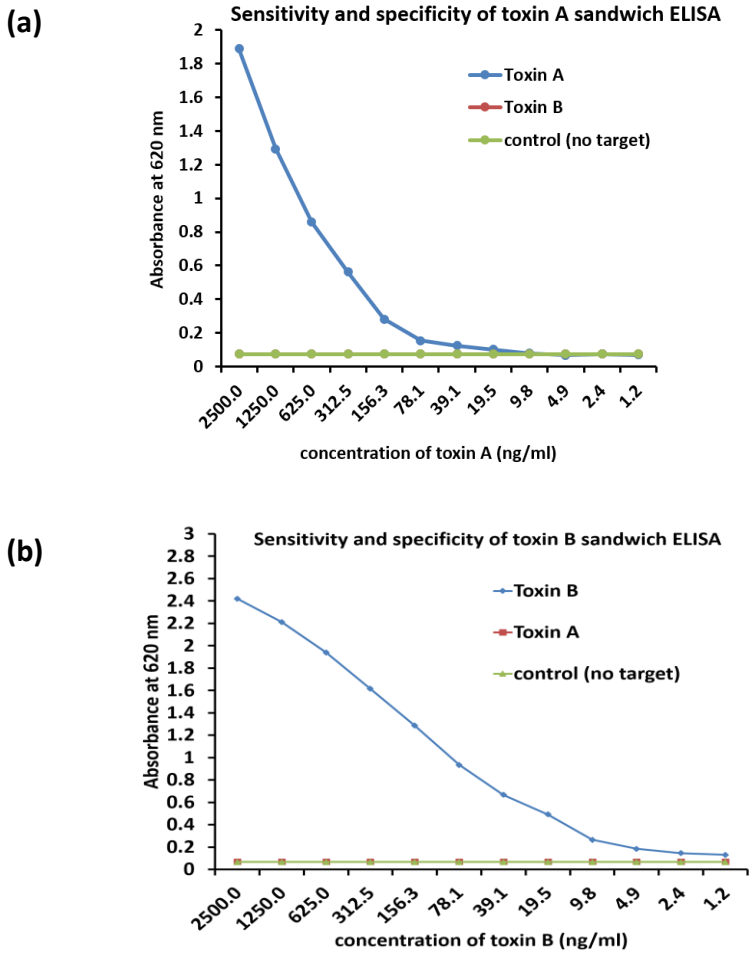

Figure 6.3. Evaluating the sensitivity and specificity for toxin A and toxin B Affimer pairs. (a) toxin A sandwich ELISA using toxin A-14 as capture and toxin A-20 phage for detection. (b) toxin B sandwich ELISA using toxin B-18 as capture and toxin B-45 for detection. In the absence of target, no binding occurred which shows the specificity of the Affimer pairs.

These results indicate that the toxin A Affimer pair and toxin B Affimer pair are highly specific for the detection of toxin A and toxin B respectively.

6.4 Determination of Limit of detection using a detection Affimer conjugated to HRP

Conjugation of a detection binder or secondary antibodies to a variety of labels including enzymes, biotin and fluorescent dyes has been reported in literature. Generally, the choice of reporter system is application-dependent. Applications such as ELISA utilise enzymes (horseradish peroxidase or alkaline phosphatase) to obtain signal amplification, while fluorescent-based applications utilise fluorescent labels.

This work focuses on the use of ELISA-based assays to develop a rapid sensitive, specific multiplex diagnostic platform for *Clostridium difficile* infection. Therefore, the detection Affimer binder could be conjugated to enzymes or biotin. As described in Section 5.6.2.2 specific orientation of capture Affimer using biotin-streptavidin interaction increases the binding efficiency of the capturing Affimer. However, results obtained from sandwich ELISA using biotinylated capture and biotinylated detection Affimers (Figure 5.20) indicates that background signals could not be abolished in the experiments. To test different labels on capture and detection binders, capture Affimers were biotinylated while detection Affimers were conjugated to HRP.

6.4.1 Conjugation of detection Affimer to HRP

The maleimide activated HRP (ThermoFisher) contains 1-3 moles of maleimide per mole of HRP. Since Affimers were modified to contain a single C-terminal cysteine residue, the conjugation reaction would result in a mixture of different ratios of Affimer: HRP with up to 3 molecules of Affimer per HRP molecule. In addition, unconjugated Affimer or HRP would be present. The presence of unlabelled detection Affimer during sandwich ELISA would compete with conjugated detection Affimer which would decrease the signal intensity obtained, hence it was necessary to remove unlabelled Affimer from the reaction. Unconjugated HRP on the other hand would easily be removed during the washing steps. Therefore, the

conjugation reaction mixture was resolved on Superdex 200 10/300 high resolution matrix as described in Section 2.12.2 to fractionate the reaction mixture based on size. HRP (ca. 44 kDa) and Affimer-HRP (>56.5 kDa) would be separated from unconjugated Affimer (ca. 12.5 kDa). Protein and peroxidase in the elution fractions were detected by simultaneous by monitoring the absorbance at 280 nm and 403 nm, the latter wavelength corresponding to the absorbance Soret peak for heme-containing peroxidase.

Figure 6.4 shows the result obtained from the conjugation of Toxin A-14, Toxin B-18 and Toxin B-45 to HRP. From the chromatogram of Toxin A-14-HRP, a major peak eluting at 15.5 mL, a shoulder at 14 mL and a minor peak at 12.5 mL was observed at 403 nm while two major peaks eluting at 15.5mL and 19 mL were observed at 280 nm wavelength. Toxin A-45-HRP chromatogram shows a major peak eluting at 15.5 mL and a shoulder at 14mL at 403 nm with a major peak at 15.5 mL and a minor peak at 19 mL at 280 nm. By contrast, the chromatogram of Toxin B-18-HRP shows a major peak with a broad shoulder and a minor shoulder eluting from 14 mL to 18 mL at 403 nm wavelength. Similar peaks were observed at 280 nm with an additional minor peak at 20.5 mL. Approximately 0.5 mL fractions were collected and 15 µL of fractions from major and minor peaks at 403 nm and 280nm and maleimide-activated HRP were analysed by 4-20 % SDS-PAGE.

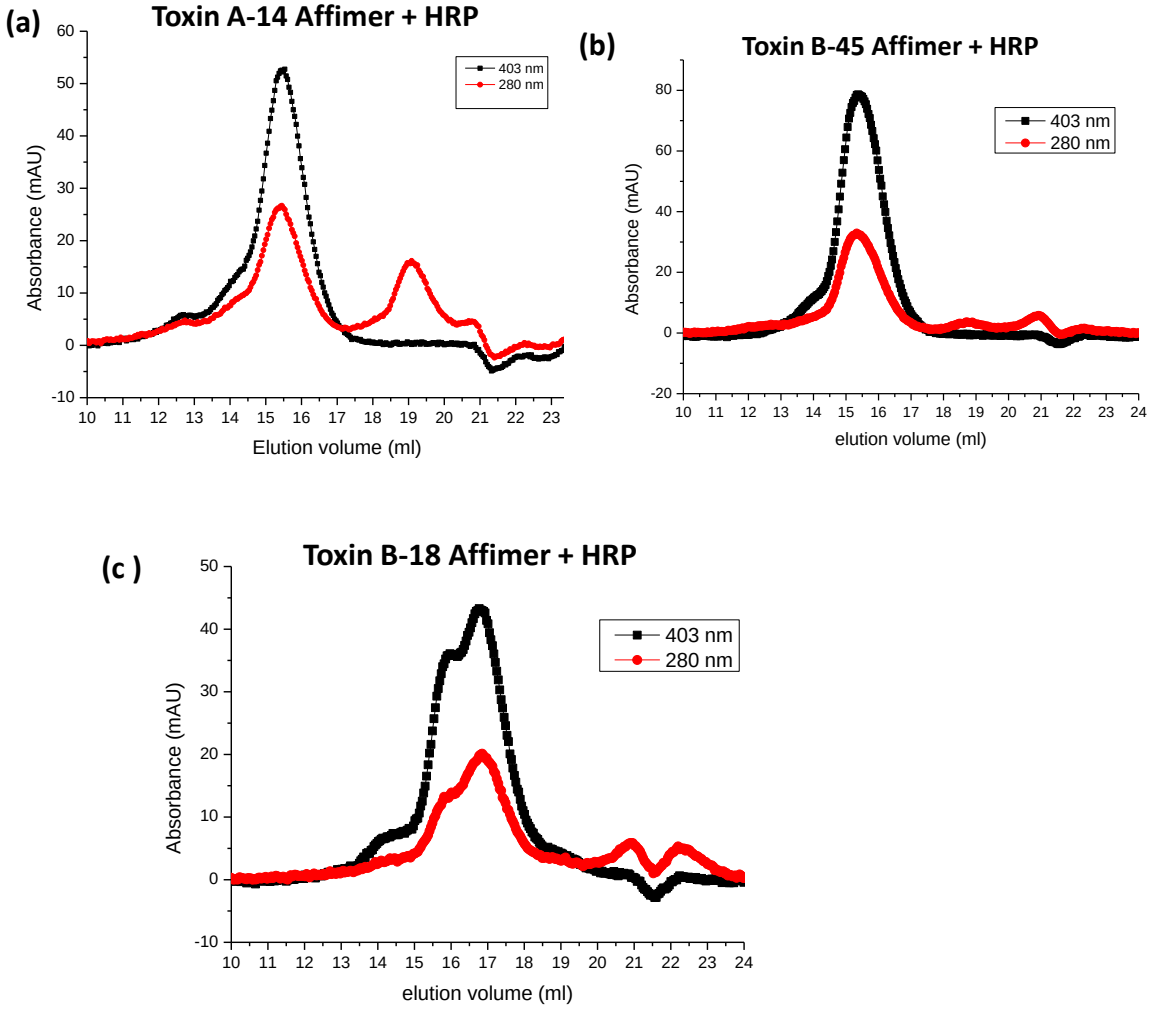

Figure 6.4: Size exclusion of Affimer binders conjugated to maleimide HRP. Three binders: (a) Toxin A-14, (b) Toxin B-45, (c) Toxin B-18, were conjugated to maleimide HRP. The chromatograms using Superdex^{TM} 200 reveals the absorption profile of the conjugate at 403 nm and 280 nm. For all conjugated binders, a major peak at 403 nm corresponds to the absorbance of HRP, while a minor double peak at 280 nm eluting later corresponds to unconjugated Affimer. Elution fractions were collected and analysed by SDS-PAGE.

Gel images of the analysed fractions for (a) A-14-HRP, (b) B-45- HRP, and (c) B-18-HRP are shown in Figure 6.5. Bands were labelled a-g for ease of identification. From band migration, molecular mass determination identified that band (a) was the unconjugated HRP with size (~ 44kDa) which migrated to the same position as the unconjugated HRP (e). Band (b) migrated at ~56.5 kDa which could correspond to HRP conjugated to Affimer in 1:1 ratio. Band (c) migrated at ~69kDa which could correspond to HRP-Affimer in a 1:2 ratio. Unconjugated Affimer migrated as band (d) with mass (~12.5 kDa). Multimeric HRP migrating at ~132 kDa is band (f). The

presence of his-tagged Affimer in the Adh-HRP samples were confirmed by western blot as shown in Figure 6.5(d). As expected conjugated Adh-HRP and toxin B-45 protein sample used as positive controls were detected. No band was observed for unconjugated HRP.

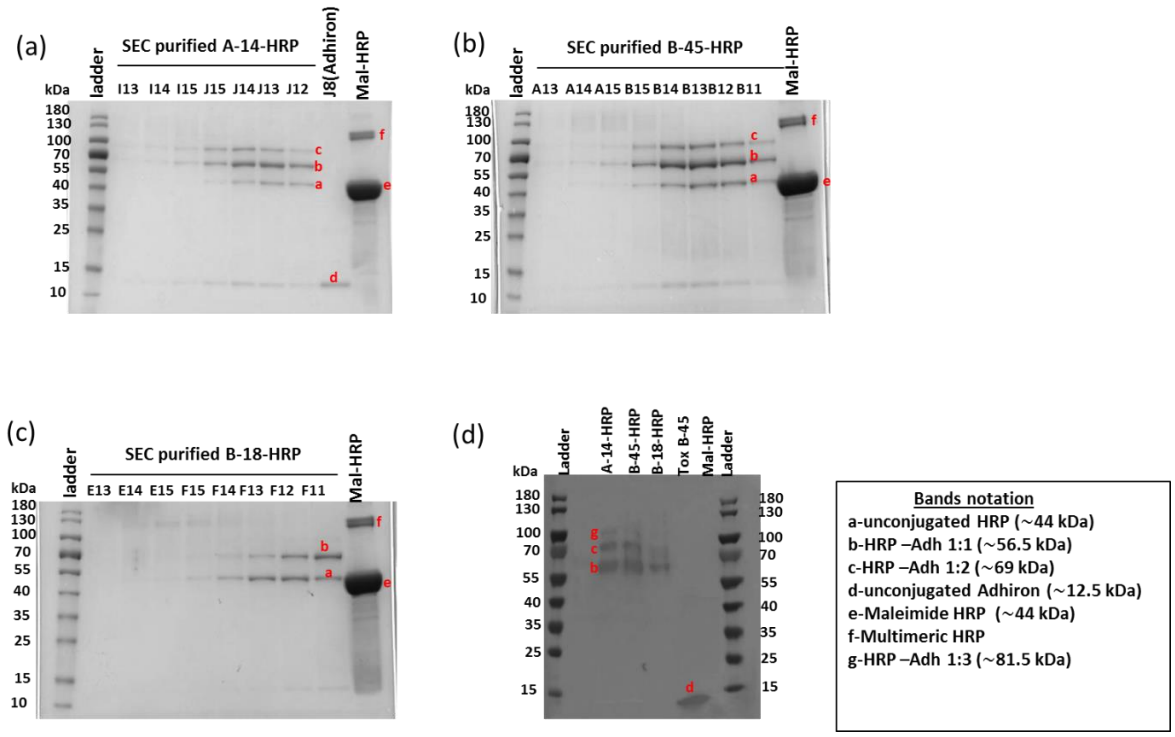

Figure 6.5: SDS-PAGE of fractions eluted from SEC of Affimer-HRP conjugation reaction. Each panel represents a separate SEC analysis for a specific Affimer binder: (a) A-14-HRP, (b) B-45-HRP, (c) B-18-HRP. Fractions corresponding to conjugated sample from each panel was analysed by western blotting (panel (d)) to confirm the presence of his-tagged protein. Bands were identified based on size and were labelled a-g.

The results obtained from Figure 6.4 and 6.5 shows that the conjugation of Affimer to HRP was successful and free unlabelled Affimer was successfully removed through size exclusion chromatography. Fractions confirmed as Affimer-HRP conjugate were pooled and concentrated using an Amicon concentrator for use in further assays.

6.4.2 Direct ELISA for the detection of target by Affimer-HRP conjugate

Affimers conjugated to HRP were tested by direct ELISA for their ability to bind immobilized target before using them in sandwich ELISA assays. Biotinylated target were immobilised on to streptavidin plates then a 50 µL aliquot of Affimer-HRP conjugate were added. Binding was detected by colour formation upon the addition of TMB substrate and the results obtained are presented in Figure 6.6. A-14 HRP successfully detected immobilised toxin A while no signal was seen in the negative control well containing immobilized toxin B. Similarly, B-18-HRP and B-45 HRP detected immobilized toxin B with no observed signal in the control well. The signal intensity observed for A-14-HRP was about 60 % lower than those from B-18-HRP and B-45-HRP. Possible reasons for this could be inefficient labelling of A-14 with HRP or the affinity of A-14 Affimer to toxin A is lower than those of B-18 and B-45 to toxin B. Since the apparent conjugation efficiency for A-14 was similar to B-18 and B-45 (>80 %) then it seems likely that the lower signal intensity relates to A-14 having a weaker affinity for toxin A. than either toxin B binder for toxin B. This is supported by the binding kinetics obtained through SPR analysis (Section 5.7).

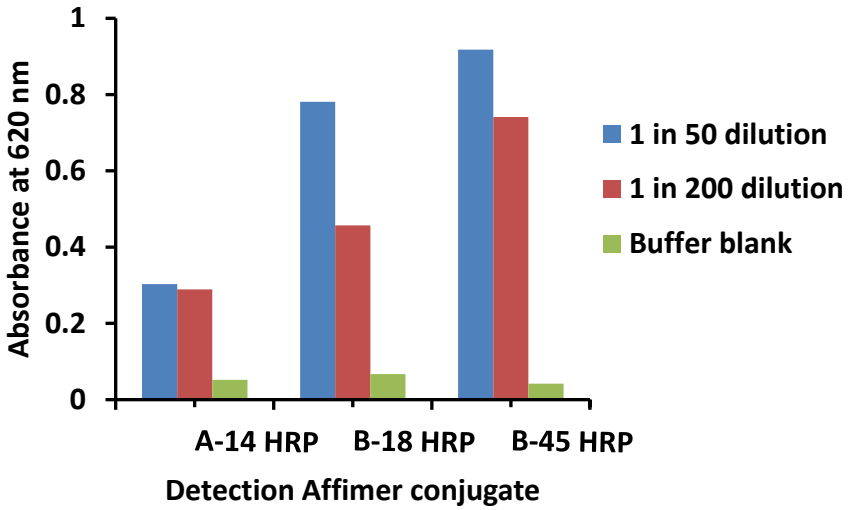

Figure 6.6: ELISA to show binding of Affimer-HRP conjugate to target. The binding of immobilised biotinylated toxin A and toxin B to Affimer-HRP was detected using TMB substrate and absorbance reading at 620 nm. The conjugates were added either in 1:50 dilution of 1:200 dilution.

Toxin B Affimers conjugated to HRP were tested for their ability to bind captured target in a sandwich ELISA format. The result presented in Figure 6.7 show that B-

18-HRP and B-45-HRP bind toxin B in a sandwich format. With 10 µg/mL of toxin B, B-18/B-45-HRP capture/detection pair (OD_{620nm} = 1.45) showed a 5-fold higher signal intensity compared to the reverse B-45/B-18-HRP pair (OD_{620nm} = 0.28), this result further substantiates the claim (Section 5.6.2) that B-18 is best utilised as a capture Affimer while B-45 is best suited as a detection Affimer.

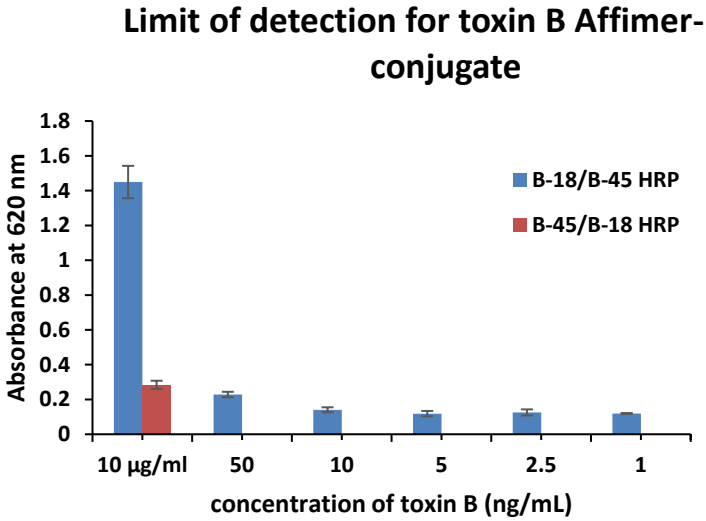

Figure 6.7. Evaluating the sensitivity for toxin B unsing Affimer-HRP conjugate. Toxin B sandwich ELISA was performed using toxin B-18 as capture and toxin B-45 conjugated to HRP for detection and data presented as blue bars. Binding was also observed when B-45 was used as capture and B-18-HRP as detection Affimer (red bar).

To determine the limit of detection for toxin B using B-18/B-45-HRP pair, a serial dilution of toxin B was prepared from 50 ng/mL to 1 ng/mL. The data show that Affimer-HRP conjugate did not give any substantial difference in signal intensity for concentrations less than 10 ng/mL. Though the conjugation of Affimer to HRP was successful and could detect its target in a sandwich assay format, the limiting factor to the sensitivity of Affimer-HRP sandwich assay is the fact that Affimer could only be labelled with one HRP per molecule thereby limiting signal amplification.

6.5 Replacing the capture antibody with a capture Affimer improves specificity and sensitivity of a commercially available kit (Techlab kit)

The diagnosis of *Clostridium difficile* infection (CDI) is strongly associated with the presence and detection of its exotoxins. Having reviewed the currently available

platforms for CDI diagnosis in Chapter 1, it is an established fact that nucleic acid amplification tests detect only the genes responsible for potential toxin production but they clearly cannot detect the presence of biologically active toxin in stool specimens, leading to potential over-diagnosis of CDI. In the same vein, though it is evident that toxin immunoassays detect the presence of toxins in clinical samples, they cannot be used as a stand-alone test for the diagnosis of CDI due to low sensitivity of the assays. Therefore, there remains the question of how to improve the sensitivity of toxin immunoassays.

Since the sensitivity of any ELISA based assay is dependent on the sensitivity and specificity of the capturing and detection molecules, an analysis of the capturing and detection molecules used in toxin A and B ELISA kits as listed on the Public Health England website and commercially available in the UK was carried out. It was revealed that >85 % of the toxin A and/B ELISA kits for the diagnosis of CDI utilises polyclonal antibodies as the capture reagent and monoclonal anti-toxin A antibody but polyclonal anti-toxin B antibody as the detection reagent as shown in Table 6.2.

Table 6.2: List of capture and detection antibodies used in commercially available clinically used *C. difficile* toxin kit.

	Capture	Detection	References
Meridian Premier Toxin A&B	Toxin specific monoclonal and polyclonal antibodies	HRP conjugated anti-Toxin A Toxin B polyclonal antibodies	www.meridianbioscience.com › C. difficile
DRG clostridium difficile Toxin A + B	Monoclonal anti-Toxin A polyclonal Toxin B antibody	Biotinylated polyclonal anti-Toxin A, monoclonal anti-Toxin B Detected with strep-HRP	http://www.drg-international.com/ifu/eia-4448.pdf
Serazym	Monoclonal anti-Toxin A Polyclonal anti-Toxin B	Biotinylated polyclonal anti-Toxin A, monoclonal anti-Toxin B Detected with strep-HRP	http://www.sekisuidiagnostics.com/products/376-serazym-clostridium-difficile-toxin-a-b-seramun
Techlab	Polyclonal goat antibody against Toxin A and B	HRP conjugated Toxin A Monoclonal mouse antibody Toxin B polyclonal goat antibody	http://www.techlab.com/wp-content/uploads/2013/06/t5015insert_rev_0308.pdf
ridascreen Xpect	Monoclonal antibodies against A +B	Biotinylated antibodies for Toxin A and B Strep-HRP	

The use of polyclonal antibodies for the development of an ELISA-based diagnostic provides the ability to recognise multiple epitopes and they are easy to generate. Nevertheless, they are plagued by the inherent limitations of polyclonal antibodies

such as batch-to-batch variation, which explains why reagents from different kits should not be mixed, and by decreased specificity since they are polyclonal. A logical explanation for the use of polyclonal anti-Toxin B antibody was provided by Deng *et al*., (2003), who found that antibodies against toxin B are difficult to generate. Analysis of the capture antibodies used in most of the kits (Table 6.2) suggests that the sensitivity and specificity of *C. difficile* ELISA kits may be limited due to use of polyclonal antibodies.

In this work, it was hypothesised that "Introducing an Affimer as a capture or detection molecule will improve the sensitivity and specificity of commercially available kits". An Affimer has the potential to complement antibodies in a hybrid-ELISA, resulting in an Affimer-sorbent Assay (AFFISA). To test this hypothesis, the Techlab Tox A/B Quick Chek ELISA kit was selected based on two criteria: First, it has high specificity (98.6 %) and sensitivity (84.3 %) according to the data published by the Public Health England (Figure 6.8) and second, it is one of the routinely used kits for *C. diff* diagnosis in the Leeds Teaching Hospitals NHS Trust clinical microbiology laboratories. The results obtained are discussed in this Section

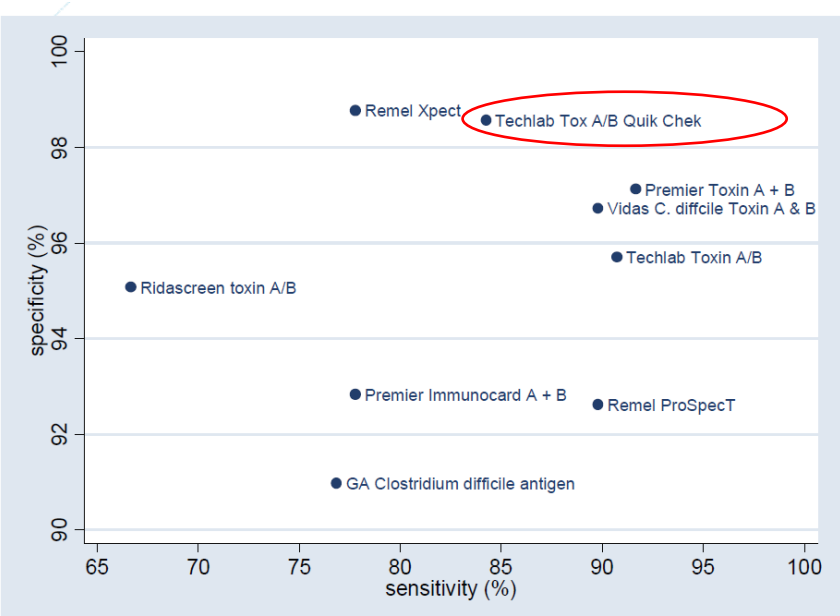

Figure 6.8. Scatter plot of estimated specificity against sensitivity (cytotoxin assay comparator). Figure was taken from the UK Department of health guideline for *C. difficile* diagnosis (2012).

6.5.1 Determination of the limit of detection for Techlab Tox A/B kit

Techlab's *C. difficile* TOX A/B II kits were purchased from Alere (UK) and ELISA was carried out as described by the manufacturer (Section 2.13.2). The kit is a sandwich ELISA format, the microwells are coated with a mixture of polyclonal antibodies against toxin A and toxin B, while the conjugate solution contains HRP conjugated monoclonal anti-toxin A and polyclonal anti-toxin B. It was essential to determine the limit of detection (LOD) of the kit for toxin A and B and compare with the LOD described in the product insert (toxin A ≥ 0.8ng/mL, toxin B ≥ 2.5 ng/mL) (*C. difficile* TOX A/B II product insert; TechLab, Inc.). To this end, serial dilutions of purified toxin A and B, spiked into PBS were prepared from 50 ng/mL to 1 ng/mL as described in Section (2.13.1) and exposed to the assay. The absorbance values at 620 nm were recorded after 10 min incubation with TMB substrate (Figure 6.9).

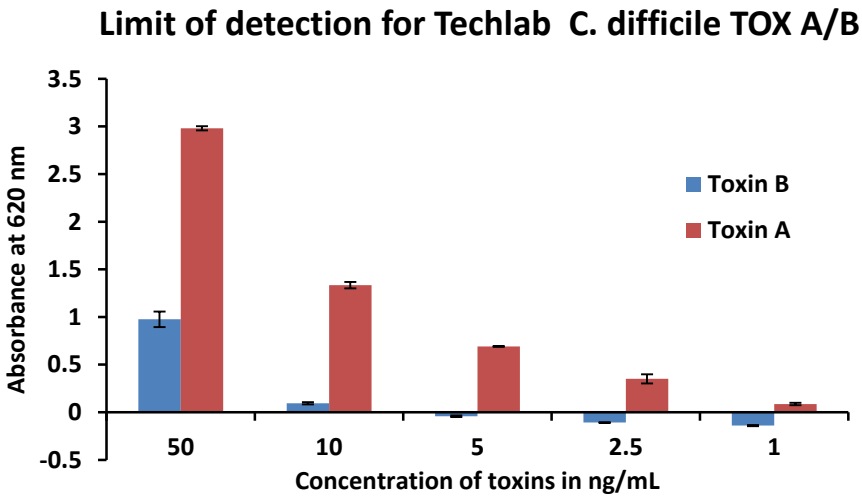

Figure 6.9. Determination of limit of detection using the *C. difficile* Tox A/B II for toxin A and B: The kit detects toxin A to ca. 1 ng/mL (red bar) while it detects toxin B to ca. 10 ng/mL.

From the results shown in Figure 6.9, the *C. difficile* TOX A/B II assay detects toxin A to ca. 1 ng/mL although lower concentrations were not tested, however it only detected toxin B to ca. 10 ng/mL. This implies that the kit has higher affinity for and is more sensitive to toxin A than toxin B. The lower sensitivity of the kit to toxin B has also been previously reported by Novak-Weekley and Hollingsworth, (2008). They found that the kit detected toxin B with weaker signals at every dilution point

they tested and declined to negative values at concentration below 250 pg/100 µL (=2.5 ng/mL).

6.5.2 Selection of the best capture Affimer to complement the *C. difficile* TOX A/B II ELISA

It was proposed to replace the capturing polyclonal anti-toxin B with and anti-toxin B Affimer. Panels of toxin B binders were tested in sandwich assay format with the kit's conjugate solution containing toxin A monoclonal antibody and toxin B polyclonal antibody (Section 2.13.3).

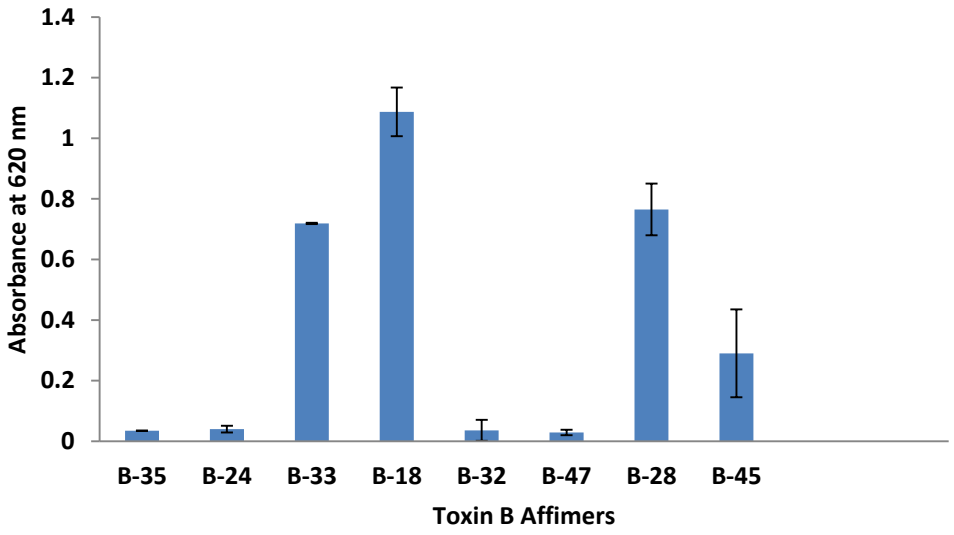

Figure 6.10: Selection of the best capture Affimer for an Affimer-Antibody hybrid assay.

Four of the eight toxin B Affimers tested gave a signal when paired with the kit detection antibody (Figure 6.10). These were B-33, B-18, B-28 and B-45 with OD_{620} nm of 0.72, 1.09, 0.77, 0.29 respectively. This implies that these whilst Affimers will recognise a specific epitope, the polyclonal antibodies clearly detect other epitopes and thus these reagents can be combined to form a hybrid assay. Toxin B-18 Affimer gave the highest signal in the hybrid assay and thus it was identified as the best capturing Affimer to be used for a toxin B hybrid assay.

6.5.3 Improved sensitivity and specificity with toxin B Affimer-antibody hybrid ELISA

In the Affimer-Antibody hybrid assay, the effect of introducing Affimer B-18 as the capture molecule was assessed. For this, the microwell containing immobilised polyclonal antitoxin A and B in the Techlab kit was replaced with biotinylated Toxin B-18 immobilised on streptavidin-coated wells. Then serial dilutions of toxin B from 50 ng/mL to 1 ng/mL was added to each well. Cross-reactivity of the hybrid assay to toxin A was tested using 50 ng/mL of purified toxin A spiked into PBS. The conjugate solution from the Techlab kit containing HRP-conjugated polyclonal anti-toxin B and monoclonal toxin A were used as for detection.

Initially, protocol 1, which is the usual protocol to perform sandwich ELISA (Section 2.11.2.) was used for the hybrid assay, while the Antibody-antibody ELISA was carried out using protocol 2 which is the optimised protocol described in the product insert (Table 6.3).

Table 6.3: Difference between Lab-based protocol and the optimised protocol based on the commercial kit assay.

Protocol 1	**Protocol 2- Optimised protocol from the kit**
Prepared microwells containing immobilised capture Affimer (toxin B-18)	Prepared microwells containing immobilised capture molecule
Add target and incubate for at room temperature for 1 hr	Add target and detection molecule and incubate at 37 ^{o}C, 1,200 rpm for 20 min
Wash-1x- (2 min)	-
Add detection molecule- incubate for 1 hr	-
Wash -6x –(6 min)	Wash 5x (5 min)
Add TMB substrate-incubate for 10 min	Add TMB substrate-Incubate for 10 min
Total time- **2 hours 18 min**	Total time- **35 min**

The result obtained from this experiment (Figure 6.11a) substituting the capturing antibody with toxin B-18 Affimer, the sensitivity of the assay was increased across all concentration tested. Importantly, the limit of detection for the techlab *C. difficile* TOX A/B II was significantly increased from 10 ng/ mL (blue bar) to 1 ng/mL in the hybrid assay (red bar). This result strongly infers that the hypothesis -

“Introducing an Affimer as a capture or detection molecule will improve the sensitivity and specificity of commercially available kits” is correct.

As shown in Table 6.3 the protocol described in the package insert (protocol 2) is optimised for the kit with total assay time of 35 min compared to protocol 1, with total assay time of 2 hours 18 min. It is seen that instead of a separate step for target addition and incubation, a wash step, and conjugate solution addition and incubation (step 1 to 3) in protocol 1, protocol 2 contains a single step of target and conjugate solution addition. Therefore, the experiment was repeated using protocol 2. The result is shown in Figure 6.11a as the green bars. Using the optimised protocol from the kit eliminated 103 min from the incubation time in protocol 1. Interestingly, there was an increase in sensitivity of the hybrid assay by almost 2.5-fold at 50 ng/mL, 5.3-fold at 10 ng/mL, 7.5-fold at 5 ng/mL, 3.3-fold at 2.5 ng/mL and 5.4-fold at 1 ng/mL.

(a)

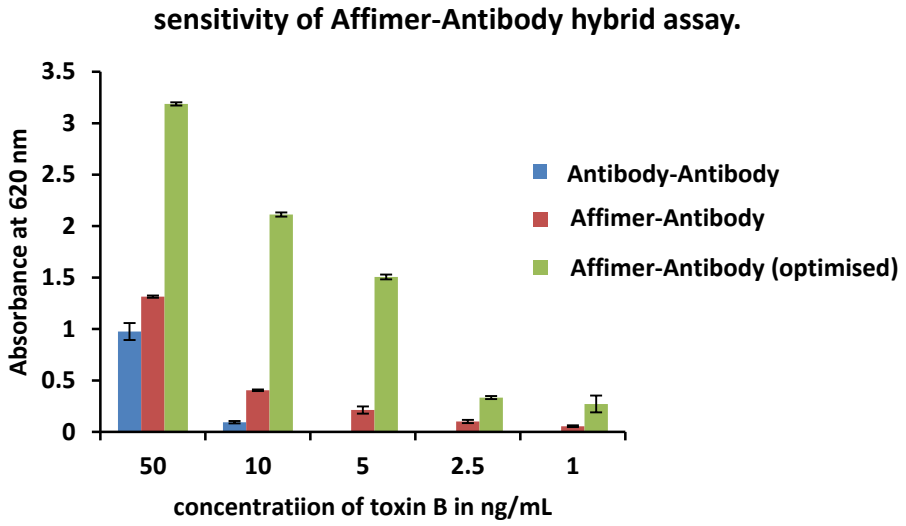

(b)

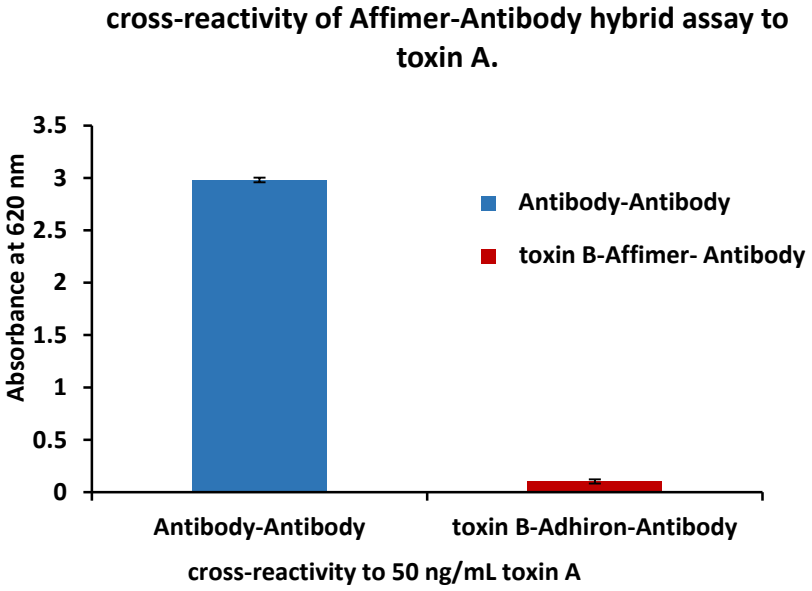

Figure 6.11: Effect of using Affimer B-18 as capture molecule on the sensitivity and cross-reactivity of Techlab *C. difficile* TOX A/B II. The comparison of the sensitivity of an Affimer-Antibody hybrid assay using protocol 1 (red bar) and 2 (green bar) with Antibody-Antibody assay (blue bar) is presented in (a), while the cross-reactivity of the two assays to toxin A is presented in (b).

The result from the cross-reactivity of the hybrid assay and the antibody-antibody ELISA assay at 50 ng/mL of toxin A is presented in Figure 6.11b. While the antibody-antibody ELISA kit binds strongly to toxin A, replacing the capturing molecule by the high affinity toxin B-18 Affimer which displays high specificity for toxin B, increases the specificity of Techlab *C. difficile* TOX A/B II the kit to toxin B by 30-fold. A hybrid assay with enhanced sensitivity and specificity to toxin B has been developed using

toxin B-18 Affimer as capturing Affimer and antibodies from Techlab *C. difficile* TOX A/B II kit as the detection molecule.

6.6 Summary

This chapter describes a hybrid assay that was developed for the detection of toxin B which is based on the combination of Affimer B-18 as capturing molecule and antibody (Techlab *C. difficile* Tox A/B II) as the detection molecule. It is a positive demonstration that can be subjected to further optimisation. Also, toxin A assay could either use the current approach, or higher affinity Affimers against toxin A be identified in further studies.

Chapter 7: General Discussion

7.1 Comparison with similar studies by other groups

7.1.1 Toxin A and Toxin B

Clostridium difficile infection remains a threat to public health with recent reports of the infection not just limited to nosocomial settings but also in animals, foods and in the environment (Ghose, 2013). Therefore, the place of accurate and rapid diagnosis cannot be over-emphasised for *Clostridium difficile* infection, as it ensures that: only the right patient with the infection are correctly identified, isolated and started on the appropriate treatment at the earliest possible time (Planche *et al*., 2008). In addition, epidemiological studies would provide a true reflection of the state of infection (Dingle *et al*., 2017).

it has ben shown that current diagnostic methods for *Clostridium difficile* infection have limitations (as stated in the introductory chapter, Section 1.3). The toxigenic cultures and the cytotoxicity neutralisation assays remain the two gold standards for diagnosing CDI but they have long turnaround times of 48 - 72 hours. They are also complex, labour intensive and require specialised training. Detection of toxins in faecal samples of patients suffering from CDI is a highly significant and necessary criterion for the diagnosis of CDI. Rapid enzyme immunoassays are used for toxin detection and can be completed in less than an hour. However, low sensitivities shown by these diagnostic EIA makes them unacceptable for use as a stand-alone test. Development of DNA-based tests are proposed to be quick and showing higher sensitivity compared to the gold standard. Nevertheless, the costs and the inability of such molecular tests to differentiate between asymptomatic carriers of toxigenic strains and patients suffering from *C. diff* infection raises concern for their routine use in CDI diagnosis due to over-diagnosis (Polage *et al*., 2015). Therefore, there remains a huge desire for an optimum diagnostic for CDI.

7.2 Replacing antibodies- why Affimers?

Non-antibody binding proteins are increasingly being used as alternatives to antibodies as binders because they display high affinity, specificity and stability against a wide range of targets. For example, Lee *et al*., (2008) identified a specific peptide aptamer to retinol binding protein 4 (RBP4), a biomarker for the diagnosis

of type 2 diabetes. This aptamer displayed high affinity and sensitivity compared to conventional ELISA detection methods (Lee *et al*., 2008). Similarly, Lofblom *et al*., (2010) employed Affibody molecules as capture agents for analytes in serum or plasma sample.

Peptides have also been utilised successfully as inhibitors against bacterial toxins such as anthrax toxin (Basha *et al*., 2006). The Affimer-phage display libraries (Chapter 1, Section 1.6.4.5) have also been used to identify binding proteins against >350 targets. However, published articles for the use of non-antibody binding proteins identified for the diagnosis of *C. difficile* infection are scarce (in fact, only aptamers have been reported). The work presented in this thesis has implications for our understanding and seeks to address this deficiency.

Can we improve the sensitivity and specificity of toxin-based detection assays for diagnosing *Clostridium difficile* infection?

For discussion purposes, results obtained in this thesis will be compared with similar studies by other groups. Work was reported by Hussack and colleagues on the isolation and characterisation of toxin specific single domain antibodies (Hussack *et al*., 2012), and the use of single domain antibodies for neutralisation of *C. difficile* toxin A (Hussack *et al*., 2011). On the other hand, Ochsner *et al*., (2014) focussed on the use of slow-off rate aptamers (SOMAmers) as replacement for antibody for toxin A and B detection in CDI diagnosis.

In Chapters 4 and 5, Affimer phage display library was used for the identification of specific and high affinity binders against GDH, toxin A and toxin B of *Clostridium difficile* that were characterised for binding, specificity, aggregation, and thermostability. This project further supports the versatility of the Affimer phage display library to select binders against a wide range of targets within a one month timeframe. This is in contrast with VH phage libraries used in Hussack's paper, which required specific phage libraries to be constructed for each target (Hussack *et al*., 2012) and could take no less than six months.

The panning rounds used in this thesis were designed to enrich for specific Affimers binding to each target. To enhance specificity, the phage for GDH was pre-panned

against *E. coli* cell lysate to exclude binders against any endogenous GDH. For toxin A, bound phage in biopanning round 2 and 3 were challenged with free toxin B to eliminate cross-reactive phage. This was done similarly for toxin B binders. The 10 unique binders for toxin A, 12 unique binders for toxin B and 9 for GDH were sub-cloned into a bacterial expression vector and were well expressed in *E. coli,* yielding up to 300 mg/L of culture and was not optimised for high level expression. To date, this is the best expression level obtained from binders against *Clostridium difficile* toxins as compared to (1.2 to 72.3 mg/L) from single domain antibodies (Hussack *et al*., 2011). For specific orientation of the binders during characterisation, a single cysteine was introduced at the C-terminal end of the Affimer. Therefore, binders were produced separately both with and without cysteine.

Toxin A and toxin B share over 63 % amino acid homology, nevertheless, highly specific and non-cross reacting Affimers were selected against toxin B and toxin A respectively. The specificity of Affimers is consistent with previous studies (Ochsner *et al*., 2014, Hussack *et al*., 2012). Most toxigenic strains reported in the literature are Toxin A^+/B^+, although incidence of Toxin A^-/B^+ have appeared in several studies, but no cases of Toxin A^+/B^- strains have been reported (Kuehne *et al*., 2010). Therefore, specific binders against each toxin could provide preliminary information about strain types. The thermostability, and non-aggregating profile of identified Affimers at temperatures greater than 80 ^oC makes them suitable for incorporation into various biosensor platforms which further validates the robustness of the Affimer scaffold, potentially allowing distribution without need for refrigeration.

7.3 Selection of pairs

Diagnostic kits used in clinical settings for diagnosing infection and diseases rely on the use of molecular recognition elements (MRE) that bind to the target(s) of interest with high affinity and specificity, and antibodies remain the most widely used MRE for this purpose (Su *et al*., 2013). To enhance sensitivity and specificity, capture antibodies are immobilised onto suitable surfaces to capture the target, then detection antibodies are added in a sandwich assay format. Beyond clinical diagnoses, sandwich ELISA are widely used in many scientific, industrial and

research applications. However, selection of MRE pair that binds to non-overlapping epitopes is critical for the development of a sandwich-type of diagnostic assay. A widely used approach for selection of pairs is to immobilise the capture MRE onto the surface of a 96-well plate, and then test different combinations of MRE to identify the best pair. This method has been used to identify monoclonal antibody (mAb) pairs against many targets (Qiu *et al*., 2009, Ding *et al*., 2014); aptamers that target hepatitis C virus (HCV) (Park *et al*., 2013); and single domain antibody against *C. diff* toxin A and B (Hussack *et al.,* 2010).

Ki *et al*., (2010) described an alternative method for identification of pairs. In this method, the capture molecule is complexed with the target and immobilised onto the surface before panning for a suitable detection molecule via phage display. The limitation of Ki's approach is that it is time consuming since it would require phage display screening, selection and characterisation of a high affinity binder that would be used as the capture molecule, to be carried out before a second phage display is undertaken to identify the detection molecule. Also, it is not guaranteed that pairs would be identified.

In this thesis, a direct absorption of capture binder was used as the first attempt to identify pairs of Affimer binders. However, the results obtained in Figures 5.19 to 5.24 indicate that identification of binders by direct absorption of a capturing Affimer may prevent the selection of the best pair. Therefore, oriented immobilisation of capture Affimer and testing different combinations of binders for pair identification, provides a better method for selection of pairs. In contrast to the method described by Ki *et al.* (2010), sandwich phage ELISA was used as a technique for identifying Affimer pairs against toxin A, toxin B and GDH. In particular, sandwich phage ELISA described in this thesis has three major advantages for the identification of pairs: (i) oriented immobilisation of capture Affimer, (ii) the avidity provided by using Affimer phage for detection improved the signal intensity obtained, and (iii) reduced time spent for the identification of pairs. Through this method, a panel of potential pairs were identified.

This thesis has successfully identified the optimal pair of binders against toxin B from the limited number of clones tested. Toxin B-18 (K_D 4.04nM) as the best

capture Affimer and Toxin B-45 (5.7 nM) as the best detection Affimer for toxin B with no cross-reactivity to toxin A as shown in the phage ELISA and SPR data. The Affimer pair was used to design a toxin B sandwich phage ELISA to determine the limit of detection. As described previously (Chapter 6, Section 6.5, Table 6.2), >85 % of the commercial toxin detection assays uses polyclonal antibodies as the capture reagent paired with monoclonal. With the Affimer pair, a viable alternative to the use of antibodies in the detection assay is provided. Affimers do not have lot-to-lot variations, they are easily expressed as soluble non-aggregating protein, their thermostability (up to 80 ^{o}C) simplifies their storage (Zhang *et al*., 2013).

7.3.1 Performance of Affimer pairs

The limit of detection for the Affimer toxin B-18 and toxin B-45 pair using sandwich phage ELISA was calculated to be 1.2 ng/mL which is 4.5pM of toxin B. This is similar to the limit of detection reported for clinically used diagnostics kits for *C. difficile;* toxin A/B of 1-5 ng/mL (Novak-Weekley, 2008, Eastwood *et al*., 2009). However, this limit of detection could not be reproduced when toxin B-45-HRP was used in place of toxin B-45 phage. The reason for this is unclear, however, it is almost certainly related to the fact that multiple anti-phage antibodies used to detect the phage would provide a more sensitive detection signal than the single HRP conjugated to toxin B-45 Affimer. Also, the avidity of B-45 phage enhances the sensitivity of the sandwich assay, while the sensitivity of B-45-HRP was impeded due to the 1:1 conjugation ratio of HRP per B-45 Affimer molecule. This avidity effect of multicopy display of peptide on the surface of the phage has been reported to enhance affinity and specificity of displayed probes (Murase *et al*., 2003, Han *et al*., 2016). Further studies are therefore needed to increase the sensitivity of protein-based toxin B-18/B-45 Affimer pair. Suggested methods would include:

(1) Oriented immobilisation of capture Affimer using Maleimide chemistry on maleimide activated plates while the target is detected using biotinylated Affimer, as described by Hortigüela and wall (2013), and Kang *et al*., (2013).

(2) Oligomerisation of the detection probes, which has been shown to be an effective way of increasing their avidity. Park *et al*., 2013 described higher

sensitivity when biotinylated detection aptamer was pre-incubated with streptavidin-HRP to generate multimers of the detection aptamer.

(3) Engineering a multivalent detection Affimer to enhance avidity effect (Deyev and Lebedenko, 2008). Cuesta *et al*., (2010) described the design of multivalent antibodies with multiple binding sites.

(4) Display of detection Affimer on pVIII coat protein then used in assay since the major coat protein PVIII of the filamentous M13 phage is present in 2500 copies. This could provide the avidity needed for signal amplification (Williams *et al*., 2015)

These methods could be adopted to generate a better sensitivity for the Affimer-based detection assay called Affimer-sorbent assay (AFFISA).

7.3.2 Performance of Affimer-based hybrid assay for CDI diagnosis

Analysis of the types of molecular recognition elements used in *C. difficile* toxin diagnostic kits revealed that >85 % utilise polyclonal anti-toxin B antibody as the capturing molecule for toxin B (Table 6.2). With the inherent disadvantages of polyclonal antibody such as low specificity, lot-to-lot batch variation, and the amount of time to generate them, it was therefore hypothesised in this project that substituting the capturing polyclonal antibodies with Affimers will improve the sensitivity and specificity of diagnostic kits. *C. difficile* TOX A/B II™ kit (Techlab) which detects both toxin A and toxin B in a patient's sample, was used as a proof-of-concept. Replacing capturing agent in sandwich assay has been reported in literature. Ochsner *et al*., (2013) used low off rate Aptamers (SOMAmers) as capture while a commercially available polyclonal antibody was used for the detection of *C. difficile* toxin B. The binding equilibrium of the binders were determined by radioactively labelling the SoMAmers. The toxin B aptamer-antibody sandwich assay showed no cross-reactivity to toxin A, but it detected toxin B up to 100 ng/mL (0.3 nM). Comparing Ochsner's data with the results described in this thesis, the Affimer-based hybrid assay used the conjugate antibody present in the Techlab kit for detection which has already been optimised for CDI diagnosis. It detected toxin B at 1 ng/mL which is a 100-fold better sensitivity compared to the detection level described by Ochsner.

Novak-Weekley and Hollingsworth (2008) assessed the sensitivity and specificity of Techlab's *C. difficile* toxA/B II™ kit and reported the lower sensitivity of the kit for toxin B. The work presented in this thesis also confirms that the Techlab tox A/B II™ kit detects toxin A better than toxin B. It detects toxin A down to 1 ng/mL but could not detect toxin B below 10 ng/mL (Figure 6.9). While the signals declined to negative values at concentration below 10 ng/mL when Techlab antibody-antibody was used, replacing the capturing antibody with toxin B-18 Affimer allowed toxin B to be detected down to 1 ng/mL. This implies that the Affimer-based hybrid assay led to a 10-fold increase in the sensitivity of the kit to toxin B.

The cross-reactivity of Techlab tox A/B II™ kit indicates that it can detect both toxin A and toxin B in clinical samples. However, the lower sensitivity of the kit for toxin B implies that toxigenic strains that are toxin A^-B^+ (Alfa, 2000) could be missed by this assay. In fact, no toxigenic *C. diff* strain producing only toxin A (toxin A^+B^-) has been reported in the literature. With the Affimer-based hybrid assay, the cross-reactivity of the kit to toxin A was eliminated. This provides a way to discriminate between toxin A and toxin B in samples. The work reported here developed a more sensitive assay for toxin B, however, further studies are required to:

(a) establish the same for toxin A.
(b) simplify the use of the capture Affimer and make it more cost-effective.
(c) explore the potential for a higher sensitive Affimer detection reagents, by combining one or more Affimer(s) to form a polyclonal Affimer mix.

7.4 Future work and recommendation

7.4.1 GDH

Glutamate dehydrogenase from *C. difficile* remains a useful screening biomarker in CDI diagnosis. This thesis has successfully identified Affimer binders that bind GDH with high affinity and specificity. GDH-4 Affimer was identified as a potential affinity reagent that is sufficient to act as both a capture molecule and a detection molecule simultaneously due to the hexameric nature of the GDH target. If the project were to be extended, a number of experiments could be carried out such as kinetic studies of the selected GDH Affimer binders to determine the K_D, further

optimisation of the Affimer-based sandwich ELISA for GDH to achieve better sensitivity compared to commercially available ELISA. The important aspect is that the simplicity of the Affimer approach would allow routine testing of GDH, toxin A and toxin B in a single multiplexed assay.

Inhibition studies: The Govind group has published some research papers (Girinathan *et al*., 2014, 2016) on the significance of *C. difficile*-derived glutamate dehydrogenase and they reported that the *C. difficile* strain gluD mutant (which does not produce GDH) was found to be more susceptible to hydrogen peroxide than the parent strain. In addition, they were able to detect *C. difficile*-derived GDH extracellularly (Girinathan *et al*., 2014). A more recent report by this group (Girinathan *et al*., 2016) showed for the first time that extracellular GDH produced by *C. difficile* supports bacterial colonisation in the gut and improves disease progression. Therefore, a useful follow-on project would be to investigate the inhibition studies of the identified Affimers against *C. difficile*-derived glutamate dehydrogenase.

7.4.2 Toxin A and Toxin B

In this project, high affinity binders against full-length native toxin B have been identified and characterised. Given the time limit of this research, focus was placed on the promising toxin B Affimer pair (Toxin B-18 and toxin B-45), therefore they were the most thoroughly characterised.

For toxin A, the best capture Affimer toxin A-14 has a K_D of 81.4 nM. Better low nanomolar or high picomolar affinity binders could be selected by including competitive elution during phage display screening, if repeated. Furthermore, though a panel of detection Affimers were identified as possible pair for toxin A-14, further studies and optimisation are needed to characterise each pair in order to identify the best pair. This would then be useful for the development of an Affimer-based hybrid assay for toxin A.

In practice, rescreening the Affimer phage library against toxins A and B under competitive elution conditions would likely be of value. Potentially, affinity maturation could be used to select variants based on existing Affimers for

enhanced affinity specifically through slower off-rate selection. Also, the exploration of the use of polyclonal Affimers for detection and the engineering of di- and multi-meric Affimers would be useful. The use of a streptavidin-based plates for oriented immobilisation is not cost-effective as a clinical diagnostic tool and so, exploring alternative systems such as CLICK chemistry approaches would be valuable. Previous work at Leeds has demonstrated the enhanced sensitivity that can be provided by using an electronic impedance-based system for detection of a cytokine in a complex biological sample (Sharma *et al*., 2016). Experiments to test the toxin B Affimers using such a platform would be very valuable as a comparison with EIA approaches in terms of detection sensitivity.

Currently, patient samples have not been tested to measure the affinity and specificity of the binders. However, this work has collaborated with scientists at Public Health England and with clinical microbiologists at Leeds to assess the detection limits of binders on clinically relevant specimens. Similarly, aside from toxin A and toxin B, other potential toxins reported to show cross-reactivity in *C. diff* toxin immunoassay needs to be included in further studies. For proper analysis, comparison studies need to be carried out using the gold standard for toxins A and B diagnosis. Further experiments that incorporate Affimers against GDH, toxin A and toxin B for use as a polyclonal mixture of Affimer monoclonal reagents may enhance the specificity of diagnostic tests.

7.4.3 Crystallisation of toxin A and B using the high affinity Affimers as crystallisation chaperones

C. difficile toxin A and B are high molecular mass proteins (308 kDa and 270 kDa respectively). To date, crystal structures for full-length toxin A and B have not been solved, although crystal structures have been determined for some of the individual domains (Pruitt, *et al*, 2010, Albesa-Jove *et al*., 2010, Chumbler *et al*., 2016). One possible reason for this has been ascribed to the heterogeneity of the sample as observed in electron micrographs of toxin B (Pruitt, *et al*., 2010). High affinity Affimers identified in this study, look promising and may be used as chaperones to obtain high resolution crystal structure for full length native toxin A and B.

7.4.4 Potential applications of toxin B pairs.

The characterisation of toxin B pairs described in this project has made it a useful reagent for proof-of-concept for some other detection platforms.

The Millner' group at Leeds are currently using the toxin B-pairs from this work as a proof-of concept to develop a gold nanoparticles-based sandwich assay. In the assay, biotinylated B-18c and B-45c Affimers were individually conjugated to streptavidin gold nanoparticles (AuNPs). Using Dynamic Light Scattering (DLS), preliminary data showed that there was a significant increase in the size of gold particles caused by the formation of aggregate in the presence of toxin B. As shown in Figure 7.1, no significant size shift was observed with either B-18c only, B-45c only or a mixture of B-18c-AuNPs and B-45c-AuNPs in the absence of toxin B.

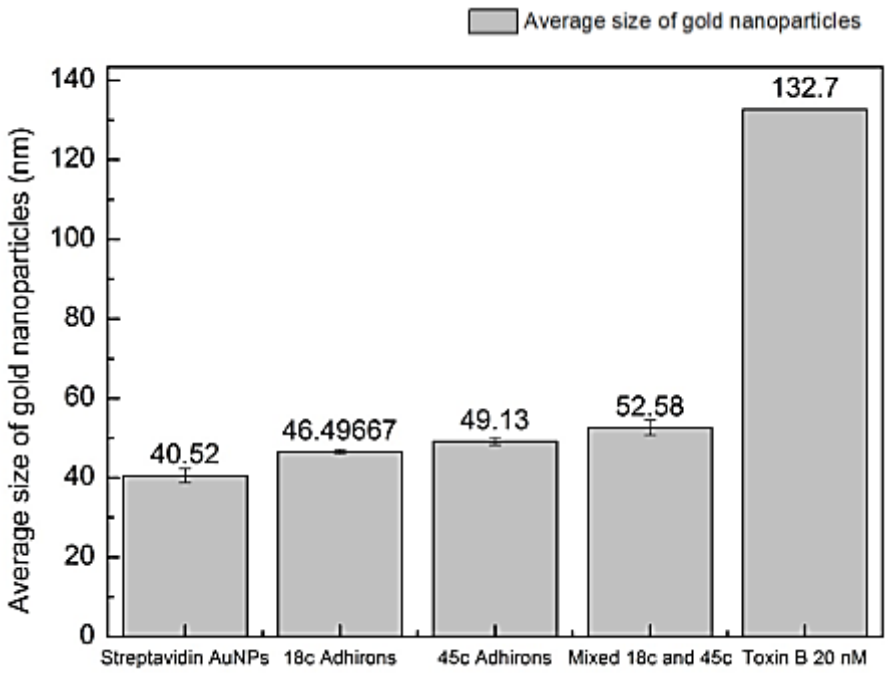

Figure 7.1: Use of Affimer pairs to monitor size shift of aggregate by dynamic light scattering (Provided by Thanisorn Mahatnirunkul).

7.4.5 Diagnosis of CDI: developing a generally acceptable gold standard for toxin A and B.

The best diagnostic method for *C. difficile* has not been defined (Gerding *et al*., 2016) even though researchers are increasingly supporting the claim that the presence of toxins in clinical sample is critical for the diagnosis of CDI. However, a

closer look at the inherent properties of the available diagnostic methods could give us a clue (see Table 7.1).

Table 7.1: Comparison of the diagnostic methods based on toxin detection

Method	sensitivity	characteristics	Detect toxin in faecal sample
Toxigenic culture	Gold standard	Isolate spores, then test for toxin production	**No**
NAATs	very sensitive, has low turnaround time	Detect tcdB gene	**No**
GDH EIA	Very sensitive, fast but not specific	Detects GDH common antigen	**No**
Toxin EIA	Low sensitivity	Detect toxin in clinical sample	**Yes**

Clostridium difficile infection diagnosis requires the identification of *C. diff* toxins as the causal agent in symptomatic patients with cell culture neutralization assay and toxigenic culture referred to as the gold standards. For toxigenic culture, however, it is important to bear in mind that the method involves isolation of spores from faecal samples and then testing if the spores are from toxigenic strains. Therefore, toxigenic cultures do not detect toxins directly from clinical samples. This important fact suggests the reason why the sensitivity of NAATs are comparable to the sensitivity of toxigenic cultures and not to cell culture neutralisation assay (CCNA), since both NAATs and toxigenic culture only detects toxigenic strains capable of producing toxins. CCNA on the other hand is also used as a gold standard but it is time consuming and it detects the presence of toxin B that can be neutralised by antitoxin.

Enzyme immunoassay is the only method that can directly detect the presence of toxins in faecal samples and if EIA toxin testing is being used, it is more likely that a positive test represents CDI, but EIA testing may yield false negatives in patients with CDI because of lack of sensitivity.

This thesis has opened a better understanding of the limited sensitivity and specificity observed in EIA (use of polyclonal antibodies for toxin B). Therefore, if the sensitivity of EIA for toxin A and B is enhanced by replacing antibodies with

Affimers, and further studies are carried out to identify Affimers that can recognise both conformational and denatured toxins in faecal samples, this would be a step in the right direction. Affimer-based toxin detection assays promise to be able to deliver a stand-alone diagnostic method that is sensitive, specific, reproducible, rapid, low cost, point-of-care and capable of replacing the current gold standards for the diagnosis of *C. difficile* infection.

7.5 Conclusion

Affimers with high sensitivity and specificity against the three validated biomarkers (toxin A, toxin B and glutamate dehydrogenase) of *Clostridium difficile* infection have been successfully identified and extensively characterised. This thesis has also explored the ability of Affimers to function as novel reagents for the potential development of point-of-care diagnostic tool for *C. difficile* infection.

References

ADEY, N. B., MATARAGNON, A. H., RIDER, J. E., CARTER, J. M. & KAY, B. K. 1995. Characterization of phage that bind plastic from phage-displayed random peptide libraries. *Gene,* 156**,** 27-31.

ALBESA-JOVÉ, D., BERTRAND, T., CARPENTER, E. P., SWAIN, G. V., LIM, J., ZHANG, J., HAIRE, L. F., VASISHT, N., BRAUN, V. & LANGE, A. 2010. Four distinct structural domains in *Clostridium difficile* toxin B visualized using SAXS. *Journal of molecular biology,* 396**,** 1260-1270.

ALFA, M. J., KABANI, A., LYERLY, D., MONCRIEF, S., NEVILLE, L. M., AL-BARRAK, A., HARDING, G. K., DYCK, B., OLEKSON, K. & EMBIL, J. M. 2000. Characterization of a toxin A-negative, toxin B-positive strain of *Clostridium difficile* responsible for a nosocomial outbreak of Clostridium difficile-associated diarrhea. *Journal of clinical microbiology,* 38**,** 2706-2714.

ANDERSON, B. M., ANDERSON, C. D., VAN TASSELL, R. L., LYERLY, D. M. & WILKINS, T. D. 1993. Purification and characterization of *Clostridium difficile* glutamate dehydrogenase. *Arch Biochem Biophys,* 300**,** 483-8.

ANDROGA, G. O., HART, J., FOSTER, N. F., CHARLES, A., FORBES, D. & RILEY, T. V. 2015. Infection with toxin A-negative, toxin B-negative, binary toxin-positive *Clostridium difficile* in a young patient with ulcerative colitis. *Journal of clinical microbiology,* 53**,** 3702-3704.

ANTONARA, S. & LEBER, A. L. 2016. Diagnosis of *Clostridium difficile* Infections in Children. *Journal of Clinical Microbiology,* 54**,** 1425-1433.

ARNOLD, F. H. 1998. Design by directed evolution. *Accounts of Chemical Research,* 31**,** 125-131.

AUBRY, A., HUSSACK, G., CHEN, W., KUOLEE, R., TWINE, S. M., FULTON, K. M., FOOTE, S., CARRILLO, C. D., TANHA, J. & LOGAN, S. M. 2012. Modulation of toxin production by the flagellar regulon in *Clostridium difficile*. *Infection and immunity,* 80**,** 3521-3532.

AVILA, M. B., AVILA, N. P. & DUPONT, A. W. 2016. Recent Advances in the Diagnosis and Treatment of *Clostridium difficile* Infection. *F1000Research,* 5**,** F1000 Faculty Rev-118.

BACCI, S., MOLBAK, K., KJELDSEN, M. K. & OLSEN, K. E. P. 2011. Binary Toxin and Death after *Clostridium difficile* Infection. *Emerging Infectious Diseases,* 17**,** 976-982.

BAKER, P. J., BRITTON, K. L., ENGEL, P. C., FARRANTS, G. W., LILLEY, K. S., RICE, D. W. & STILLMAN, T. J. 1992. Subunit assembly and active site location in the structure of glutamate dehydrogenase. *Proteins: Structure, Function, and Bioinformatics,* 12**,** 75-86.

BALOCH, A. R., BALOCH, A. W., SUTTON, B. J. & ZHANG, X. 2016. Antibody mimetics: promising complementary agents to animal-sourced antibodies. *Crit Rev Biotechnol,* 36**,** 268-75.

BANTA, S., DOOLEY, K. & SHUR, O. 2013. Replacing Antibodies: Engineering New Binding Proteins. *Annual review of biomedical engineering*.

BARBUT, F., BRAUN, M., BURGHOFFER, B., LALANDE, V. & ECKERT, C. 2009. Rapid detection of toxigenic strains of *Clostridium difficile* in diarrheal stools by real-time PCR. *Journal of clinical microbiology,* 47**,** 1276-1277.

BARBUT, F., SURGERS, L., ECKERT, C., VISSEAUX, B., CUINGNET, M., MESQUITA, C., PRADIER, N., THIRIEZ, A., AIT-AMMAR, N., AIFAOUI, A., GRANDSIRE, E. & LALANDE, V. 2014. Does a rapid diagnosis of *Clostridium difficile* infection impact on quality of patient management? *Clinical Microbiology and Infection,* 20**,** 136-144.

BARTH, H., AKTORIES, K., POPOFF, M. R. & STILES, B. G. 2004. Binary bacterial toxins: Biochemistry, biology, and applications of common Clostridium and Bacillus proteins. *Microbiology and Molecular Biology Reviews,* 68**,** 373-+.

BARTLETT, J. G., CHANG, T. W., GURWITH, M., GORBACH, S. L. & ONDERDONK, A. B. 1978. Antibiotic-associated pseudomembranous colitis due to toxin-producing clostridia. *New England Journal of Medicine,* 298**,** 531-534.

BASHA, S., RAI, P., POON, V., SARAPH, A., GUJRATY, K., GO, M. Y., SADACHARAN, S., FROST, M., MOGRIDGE, J. & KANE, R. S. 2006. Polyvalent inhibitors of anthrax toxin that target host receptors. *Proceedings of the National Academy of Sciences,* 103**,** 13509-13513.

BAUER, M. P., KUIJPER, E. J. & VAN DISSEL, J. T. 2009. European Society of Clinical Microbiology and Infectious Diseases (ESCMID): treatment guidance document for *Clostridium difficile* infection (CDI). *Clinical Microbiology and Infection,* 15**,** 1067-1079.

BECK, A., WURCH, T. & CORVAIA, N. 2008. Editorial: Therapeutic Antibodies and Derivatives: From the Bench to the Clinic. *Current Pharmaceutical Biotechnology,* 9**,** 421-422.

BERTONE, P., KLUGER, Y., LAN, N., ZHENG, D. Y., CHRISTENDAT, D., YEE, A., EDWARDS, A. M., ARROWSMITH, C. H., MONTELIONE, G. T. & GERSTEIN, M. 2001. SPINE: an integrated tracking database and data mining approach for identifying feasible targets in high-throughput structural proteomics. *Nucleic Acids Research,* 29**,** 2884-2898.

BINZ, H. K., AMSTUTZ, P., KOHL, A., STUMPP, M. T., BRIAND, C., FORRER, P., GRUTTER, M. G. & PLUCKTHUN, A. 2004. High-affinity binders selected from designed ankyrin repeat protein libraries. *Nat Biotechnol,* 22**,** 575-82.

BINZ, H. K., AMSTUTZ, P. & PLUCKTHUN, A. 2005. Engineering novel binding proteins from nonimmunoglobulin domains. *Nature Biotechnology,* 23**,** 1257-1268.

BIRD, R. E., HARDMAN, K. D., JACOBSON, J. W., JOHNSON, S., KAUFMAN, B. M., LEE, S.-M., LEE, T., POPE, S. H., RIORDAN, G. S. & WHITLOW, M. 1988. Single-chain antigen-binding proteins. *Science,* 242**,** 423-427.

BOETTNER, M., STEFFENS, C., VON MERING, C., BORK, P., STAHL, U. & LANG, C. 2007. Sequence-based factors influencing the expression of heterologous genes in the yeast Pichia pastoris--A comparative view on 79 human genes. *J Biotechnol,* 130**,** 1-10.

BOLTON, R., TAIT, S., DEAR, P. & LOSOWSKY, M. 1984. Asymptomatic neonatal colonisation by Clostridium difficile. *Archives of disease in childhood,* 59**,** 466-472.

BREKKE, O. H. & SANDLIE, I. 2003. Therapeutic antibodies for human diseases at the dawn of the twenty-first century. *Nat Rev Drug Discov,* 2**,** 52-62.

BURNHAM, C.-A. D. & CARROLL, K. C. 2013. Diagnosis of *Clostridium difficile* infection: an ongoing conundrum for clinicians and for clinical laboratories.

Clinical microbiology reviews, 26**,** 604-630.

CARAVELLA, J. & LUGOVSKOY, A. 2010. Design of next-generation protein therapeutics. *Curr Opin Chem Biol,* 14**,** 520-8.

CARMAN, R., WICKHAM, K., CHEN, L., LAWRENCE, A., BOONE, J., WILKINS, T., KERKERING, T. M. & LYERLY, D. 2012. Glutamate dehydrogenase is highly conserved among *Clostridium difficile* ribotypes. *Journal of clinical microbiology,* 50**,** 1425-1426.

CARROLL, K. C. 2011. Tests for the diagnosis of *Clostridium difficile* infection: The next generation. *Anaerobe,* 17**,** 170-174.

CARTER, G. P., ROOD, J. I. & LYRAS, D. 2010. The role of toxin A and toxin B in Clostridium difficile-associated disease: past and present perspectives. *Gut microbes,* 1**,** 58-64.

CARTER, P. J. 2011. Introduction to current and future protein therapeutics: a protein engineering perspective. *Experimental cell research,* 317**,** 1261-1269.

CERQUETTI, M., LUZZI, I., CAPRIOLI, A., SEBASTIANELLI, A. & MASTRANTONIO, P. 1995. Role of *Clostridium difficile* in childhood diarrhea. *The Pediatric infectious disease journal,* 14**,** 598-602.

CHAMES, P., VAN REGENMORTEL, M., WEISS, E. & BATY, D. 2009. Therapeutic antibodies: successes, limitations and hopes for the future. *British Journal of Pharmacology,* 157**,** 220-233.

CHAN, C. P. Y., MAK, W. C., CHEUNG, K. Y., SIN, K. K., YU, C. M., RAINER, T. H. & RENNEBERG, R. 2013. Evidence-Based Point-of-Care Diagnostics: Current Status and Emerging Technologies. *Annual Review of Analytical Chemistry*.

CHANG, T., LIN, P., GORBACH, S. & BARTLETT, J. 1979. Ultrastructural changes of cultured human amnion cells by *Clostridium difficile* toxin. *Infection and immunity,* 23**,** 795-798.

CHANG, T.-W., BARTLETT, J., GORBACH, S. & ONDERDONK, A. 1978. Clindamycin-induced enterocolitis in hamsters as a model of pseudomembranous colitis in patients. *Infection and immunity,* 20**,** 526-529.

CHAPIN, K. C., DICKENSON, R. A., WU, F. & ANDREA, S. B. 2011. Comparison of five assays for detection of *Clostridium difficile* toxin. *The Journal of Molecular Diagnostics,* 13**,** 395-400.

CHUMBLER, N. M., RUTHERFORD, S. A., ZHANG, Z., FARROW, M. A., LISHER, J. P., FARQUHAR, E., GIEDROC, D. P., SPILLER, B. W., MELNYK, R. A. & LACY, D. B. 2016. Crystal structure of *Clostridium difficile* toxin A. *Nature Microbiology,* 1**,** 15002.

CLEMENTS, A. C., MAGALHÃES, R. J. S., TATEM, A. J., PATERSON, D. L. & RILEY, T. V. 2010. *Clostridium difficile* PCR ribotype 027: assessing the risks of further worldwide spread. *The Lancet infectious diseases,* 10**,** 395-404.

COHEN, S. H., GERDING, D. N., JOHNSON, S., KELLY, C. P., LOO, V. G., MCDONALD, L. C., PEPIN, J. & WILCOX, M. H. 2010. Clinical Practice Guidelines for *Clostridium difficile* Infection in Adults: 2010 Update by the Society for Healthcare Epidemiology of America (SHEA) and the Infectious Diseases Society of America (IDSA). *Infection Control and Hospital Epidemiology,* 31**,** 431-455.

CORPET, F. 1988. Multiple sequence alignment with hierarchical clustering. *Nucleic Acids Research,* 16**,** 10881-10890.

CROBACH, M., DEKKERS, O., WILCOX, M. & KUIJPER, E. 2009. European Society of Clinical Microbiology and Infectious Diseases (ESCMID): data review and recommendations for diagnosing *Clostridium difficile*-infection (CDI). *Clinical Microbiology and Infection,* 15**,** 1053-1066.

CROOKS, G. E., HON, G., CHANDONIA, J. M. & BRENNER, S. E. 2004. WebLogo: A sequence logo generator. *Genome Research,* 14**,** 1188-1190.

CUESTA, A. M., SAINZ-PASTOR, N., BONET, J., OLIVA, B. & ALVAREZ-VALLINA, L. 2010. Multivalent antibodies: when design surpasses evolution. *Trends in Biotechnology,* 28**,** 355-362.

DALE, G. E., BROGER, C., LANGEN, H., D'ARCY, A. & STUBER, D. 1994. Improving protein solubility through rationally designed amino acid replacements: Solubilization of the trimethoprim-resistant type S1 dihydrofolate reductase. *Protein Engineering,* 7**,** 933-939.

DE JONG, E., DE JONG, A., BARTELS, C., MELCHERS, W. & STURM, P. 2012. Clinical and laboratory evaluation of a real-time PCR for *Clostridium difficile* toxin A and B genes. *European journal of clinical microbiology & infectious diseases,* 31**,** 2219-2225.

DEACON, S. E. & MCPHERSON, M. J. 2011. Enhanced Expression and Purification of Fungal Galactose Oxidase in Escherichia coli and Use for Analysis of a Saturation Mutagenesis Library. *Chembiochem,* 12**,** 593-601.

DELMÉE, M., VAN BROECK, J., SIMON, A., JANSSENS, M. & AVESANI, V. 2005. Laboratory diagnosis of Clostridium difficile-associated diarrhoea: a plea for culture. *Journal of Medical Microbiology,* 54**,** 187-191.

DENG, X. K., NESBIT, L. A. & MORROW, K. J. 2003. Recombinant Single-Chain Variable Fragment Antibodies Directed against *Clostridium difficile* Toxin B Produced by Use of an Optimized Phage Display System. *Clinical and Diagnostic Laboratory Immunology,* 10**,** 587-595.

DENNIS, M. S., HERZKA, A. & LAZARUS, R. A. 1995. Potent and Selective Kunitz Domain Inhibitors of Plasma Kallikrein Designed by Phage Display. *Journal of Biological Chemistry,* 270**,** 25411-25417.

DEPARTMENT OF HEALTH, U. K. 2012 Updated guidance on the diagnosis and reporting of Clostridium difficile.

DEPESTEL, D. D. & ARONOFF, D. M. 2013. Epidemiology of *Clostridium difficile* Infection. *Journal of pharmacy practice,* 26**,** 464-475.

DEYEV, S. M. & LEBEDENKO, E. N. 2008. Multivalency: the hallmark of antibodies used for optimization of tumor targeting by design. *Bioessays,* 30**,** 904-918.

DI BELLA, S., ASCENZI, P., SIARAKAS, S., PETROSILLO, N. & DI MASI, A. 2016. *Clostridium difficile* Toxins A and B: Insights into Pathogenic Properties and Extraintestinal Effects. *Toxins,* 8.

DING, X.-X., LI, X.-F., DENG, Y.-Q., GUO, Y.-H., HAO, W., CHE, X.-Y., QIN, C.-F. & FU, N. 2014. Development of a double antibody sandwich ELISA for West Nile virus detection using monoclonal antibodies against non-structural protein 1. *PloS one,* 9**,** e108623.

DINGLE, K. E., DIDELOT, X., QUAN, T. P., EYRE, D. W., STOESSER, N., GOLUBCHIK, T., HARDING, R. M., WILSON, D. J., GRIFFITHS, D., VAUGHAN, A., FINNEY, J. M., WYLLIE, D. H., OAKLEY, S. J., FAWLEY, W. N., FREEMAN, J., MORRIS, K., MARTIN, J., HOWARD, P., GORBACH, S., GOLDSTEIN, E. J. C., CITRON, D. M.,

HOPKINS, S., HOPE, R., JOHNSON, A. P., WILCOX, M. H., PETO, T. E. A., WALKER, A. S. & CROOK, D. W. 2017. Effects of control interventions on *Clostridium difficile* infection in England: an observational study. *The Lancet Infectious Diseases*.

DUBBERKE, E. R. & OLSEN, M. A. 2012. Burden of *Clostridium difficile* on the healthcare system. *Clinical Infectious Diseases,* 55**,** S88-S92.

EASTWOOD, K., ELSE, P., CHARLETT, A. & WILCOX, M. 2009. Comparison of Nine Commercially Available *Clostridium difficile* Toxin Detection Assays, a Real-Time PCR Assay for *C. difficile* tcdB, and a Glutamate Dehydrogenase Detection Assay to Cytotoxin Testing and Cytotoxigenic Culture Methods. *Journal of Clinical Microbiology,* 47**,** 3211-3217.

EGLOW, R., POTHOULAKIS, C., ITZKOWITZ, S., ISRAEL, E., O'KEANE, C., GONG, D., GAO, N., XU, Y., WALKER, W. & LAMONT, J. 1992. Diminished *Clostridium difficile* toxin A sensitivity in newborn rabbit ileum is associated with decreased toxin A receptor. *Journal of Clinical Investigation,* 90**,** 822.

EHRLICH, G. K., BERTHOLD, W. & BAILON, P. 2000. Phage display technology. Affinity selection by biopanning. *Methods Mol Biol,* 147**,** 195-208.

ENGVALL, E. 2010. The ELISA, Enzyme-Linked Immunosorbent Assay. *Clinical Chemistry,* 56**,** 319.

ENGVALL, E. & PERLMANN, P. 1971. ENZYME-LINKED IMMUNOSORBENT ASSAY (ELISA) QUANTITATIVE ASSAY OF IMMUNOGLOBULIN-G. *Immunochemistry,* 8**,** 871-&.

FONG, K. S., FATICA, C., HALL, G., PROCOP, G., SCHINDLER, S., GORDON, S. M. & FRASER, T. G. 2011. Impact of PCR Testing for Clostridium difficile on Incident Rates and Potential on Public Reporting: Is the Playing Field Level? *Infection Control and Hospital Epidemiology,* 32**,** 932-933.

FRANCIS, M. B., ALLEN, C. A., SHRESTHA, R. & SORG, J. A. 2013. Bile acid recognition by the *Clostridium difficile* germinant receptor, CspC, is important for establishing infection. *PLoS Pathog,* 9**,** e1003356.

FREEMAN, J., BAUER, M. P., BAINES, S. D., CORVER, J., FAWLEY, W. N., GOORHUIS, B., KUIJPER, E. J. & WILCOX, M. H. 2010. The Changing Epidemiology of *Clostridium difficile* Infections. *Clinical Microbiology Reviews,* 23**,** 529-549.

FRENZEL, A., HUST, M. & SCHIRRMANN, T. 2013. Expression of recombinant antibodies. *Front Immunol,* 4**,** 217.

GAN, S. D. & PATEL, K. R. 2013. Enzyme immunoassay and enzyme-linked immunosorbent assay. *J Invest Dermatol,* 133**,** 287.

GASTEIGER, E., GATTIKER, A., HOOGLAND, C., IVANYI, I., APPEL, R. D. & BAIROCH, A. 2003. ExPASy: the proteomics server for in-depth protein knowledge and analysis. *Nucleic Acids Research,* 31**,** 3784-3788.

GEBAUER, M. & SKERRA, A. 2009. Engineered protein scaffolds as next-generation antibody therapeutics. *Current Opinion in Chemical Biology,* 13**,** 245-255.

GEORGE, W., SUTTER, V., CITRON, D. & FINEGOLD, S. 1979. Selective and differential medium for isolation of Clostridium difficile. *Journal of clinical microbiology,* 9**,** 214-219.

GERDING, D. N. 2009. *Clostridium difficile* 30 years on: what has, or has not, changed and why? *International Journal of Antimicrobial Agents,* 33, Supplement 1**,** S2-S8.

GERDING, D. N., FILE JR, T. M. & MCDONALD, L. C. 2016. Diagnosis and treatment of *Clostridium difficile* infection. *Infectious Diseases in Clinical Practice,* 24**,** 3-10.

GERIC, B., CARMAN, R. J., RUPNIK, M., GENHEIMER, C. W., SAMBOL, S. P., LYERLY, D. M., GERDING, D. N. & JOHNSON, S. 2006. Binary toxin-producing, large clostridial toxin-negative *Clostridium difficile* strains are enterotoxic but do not cause disease in hamsters. *Journal of Infectious Diseases,* 193**,** 1143-1150.

GHOSE, C. 2013. *Clostridium difficile* infection in the twenty-first century. *Emerg Microbes Infect,* 2**,** e62.

GIRINATHAN, B. P., BRAUN, S., SIRIGIREDDY, A. R., LOPEZ, J. E. & GOVIND, R. 2016. Importance of Glutamate Dehydrogenase (GDH) in *Clostridium difficile* Colonization In Vivo. *PloS one,* 11**,** e0160107.

GIRINATHAN, B. P., BRAUN, S. E. & GOVIND, R. 2014. *Clostridium difficile* glutamate dehydrogenase is a secreted enzyme that confers resistance to H_2O_2. *Microbiology,* 160**,** 47-55.

GIVER, L. & ARNOLD, F. H. 1998. Combinatorial protein design by in vitro recombination. *Current Opinion in Chemical Biology,* 2**,** 335-338.

GOLDENBERG, S., CLIFF, P., SMITH, S., MILNER, M. & FRENCH, G. 2010. Two-step glutamate dehydrogenase antigen real-time polymerase chain reaction assay for detection of toxigenic Clostridium difficile. *Journal of Hospital Infection,* 74**,** 48-54.

GOLDENBERG, S. D., DIERINGER, T. & FRENCH, G. L. 2010. Detection of toxigenic *Clostridium difficile* in diarrheal stools by rapid real-time polymerase chain reaction. *Diagnostic Microbiology and Infectious Disease,* 67**,** 304-307.

GOLDENBERG, S. D., GUMBAN, M., HALL, A., PATEL, A. & FRENCH, G. L. 2011. Lack of effect of strain type on detection of toxigenic *Clostridium difficile* by glutamate dehydrogenase and polymerase chain reaction. *Diagnostic Microbiology and Infectious Disease,* 70**,** 417-419.

GOULD, C. V. & MCDONALD, L. C. 2008. Bench-to-bedside review: *Clostridium difficile* colitis. *Critical Care,* 12**,** 203-203.

GOVIND, R. & DUPUY, B. 2012. Secretion of *Clostridium difficile* toxins A and B requires the holin-like protein TcdE. *PLoS pathogens,* 8**,** e1002727.

GRÖNWALL, C. & STÅHL, S. 2009. Engineered affinity proteins—Generation and applications. *Journal of Biotechnology,* 140**,** 254-269.

HALL, A. J., CURNS, A. T., MCDONALD, L. C., PARASHAR, U. D. & LOPMAN, B. A. 2012. The Roles of *Clostridium difficile* and Norovirus Among Gastroenteritis-Associated Deaths in the United States, 1999–2007. *Clinical Infectious Diseases,* 55**,** 216-223.

HALL, I. C. & O'TOOLE, E. 1935. Intestinal flora in new-born infants: with a description of a new pathogenic anaerobe, Bacillus difficilis. *American journal of diseases of children,* 49**,** 390-402.

HAMERSCASTERMAN, C., ATARHOUCH, T., MUYLDERMANS, S., ROBINSON, G., HAMERS, C., SONGA, E. B., BENDAHMAN, N. & HAMERS, R. 1993. NATURALLY-OCCURRING ANTIBODIES DEVOID OF LIGHT-CHAINS. *Nature,* 363**,** 446-448.

HAN, L., LIU, P., PETRENKO, V. A. & LIU, A. 2016. A Label-Free Electrochemical

Impedance Cytosensor Based on Specific Peptide-Fused Phage Selected from Landscape Phage Library. *Scientific Reports,* 6**,** 22199.

HEY, T., FIEDLER, E., RUDOLPH, R. & FIEDLER, M. 2005. Artificial, non-antibody binding proteins for pharmaceutical and industrial applications. *Trends Biotechnol,* 23**,** 514-522.

HO, J. G., GRECO, A., RUPNIK, M. & NG, K. K.-S. 2005. Crystal structure of receptor-binding C-terminal repeats from *Clostridium difficile* toxin A. *Proceedings of the National Academy of Sciences of the United States of America,* 102**,** 18373-18378.

HOFFMANN, T., STADLER, L. K., BUSBY, M., SONG, Q., BUXTON, A. T., WAGNER, S. D., DAVIS, J. J. & KO FERRIGNO, P. 2010. Structure-function studies of an engineered scaffold protein derived from stefin A. I: Development of the SQM variant. *Protein Eng Des Sel,* 23**,** 403-13.

HONG, K. L. & SOOTER, L. J. 2015. Single-stranded DNA aptamers against pathogens and toxins: identification and biosensing applications. *BioMed research international,* 2015.

HONG, P., KOZA, S. & BOUVIER, E. S. P. 2012. Size-Exclusion Chromatography for the Analysis of Protein Biotherapeutics and their Aggregates. *Journal of Liquid Chromatography & Related Technologies,* 35**,** 2923-2950.

HOOGENBOOM, H. R. 1997. Designing and optimizing library selection strategies for generating high-affinity antibodies. *Trends in Biotechnology,* 15**,** 62-70.

HORNBECK, P. 2001. Enzyme-Linked Immunosorbent Assays. *Current Protocols in Immunology.* John Wiley & Sons, Inc.

HORNBECK, P., WINSTON, S. E. & FULLER, S. A. 2001. Enzyme-linked immunosorbent assays (ELISA). *Curr Protoc Mol Biol,* 11.

HORTIGÜELA, M. J. & WALL, J. G. 2013. Improved detection of domoic acid using covalently immobilised antibody fragments. *Marine drugs,* 11**,** 881-895.

HOSSE, R. J., ROTHE, A. & POWER, B. E. 2006. A new generation of protein display scaffolds for molecular recognition. *Protein Science,* 15**,** 14-27.

HUSSACK, G., ARBABI-GHAHROUDI, M., MACKENZIE, C. R. & TANHA, J. 2012. Isolation and Characterization of *Clostridium difficile* Toxin-Specific Single-Domain Antibodies. *In:* SAERENS, D. & MUYLDERMANS, S. (eds.) *Single Domain Antibodies.* Humana Press.

HUSSACK, G., ARBABI-GHAHROUDI, M., VAN FAASSEN, H., SONGER, J. G., NG, K. K.-S., MACKENZIE, R. & TANHA, J. 2011. Neutralization of *Clostridium difficile* Toxin A with Single-domain Antibodies Targeting the Cell Receptor Binding Domain. *Journal of Biological Chemistry,* 286**,** 8961-8976.

HUSSACK, G. & TANHA, J. 2010. Toxin-specific antibodies for the treatment of Clostridium difficile: current status and future perspectives. *Toxins,* 2**,** 998-1018.

JACKEL, C., KAST, P. & HILVERT, D. 2008. Protein design by directed evolution. *Annu Rev Biophys,* 37**,** 153-73.

JACOBS, S. A., DIEM, M. D., LUO, J. Q., TEPLYAKOV, A., OBMOLOVA, G., MALIA, T., GILLILAND, G. L. & O'NEIL, K. T. 2012. Design of novel FN3 domains with high stability by a consensus sequence approach. *Protein Engineering Design & Selection,* 25**,** 107-117.

JANGI, S. & LAMONT, J. T. 2010. Asymptomatic colonization by *Clostridium difficile*

in infants: implications for disease in later life. *Journal of pediatric gastroenterology and nutrition,* 51**,** 2-7.

JONES, D. S., SILVERMAN, A. P. & COCHRAN, J. R. 2008. Developing therapeutic proteins by engineering ligand-receptor interactions. *Trends Biotechnol,* 26**,** 498-505.

JONES, P. T., DEAR, P. H., FOOTE, J., NEUBERGER, M. S. & WINTER, G. 1986. REPLACING THE COMPLEMENTARITY-DETERMINING REGIONS IN A HUMAN-ANTIBODY WITH THOSE FROM A MOUSE. *Nature,* 321**,** 522-525.

JONSSON, A., WÅLLBERG, H., HERNE, N., STÅHL, S. & FREJD, F. Y. 2009. Generation of tumour-necrosis-factor-α-specific affibody1 molecules capable of blocking receptor binding in vitro. *Biotechnology and Applied Biochemistry,* 54**,** 93-103.

JUNG, D., GIALLOURAKIS, C., MOSTOSLAVSKY, R. & ALT, F. W. 2006. Mechanism and control of V(D)J recombination at the immunoglobulin heavy chain locus. *Annual Review of Immunology.*

JUST, I., SELZER, J., WILM, M., VON EICHEL-STREIBER, C., MANN, M. & AKTORIES, K. 1995. Glucosylation of Rho proteins by *Clostridium difficile* toxin B.

KANG, M., KIM, S. Y., AN, S. S. A. & JU, Y. R. 2013. Characterizing affinity epitopes between prion protein and β-amyloid using an epitope mapping immunoassay. *Experimental & molecular medicine,* 45**,** e34.

KARANICOLAS, J., CORN, J. E., CHEN, I., JOACHIMIAK, L. A., DYM, O., PECK, S. H., ALBECK, S., UNGER, T., HU, W. & LIU, G. 2011. A de novo protein binding pair by computational design and directed evolution. *Molecular cell,* 42**,** 250-260.

KAREN C, C. & JOHN G, B. 2011. Biology of Clostridium difficile: implications for epidemiology and diagnosis. *Annual review of microbiology,* 65**,** 501-521.

KARLSSON, F., BORREBAECK, C. A., NILSSON, N. & MALMBORG-HAGER, A.-C. 2003. The mechanism of bacterial infection by filamentous phages involves molecular interactions between TolA and phage protein 3 domains. *Journal of Bacteriology,* 185**,** 2628-2634.

KATO, K., HAMAGUCHI, Y., OKAWA, S., ISHIKAWA, E., KOBAYASHI, K. & KATUNUMA, N. 1977. Use of rabbit antibody IgG bound onto plain and aminoalkylsilyl glass surface for the enzyme-linked sandwich immunoassay. *Journal of Biochemistry,* 82**,** 261-266.

KELLY, C. P. & LAMONT, J. T. 2008. Clostridium difficile—more difficult than ever. *New England Journal of Medicine,* 359**,** 1932-1940.

KELLY, M., CHAMPAGNE, S., SHERLOCK, C., NOBLE, M., FREEMAN, H. & SMITH, J. 1987. Commercial latex agglutination test for detection of Clostridium difficile-associated diarrhea. *Journal of clinical microbiology,* 25**,** 1244-1247.

KELLY, M. D. C. P. & LAMONT, M. D. J. T. 1998. *CLOSTRIDIUM DIFFICILE* INFECTION. *Annual Review of Medicine,* 49**,** 375-390.

KI, M. K., KANG, K. J. & SHIM, H. 2010. Phage display selection of EGFR-specific antibodies by capture-sandwich panning. *Biotechnology and Bioprocess Engineering,* 15**,** 152-156.

KIM, H., RILEY, T. V., KIM, M., KIM, C. K., YONG, D., LEE, K., CHONG, Y. & PARK, J.-W. 2008. Increasing prevalence of toxin A-negative, toxin B-positive isolates of *Clostridium difficile* in Korea: impact on laboratory diagnosis. *Journal of*

clinical microbiology, 46**,** 1116-1117.

KISS, C., FISHER, H., PESAVENTO, E., DAI, M., VALERO, R., OVECKA, M., NOLAN, R., PHIPPS, M. L., VELAPPAN, N., CHASTEEN, L., MARTINEZ, J. S., WALDO, G. S., PAVLIK, P. & BRADBURY, A. R. 2006. Antibody binding loop insertions as diversity elements. *Nucleic Acids Res,* 34**,** e132.

KNAPPIK, A., GE, L., HONEGGER, A., PACK, P., FISCHER, M., WELLNHOFER, G., HOESS, A., WOÈLLE, J., PLÜCKTHUN, A. & VIRNEKÄS, B. 2000. Fully synthetic human combinatorial antibody libraries (HuCAL) based on modular consensus frameworks and CDRs randomized with trinucleotides. *Journal of molecular biology,* 296**,** 57-86.

KOHLER, G. & MILSTEIN, C. 1975. CONTINUOUS CULTURES OF FUSED CELLS SECRETING ANTIBODY OF PREDEFINED SPECIFICITY. *Nature,* 256**,** 495-497.

KOIDE, A., BAILEY, C. W., HUANG, X. L. & KOIDE, S. 1998. The fibronectin type III domain as a scaffold for novel binding proteins. *Journal of Molecular Biology,* 284**,** 1141-1151.

KOMOR, R. S., ROMERO, P. A., XIE, C. B. & ARNOLD, F. H. 2012. Highly thermostable fungal cellobiohydrolase I (Cel7A) engineered using predictive methods. *Protein Engineering Design and Selection,* 25**,** 827-833.

KONDO, H., ABE, K., EMORI, Y. & ARAI, S. 1991. Gene organization of oryzacystatin-II, a new cystatin superfamily member of plant origin, is closely related to that of oryzacystatin-I but different from those of animal cystatins. *FEBS Lett,* 278**,** 87-90.

KOO, H. L., VAN, J. N., ZHAO, M., YE, X., REVELL, P. A., JIANG, Z.-D., GRIMES, C. Z., KOO, D. C., LASCO, T. & KOZINETZ, C. A. 2014. Real-time polymerase chain reaction detection of asymptomatic *Clostridium difficile* colonization and rising *C. diff*icile–associated disease rates. *Infection Control,* 35**,** 667-673.

KORDIŠ, D. & TURK, V. 2009. Phylogenomic analysis of the cystatin superfamily in eukaryotes and prokaryotes. *BMC Evolutionary Biology,* 9**,** 1-22.

KRAGSTRUP, T. W., OTKJAER, K. & HOLM, C. 2008. The expression of IL-20 and IL-24 and their shared receptors are increased in rheumatoid arthritis and spondyloarthropathy. *Cytokine,* 41.

KRUMPE, L., SCHUMACHER, K., MCMAHON, J., MAKOWSKI, L. & MORI, T. 2007. Trinucleotide cassettes increase diversity of T7 phage-displayed peptide library. *BMC biotechnology,* 7**,** 65.

KUEHNE, S. A., CARTMAN, S. T., HEAP, J. T., KELLY, M. L., COCKAYNE, A. & MINTON, N. P. 2010. The role of toxin A and toxin B in *Clostridium difficile* infection. *Nature,* 467**,** 711-713.

KUFELNICKA, A. M. & KIRN, T. J. 2011. Effective Utilization of Evolving Methods for the Laboratory Diagnosis of *Clostridium difficile* Infection. *Clinical Infectious Diseases,* 52**,** 1451-1457.

KUIJPER, E., COIGNARD, B. & TÜLL, P. 2006. Emergence of Clostridium difficile-associated disease in North America and Europe. *Clinical Microbiology and Infection,* 12**,** 2-18.

KYLE, H. F., WICKSON, K. F., STOTT, J., BURSLEM, G. M., BREEZE, A. L., TIEDE, C., TOMLINSON, D. C., WARRINER, S. L., NELSON, A. & WILSON, A. J. 2015. Exploration of the HIF-1α/p300 interface using peptide and Affimer phage display technologies. *Molecular BioSystems,* 11**,** 2738-2749.

KYNE, L. 2010. Clostridium difficile—beyond antibiotics. *N Engl J Med,* 362**,** 264-265.
LAEMMLI, U. K. 1970. Cleavage of structural proteins during the assembly of the head of bacteriophage T4. *Nature,* 227**,** 680-5.
LEE, J., KIM, H. J., YANG, C. S., KYEONG, H. H., CHOI, J. M., HWANG, D. E., YUK, J. M., PARK, K., KIM, Y. J., LEE, S. G., KIM, D., JO, E. K., CHEONG, H. K. & KIM, H. S. 2014. A High-Affinity Protein Binder that Blocks the IL-6/STAT3 Signaling Pathway Effectively Suppresses Non–Small Cell Lung Cancer. *Mol Ther,* 22**,** 1254-65.
LEE, S. J., YOUN, B.-S., PARK, J. W., NIAZI, J. H., KIM, Y. S. & GU, M. B. 2008. ssDNA aptamer-based surface plasmon resonance biosensor for the detection of retinol binding protein 4 for the early diagnosis of type 2 diabetes. *Analytical chemistry,* 80**,** 2867-2873.
LEFFLER, D. A. & LAMONT, J. T. 2015. *Clostridium difficile* Infection. *New England Journal of Medicine,* 372**,** 1539-1548.
LEHMANN, M., PASAMONTES, L., LASSEN, S. F. & WYSS, M. 2000. The consensus concept for thermostability engineering of proteins. *Biochimica et Biophysica Acta (BBA) - Protein Structure and Molecular Enzymology,* 1543**,** 408-415.
LESSA, F. C., GOULD, C. V. & MCDONALD, L. C. 2012. Current Status of *Clostridium difficile* Infection Epidemiology. *Clinical Infectious Diseases,* 55**,** S65-S70.
LESSA, F. C., MU, Y., BAMBERG, W. M., BELDAVS, Z. G., DUMYATI, G. K., DUNN, J. R., FARLEY, M. M., HOLZBAUER, S. M., MEEK, J. I., PHIPPS, E. C., WILSON, L. E., WINSTON, L. G., COHEN, J. A., LIMBAGO, B. M., FRIDKIN, S. K., GERDING, D. N. & MCDONALD, L. C. 2015. Burden of *Clostridium difficile* Infection in the United States. *New England Journal of Medicine,* 372**,** 825-834.
LIM, S. K., STUART, R. L., MACKIN, K. E., CARTER, G. P., KOTSANAS, D., FRANCIS, M. J., EASTON, M., DIMOVSKI, K., ELLIOTT, B. & RILEY, T. V. 2014. Emergence of a ribotype 244 strain of *Clostridium difficile* associated with severe disease and related to the epidemic ribotype 027 strain. *Clinical Infectious Diseases,* 58**,** 1723-1730.
LIN, A. V. 2015. Indirect ELISA. *Methods Mol Biol,* 1318**,** 51-9.
LIPOVŠEK, D. 2011. Adnectins: engineered target-binding protein therapeutics. *Protein Engineering Design and Selection,* 24**,** 3-9.
LLOYD, A., PASUPULETI, V., THOTA, P., PANT, C., ROLSTON, D. D. K., HERNANDEZ, A. V., BENITES-ZAPATA, V. A., FRASER, T. G., DONSKEY, C. J. & DESHPANDE, A. 2015. Accuracy of loop-mediated isothermal amplification for the diagnosis of *Clostridium difficile* infection: a systematic review. *Diagnostic Microbiology and Infectious Disease*.
LÖFBLOM, J., FELDWISCH, J., TOLMACHEV, V., CARLSSON, J., STÅHL, S. & FREJD, F. Y. 2010. Affibody molecules: Engineered proteins for therapeutic, diagnostic and biotechnological applications. *FEBS Letters,* 584**,** 2670-2680.
LÖFBLOM, J., FREJD, F. Y. & STÅHL, S. 2011. Non-immunoglobulin based protein scaffolds. *Curr Opin Biotechnol,* 22**,** 843-848.
LYERLY, D. M., BARROSO, L. A. & WILKINS, T. D. 1991. Identification of the latex test-reactive protein of *Clostridium difficile* as glutamate dehydrogenase. *Journal of clinical microbiology,* 29**,** 2639-2642.
LYERLY, D. M., KRIVAN, H. C. & WILKINS, T. D. 1988. Clostridium difficile: its disease

and toxins. *Clinical microbiology reviews,* 1**,** 1-18.

LYERLY, D. M., SAUM, K. E., MACDONALD, D. K. & WILKINS, T. D. 1985. Effects of *Clostridium difficile* toxins given intragastrically to animals. *Infection and immunity,* 47**,** 349-352.

LYERLY, D. M., SULLIVAN, N. M. & WILKINS, T. D. 1983. Enzyme-linked immunosorbent assay for *Clostridium difficile* toxin A. *Journal of clinical microbiology,* 17**,** 72-78.

LYERLY, D. M. & WILKINS, T. D. 1986. Commercial latex test for *Clostridium difficile* toxin A does not detect toxin A. *Journal of Clinical Microbiology,* 23**,** 622-623.

LYRAS, D., O/'CONNOR, J. R., HOWARTH, P. M., SAMBOL, S. P., CARTER, G. P., PHUMOONNA, T., POON, R., ADAMS, V., VEDANTAM, G., JOHNSON, S., GERDING, D. N. & ROOD, J. I. 2009. Toxin B is essential for virulence of Clostridium difficile. *Nature,* 458**,** 1176-1179.

MAMLUK, R., CARVAJAL, I. M., MORSE, B. A., WONG, H., ABRAMOWITZ, J., ASLANIAN, S., LIM, A. C., GOKEMEIJER, J., STOREK, M. J., LEE, J., GOSSELIN, M., WRIGHT, M. C., CAMPHAUSEN, R. T., WANG, J., CHEN, Y., MILLER, K., SANDERS, K., SHORT, S., SPERINDE, J., PRASAD, G., WILLIAMS, S., KERBEL, R., EBOS, J., MUTSAERS, A., MENDLEIN, J. D., HARRIS, A. S. & FURFINE, E. S. 2010. Anti-tumor effect of CT-322 as an adnectin inhibitor of vascular endothelial growth factor receptor-2. *MAbs,* 2**,** 199-208.

MATAMOUROS, S., ENGLAND, P. & DUPUY, B. 2007. *Clostridium difficile* toxin expression is inhibited by the novel regulator TcdC. *Molecular microbiology,* 64**,** 1274-1288.

MCCAFFERTY, J., GRIFFITHS, A. D., WINTER, G. & CHISWELL, D. J. 1990. PHAGE ANTIBODIES - FILAMENTOUS PHAGE DISPLAYING ANTIBODY VARIABLE DOMAINS. *Nature,* 348**,** 552-554.

MCDONALD, L. C., KILLGORE, G. E., THOMPSON, A., OWENS JR, R. C., KAZAKOVA, S. V., SAMBOL, S. P., JOHNSON, S. & GERDING, D. N. 2005. An epidemic, toxin gene–variant strain of Clostridium difficile. *New England Journal of Medicine,* 353**,** 2433-2441.

MCFARLAND, L. V., MULLIGAN, M. E., KWOK, R. Y. & STAMM, W. E. 1989. Nosocomial acquisition of *Clostridium difficile* infection. *New England journal of medicine,* 320**,** 204-210.

MCGLONE, S., BAILEY, R., ZIMMER, S., POPOVICH, M., TIAN, Y., UFBERG, P., MUDER, R. & LEE, B. 2012. The economic burden of Clostridium difficile. *Clinical Microbiology and Infection,* 18**,** 282-289.

MCPHERSON, M. J. & WOOTTON, J. C. 1983. Complete nucleotide sequence of the Escherichia coli gdhA gene. *Nucleic Acids Res,* 11**,** 5257-66.

MICHNICK, S. W., REMY, I., CAMPBELL-VALOIS, F. X., VALLEE-BELISLE, A. & PELLETIER, J. N. 2000. Detection of protein-protein interactions by protein fragment complementation strategies. *Applications of Chimeric Genes and Hybrid Proteins, Pt C,* 328**,** 208-230.

MINO, G., BAEZ, M. & GUTIERREZ, G. 2013. Effect of mutation at the interface of Trp-repressor dimeric protein: a steered molecular dynamics simulation. *European Biophysics Journal with Biophysics Letters,* 42**,** 683-690.

MOEHRING, R. W., LOFGREN, E. T. & ANDERSON, D. J. 2013. Impact of Change to

Molecular Testing for *Clostridium difficile* Infection on Healthcare Facility–Associated Incidence Rates. *Infection control and hospital epidemiology : the official journal of the Society of Hospital Epidemiologists of America,* 34**,** 1055-1061.

MORRISON, S. L., JOHNSON, M. J., HERZENBERG, L. A. & OI, V. T. 1984. CHIMERIC HUMAN-ANTIBODY MOLECULES - MOUSE ANTIGEN-BINDING DOMAINS WITH HUMAN CONSTANT REGION DOMAINS. *Proceedings of the National Academy of Sciences of the United States of America-Biological Sciences,* 81**,** 6851-6855.

MROSS, K., RICHLY, H., FISCHER, R., SCHARR, D., BÜCHERT, M., STERN, A., GILLE, H., AUDOLY, L. P. & SCHEULEN, M. E. 2013. First-in-Human Phase I Study of PRS-050 (Angiocal), an Anticalin Targeting and Antagonizing VEGF-A, in Patients with Advanced Solid Tumors. *PLOS ONE,* 8**,** e83232.

MURASE, K., MORRISON, K. L., TAM, P. Y., STAFFORD, R. L., JURNAK, F. & WEISS, G. A. 2003. EF-Tu binding peptides identified, dissected, and affinity optimized by phage display. *Chem Biol,* 10**,** 161-8.

NILSSON, B., MOKS, T., JANSSON, B., ABRAHMSEN, L., ELMBLAD, A., HOLMGREN, E., HENRICHSON, C., JONES, T. A. & UHLEN, M. 1987. A synthetic IgG-binding domain based on staphylococcal protein A. *Protein Eng,* 1**,** 107-13.

NORDBERG, E., FRIEDMAN, M., GOSTRING, L., ADAMS, G. P., BRISMAR, H., NILSSON, F. Y., STAHL, S., GLIMELIUS, B. & CARLSSON, J. 2007. Cellular studies of binding, internalization and retention of a radiolabeled EGFR-binding affibody molecule. *Nucl Med Biol,* 34**,** 609-18.

NOVAK-WEEKLEY, S. M. & HOLLINGSWORTH, M. H. 2008. Comparison of the Premier Toxin A and B Assay and the TOX A/B II Assay for Diagnosis of *Clostridium difficile* Infection. *Clinical and Vaccine Immunology : CVI,* 15**,** 575-578.

NOVAK-WEEKLEY, S. M., MARLOWE, E. M., MILLER, J. M., CUMPIO, J., NOMURA, J. H., VANCE, P. H. & WEISSFELD, A. 2010. *Clostridium difficile* testing in the clinical laboratory by use of multiple testing algorithms. *J Clin Microbiol,* 48**,** 889-93.

NUTTALL, S. D. & WALSH, R. B. 2008. Display scaffolds: protein engineering for novel therapeutics. *Current Opinion in Pharmacology,* 8**,** 609-615.

NYGREN, P.-Å. & SKERRA, A. 2004. Binding proteins from alternative scaffolds. *Journal of Immunological Methods,* 290**,** 3-28.

OCHSNER, U. A., GREEN, L. S., GOLD, L. & JANJIC, N. 2014. Systematic selection of modified aptamer pairs for diagnostic sandwich assays. *Biotechniques,* 56**,** 125-133.

OCHSNER, U. A., KATILIUS, E. & JANJIC, N. 2013. Detection of *Clostridium difficile* toxins A, B and binary toxin with slow off-rate modified aptamers. *Diagn Microbiol Infect Dis,* 76**,** 278-85.

ODEGRIP, R., COOMBER, D., ELDRIDGE, B., HEDERER, R., KUHLMAN, P. A., ULLMAN, C., FITZGERALD, K. & MCGREGOR, D. 2004. CIS display: In vitro selection of peptides from libraries of protein-DNA complexes. *Proceedings of the National Academy of Sciences of the United States of America,* 101**,** 2806-2810.

OWENS, J. R. C., DONSKEY, C. J., GAYNES, R. P., LOO, V. G. & MUTO, C. A. 2008.

Antimicrobial-Associated Risk Factors for *Clostridium difficile* Infection. *Clinical Infectious Diseases,* 46**,** S19-S31.

PACE, C. N., VAJDOS, F., FEE, L., GRIMSLEY, G. & GRAY, T. 1995. How to measure and predict the molar absorption coefficient of a protein. *Protein Science,* 4**,** 2411-2423.

PALCHETTI, I. & MASCINI, M. 2012. Aptamer-based Biosensors for Cancer Studies. *Biosensors and Cancer***,** 85.

PARK, J. H., JEE, M. H., KWON, O. S., KEUM, S. J. & JANG, S. K. 2013. Infectivity of hepatitis C virus correlates with the amount of envelope protein E2: development of a new aptamer-based assay system suitable for measuring the infectious titer of HCV. *Virology,* 439**,** 13-22.

PASQUO, A., BRITTON, K. L., STILLMAN, T. J., RICE, D. W., COLFEN, H., HARDING, S. E., SCANDURRA, R. & ENGEL, P. C. 1996. Construction of a dimeric form of glutamate dehydrogenase from Clostridium symbiosum by site-directed mutagenesis. *Biochim Biophys Acta,* 1297**,** 149-58.

PÉPIN, J., SAHEB, N., COULOMBE, M.-A., ALARY, M.-E., CORRIVEAU, M.-P., AUTHIER, S., LEBLANC, M., RIVARD, G., BETTEZ, M. & PRIMEAU, V. 2005. Emergence of fluoroquinolones as the predominant risk factor for Clostridium difficile–associated diarrhea: a cohort study during an epidemic in Quebec. *Clinical Infectious Diseases,* 41**,** 1254-1260.

PÉPIN, J., VALIQUETTE, L. & COSSETTE, B. 2005. Mortality attributable to nosocomial Clostridium difficile–associated disease during an epidemic caused by a hypervirulent strain in Quebec. *Canadian Medical Association Journal,* 173**,** 1037-1042.

PERCHIACCA, J. M., BHATTACHARYA, M. & TESSIER, P. M. 2011. Mutational analysis of domain antibodies reveals aggregation hotspots within and near the complementarity determining regions. *Proteins: Structure, Function, and Bioinformatics,* 79**,** 2637-2647.

PETRENKO, V., SMITH, G., GONG, X. & QUINN, T. 1996. A library of organic landscapes on filamentous phage. *Protein Engineering,* 9**,** 797-801.

PLANCHE, T., AGHAIZU, A., HOLLIMAN, R., RILEY, P., POLONIECKI, J., BREATHNACH, A. & KRISHNA, S. 2008. Diagnosis of *Clostridium difficile* infection by toxin detection kits: a systematic review. *The Lancet infectious diseases,* 8**,** 777-784.

PLANCHE, T. & WILCOX, M. 2011. Reference assays for *Clostridium difficile* infection: one or two gold standards? *Journal of Clinical Pathology,* 64**,** 1-5.

PLANCHE, T. D., DAVIES, K. A., COEN, P. G., FINNEY, J. M., MONAHAN, I. M., MORRIS, K. A., O'CONNOR, L., OAKLEY, S. J., POPE, C. F. & WREN, M. W. 2013. Differences in outcome according to *Clostridium difficile* testing method: a prospective multicentre diagnostic validation study of C difficile infection. *The Lancet infectious diseases,* 13**,** 936-945.

POLAGE, C. R., CHIN, D. L., LESLIE, J. L., TANG, J., COHEN, S. H. & SOLNICK, J. V. 2012. Outcomes in patients tested for *Clostridium difficile* toxins. *Diagnostic microbiology and infectious disease,* 74**,** 369-373.

POLAGE, C. R., GYORKE, C. E., KENNEDY, M. A., LESLIE, J. L., CHIN, D. L., WANG, S., NGUYEN, H. H., HUANG, B., TANG, Y. W., LEE, L. W., KIM, K., TAYLOR, S., ROMANO, P. S., PANACEK, E. A., GOODELL, P. B., SOLNICK, J. V. & COHEN, S.

H. 2015. Overdiagnosis of *Clostridium difficile* Infection in the Molecular Test Era. *JAMA Intern Med,* 175**,** 1792-801.

PRUITT, R. N., CHAMBERS, M. G., NG, K. K.-S., OHI, M. D. & LACY, D. B. 2010. Structural organization of the functional domains of *Clostridium difficile* toxins A and B. *Proceedings of the National Academy of Sciences,* 107**,** 13467-13472.

PRUITT, R. N. & LACY, D. B. 2012. Toward a structural understanding of *Clostridium difficile* toxins A and B. *Frontiers in cellular and infection microbiology,* 2.

QIU, L.-W., DI, B., WEN, K., WANG, X.-S., LIANG, W.-H., WANG, Y.-D., PAN, Y.-X., WANG, M., DING, Y.-Q. & CHE, X.-Y. 2009. Development of an Antigen Capture Immunoassay Based on Monoclonal Antibodies Specific for Dengue Virus Serotype 2 Nonstructural Protein 1 for Early and Rapid Identification of Dengue Virus Serotype 2 Infections. *Clinical and Vaccine Immunology,* 16**,** 88-95.

QUINN, C. D., SEFERS, S. E., BABIKER, W., HE, Y., ALCABASA, R., STRATTON, C. W., CARROLL, K. C. & TANG, Y. W. 2010. *C. diff* Quik Chek complete enzyme immunoassay provides a reliable first-line method for detection of *Clostridium difficile* in stool specimens. *Journal of Clinical Microbiology,* 48**,** 603-605.

RAINA, M., SHARMA, R., DEACON, S. E., TIEDE, C., TOMLINSON, D., DAVIES, A. G., MCPHERSON, M. J. & WALTI, C. 2015. Antibody mimetic receptor proteins for label-free biosensors. *Analyst,* 140**,** 803-810.

REICHERT, J. M. Antibodies to watch in 2010. MAbs, 2010. Landes Bioscience, 2, 84-100.

RILEY, T., BRAZIER, J., HASSAN, H., WILLIAMS, K. & PHILLIPS, K. 1987. Comparison of alcohol shock enrichment and selective enrichment for the isolation of Clostridium difficile. *Epidemiology and infection,* 99**,** 355-359.

ROBERTS, B. L., MARKLAND, W., LEY, A. C., KENT, R. B., WHITE, D. W., GUTERMAN, S. K. & LADNER, R. C. 1992. DIRECTED EVOLUTION OF A PROTEIN - SELECTION OF POTENT NEUTROPHIL ELASTASE INHIBITORS DISPLAYED ON M13 FUSION PHAGE. *Proceedings of the National Academy of Sciences of the United States of America,* 89**,** 2429-2433.

ROUX, K. H., GREENBERG, A. S., GREENE, L., STRELETS, L., AVILA, D., MCKINNEY, E. C. & FLAJNIK, M. F. 1998. Structural analysis of the nurse shark (new) antigen receptor (NAR): Molecular convergence of NAR and unusual mammalian immnnoglobulins. *Proceedings of the National Academy of Sciences of the United States of America,* 95**,** 11804-11809.

RUBIN, M. S., BODENSTEIN, L. E. & KENT, K. C. 1995. Severe*Clostridium difficile* colitis. *Diseases of the Colon & Rectum,* 38**,** 350-354.

RUIGROK, V. J. B., LEVISSON, M., EPPINK, M. H. M., SMIDT, H. & VAN DER OOST, J. 2011. Alternative affinity tools: more attractive than antibodies? *Biochemical Journal,* 436**,** 1-13.

RUPNIK, M., AVESANI, V., JANC, M., VON EICHEL-STREIBER, C. & DELMÉE, M. 1998. A Novel Toxinotyping Scheme and Correlation of Toxinotypes with Serogroups of Clostridium difficileIsolates. *Journal of clinical microbiology,* 36**,** 2240-2247.

RUPNIK, M., WILCOX, M. H. & GERDING, D. N. 2009. *Clostridium difficile* infection:

new developments in epidemiology and pathogenesis. *Nat Rev Micro,* 7**,** 526-536.

SAXENA, D., KUMAR, J. S., PARIDA, M., SIVAKUMAR, R. R. & PATRO, I. K. 2013. Development and evaluation of NS1 specific monoclonal antibody based antigen capture ELISA and its implications in clinical diagnosis of West Nile virus infection. *Journal of Clinical Virology,* 58**,** 528-534.

SCHELLENBERGER, V., WANG, C.-W., GEETHING, N. C., SPINK, B. J., CAMPBELL, A., TO, W., SCHOLLE, M. D., YIN, Y., YAO, Y. & BOGIN, O. 2009. A recombinant polypeptide extends the in vivo half-life of peptides and proteins in a tunable manner. *Nature biotechnology,* 27**,** 1186-1190.

SCHLEHUBER, S., BESTE, G. & SKERRA, A. 2000. A novel type of receptor protein, based on the lipocalin scaffold, with specificity for digoxigenin11Edited by R. Huber. *Journal of Molecular Biology,* 297**,** 1105-1120.

SCHROEDER JR, H. W. & CAVACINI, L. 2010. Structure and function of immunoglobulins. *Journal of Allergy and Clinical Immunology,* 125**,** S41-S52.

SCHROEDER, L. F., ROBILOTTI, E., PETERSON, L. R., BANAEI, N. & DOWDY, D. W. 2014. Economic Evaluation of Laboratory Testing Strategies for Hospital-Associated *Clostridium difficile* Infection. *Journal of Clinical Microbiology,* 52**,** 489-496.

SCOTT, J. K. & SMITH, G. P. 1990. Searching for peptide ligands with an epitope library. *Science,* 249**,** 386-390.

SHARMA, R., DEACON, S. E., NOWAK, D., GEORGE, S., SZYMONIK, M., TANG, A., TOMLINSON, D., DAVIES, A., MCPHERSON, M. & WÄLTI, C. 2016. Label-free electrochemical impedance biosensor to detect human interleukin-8 in serum with sub-pg/ml sensitivity. *Biosensors and Bioelectronics,* 80**,** 607-613.

SHARP, S. E., RUDEN, L. O., POHL, J. C., HATCHER, P. A., JAYNE, L. M. & IVIE, W. M. 2010. Evaluation of the *C. diff* Quik Chek Complete Assay, a New Glutamate Dehydrogenase and A/B Toxin Combination Lateral Flow Assay for Use in Rapid, Simple Diagnosis of *Clostridium difficile* Disease. *Journal of Clinical Microbiology,* 48**,** 2082-2086.

SHERWOOD, L. J. & HAYHURST, A. 2012. Hapten Mediated Display and Pairing of Recombinant Antibodies Accelerates Assay Assembly for Biothreat Countermeasures. 2**,** 807.

SHETTY, N., WREN, M. & COEN, P. 2011. The role of glutamate dehydrogenase for the detection of *Clostridium difficile* in faecal samples: a meta-analysis. *Journal of Hospital Infection,* 77**,** 1-6.

SHIN, B.-M., KUAK, E. Y., YOO, S. J., SHIN, W. C. & YOO, H. M. 2008. Emerging toxin A− B+ variant strain of *Clostridium difficile* responsible for pseudomembranous colitis at a tertiary care hospital in Korea. *Diagnostic Microbiology and Infectious Disease,* 60**,** 333-337.

SIDDIQUI, M. Z. 2010. Monoclonal Antibodies as Diagnostics; an Appraisal. *Indian Journal of Pharmaceutical Sciences,* 72**,** 12-17.

SIDHU, S. S., WEISS, G. A. & WELLS, J. A. 2000. High copy display of large proteins on phage for functional selections. *J Mol Biol,* 296**,** 487-95.

SIMOR, A. E., BRADLEY, S. F., STRAUSBAUGH, L. J., CROSSLEY, K. & NICOLLE, L. E. 2002. *Clostridium difficile* in long-term-care facilities for the elderly. *Infect Control Hosp Epidemiol,* 23**,** 696-703.

SKERRA, A. 2000. Engineered protein scaffolds for molecular recognition. *Journal of Molecular Recognition,* 13**,** 167-187.

SKERRA, A. 2000. Lipocalins as a scaffold. *Biochimica Et Biophysica Acta-Protein Structure and Molecular Enzymology,* 1482**,** 337-350.

SKERRA, A. 2003. Imitating the humoral immune response. *Current Opinion in Chemical Biology,* 7**,** 683-693.

SKERRA, A. 2007. Alternative non-antibody scaffolds for molecular recognition. *Curr Opin Biotechnol,* 18**,** 295-304.

ŠKRLEC, K., ŠTRUKELJ, B. & BERLEC, A. 2015. Non-immunoglobulin scaffolds: a focus on their targets. *Trends in Biotechnology,* 33**,** 408-418.

SLOAN, L. M., DURESKO, B. J., GUSTAFSON, D. R. & ROSENBLATT, J. E. 2008. Comparison of Real-Time PCR for Detection of the tcdC Gene with Four Toxin Immunoassays and Culture in Diagnosis of *Clostridium difficile* Infection. *Journal of clinical microbiology,* 46**,** 1996-2001.

SMIALOWSKI, P., MARTIN-GALIANO, A. J., MIKOLAJKA, A., GIRSCHICK, T., HOLAK, T. A. & FRISHMAN, D. 2007. Protein solubility: sequence based prediction and experimental verification. *Bioinformatics,* 23**,** 2536-2542.

SMITH, G. P. 1985. FILAMENTOUS FUSION PHAGE - NOVEL EXPRESSION VECTORS THAT DISPLAY CLONED ANTIGENS ON THE VIRION SURFACE. *Science,* 228**,** 1315-1317.

SMITH, G. P. & PETRENKO, V. A. 1997. Phage display. *Chemical Reviews,* 97**,** 391-410.

SONG, L., ZHAO, M., DUFFY, D. C., HANSEN, J., SHIELDS, K., WUNGJIRANIRUN, M., CHEN, X., XU, H., LEFFLER, D. A., SAMBOL, S. P., GERDING, D. N., KELLY, C. P. & POLLOCK, N. R. 2015. Development and Validation of Digital Enzyme-Linked Immunosorbent Assays for Ultrasensitive Detection and Quantification of *Clostridium difficile* Toxins in Stool. *Journal of Clinical Microbiology,* 53**,** 3204-3212.

STADLER, L. K. J., HOFFMANN, T., TOMLINSON, D. C., SONG, Q., LEE, T., BUSBY, M., NYATHI, Y., GENDRA, E., TIEDE, C., FLANAGAN, K., COCKELL, S. J., WIPAT, A., HARWOOD, C., WAGNER, S. D., KNOWLES, M. A., DAVIS, J. J., KEEGAN, N. & KO FERRIGNO, P. 2011. Structure–function studies of an engineered scaffold protein derived from Stefin A. II: Development and applications of the SQT variant. *Protein Engineering Design and Selection,* 24**,** 751-763.

STAHL, S., KRONQVIST, N., JONSSON, A. & LOFBLOM, J. 2013. Affinity proteins and their generation. *Journal of Chemical Technology and Biotechnology,* 88**,** 25-38.

STEELE, J., CHEN, K., SUN, X., ZHANG, Y., WANG, H., TZIPORI, S. & FENG, H. 2012. Systemic dissemination of *Clostridium difficile* toxins A and B is associated with severe, fatal disease in animal models. *Journal of Infectious Diseases,* 205**,** 384-391.

STEIPE, B., SCHILLER, B., PLUCKTHUN, A. & STEINBACHER, S. 1994. Sequence statistics reliably predict stabilizing mutations in a protein domain. *J Mol Biol,* 240**,** 188-92.

STEMMER, W. P. C. 1994. RAPID EVOLUTION OF A PROTEIN IN-VITRO BY DNA SHUFFLING. *Nature,* 370**,** 389-391.

STUDIER, F. W. & MOFFATT, B. A. 1986. Use of bacteriophage T7 RNA polymerase

to direct selective high-level expression of cloned genes. *Journal of molecular biology,* 189**,** 113-130.

SU, W.-Y., MERCER, J., VAN HAL, S. J. & MALEY, M. 2013. *Clostridium difficile* Testing: Have We Got It Right? *Journal of Clinical Microbiology,* 51**,** 377-378.

SURAWICZ, C. M., BRANDT, L. J., BINION, D. G., ANANTHAKRISHNAN, A. N., CURRY, S. R., GILLIGAN, P. H., MCFARLAND, L. V., MELLOW, M. & ZUCKERBRAUN, B. S. 2013. Guidelines for diagnosis, treatment, and prevention of *Clostridium difficile* infections. *The American journal of gastroenterology,* 108**,** 478.

SWINDELLS, J., BRENWALD, N., READING, N. & OPPENHEIM, B. 2010. Evaluation of diagnostic tests for *Clostridium difficile* infection. *Journal of clinical microbiology,* 48**,** 606-608.

TEDESCO, F. J., BARTON, R. W. & ALPERS, D. H. 1974. Clindamycin associated colitis. A prospective study. *Annals of Internal Medicine,* 81**,** 429-433.

TERPE, K. 2006. Overview of bacterial expression systems for heterologous protein production: from molecular and biochemical fundamentals to commercial systems. *Applied microbiology and biotechnology,* 72**,** 211-222.

THOMPSON, J. D., HIGGINS, D. G. & GIBSON, T. J. 1994. CLUSTAL-W - IMPROVING THE SENSITIVITY OF PROGRESSIVE MULTIPLE SEQUENCE ALIGNMENT THROUGH SEQUENCE WEIGHTING, POSITION-SPECIFIC GAP PENALTIES AND WEIGHT MATRIX CHOICE. *Nucleic Acids Research,* 22**,** 4673-4680.

TICEHURST, J. R., AIRD, D. Z., DAM, L. M., BOREK, A. P., HARGROVE, J. T. & CARROLL, K. C. 2006. Effective detection of toxigenic *Clostridium difficile* by a two-step algorithm including tests for antigen and cytotoxin. *Journal of clinical microbiology,* 44**,** 1145-1149.

TIEDE, C., TANG, A. A. S., DEACON, S. E., MANDAL, U., NETTLESHIP, J. E., OWEN, R. L., GEORGE, S. E., HARRISON, D. J., OWENS, R. J., TOMLINSON, D. C. & MCPHERSON, M. J. 2014. Affimer: a stable and versatile peptide display scaffold for molecular recognition applications. *Protein Engineering Design and Selection*.

TLEYJEH, I. M., ABDULHAK, A. A. B., RIAZ, M., ALASMARI, F. A., GARBATI, M. A., ALGHAMDI, M., KHAN, A. R., AL TANNIR, M., ERWIN, P. J. & IBRAHIM, T. 2012. Association between proton pump inhibitor therapy and *Clostridium difficile* infection: a contemporary systematic review and meta-analysis. *PloS one,* 7**,** e50836.

TREVINO, S. R., SCHOLTZ, J. M. & PACE, C. N. 2007. Amino acid contribution to protein solubility: Asp, Glu, and Ser contribute more favorably than the other hydrophilic amino acids in RNase Sa. *Journal of molecular biology,* 366**,** 449-460.

VAN DEN BERG, R. J., BRUIJNESTEIJN VAN COPPENRAET, L. S., GERRITSEN, H.-J., ENDTZ, H. P., VAN DER VORM, E. R. & KUIJPER, E. J. 2005. Prospective Multicenter Evaluation of a New Immunoassay and Real-Time PCR for Rapid Diagnosis of Clostridium difficile-Associated Diarrhea in Hospitalized Patients. *Journal of clinical microbiology,* 43**,** 5338-5340.

VAN DEN BERG, R. J., VAN COPPENRAET, L. S. B., GERRITSEN, H.-J., ENDTZ, H. P., VAN DER VORM, E. R. & KUIJPER, E. J. 2005. Prospective multicenter evaluation of a new immunoassay and real-time PCR for rapid diagnosis of Clostridium difficile-associated diarrhea in hospitalized patients. *Journal of*

clinical microbiology, 43**,** 5338-5340.
VAN DIJK, M. A. & VAN DE WINKEL, J. G. 2001. Human antibodies as next generation therapeutics. *Curr Opin Chem Biol,* 5**,** 368-74.
VAN WEEMEN, B. K. & SCHUURS, A. H. 1971. Immunoassay using antigen-enzyme conjugates. *FEBS Lett,* 15**,** 232-236.
VANPOUCKE, H., DE BAERE, T., CLAEYS, G., VANEECHOUTTE, M. & VERSCHRAEGEN, G. 2001. Evaluation of six commercial assays for the rapid detection of *Clostridium difficile* toxin and/or antigen in stool specimens. *Clinical Microbiology and Infection,* 7**,** 55-64.
VODNIK, M., ZAGER, U., STRUKELJ, B. & LUNDER, M. 2011. Phage display: selecting straws instead of a needle from a haystack. *Molecules,* 16**,** 790-817.
VON EICHEL-STREIBER, C., LAUFENBERG-FELDMANN, R., SARTINGEN, S., SCHULZE, J. & SAUERBORN, M. 1992. Comparative sequence analysis of the*Clostridium difficile* toxins A and B. *Molecular and General Genetics MGG,* 233**,** 260-268.
VON EICHEL-STREIBER, C., WARFOLOMEOW, I., KNAUTZ, D., SAUERBORN, M. & HADDING, U. 1991. Morphological changes in adherent cells induced by *Clostridium difficile* toxins. *Biochem Soc Trans,* 19**,** 1154-60.
VOTH, D. E. & BALLARD, J. D. 2005. *Clostridium difficile* toxins: mechanism of action and role in disease. *Clinical microbiology reviews,* 18**,** 247-263.
WANG, W., SINGH, S., ZENG, D. L., KING, K. & NEMA, S. 2007. Antibody structure, instability, and formulation. *Journal of Pharmaceutical Sciences,* 96**,** 1-26.
WESOLOWSKI, J., ALZOGARAY, V., REYELT, J., UNGER, M., JUAREZ, K., URRUTIA, M., CAUERHFF, A., DANQUAH, W., RISSIEK, B. & SCHEUPLEIN, F. 2009. Single domain antibodies: promising experimental and therapeutic tools in infection and immunity. *Medical microbiology and immunology,* 198**,** 157-174.
WILCOX, M. H. 2012. Overcoming barriers to effective recognition and diagnosis of *Clostridium difficile* infection. *Clinical Microbiology and Infection,* 18**,** 13-20.
WILLATS, W. G. 2002. Phage display: practicalities and prospects. *Plant molecular biology,* 50**,** 837-854.
WILLIAMS, S., SCHULZ, P. & SIERKS, M. R. 2015. A sensitive phage-based capture ELISA for sub-femtomolar detection of protein variants directly from biological samples. *Biotechnol Prog,* 31**,** 289-98.
WOJCIK, J., HANTSCHEL, O., GREBIEN, F., KAUPE, I., BENNETT, K. L., BARKINGE, J., JONES, R. B., KOIDE, A., SUPERTI-FURGA, G. & KOIDE, S. 2010. A potent and highly specific FN3 monobody inhibitor of the Abl SH2 domain. *Nature Structural & Molecular Biology,* 17**,** 519-U173.
WONG, S., SANTULLO, P., O'DRISCOLL, J., JAMOUS, A., HIRANI, S. P. & SAIF, M. 2017. Use of antibiotic and prevalence of antibiotic-associated diarrhoea in-patients with spinal cord injuries: a UK national spinal injury centre experience. *Spinal Cord*.
WOODMAN, R., YEH, J. T. H., LAURENSON, S. & FERRIGNO, P. K. 2005. Design and Validation of a Neutral Protein Scaffold for the Presentation of Peptide Aptamers. *Journal of Molecular Biology,* 352**,** 1118-1133.
WURCH, T., LOWE, P., CAUSSANEL, V., BES, C., BECK, A. & CORVAIA, N. 2008. Development of Novel Protein Scaffolds as Alternatives to Whole Antibodies for Imaging and Therapy: Status on Discovery Research and

Clinical Validation. *Current Pharmaceutical Biotechnology,* 9**,** 502-509.

WURCH, T., LOWE, P., CAUSSANEL, V., BES, C., BECK, A. & CORVAIA, N. 2008. Development of Novel Protein Scaffolds as Alternatives to Whole Antibodies for Imaging and Therapy: Status on Discovery Research and Clinical Validation. *Current Pharmaceutical Biotechnology,* 9**,** 502-509.

XU, H., DI, B., PAN, Y.-X., QIU, L.-W., WANG, Y.-D., HAO, W., HE, L.-J., YUEN, K.-Y. & CHE, X.-Y. 2006. Serotype 1-Specific Monoclonal Antibody-Based Antigen Capture Immunoassay for Detection of Circulating Nonstructural Protein NS1: Implications for Early Diagnosis and Serotyping of Dengue Virus Infections. *Journal of Clinical Microbiology,* 44**,** 2872-2878.

YALOW, R. S. & BERSON, S. A. 1960. Immunoassay of endogenous plasma insulin in man. *The Journal of clinical investigation,* 39**,** 1157-1175.

ZHANG, C., JIN, K., XIAO, Y., CHENG, Y., HUANG, Z., WANG, S. & LU, S. 2013. Potent monoclonal antibodies against *Clostridium difficile* toxin A elicited by DNA immunization. *Human Vaccines & Immunotherapeutics,* 9**,** 2157-2164.

ZIMLICHMAN, E., HENDERSON, D., TAMIR, O., FRANZ, C., SONG, P., YAMIN, C. K., KEOHANE, C., DENHAM, C. R. & BATES, D. W. 2013. Health care–associated infections: a meta-analysis of costs and financial impact on the US health care system. *JAMA internal medicine,* 173**,** 2039-2046.